

# Next Generation Risk Assessment of Androgens and Estrogens



Tessa C.A. van Tongeren

## **Propositions**

1. The Dietary Comparator Ratio approach is an adequate new approach methodology for the safety assessment of human chemical exposures.  
(this thesis)
2. Biologically active metabolites must be taken into account in the physiologically based kinetic modelling-facilitated quantitative in vitro to in vivo extrapolation for evaluating the safety of a parent compound.  
(this thesis)
3. Medical science has a gender problem.
4. Risk analysis is required before adopting artificial intelligence in technology.
5. Educational school visits to slaughterhouses will benefit a more sustainable meat consuming society.
6. The race car track in Zandvoort must be repurposed to a Natura 2000 area.

Propositions belonging to the thesis, entitled  
Next Generation Risk Assessment of Androgens and Estrogens.

Tessa C. A. van Tongeren  
Wageningen, 05 September 2023

# **Next Generation Risk Assessment of Androgens and Estrogens**

**Tessa C.A. van Tongeren**

## **Thesis committee**

### **Promotors**

Prof. Dr I.M.C.M Rietjens  
Professor of Toxicology  
Wageningen University & Research

Prof. Dr P.L. Carmichael  
Special Professor, Next Generation Risk Assessment Approaches for Human and  
Environmental Health  
Wageningen University & Research  
Unilever Safety and Environmental Assurance Centre (SEAC), Sharnbrook, United  
Kingdom

### **Co-promotor**

Dr H. Li  
Toxicologist  
Unilever SEAC, Sharnbrook, United Kingdom

### **Other members**

Prof. Dr R.F. Witkamp, Wageningen University & Research  
Dr.P. Kukic, Unilever SEAC, Sharnbrook, United Kingdom  
Prof. Dr J. Legler, Utrecht University  
Dr A. Paini, esqLABS GmbH, Saterland, Germany

This research was conducted under the auspices of VLAG Graduate School (Biobased, Biomolecular, Chemical, Food, and Nutrition sciences)

# **Next Generation Risk Assessment of Androgens and Estrogens**

**Tessa C.A. van Tongeren**

## **Thesis**

submitted in fulfilment of the requirements for the degree of doctor

at Wageningen University

by the authority of the Rector Magnificus,

Prof. Dr A.P.J. Mol,

in the presence of the

Thesis Committee appointed by the Academic Board

to be defended in public

on Tuesday 05 September 2023

at 1.30 p.m. in the Omnia Auditorium.

Tessa C.A. van Tongeren

Next Generation Risk Assessment of Androgens and Estrogens, 259 pages.

PhD thesis, Wageningen University, Wageningen, the Netherlands (2023)

With references, with summary in English and Dutch

ISBN 978-94-6447-775-7

DOI <https://doi.org/10.18174/633853>

# Contents

<b>Chapter 1</b>	General introduction	<b>7</b>
<b>Chapter 2</b>	Next generation risk assessment of human exposure to anti-androgens using newly defined comparator compound values	<b>27</b>
<b>Chapter 3</b>	Next generation risk assessment of human exposure to estrogens using safe comparator compound values based on <i>in vitro</i> bioactivity assays	<b>55</b>
<b>Chapter 4</b>	Next generation risk assessment of the anti-androgen flutamide including the contribution of its active metabolite hydroxyflutamide	<b>117</b>
<b>Chapter 5</b>	A two-chamber co-culture system with human liver and reporter cells for evaluating androgenic responses	<b>151</b>
<b>Chapter 6</b>	General discussion	<b>183</b>
<b>Chapter 7</b>	Summary	<b>209</b>
<b>Chapter 8</b>	Samenvatting	<b>213</b>
<b>Chapter 9</b>	References	<b>217</b>
<b>Appendix</b>	Acknowledgment	<b>250</b>
	Biography	<b>255</b>
	List of Publications	<b>256</b>
	Overview of completed training activities	<b>257</b>



# Chapter 1



# Chapter 1. General introduction

## 1.1 General introduction and aim of the thesis

The purpose of toxicological risk assessment is to assure safe levels of human exposure to chemicals. An important group of chemicals to evaluate in risk assessment are putative endocrine disrupting chemicals (EDCs). EDCs are defined by the World Health Organization (WHO) as *an exogenous substance or mixture that alters function(s) of the endocrine system and consequently causes adverse health effects in an intact organism, or its progeny, or (sub)populations* (Damstra et al., 2002). Exposure to putative EDCs, or endocrine acting chemicals (EACs), is of concern because of increasing incidences of endocrine-related diseases in humans (Bergman et al., 2013). These pathologies include infertility, cardiovascular disease, and elevated rates of endocrine-related cancers such as breast, endometrial, ovarian, prostate, testicular, and thyroid cancer over a time-scale that could not be causing increasing incidence of these effects by genetic factors (Bergman et al., 2013; Damstra et al., 2002). There is however controversy in the scientific assessment of EDC-induced health problems due to limited human data correlating EDC exposure to human disease (Safe, 2020). Still, recently, an estimation was presented that up to 800 chemicals are expected or suspected to act as EDCs (Bergman et al., 2013).

The European Union presented REACH (Registration, Evaluation, Authorization and restriction of CHemicals), in which the regulation of the safety assessment of existing or new chemicals and consumer products, produced or marketed in quantities of more than one ton per year, is established (European Commission, 2006). It was estimated that to meet the REACH requirements, in the best-case scenario, up to 54 million vertebrate animals would be required for toxicity testing and costs would be up to 9.5 billion euros (Rovida & Hartung, 2009). However in REACH, there are not yet standard toxicity tests for EACs defined (Rovida & Hartung, 2009). The Organisation for Economic Co-operation and Development (OECD) defined the Conceptual Framework for the Testing and Assessment of Endocrine Disrupting Chemicals (the 'OECD Conceptual Framework') which includes a tiered approach of *in vitro* screening tests to prioritize chemicals for further *in vivo* testing (OECD, 2018b), the latter used to evaluate safe exposure levels. *In vivo* tests, among others, include the uterotrophic, Hershberger, 28- and 90-day repeat-dose toxicity, and the extended one- and two-generation reproductive toxicity assays in rats. In the uterotrophic assay, the chemical-dependent increase in the weight of the uterus in ovariectomized or intact immature female rats is

measured. The increase in wet and blotted (dry) uterine weight is related to the chemical exposure (Hyung et al., 2005). In the Hershberger assay, the chemical-dependent response is measured by the weight change of the ventral prostate, seminal vesicle (plus fluids and coagulating glands), levator ani-bulbocavernosus muscle, paired Cowper's glands, and the glans penis in castrated or peripubertal male rats (OECD, 2009). In both assays, the treatment period is short and the doses of the tested chemical are high. The 28- and 90-day repeat-dose toxicity studies in rodents are performed to look at changes in growth, organ weights, and histopathology that could be related to chemical-dependent endocrine disruption (OECD-407, 2008; *Repeated Dose 90-Day Oral Toxicity Study in Rodents (OECD TG 408)*, 2018). In the one- and two-generation reproductive toxicity assays, male and female rats are dosed pre- and postnatal (male rats in the one-generation study are only dosed prenatal) to evaluate reproductive endpoints like spermatogenesis and oestrus cycle by testicular and ovarian histopathology and development of the F1 (and F2) generation offspring (*Extended One-Generation Reproductive Toxicity Study (EOGRTS) (OECD TG 443)*, 2018; *Two-Generation Reproduction Toxicity Study (OECD TG 416)*, 2018). In the Endocrine Disruptor Screening Program (EDSP), tiered *in vitro* and *in vivo* tests are presented to evaluate endocrine activity of pesticides, industrial chemicals, and environmental contaminants (The Endocrine Disruptor Screening and Testing Advisory Committee, 1998).

In the *in vivo* assays, animals are exposed to an increasing dose of the chemical of interest, generating a dose-response curve from which the point of departure (PoD) is determined to set a safe exposure level for humans taking into account adequate uncertainty factors (UFs). The PoD can be the no-observed-adverse-effect level (NOAEL), the highest level that is not associated with any significant adverse changes compared to controls or the 95% lower confidence limit of the Benchmark dose (BMD) causing 5% extra response above background level (BMDL<sub>05</sub>) which is considered to result in a similar level of protection as the NOAEL (Hardy et al., 2017). The difference is that benchmark dose modelling is a statistical technique that takes the whole dose-response curve into account (Edler et al., 2002), enabling a more precise and advanced estimation of the PoD. Another advantage is that when using the BMDL, a bad study design with a lot of uncertainty in the data will result in a lower and thus more conservative PoD, while the NOAEL approach would result in a higher PoD. Animal-based PoDs are converted to human safe levels using UFs for interspecies and interindividual differences, and, when indicated by gaps in the database, extra UFs.

However as stated, the large amount of chemicals to be tested will require a high number of animals in the *in vivo* tests (Rovida & Hartung, 2009). Furthermore, the *in*

*vivo* test guideline endpoints may not be relevant or are insufficient to identify human pathologies. Changes in organ weight, for example, are seldom used in the diagnosis of human diseases and endometriosis is not covered as an endpoint in the animal studies (Vandenberg, 2021). Other disadvantages often encountered in *in vivo* guideline studies are the insensitivity (high dosing), lack of reproducibility, or insufficient use of positive or negative controls (Vandenberg, 2021).

It is therefore of no surprise that, in both science and society, controversy arises around the use of animal-based testing strategies because of the ethical, economic, and legislative issues, while at the same time experimental animals may thus not adequately represent the human body and animal test guidelines may not cover human pathologies. This drives the need for alternative testing strategies to replace, reduce, and refine (3Rs) the use of experimental animals (Russell & Burch, 1959) for risk assessment purposes. This is further highlighted in the publication of *Toxicity Testing in the 21st Century: A Vision and a Strategy* (NRC, 2007), where a paradigm shift is presented away from animal-based testing strategies towards the use of *in vitro* and *in silico* approaches to assess chemical-induced biological changes in the human physiology. Next Generation Risk Assessment (NGRA) offers opportunities to reach this goal (US EPA, 2018). In NGRA, the development and use of non-animal based new approach methodologies (NAMs) aims not to predict chemical-induced pathologies in animals but to assure human safety, eliminating the need for animal data (Baltazar et al., 2020; Carmichael et al., 2022; Carmichael et al., 2009; NRC, 2007). The aim of this thesis is to perform NGRA to establish human relevant safe levels of chemical exposure to EACs with androgenic and estrogenic properties, by integrating *in vitro* and *in silico* approaches.

## **1.2 Xenobiotic androgenic and estrogenic compounds may interfere with the endocrine system**

Xenobiotic androgenic and estrogenic compounds are EACs which may mimic steroid sex hormones like testosterone (T, **Figure 1.1**) or estradiol (E2, **Figure 1.1**) in causing androgenic and estrogenic effects (Marcocchia et al., 2017). These endogenous hormones are responsible for the development of the male and female phenotype, respectively. Androgens, from the Greek word *Andro* meaning male, regulate the development, maturation, and functioning of predominantly the male reproductive system (US EPA, 2011; Marcocchia et al., 2017; Schiffer et al., 2018). The main androgen is T which is converted by 5 alpha-reductases (5 $\alpha$ Rs) to the more bioactive metabolite 5 $\alpha$ -dihydrotestosterone (DHT, **Figure 1.1**) (Srivilai et al., 2019). The word estrogen

comes from the Latin word *Oestrus* or the Greek *Oistros* which describes a gadfly: it was observed that when female cattle were sexually receptive, they acted like they were being annoyed by gadflies (Shoham & Schachter, 1996). Estrogens regulate the development, maturation, and maintenance of predominantly the female reproductive system and the menstrual cycle. Estrone (E1), E2, and estriol (E3) are the main endogenous estrogens, E2 being the most active (Kiyama & Wada-Kiyama, 2015; Marcoccia et al., 2017)

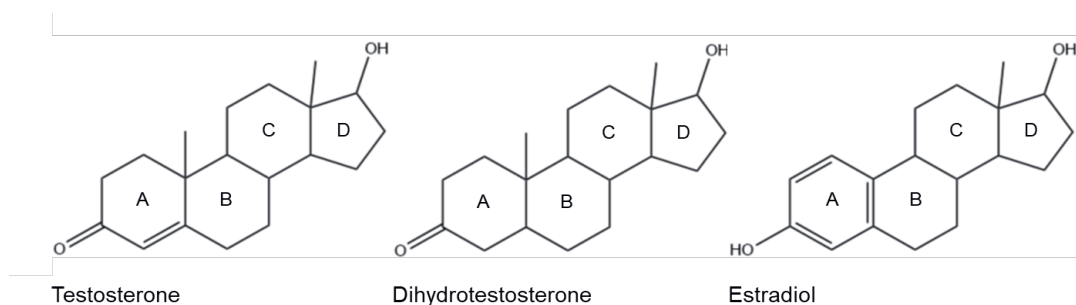


**Figure 1.1.** Structural formulas of main androgens testosterone (T) and dihydrotestosterone (DHT) and the main estrogen estradiol (E2).

The androgenic or estrogenic hormones dimerize on the androgen receptor (AR) or estrogenic receptor (ER), respectively, which are members of the nuclear receptor superfamily of ligand inducible transcription factors, expressed in the cytosol in a variety of tissues. Upon this activation, the receptors dimerize and translocate to the nucleus where they bind to hormone responsive elements in the DNA of androgen/estrogen-responsive genes and act as transcription factors. The AR is expressed in the prostate, testes, hypothalamus, pituitary gland, and liver (Matsumoto et al., 2008). There are two subtypes of the ER, the ER $\alpha$  and ER $\beta$  (Baker, 2013; Deroo & Korach, 2006). The ER $\alpha$  is expressed in the mammary gland, uterus, ovary (thecal cells), bone, testes, epididymis, prostate (stroma), liver, adipose tissue, the cardiovascular and central nervous system. The ER $\beta$  is expressed in the ovary (granulosa cells), bladder, prostate (epithelium), colon, adipose tissue, and the immune, cardiovascular, and central nervous systems (Paterni et al., 2014). Activation of the ER $\alpha$  by xenobiotics induces a classic estrogenic response and is suggested to be a molecular initiation event (MIE) that drives estrogen-related pathologies (OECD, 2016), and ER $\alpha$ -knockout mice have an altered functioning of the reproductive system (Couse & Korach, 1999). The ER $\alpha$  is thus a target of interest in the research on endocrine-related diseases. Males have higher plasma levels of androgens whereas females have higher plasma levels of estrogens (Sohoni & Sumpter, 1998). However, both groups of steroids are essential for

the physiological development of the male and female reproductive systems (Marcoccia et al., 2017).

Androgenic and estrogenic compounds have a chemical structure that shows similarities to the structure of the endogenous steroid sex hormones, enabling them to bind to the respective receptors and act as EACs. Androgenic and estrogenic compounds are a diverse group of chemicals with a variety of functions including pharmaceuticals, plasticizers, food additives, pesticides, industrial chemicals, fungicides, pollutants, cosmetics, and bioactive molecules present in plants and exposure can result from ingestion, inhalation or skin absorption (Kiyama & Wada-Kiyama, 2015). The molecular mechanism of these compounds includes agonism or antagonism of the AR or ER, thus affecting the target gene expression and having (anti)androgenic or (anti)estrogenic effects, and thereby potentially disrupting androgenic or estrogenic functioning (Franssen et al., 2022; Kiyama & Wada-Kiyama, 2015). Consequently this can lead to adverse health effects including increased cancer risk in androgen- and estrogen-responsive tissues. Furthermore, reproductive and developmental related pathologies such as adverse pregnancy outcomes, endometriosis, reduced semen quality, genital malformations, decreased age at menarche, irregular menstruation, disturbed puberty, and infertility have been associated with exposure to (anti)androgenic and (anti)estrogenic compounds (Basak et al., 2020; Bergman et al., 2013; Buck Louis et al., 2011; Cooper et al., 2005; Damstra et al., 2002; Franssen et al., 2022; Gaspari et al., 2011; Rumph et al., 2020; Varnell et al., 2021).

### **1.3 New approach methodologies (NAMs) for androgenic and estrogenic compounds**

In recent years, there have been significant advances to identify and quantify the toxicodynamic responses of (anti)androgenic and (anti)estrogenic compounds using *in vitro* bioactivity assays. These can be used as NAMs in an NGRA context. The *in vitro* AR-Chemically Activated LUCiferase eXpression (CALUX) and ER-CALUX assay are validated reported gene assays (Sonneveld et al., 2005; van der Burg, Winter, Man, et al., 2010). These reporter gene assays use human osteosarcoma (U2OS) cells transfected with the human AR, ER $\alpha$ , or ER $\beta$  (Sonneveld et al., 2005) or human breast carcinoma T47D cells endogenously expressing the ER $\alpha$  and ER $\beta$  (Legler et al., 1999) and a luciferase reporter construct containing hormone-responsive elements coupled to a TATA promoter. Upon binding to the AR or ERs, the nuclear receptors undergo a conformational change leading to dimerization and translocation to the nucleus, where

they bind the hormone-responsive elements in the DNA. The conformational change of the receptors also leads to recruitment of transcription factors and consequently the hormone-responsive elements in the DNA and also the luciferase reporter gene gets activated, the latter resulting in the production of luciferase. This enzyme catalyses the oxidation of substrate luciferin using energy from ATP whereby photons are released and the emitted light can be measured by a luminometer (Legler et al., 1999; Sonneveld et al., 2005). The CALUX assays can discriminate between agonists and antagonists, contrary to receptor binding assays (US EPA, 2011\_ref 2). A similar reporter gene assay uses CV-1 cells expressing the human AR (INDIGO Biosciences, Inc., State Collage, PA, USA). Another *in vitro* bioactivity assay uses the human breast cancer estrogenic-sensitive MCF-7 cells (Soule et al., 1973), measuring cell proliferation as DNA per well after 6 days of exposure to the compounds of interest in the MCF-7/Bos proliferation assay (Burton, 1956; Natarajan et al., 1994; Soto et al., 1995).

However, a limitation of using such NAMs in an NGRA context is that they cannot directly be used to determine the PoD to set safe exposure levels for humans, since the cells employed are not an intact body where the *in vivo* absorption, distribution, metabolism, and excretion (ADME) characteristics of the chemical are captured. For instance, cell-based bioassays seldom capture metabolism due to the lack of expression of hepatic enzymes such as in the human body and consequently they also do not capture the role of active metabolites in the toxicodynamic response at the biological *in vivo* target site (Coecke et al., 2006; Hartung, 2018; Mazzoleni et al., 2009).

## 1.4 The Dietary Comparator Ratio approach

One way to use NAM *in vitro* bioactivity data in NGRA to evaluate the safety of chemical exposure to humans is the so-called Dietary Comparator Ratio (DCR) approach (Becker et al., 2015; Dent et al., 2019). The DCR compares the Exposure Activity Ratio (EAR) for exposure to the compound of interest ( $EAR_{\text{test}}$ ) to the EAR of an established safe level of human exposure to a comparator compound ( $EAR_{\text{comparator}}$ ) exhibiting the same mode of action, *e.g.* the antagonism of the AR or agonism of the ER. In the EAR, the internal exposure to the compound at the dose level to be evaluated is compared to the effect concentration (*e.g.*  $IC_{50}$  or  $EC_{50}$ ) from a relevant *in vitro* bioactivity assay, *e.g.* the AR-CALUX or ER-CALUX assay. The  $EAR_{\text{test}}$  is calculated using Eq. 1.

$$\text{Eq.1. } EAR_{\text{test}} = \frac{\text{internal concentration at defined exposure level (test)}}{EC_{50} \text{ or } IC_{50} \text{ (test)}}$$

The internal concentration at the defined exposure level of the test compound is taken from reported human pharmacokinetic data in literature or predicted using physiologically based kinetic (PBK) modelling (see next section) and the EC<sub>50</sub> or IC<sub>50</sub> values are derived from the concentration-response curve in the respective *in vitro* bioactivity assay. The EAR<sub>comparator</sub> is calculated following Eq. 2.

$$\text{Eq. 2. } \text{EAR}_{\text{comparator}} = \frac{\text{internal concentration at an established safe exposure level (comparator)}}{\text{EC}_{50} \text{ or IC}_{50} \text{ (comparator)}}$$

The internal concentration at an established safe exposure level is taken from reported human pharmacokinetic data in literature or predicted using PBK modelling and the EC<sub>50</sub> or IC<sub>50</sub> values are derived from the concentration-response curve in the respective *in vitro* bioactivity assay. The DCR is calculated using Eq. 3, comparing the EAR<sub>test</sub> to the EAR<sub>comparator</sub>.

$$\text{Eq. 3. } \text{DCR} = \frac{\text{EAR}_{\text{test}}}{\text{EAR}_{\text{comparator}}}$$

When the EAR<sub>comparator</sub> is defined at a safe level of human exposure this implies that, when the derived DCR of the exposure to a compound under evaluation is ≤ 1, this exposure can also be considered safe.

Initial examples of applications of the DCR approach to evaluate anti-androgenic and estrogenic exposures in humans have been presented previously (Becker et al., 2015; Dent et al., 2019). To establish the EAR<sub>comparator</sub> (Eq. 2) these studies used the internal concentration at an established safe exposure level of the comparator compound taken from reported human pharmacokinetic data in literature or predicted using PBK modelling. Dent et al. (2019) evaluated human exposure to putative anti-androgens, using the internal concentration of 3,3-diindolylmethane (DIM, Table 1) from the intake of 50 grams of Brussels sprouts, in order to set the EAR<sub>comparator</sub>, based on the history of safe use from that intake. However, using the consumption of 50 grams of Brussels sprouts as safe comparator exposure resulted in DCR values for the 12 tested exposure scenarios to the anti-androgenic compounds that were all > 1. This suggested that all 12 exposure scenarios were to result in *in vivo* anti-androgenicity in humans, even the exposure scenarios known to not result in *in vivo* anti-androgenicity. Thus, the comparator exposure scenario of DIM intake from 50 grams of Brussels sprouts appeared too conservative, making the approach overprotective for human health and thus not suitable for adequate evaluation of human exposure scenarios. The study of

Becker et al. (2015), evaluating human exposures to putative estrogens, used internal human exposures to genistein (GEN, **Table 1.1**), present in, for example, soybeans (Elsenbrand, 2007) following the intake of different diets, to set the  $EAR_{\text{comparator}}$ . These intakes were considered conservative and health protective in humans. Results revealed that 6 from the 30 included exposure scenarios to the estrogenic test compounds had a  $DCR > 1$ , thus expected to result in *in vivo* estrogenicity prioritizing them for further safety testing (Becker et al., 2015). Since there was no comparison made to actual information regarding the onset of *in vivo* estrogenicity of those exposure scenarios in humans, the predictions made based on the  $DCR$  values were not verified.

In this thesis, the  $DCR$  approach is further developed by tackling the aforementioned issues. To this purpose, putative anti-androgenic human exposure scenarios were evaluated with a newly defined  $EAR_{\text{comparator}}$  value for the comparator compounds DIM and bicalutamide (BIC, **Table 1.1**), a prostate cancer drug. Putative estrogenic human exposure scenarios were evaluated against a newly defined  $EAR_{\text{comparator}}$  value for GEN. To define these new  $EAR_{\text{comparator}}$  values a new approach was applied. The  $EAR_{\text{comparator}}$  was defined at an established safe level of exposure, predicted by PBK modelling reverse dosimetry to result in an internal concentration equal to the 95% lower confidence limit of the Benchmark Concentration (BMC) causing 5% extra response above the background level ( $BMCL_{05}$ ) in the *in vitro* androgenic (for DIM and BIC) or estrogenic (for GEN) bioactivity assays. In this approach it is assumed that when the internal plasma concentration matches the  $BMCL_{05}$ , no AR- or ER-mediated effects following compound exposure are expected and thus this exposure is considered safe. This newly defined approach the  $EAR_{\text{comparator}}$  is solely based on *in vitro* data and calculated following Eq. 4.

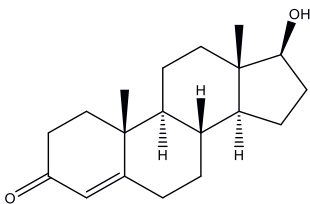
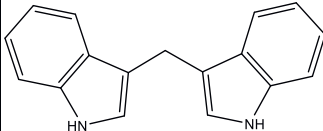
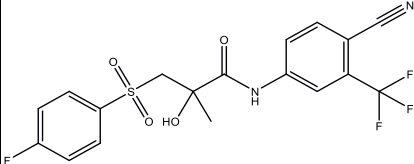
$$\text{Eq. 4. } EAR_{\text{comparator}} (\textit{in vitro} \text{ based}) = \frac{BMCL_{05} (\text{comparator})}{EC_{50} \text{ or } IC_{50} (\text{comparator})}$$

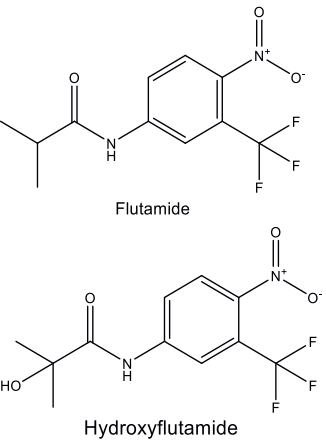
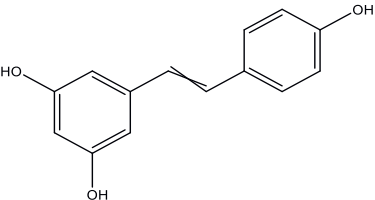
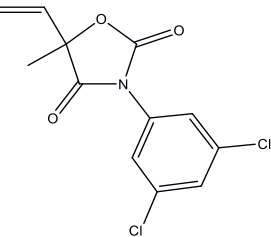
The  $BMCL_{05}$  and  $EC_{50}$  or  $IC_{50}$  are both derived from the concentration-response curve obtained for the selected comparator compound using the respective *in vitro* bioactivity assay. It is of interest to note that defining the safe level of exposure and the  $EAR_{\text{comparator}}$  in this way, formally it would call for a redefinition of the term  $DCR$  which means dietary comparator ratio, since in this new approach the  $EAR_{\text{comparator}}$  is no longer defined based on a safe level of dietary intake. However, for clarity and because the principle idea behind the methodology was not modified, in the present thesis the terminology was not modified.

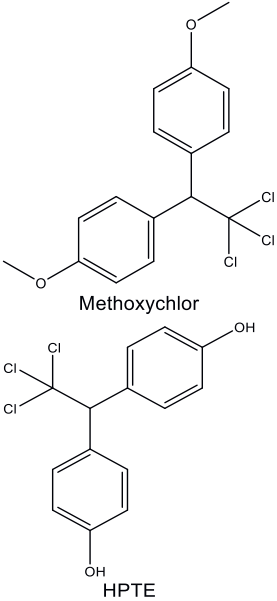
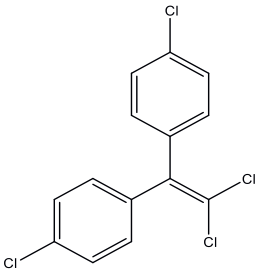
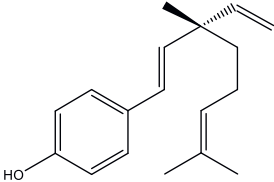
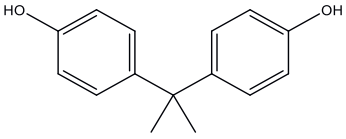


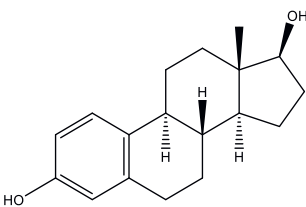
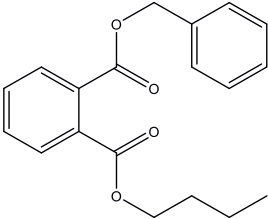
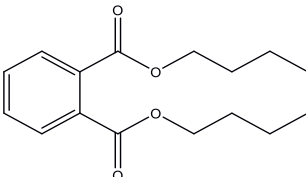
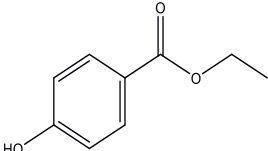
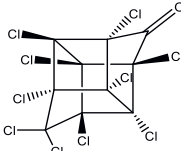
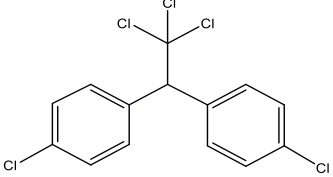
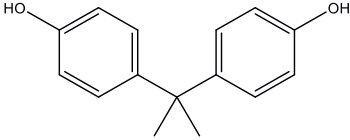
Comparison of the DCR values obtained with the newly defined  $EAR_{\text{comparator}}$  for exposure scenarios with known health outcome in terms of anti-androgenic or estrogenic activity can be used to evaluate the new predictions. When correctly predicted, the approach can be used to make a DCR-based safety estimation of exposures for which it is not known whether they would result in anti-androgenic or estrogenic effects in humans. The data set used for this evaluation in the present thesis regarding anti-androgenic exposures are taken as reported by Dent et al. (2019) whereas the estrogenic exposures are taken from literature. In both cases exposure scenarios used for the evaluation included positive, negative or unknown scenarios for exposures. For the evaluation of the anti-androgens it included exposures to plant-based compounds, pesticides, bisphenol A, and drugs and for evaluation of the estrogens it included exposures to endogenous hormones, plant-based compounds, phthalates, ethyl paraben, pesticides, bisphenol A, a mycotoxin, and drugs (**Table 1.1**).

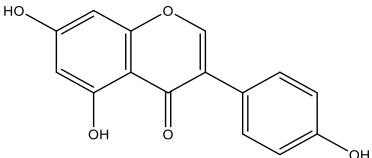
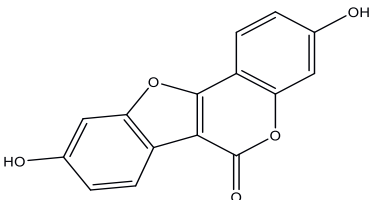
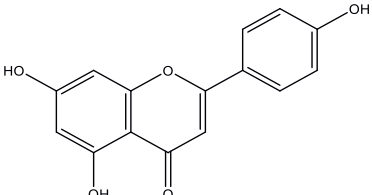
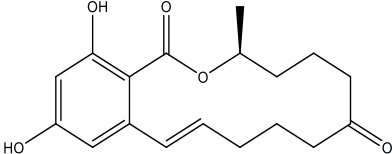
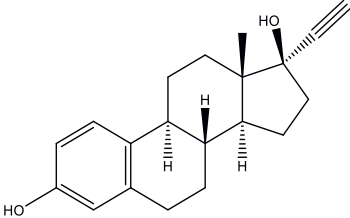
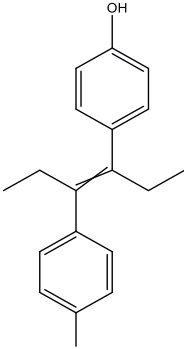
**Table 1.1.** The (anti)androgenic and estrogenic comparator and test compounds with their structure formula included in this thesis.

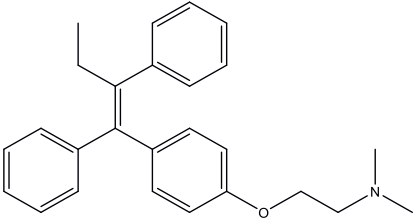
Androgens	Compound	Structure formula
Testosterone (T)	Endogenous hormone	
Anti-androgens	Compound	Structure formula
3,3-Diindolylmethane (DIM)	Bioactive molecule from cruciferous vegetables	
Bicalutamide (BIC)	Pharmaceutical for the treatment of prostate cancer	

<p>Flutamide (FLU &amp; its metabolite hydroxyflutamide (HF))</p>	<p>Pharmaceuticals for the treatment of prostate cancer and hirsutism</p>	 <p>Flutamide</p> <p>Hydroxyflutamide</p> <p>The image shows two chemical structures. The top structure is Flutamide, which consists of a benzene ring with a nitro group (-NO2) at the 1-position, a trifluoromethyl group (-CF3) at the 2-position, and an isobutyramide group (-NH-CO-CH2-CH(CH3)2) at the 4-position. The bottom structure is Hydroxyflutamide, which is identical to Flutamide but has a hydroxyl group (-OH) attached to the alpha-carbon of the isobutyramide side chain.</p>
<p>Resveratrol (RES)</p>	<p>Bioactive molecule present in fruits and berries, mostly grapes and thus red wine.</p>	 <p>Resveratrol</p> <p>The image shows the chemical structure of Resveratrol, a stilbenoid. It features a central trans-stilbene core (two phenyl rings connected by a double bond). The left phenyl ring has hydroxyl groups (-OH) at the 3 and 4 positions. The right phenyl ring has a hydroxyl group (-OH) at the 4 position.</p>
<p>Vinclozolin (VIN)</p>	<p>Pesticide</p>	 <p>Vinclozolin</p> <p>The image shows the chemical structure of Vinclozolin, a fungicide. It consists of a five-membered oxazolidinone ring system. The ring has a vinyl group (-CH=CH2) attached to the 2-position, a carbonyl group (=O) at the 3-position, and a nitrogen atom at the 4-position. The nitrogen atom is substituted with a 3,5-dichlorophenyl group (-C6H3Cl2).</p>

Methoxychlor (MX) & its metabolite hydroxychlor (HPTE)	Pesticide	 <p>Methoxychlor</p> <p>HPTE</p>
Dichlorodiphenyldichloroethylene (DDE)	Pesticide	
Bakuchiol (BAK)	Bioactive molecule from babchi plant	
Bisphenol A	Industrial chemical, used in <i>e.g.</i> plastics (exerts also estrogenic activity)	
<b>Estrogens</b>	<b>Compound</b>	<b>Structure formula</b>

17 $\beta$ -Estradiol (E2)	Endogenous hormone	
Butylbenzyl phthalate (BBzP)	Phthalates	
Di-n-butyl phthalate (DBP)	Phthalates	
Ethyl paraben (EP)	Paraben	
Kepone (KEP)	Pesticide	
Dichlorodiphenyltrichloroethane (DDT)	Pesticide	
Bisphenol A	industrial chemical, used in <i>e.g.</i> plastics (exerts also anti-androgenic activity)	

Genistein (GEN)	Bioactive molecule present in soy	
Coumestrol (COU)	Bioactive molecule present in plants, such as cabbage and alfalfa beans	
Apigenin (API)	Bioactive molecule present in plants, such as parsley and celery	
Zearalenone (ZEA)	Mycotoxin	
17 $\alpha$ -Ethinyl estradiol (EE)	Contraceptive	
Diethylstilbesterol (DES)	Pharmaceutical, restricted for the treatment certain types of cancer	

Tamoxifen (TAM)	Pharmaceutical for the treatment of breast cancer	
-----------------	---	--

## 1.5 Physiologically based kinetic (PBK) modelling

The DCR approach requires the internal concentration of the compound of interest at the exposure level to be evaluated. However, when only the external dose is available, PBK modelling can be used to predict the internal concentration at that defined external dose level, required for definition of the respective EAR. In a PBK model, the animal or human body is described as different tissue compartments and with mathematical equations the ADME characteristics of a chemical in those compartments is simulated based on physiological, physico-chemical and biochemical parameters using computational software like GastroPlus (Simulation Plus Inc., Lancaster, CA, United States) or Berkeley Madonna (Macey and Oster, UC Berkeley, CA, USA). Physiological parameters include e.g. tissue volumes, tissue blood flows, and the cardiac output, which can be derived from literature. Physico-chemical parameters include e.g. blood/tissue partition coefficients which can be literature derived or predicted (Rodgers et al., 2005; Rodgers & Rowland, 2006) or the fraction unbound ( $f_{ub}$ ) for plasma protein binding which can be derived from literature, predicted or determined by *in vitro* incubations with human plasma. Kinetic parameters like kinetic constants for the rate of dermal or intestinal absorption can be literature derived or *in vitro* determined using, for example, skin penetration assays or the Caco-2 permeability assay. Kinetic parameters for metabolic reactions like Michaelis-Menten kinetic parameters  $V_{max}$  and  $K_m$ , or the hepatic clearance can be, if not reported in literature, determined *in vitro* by incubation with the relevant biological samples like human liver cells or tissue fractions. The PBK model allows the simulation of the concentrations of a parent compound and its metabolites in specific target organs at a certain dose, time-point, and following a specific route of administration. Different human populations can be included in the modelling based on for instance sex, ethnicity (e.g. Caucasian or Asian), age (e.g. paediatric or geriatric), health status (e.g. obesity), or genetics (e.g. different expression of enzyme levels). Thus with PBK modelling, the internal concentrations at external high and, more realistic, low doses of a compound can be simulated and predicted in a specified target organ or blood/plasma and for a relevant

species including humans. The adequacy of the PBK model predictions is generally evaluated by comparing the predictions to corresponding *in vivo* pharmacokinetic (PK) data (Louisse et al., 2017; Rietjens et al., 2011). Once validated, the models can be used to make predictions for internal concentrations in relevant target organs or blood/plasma at defined external dose levels (so-called forward dosimetry).

## **1.6 Physiologically based kinetic modelling-facilitated *in vitro* to *in vivo* extrapolation to set PoDs in risk assessment**

With a validated PBK model, not only can the internal concentrations upon a certain external dose be predicted, this can also be done *vice versa* predicting the external dose that would be required to reach a certain internal concentration (so-called reverse dosimetry), which is done in PBK modelling-facilitated quantitative *in vitro* to *in vivo* extrapolation (QIVIVE) (Fabian et al., 2019; Louisse et al., 2017; Punt et al., 2019; Rietjens et al., 2011; Wetmore et al., 2015; Yoon et al., 2012). In reverse dosimetry, the unbound *in vitro* effect concentrations of a compound in a bioactivity assay, e.g. the AR-CALUX assay, are considered equal to the unbound *in vivo* tissue or blood/plasma concentrations that would cause a corresponding e.g. androgenic effect in the *in vivo* situation, thereby correcting the total *in vivo* concentration for the difference in protein binding between the *in vitro* and *in vivo* situation. With the PBK model, the doses are predicted that would be required to result in those corrected total *in vivo* internal concentrations, enabling translation of the *in vitro* concentration-response curve to an *in vivo* dose-response curve. With the *in vivo* dose-response data, the PoD can be set for the corresponding biological effect to be used in risk assessment (Rietjens et al., 2011).

## **1.7 Approaches to include biotransformation in the *in vitro* and *in silico* tools**

Biotransformation leads to bioactivation or detoxication of compounds, thus changing the potency to their biological target in the human body (Coecke et al., 2006; Gu & Manautou, 2012; OECD DRP 97, 2008). Performing PBK modelling-facilitated QIVIVE based on the *in vitro* bioactivity data of only a parent compound, the activity of potentially active metabolites is not included and the predicted dose-response curve might underestimate or overestimate the toxic response that would occur *in vivo* in humans. In this thesis, two approaches are explored to include biotransformation in an NGRA context: 1) Using a toxic equivalency factor (TEF) approach in the PBK modelling-

facilitated QIVIVE to include the role of an active metabolite and 2) Development of a new *in vitro* technology enabling co-cultivation of metabolically competent cells and reporter gene cells to include the metabolite formation in the *in vitro* bioactivity assays.

## **1.8 Including the contribution of the bioactivity of relevant metabolites using a TEF approach in the PBK modelling-facilitated QIVIVE of a parent compound**

The pharmaceutical anti-androgen flutamide (FLU) is hepatically activated to hydroxyflutamide (HF). When performing PBK modelling-facilitated QIVIVE based on only the *in vitro* bioactivity data of FLU, the bioactivity of HF is not captured and the predicted dose-response might underestimate the *in vivo* anti-androgenicity of FLU. With the toxic equivalency factor (TEF) approach and the TEF values determined in an *in vitro* bioactivity assay, the *in vivo* internal effect concentrations of both a parent compound and a relevant metabolite can be expressed in parent compound equivalents (Zhao et al., 2021). With a PBK model, including the kinetics of the conversion of the parent compound to the metabolite, the doses of the parent compound can be simulated that are required to reach those combined internal concentrations of both parent compound and metabolite expressed in parent compound equivalents. In the present thesis this approach was used to predict the *in vivo* anti-androgenic response towards FLU taking the anti-androgenic bioactivity of HF into account using its TEF value relative to FLU as determined in the AR-CALUX assay. This enabled the estimation of the PoD from the predicted dose-response curve for FLU taking the toxicokinetics and toxicodynamics of HF into account.

## **1.9 New technology: Development of two-chamber liver-target cell co-culture system**

New technologies are developed to include biotransformation of a parent compound in *in vitro* bioactivity assays, such as *in vitro* tissue co-cultures that include a biotransformation-competent cell line. Hepatic biotransformation can be measured *in vitro* by incubating the compound under study over time with primary human hepatocytes (PHHs), whereafter concentrations of the parent compound and relevant metabolite(s) are measured to obtain hepatic kinetic parameters. PHHs are considered the gold standard for *in vitro* hepatic metabolism due to the functional preservation of



metabolism, transport, and receptor signalling pathways, as they are directly obtained from the human liver (Jackson et al., 2016; Stanley & Wolf, 2022). However, simultaneously, this is one of the limitations in using PHHs for *in vitro* kinetic studies since human liver samples must be available. Other disadvantages are that PHHs taken from liver donors can show large inter-donor variations in enzyme levels and that PHHs have a limited lifetime when cultured (Ramaiahgari et al., 2017). An alternative *in vitro* approach to measure biotransformation is using the immortalized human hepatocellular carcinoma derived (HepaRG) cell line, which is *in vitro* differentiated to hepatocyte- and cholangiocyte-like cells in 2D co-culture (1:1) (Aninat et al., 2006; Gripon et al., 2002) or even three dimensional (3D) culture (Gunness et al., 2013; Jackson et al., 2016; Leite et al., 2012; Ramaiahgari et al., 2017). Differentiation of the cells is initiated and maintained by treatment with 2% dimethyl sulfoxide (DMSO) and hydrocortisone for up to 4 weeks (Gripon et al., 2002; Jackson et al., 2016; Stanley & Wolf, 2022). In the present thesis, hepatic biotransformation *in vitro* was studied using 3D HepaRG microtissues. 3D HepaRG microtissues have prolonged and stable liver functionality including activities of biotransformation enzymes and are less susceptible to dedifferentiation than 2D HepaRGs (Gunness et al., 2013; Jackson et al., 2016; Leite et al., 2012; Ramaiahgari et al., 2017). Using histology and electronic microscopy it was shown that the microtissues display a hepatocyte phenotype with bile canaliculi with microvilli and tight junctions, and abundant mitochondria. Hepatic zonation was characterized in the microtissues. Enzyme activities were similar to those of *in vivo* liver tissues (Ip et al., submitted).

To capture hepatic biotransformation in *in vitro* AR reporter assays, an *in vitro* two-chamber liver-target co-culture system was developed (**Figure 1.2**). The use of the same medium in both chambers allows the free diffusion of chemicals throughout the system (Ip et al., submitted). In a 96 wells plate platform, an agarose mold system is used to create a hydrogel in each well consisting of a base platform with pegs of a circular ring and a central peg as a cylinder that touches the bottom of the well plate. This generates an outer ring-shaped trough in the agarose hydrogel around a central chamber in each well of the 96 wells plate. In the outer ring-shaped trough of the agarose two-chamber system, differentiated HepaRGs are seeded which will form 3D HepaRG microtissues. Seeding AR reporter gene target cells in the central chamber of the system will complement the microenvironment where the chemically-induced androgenic response in the presence of hepatic metabolism can be measured.

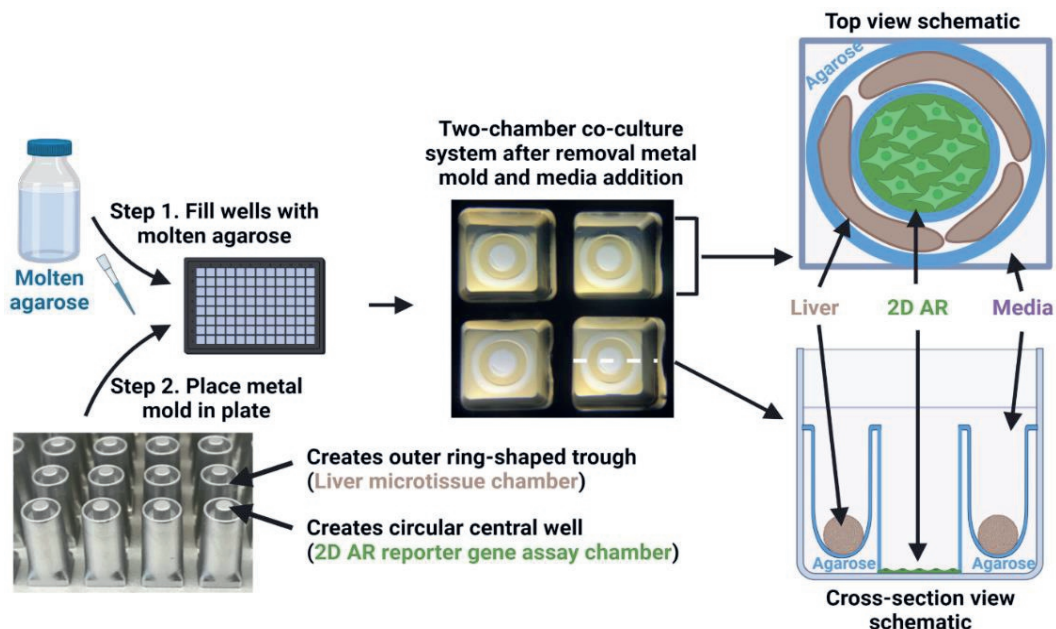


**Figure 1.2.** Schematic representation of the two-chamber co-culture system in 96 square well plate format. In Step 1 molten agarose hydrogel is added to the wells of the plate and in Step 2 the metal mold is placed invertedly in the plate until the agarose solidifies. After removal of the metal mold and addition of media, the outer ring-shaped trough can be used for cultivation of the 3D human liver tissue chamber and the circular central chamber at the bottom of the plate for cultivation of the 2D AR reporter gene cells (adapted from Ip et al., submitted). The right panel displays a schematic top and cross-sectional view of the agarose mold with liver and AR tissue in a well. This figure was created in BioRender.com.

## 1.10 Outline of the thesis

The aim the thesis was to perform next generation risk assessment (NGRA) to inform human-relevant safe levels of chemical exposure, integrating *in vitro* and *in silico* approaches for chemicals with putative (anti)androgenic and/or estrogenic effects.

**Chapter 1** provides the aim of the thesis and general background information, including a short description of (anti)androgens and estrogens and strategies for their safety assessment in next generation risk assessment, as well as the outline of the PhD thesis.

In **Chapter 2**, the use of newly defined comparator compound values solely based on *in vitro* bioactivity data in the DCR approach was studied to investigate whether this would result in adequate predictions for the anti-androgenic effects of a series of defined exposure scenarios. The  $EAR_{\text{comparator}}$  values were defined from the *in vitro* AR-CALUX assay, using the  $BMCL_{05}$  values as alternative safe level of exposure. The adequacy of the newly defined  $EAR_{\text{comparator}}$  values was studied by PBK-modelling based translation of the  $BMCL_{05}$  values and comparison of the generated DCR values of the evaluated exposure scenarios to the anti-androgenic test compounds to actual knowledge on their safety regarding *in vivo* anti-androgenic effects.

In **Chapter 3**, the DCR approach was further developed by assessing the safety of 14 exposure scenarios to (putative) estrogenic compounds based on multiple *in vitro* bioactivity assays using a newly defined *in vitro*-based  $EAR_{\text{comparator}}$  of genistein (GEN), present in soy. The adequacy of the *in vitro*-based  $EAR_{\text{comparator}}$  to define the exposure scenarios at which no ER-mediated effects are induced was assessed by comparison to *in vivo* reported safe internal levels of GEN from different diets and comparison of the generated DCR values of the evaluated exposure scenarios to the estrogenic test compounds to actual knowledge on their safety regarding *in vivo* estrogenic effects.

In **Chapter 4**, a proof of principle was presented to include biotransformation in PBK modelling-facilitated QIVIVE in an NGRA approach, using a toxic equivalency factor (TEF) approach. It was evaluated whether including the more bioactive metabolite hydroxyflutamide (HF) in the PBK modelling-facilitated QIVIVE of anti-androgen flutamide (FLU) would provide a more appropriate NAM-based PoD than when the bioactivity of the metabolite HF was not taken into account.

In **Chapter 5**, a two-chamber co-culture system with liver and reporter cells was developed to assess androgenic responses in the absence and presence of a biotransformation system. The androgenic response of testosterone (T) and 5 $\alpha$ -dihydrotestosterone (DHT), which are hepatically detoxified, were studied using the AR-CALUX or AR-INDIGO assay in the absence or presence of HepaRG microtissues.

Finally in **Chapter 6**, a general overview of the results of the previous chapters is provided and the results obtained are discussed in a wider perspective, whereafter future perspectives of the researched animal-free *in vitro* and *in silico* tools in NGRA are presented.



# Chapter 2

## **Chapter 2. Next generation risk assessment of human exposure to anti-androgens using newly defined comparator compound values**

Tessa C. A. van Tongeren, Thomas E. Moxon, Matthew P. Dent, Hequn Li, Paul L. Carmichael, Ivonne M. C. M. Rietjens

Published in *Toxicology in vitro* (2021), 73: 105132

## Abstract

Next Generation Risk Assessment (NGRA) can use the so-called Dietary Comparator Ratio (DCR) to evaluate the safety of a defined exposure to a compound of interest. The DCR compares the Exposure Activity Ratio (EAR) for the compound of interest, to the EAR of an established safe level of human exposure to a comparator compound with the same putative mode of action. A  $DCR \leq 1$  indicates the exposure evaluated is safe. The present study aimed at defining adequate and safe comparator compound exposures for evaluation of anti-androgenic effects, using 3,3-diindolylmethane (DIM), from cruciferous vegetables, and the anti-androgenic drug bicalutamide (BIC). EAR values for these comparator compounds were defined using the AR-CALUX assay. The adequacy of the new comparator EAR values was evaluated using PBK modelling and by comparing the generated DCRs of a series of test compound exposures to actual knowledge on their safety regarding *in vivo* anti-androgenicity. Results obtained supported the use of AR-CALUX-based comparator EARs for DCR-based NGRA for putative anti-androgenic compounds. This further validates the DCR approach as an animal free *in silico/in vitro* 3Rcompliant method in NGRA.

**Key words:** Risk assessment · 3R compliant method · Androgen receptor · Dietary comparator · *In vitro/in silico* approaches

## 2.1 Introduction

At the current state-of-the-art, toxicological risk and safety assessment is in many cases still based on the traditional use of animals for systemic toxicity testing in order to obtain points of departure (PoDs) to define safe levels of human exposure. However, use of animal-based testing strategies is under debate because of ethical, economic, and legislative issues, while at the same time experimental animals may not adequately represent the human situation. This initiates the need for alternative testing strategies to reduce, replace, and refine (3Rs) the use of animals for risk assessment purposes (Russell & Burch, 1959). Next Generation Risk Assessment (NGRA) aims to not replace each existing animal test with an alternative but to assure human safety based on human data and *in vitro* and *in silico* approaches. One NGRA strategy is based on the so-called Dietary Comparator Ratio (DCR) (Becker et al., 2015).

The DCR compares the Exposure Activity Ratio (EAR) for exposure to the compound of interest to the EAR of an established safe level of human exposure to a comparator compound ( $EAR_{\text{comparator}}$ ) exhibiting the same mode of action. The EAR compares an internal human exposure concentration at a defined external dose level to a biological effect concentration such as the half maximal effective concentration ( $EC_{50}$ ) of a chemical obtained from a relevant *in vitro* assay or *in silico* prediction, leading away from the use of *in vivo* data (Becker et al., 2015). When the exposure scenario used to define the  $EAR_{\text{comparator}}$  is considered safe and the DCR of the studied compound obtained is  $\leq 1$ , it can be concluded that the exposure to the compound under study will also be safe.

Dent et al. (2019) described a proof-of-principle of the DCR approach evaluating a series of human exposure scenarios to putative dietary anti-androgenic compounds. In this study, the exposure to 3,3-diindolylmethane (DIM, **Figure 2.1**), resulting from the intake of a portion of 50 g Brussels sprouts (Fujioka et al., 2016), was used as the comparator exposure because no anti-androgenic adverse effects are expected in humans after normal dietary consumption of this amount of the cruciferous vegetable (Dent et al., 2019).

However, use of exposure to DIM from consumption of 50 g Brussels sprouts as the safe comparator exposure regimen, resulted in DCR values that exceeded the value of 1 for all test compounds evaluated. This indicated that the exposure scenarios evaluated for the 9 putative anti-androgenic compounds were all predicted to have higher chances to results in *in vivo* anti-androgenic effects than resulting from the intake of 50 g Brussels

sprouts. Whilst protective, this DCR approach was considered overly conservative, because for several of these exposure scenarios data were available supporting the absence of anti-androgenic effects.

Therefore, the aim of the present study was to explore the possibility to define less conservative comparator EARs based on alternative safe levels for human exposure to anti-androgenic active compounds and newly defined  $EAR_{\text{comparator}}$  values. To this end, an updated  $EAR_{\text{comparator}}$  was defined for DIM, as well as an  $EAR_{\text{comparator}}$  for the anti-androgenic drug bicalutamide (BIC, **Figure 2.1**). BIC is a nonsteroidal racemate anti-androgen used in the treatment for prostate cancer. The  $EAR_{\text{comparator}}$  for BIC was defined for R-BIC, since R-BIC accounts for 99% of the plasma concentration after dosing in humans and is a more potent anti-androgen than S-BIC (Cockshott, 2004); AstraZeneca Pharmaceuticals, 2005). In order to assure a 3R compliant method, in the present study the EARs were defined using the AR-CALUX assay for anti-androgenic activity. The newly defined  $EAR_{\text{comparator}}$  values were used to obtain DCRs and an updated outcome of the NGRA for the series of putative anti-androgen exposures.

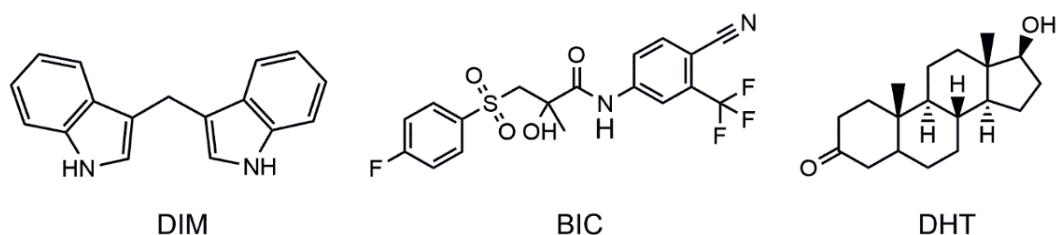


**Figure 2.1.** Structure formulas of DIM, bicalutamide (BIC), and dihydrotestosterone (DHT).

## 2.2 Material and methods

### 2.2.1 Chemicals

DHT (CAS no. 521-18-6), BIC (CAS no. 90357-06-5), FLU (CAS no. 13311-84-7), and Triton X-100 were purchased from Sigma-Aldrich Chemie B.V. (Zwijndrecht, the Netherlands). Penicillin-streptomycin solution was purchased from Invitrogen (Breda, the Netherlands). Phosphate-buffered saline (PBS), trypsin EDTA (trypsin (0.025%)/EDTA (0.01%)), Dulbecco's modified Eagle's Medium/Ham's nutrient mixture F12 (DMEM/F12), Phenol Red Free DMEM/F-12, fetal calf serum (FCS), dextran-coated charcoal-treated (DCC) FCS, MEM (100 $\times$ ) non-essential amino acids



(NEAAs), and geneticin (G-418) were purchased from Gibco (Paisley, United Kingdom). Dimethyl sulfoxide (DMSO) was purchased from Acros Organics (Geel, Belgium). Low salt buffer (LSB), consisted of 10 mM Tris (Invitrogen), 2 mM dithiothreitol (DTT) (Duchefa Biochemie bv, Haarlem, the Netherlands), and 2 mM 1, 2-diaminocyclohexanete triacetic acid monohydrate (CDTA) (Fluka, Munich, Germany). The flashmix consisted of 20 mM tricine (Jansen chemica, Landsmeer, the Netherlands), 1.07 mM ( $\text{MgCO}_3$ ) $4\text{Mg}(\text{OH})2.5\text{H}_2\text{O}$  (Sigma-Aldrich, 99% purity), 2.67 mM magnesium sulphate ( $\text{MgSO}_4$ ) (Ridel de Haën, Landsmeer, the Netherlands), 0.1 mM ethylenedinitrilotetraacetic acid disodium salt dihydrate (Titriplex III; Merck, Amsterdam, the Netherlands), 2 mM DTT (Duchefa Biochemie), 0.47 mM D-luciferin (Duchefa Biochemie), and 5 mM adenosine-5' -triphosphate (ATP, Boehringer, Alkmaar, the Netherlands).

### 2.2.2 Cell culture

Cells from the stably transfected human osteosarcoma (U2OS) cell line expressing the human androgen receptor (AR) (BioDetection Systems (BDS), Amsterdam, the Netherlands) were maintained in DMEM/F-12 supplemented with 7.5% FCS, 1% NEAAs, 10 units/mL penicillin, 10  $\mu\text{g}/\text{mL}$  streptomycin, and 0.2 mg/mL G-418 in an incubator (5%  $\text{CO}_2$ ; 37°C). The cells were routinely subcultured when reaching 85–95% confluency (i.e. every 3 to 4 days), using trypsin-EDTA.

### 2.2.3 AR-CALUX

AR-CALUX assay data of DIM were taken from the literature (Dent et al., 2019). The AR-CALUX assay of BIC was performed as described previously (Sonneveld et al., 2005; van der Burg, Winter, Man, et al., 2010) by BDS. In short, the U2OS cells were plated in the inner wells of white, clear-bottomed 96-well plates at a density of  $1 \times 10^5$  cells/mL in a volume of 100  $\mu\text{L}/\text{well}$  assay medium consisting of Phenol Red Free DMEM/F-12 supplemented with 5% DCC-FCS, 1% NEAAs, 10 units/mL penicillin, and 10  $\mu\text{g}/\text{mL}$  streptomycin. 200  $\mu\text{L}$  PBS was loaded in the outer wells to prevent evaporation of the assay medium and the plate was placed for 24 h in an incubator (5%  $\text{CO}_2$ ; 37°C). Afterwards, the assay medium was aspirated and 100  $\mu\text{L}$  fresh assay medium was added to the cells and the plate was incubated for another 24 h in an incubator (5%  $\text{CO}_2$ ; 37°C). The test compounds dissolved in DMSO (final concentration 0.1% DMSO) tested in triplicate ( $n = 3$ ), the vehicle control (0.1% DMSO) ( $n = 6$ ), and the cytotoxicity control (0.01% Triton X-100) ( $n = 6$ ) were tested in the agonism assay and antagonism assay. After the incubation time, the assay medium was removed and the cells were exposed

by adding 100  $\mu\text{L}$  fresh assay medium containing the appropriate concentration of test compound to each well. In the agonism assay, the cells were exposed to a concentration range of DHT ( $1 \times 10^{-3}$  to 100 nM) or BIC ( $1 \times 10^{-3}$  to 3  $\mu\text{M}$ ). In the antagonism assay, FLU as a quality control and BIC were tested in a concentration range of  $1 \times 10^{-2}$  to 30  $\mu\text{M}$  and  $1 \times 10^3$  to 3  $\mu\text{M}$ , respectively, in the presence of the  $\text{EC}_{50}$  (0.3 nM) of DHT as the agonist. For the specificity control, the cells were exposed to the same concentration range of FLU and BIC with  $100 \times \text{EC}_{50}$  (30 nM) of DHT. After 24 h of exposure in an incubator (5%  $\text{CO}_2$ ; 37°C), the media were removed and the cells were washed with 100  $\mu\text{L}$  PBS in nanopore water (1:1) and lysed with 30  $\mu\text{L}$  LSB. Luminescence was measured with the Infinite 200 PRO (Tecan, Männedorf, Switzerland). Cytotoxicity was measured as the lactate dehydrogenase (LDH) leakage into the culture medium quantified using the Cytotoxicity Detection Kit (Roche, 1,644,793). In short, cells were exposed as in the AR-CALUX assay ( $n = 3$ ) or to the positive control for cytotoxicity (0.01% Triton X-100) ( $n = 6$ ) for 24 h in an incubator (5%  $\text{CO}_2$ ; 37°C), after which the reaction mixture of the Cytotoxicity Detection Kit was added. After 5 to 30 min, the stop solution was added and absorbance was measured with a microplate spectrophotometer system (Spectra max190-Molecular Devices, Wokingham, UK).

### 2.2.3.1 Data analysis

Antagonism was defined as at least 20% decrease in relative induction of the DHT induced response at a non-cytotoxic concentration of the test compound and the response being confirmed as AR-specific. The test concentration was stated as cytotoxic when the percentage LDH leakage was higher than 15% compared to the positive control of cytotoxicity set at 100%, and for these samples the observed reduction in luminescence was considered not to be due to antagonism and excluded from the analysis. The  $\text{IC}_{50}$  value of DIM was taken from Dent et al. (2019) and the  $\text{IC}_{50}$  value of BIC was modelled with a nonlinear regression of log (inhibitor) vs. response (four parameters) model using GraphPad Prism 5 (GraphPad, San Diego, USA). The  $\text{BMCL}_{05}$  value of DIM and BIC were using the benchmark response (BMR) of a 5% increase in the response compared to the control. The benchmark concentration causing this BMR ( $\text{BMC}_{05}$ ) and the upper ( $\text{BMCU}_{05}$ ) and lower ( $\text{BMCL}_{05}$ ) bound of its 95% confidence interval were determined. The acceptance criteria of the  $\text{BMCL}_{05}$  values were a p-value  $> 0.05$ , indicating support for a concentration-response. Furthermore, the model should describe the data adequacy in the BMR region reflected by a  $\text{BMC}_{05}$ :  $\text{BMCL}_{05}$  ratio lower than 3 (Hardy et al., 2017).

## 2.2.4 Evaluation of the BMCL<sub>05</sub> for prediction of a safe comparator exposure level

The BMCL<sub>05</sub> values of DIM and BIC for the induction of anti-androgenic effects were considered to reflect a safe internal exposure level without AR-mediated effects. This assumption is based on the fact that a BMCL<sub>05</sub> value may be equivalent to what would be considered a no observed adverse effect level (Hardy et al., 2017). To further evaluate this assumption, these *in vitro* safe levels were translated to their corresponding human urinary excretion and exposure levels using PBK modelling-based quantitative *in vitro* to *in vivo* extrapolation (QIVIVE) and compared to the urine excretion level of DIM as a biomarker for the intake of DIM from Brussels sprouts and the therapeutic dose of BIC, respectively.

### 2.2.4.1 PBK model development

The PBK model of DIM was taken from Dent et al. (2019), linking DIM plasma concentrations to urinary excretion levels of DIM (Fujioka et al., 2016). This PBK model and the PBK model of BIC were developed using the commercially available software GastroPlus™ version 9.6 (Simulation Plus Inc., Lancaster, CA, USA). The built-in Population Estimates for Age-Related (PEAR) Physiology™ module was used to parameterize the PBK model. For validation purposes, the model was parameterized for a fasted 38 year old female with a body weight of 71.2 kg and a fed 30 year old male with a body weight of 85.53 kg of DIM and BIC, respectively, to match the corresponding pharmacokinetic data from literature (Mckillop et al., 1993; Reed et al., 2008; Tyrrell et al., 1998). For QIVIVE, both PBK models were defined for a 30 year old male with a body weight of 70 kg. The physiochemical parameters were derived from PubChem databases (Kim et al., 2016), literature or predicted from their structure with the built-in ADMET Predictor™ version 9.6 (Simulation Plus Inc., Lancaster, CA) (**Table 2.1**).

**Table 2.1.** Input parameters of the PBK model describing the kinetics of DIM and BIC in humans.

Parameter	Value DIM <sup>1</sup>	Value BIC
MW	246.31 <sup>a</sup>	430.37 <sup>a</sup>
Log P	4.17 <sup>b</sup>	2.3 <sup>a</sup>
Solubility at 25°C (µg/mL)	12 <sup>b</sup>	9.28 <sup>a</sup>
pKa		Acid 11.95 <sup>c</sup> Base -4 <sup>c</sup>
P <sub>eff</sub>	2 x 10 <sup>-4</sup> cm/s <sup>b</sup>	32 x 10 <sup>-6</sup> cm/s <sup>d</sup>
F <sub>ub</sub> <i>in vivo</i>	2.84% <sup>b</sup>	10.52% <sup>b</sup>
R <sub>b2p</sub>	0.82 <sup>b</sup>	0.63 <sup>b</sup>
CL <sub>sys</sub> (L/h)		0.32 <sup>e</sup>
CL <sub>ren</sub> (L/h)	7.27 <sup>f</sup>	0.12 <sup>e, g</sup>
CL <sub>hep</sub>	0.931 L/h/kg <sup>f, h</sup>	0.21 L/h <sup>e, g</sup>

<sup>1</sup> Taken from Dent et al. (2019)

<sup>a</sup> Kim et al. (2016)

<sup>b</sup> ADMET predictor™

<sup>c</sup> Wishart et al. (2007)

<sup>d</sup> Bassetto et al. (2016)

<sup>e</sup> AstraZeneca Pharmaceuticals (2005)

<sup>f</sup> Dent et al. (2019)

<sup>g</sup> B.C. Cancer Agency (2001)

<sup>h</sup> Tang et al. (2007); Wu et al. (2015)

The effective permeability ( $p_{\text{eff}}$ ) of BIC was simulated from the Caco-2 value reported by Bassetto et al. (2016) using the built-in conversion equation based on the Absorption Systems Caco-2 calibration (ABSCa). The distribution of both compounds into tissues was assumed to be perfusion limited and the tissue: plasma partition coefficients ( $K_{\text{ps}}$ ) were calculated with the Lucakova method (GastroPlus™) (Rodgers et al., 2005; Rodgers & Rowland, 2006). The hepatic clearance ( $\text{CL}_{\text{hep}}$ ) of DIM was scaled from rat data (Dent et al., 2019; Tang et al., 2007; Wu et al., 2015). The Extended Clearance Classification System (ECCS) method (Varma et al., 2015) predicts renal clearance as the major route of clearance for BIC, though evidence from studies also indicate metabolism can play a major role in the clearance (AstraZeneca Pharmaceuticals,

2005). Clinical studies showed that severe hepatic impairment increases the accumulation of BIC in the plasma which is indicative of the physiological involvement of hepatic clearance ( $CL_{\text{hep}}$ ) (Cockshott, 2004; AstraZeneca Pharmaceuticals, 2005). No data on the *in vitro* hepatic clearance of BIC were found in literature, but from the study of AstraZeneca Pharmaceuticals (2005) a nominal system clearance ( $CL_{\text{sys}}$ ) of 0.32 L/h was found. Since the urinary excretion of BIC was observed to be 36% (B.C. Cancer Agency, 2001), in this study the  $CL_{\text{ren}}$  was set to 0.12 L/h ( $0.36 \times 0.32$  L/h) and the  $CL_{\text{hep}}$  was calculated by subtracting  $CL_{\text{ren}}$  from the  $CL_{\text{sys}}$  resulting in a value of 0.21 L/h.

#### 2.2.4.2 PBK model validation

For validation purposes, the PBK model predicting the DIM plasma concentration upon dosing of DIM was validated previously by Dent et al. (2019) against corresponding clinical data from literature (Reed et al., 2008). For validation of the PBK model of BIC, a simulation was carried out using the GastroPlus™ Single Simulation Mode to obtain the time-dependent plasma concentration curves upon dosing a single immediate release (IR) tablet of 50 mg BIC to a male with a bodyweight of 85.53 kg with a simulation time of 25 days. The predicted time-dependent plasma concentration curve thus obtained was validated against pharmacokinetic data reported by McKillop et al. (1993) upon oral dosing of 50 mg in healthy male volunteers ( $n = 5$ ). Similar, the repeated IR tablet dosing of 10 mg/day BIC was simulated by the GastroPlus™ Repeated Simulation Mode, with a simulation time of 12 weeks and compared to corresponding pharmacokinetic data reported by Tyrrell et al. (1998) in patients with advanced prostate cancer ( $n = 140$ ).

#### 2.2.4.3 Sensitivity analysis

The PBK models were standardized by parameterizing for a 30 year old American male with a body weight of 70 kg to execute the sensitivity analysis with the built-in parameter sensitivity analysis (PSA) mode of GastroPlus™. The sensitivity analysis was conducted with the previously developed PBK model predicting the nominal plasma concentration of DIM upon an oral dose of 50 mg DIM (Dent et al., 2019), and the PBK model developed for BIC in the present study at an oral dose of 10 mg/day, both being dose levels used for the validation of the PBK models. The sensitivity coefficients (SCs) for the maximum plasma concentration ( $C_{\text{max}}$ ) and AUC were calculated as the % change in model outcome divided by the % change in parameter value (Eq. (1)).

$$\text{Eq. 1} \quad SC = \frac{\% \text{ change in model outcome}}{\% \text{ change in parameter value}}$$

The % change in parameter value was set at 5% (Moxon et al., 2020; Zhang et al., 2018), leaving the rest of the parameters unchanged. Parameters with a SC > 0.1 or < -0.1 were considered to be influential on the prediction of the  $C_{\max}$  and AUC (Zhang et al., 2018).

#### 2.2.4.4 PBK modelling-based QIVIVE

The nominal  $BMCL_{05}$  values of DIM and BIC derived from the *in vitro* AR-CALUX assay data were translated to the nominal  $C_{\max}$  correcting for differences in protein binding in the *in vitro* and *in vivo* situation following Eq. (2). This correction implies that the biological effect is related to the free concentrations and that the free *in vitro* concentration in the assay medium is set equal to the free *in vivo* concentration in the human plasma.

$$\text{Eq. 2} \quad \text{nominal } C_{\max} = \frac{\text{nominal } BMCL_{05} (\text{comparator}) * f_{ub \text{ in vitro}} (\text{comparator})}{f_{ub \text{ in vivo}} (\text{comparator})}$$

The nominal  $BMCL_{05}$  values of DIM and BIC were derived from the AR-CALUX assay and the  $f_{ub \text{ in vitro}}$  and the  $f_{ub \text{ in vivo}}$  represent the fraction unbound in the medium used in the AR-CALUX assay and in human plasma, respectively, determined as described below. With the PBK models, QIVIVE was performed to predict the urinary excretion level or the external dose level that would result in the nominal  $C_{\max}$  values of DIM and BIC, respectively, and the levels thus obtained were subsequently compared to the urinary excretion from the intake of DIM *via* consumption of Brussels sprouts and the exposure to BIC at the therapeutic dose, respectively.

#### 2.2.5 Definition of the EAR and the DCR values

In the DCR approach, the EAR of a compound under study ( $EAR_{\text{test}}$ ) is compared to the  $EAR_{\text{comparator}}$  which is based on an established safe level of human exposure to a comparator compound (Eq. (3)).

$$\text{Eq. 3} \quad DCR = \frac{EAR_{\text{test}}}{EAR_{\text{comparator}}}$$

In the present study, the  $EAR_{\text{test}}$  was calculated using Eq. (4).

Eq. 4

$$EAR_{\text{test}} = \frac{\text{nominal internal concentration at defined external dose level (test)} * f_{\text{ub in vivo}} (\text{test})}{\text{nominal IC}_{50} (\text{test}) * f_{\text{ub in vitro}} (\text{test})}$$

In which the  $f_{\text{ub in vivo}}$  represents the fraction unbound of the test compound in human plasma, the  $f_{\text{ub in vitro}}$  the fraction unbound of the test compound in the medium of the AR-CALUX assay. The  $f_{\text{ub}}$  values were determined as described below. The nominal  $IC_{50}$  was derived from the AR-CALUX concentration-response curve while the nominal internal concentration at the defined external dose level of the test compound was calculated previously using a human PBK model for the test compound or taken from reported pharmacokinetic data in literature (Dent et al., 2019). The variability of the biomarker and thus the nominal internal concentration of the test compounds were included as the mean, the 5th or 25th, and the 95th or 75th percentiles, as reported by Dent et al. (2019), resulting in distribution of the  $EAR_{\text{test}}$  values from the corresponding percentiles of the respective test compound. When no biomarker distribution data were available, no distribution in the nominal internal concentration was included and thus only one  $EAR_{\text{test}}$  value was calculated. Furthermore in the present study, the  $EAR_{\text{comparator}}$  was calculated following Eq. (5) using data obtained in the AR-CALUX assay.

Eq. 5

$$EAR_{\text{comparator (AR-CALUX based)}} = \frac{\text{nominal BMCL}_{05} (\text{comparator}) * f_{\text{ub in vitro}} (\text{comparator})}{\text{nominal IC}_{50} (\text{comparator}) * f_{\text{ub in vitro}} (\text{comparator})}$$

The nominal  $IC_{50}$  and nominal  $BMCL_{05}$  were both derived from the AR-CALUX concentration-response curve of the respective comparator compound and  $f_{\text{ub in vitro}}$  represents the fraction unbound of the comparator compound in the medium of the assay, determined as described hereafter. Since in this novel approach the  $EAR_{\text{comparator}}$  is entirely based on the *in vitro* AR-CALUX assay, using the  $f_{\text{ub in vitro}}$  for correction for protein binding does not affect the outcome of Eq. 5. The  $EAR$  values obtained were used to calculate the DCR using Eq. (3). The DCR values thus calculated were compared to the DCR values reported previously by Dent et al. (2019) using intake of DIM *via* 50 g Brussels sprouts as the comparator, with its mean, 5th, and 95th percentiles. The variability of the DCRs was calculated by comparing the  $EAR_{\text{test}}$  from the lowest percentile to the  $EAR_{\text{comparator}}$  from the highest percentile and vice versa for those test compounds with distribution data available. In addition, since the DCR values previously reported were not corrected for protein binding, these DCR values were also

considered taking the  $f_{ub \text{ in vitro}}$  and  $f_{ub \text{ in vivo}}$  for defining the EAR values into account (Eq. (4) and Eq. (6)).

Eq. 6

$EAR_{\text{comparator (50 g Brussels sprouts)}}$  with correction for protein binding

$$= \frac{\text{nominal internal concentration at defined external dose level (comparator)} * f_{ub \text{ in vivo}} \text{ (comparator)}}{\text{nominal } IC_{50} \text{ (comparator)} * f_{ub \text{ in vitro}} \text{ (comparator)}}$$

## 2.2.6 Determination of the $f_{ub \text{ in vivo}}$

The  $f_{ub \text{ in vivo}}$  values for the comparator and test compounds were predicted by the commercially available software ADMET Predictor™ version 9.6 (Simulation Plus Inc.). This software predicts chemical-dependent parameters based on SMILES using QSAR-methods.

## 2.2.7 Determination of the $f_{ub \text{ in vitro}}$

The  $f_{ub \text{ in vitro}}$  values were calculated assuming a linear relation between the fraction unbound and the protein content in a biological matrix, with the fraction unbound being 1.0 in the absence of protein. This assumption is supported by the linear relationship reported by Gülden et al. (2002) between the unbound fraction and albumin concentrations added to the *in vitro* test system for some chlorophenols (Gülden et al., 2002). The protein content of human plasma has been reported to be 8% (Mescher, 2009; Mathew et al., 2020). The assay medium used in the AR-CALUX assay contained 5% DCC-FCS (Dent et al., 2019; Sonneveld et al., 2005) which was considered as a 5% protein content. Based on these assumptions, the  $f_{ub \text{ in vitro}}$  values of the comparator and test compounds were calculated by linear extrapolation to the 5% protein content using the  $f_{ub}$  of 1.0 in the absence of protein and the respective  $f_{ub \text{ in vivo}}$  values generated with the ADMET Predictor™ at 8% protein content in *in vivo* plasma.

## 2.2.8 Definition of test compounds and their exposure scenarios

The exposure scenarios to the putative anti-androgenic test compounds evaluated in the DCR-based NGRA were the same as the ones previously selected by Dent et al.



(2019) and are summarized in **Table 2.2**. The table also presents whether at the exposure scenario evaluated anti-androgenic effects are expected to occur. This reveals that the data set consists of both putative negative as well as positive test compound exposure scenarios for anti-androgenicity.

**Table 2.2.** Exposure scenarios of putative dietary anti-androgenic test compounds in humans evaluated by the DCR approach (adapted from Dent et al., 2019), including whether or not *in vivo* anti-androgenic effects at the respective exposure scenarios are expected or where this is unknown.

Test compound	Exposure scenario	<i>In vivo</i> anti-androgenic effect expected	Source
Resveratrol (RES)	25 mg orally; corresponding to moderate intake of red wine	No	(Almeida et al., 2009; Goldberg et al., 2003)
Flutamide (FLU) & its metabolite hydroxyflutamide (HF)	Therapeutic oral dose of 250 mg/day flutamide	Yes	(Radwanski et al., 1989)
Bisphenol A (BPA), vinclozolin (VIN), and methoxychlor (MX) & its metabolite hydroxychlor (HPTE)	Oral RfD/TDI	No	Scaled by Dent et al., (2019) from the $C_{ss}$ values reported by Wetmore et al., (2012)
Dichlorodiphenyldichloroethylene (3,3'-DDE)	Serum levels in men from DDT-sprayed area in South Africa	Yes	(Aneck-Hahn et al., 2007)
Dichlorodiphenyldichloroethylene (3,3'-DDE)	Serum levels in DDT-exposed women between 1959 and 1967 in the USA,	No	(Longnecker et al., 2002); (Bhatia et al., 2005) respectively

	n=599 and n=283		
Bakuchiol (BAK)	Exposure <i>via</i> shampoo & body lotion once per day as a case- study by Dent <i>et al.</i> , (2019)	Unknown	(Dent et al., 2019)

## 2.3 Results

### 2.3.1 AR-CALUX

**Figure 2.2** presents the concentration-response curves for the anti-androgenic activity of DIM and BIC in the AR-CALUX assay. Both compounds did not show a response in the agonist AR-CALUX assay. Their anti-androgenic response was confirmed to be AR-specific by the observation of the right shift of the concentration-response curve at a higher agonist concentration (100 x EC<sub>50</sub> of DHT) (data not shown). From the concentration-response data obtained the nominal BMCL<sub>05</sub> and IC<sub>50</sub> values were derived. The results of the benchmark dose modelling to derive the BMCL<sub>05</sub> values are presented in Supplementary material S2.1. The nominal BMCL<sub>05</sub> and IC<sub>50</sub> values thus obtained amounted to 5.13 nM and 1.27 μM for DIM and to 0.10 nM and 0.07 μM for BIC, respectively.

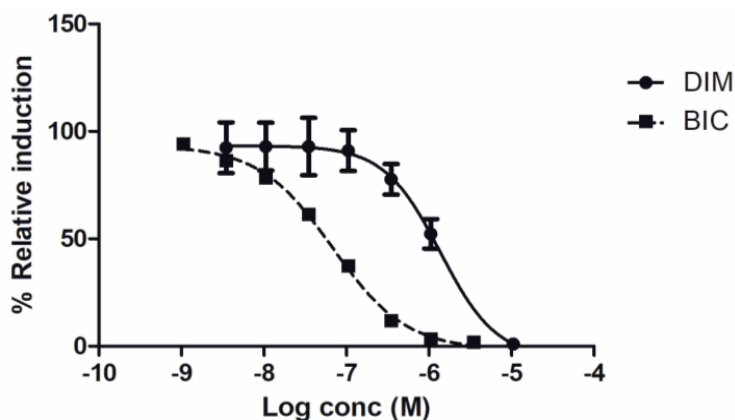


**Figure 2.2.** The concentration-dependent antagonistic activity of DIM (solid line and circles) and BIC (dashed line and squares), on the DHT-mediated luciferase induction in the U2OS AR-CALUX reporter gene assay. The data for DIM were taken from Dent et al. (2019). The symbols present the mean  $\pm$  SD values of 3 independent studies.

### 2.3.2 Determination of the $f_{ub}$ values

**Table 2.3** compiles the ADMET predicted  $f_{ub}$  *in vivo* values. Using these values at 8% protein, the protein content in human plasma, and assuming the  $f_{ub}$  to equal 1.0 at 0% protein, the  $f_{ub}$  *in vitro* values representing the fraction unbound in the assay medium of the *in vitro* AR-CALUX assay containing 5% protein were calculated for the comparator and test compounds of the present study. These values are also presented in **Table 2.3**.

**Table 2.3.** The ADMET Predictor™ generated  $f_{ub}$  *in vivo* values and the calculated  $f_{ub}$  *in vitro* values of the comparator and test compounds of the present study.

Compound	$f_{ub}$ <i>in vivo</i>	$f_{ub}$ <i>in vitro</i>
<b>DIM</b>	0.03	0.40
<b>BIC</b>	0.11	0.44
<b>BAK</b>	0.05	0.41
<b>RES</b>	0.08	0.42
<b>VIN</b>	0.12	0.45
<b>BPA</b>	0.09	0.43
<b>MX</b>	0.04	0.40
<b>HPTE</b>	0.05	0.40
<b>3,3-DDE</b>	0.03	0.39
<b>FLU</b>	0.20	0.50
<b>HF</b>	0.32	0.57

Given the lower protein concentration in the *in vitro* AR-CALUX assay medium than in human plasma, the  $f_{ub}$  *in vitro* values were all higher than the  $f_{ub}$  *in vivo* values. The method applied to obtain the  $f_{ub}$  *in vitro* data was verified by comparison of the calculated  $f_{ub}$  *in vitro* of BPA of 0.43 to the value obtained in the same *in vitro* medium using the Rapid Equilibrium Device (RED) assay amounting to  $0.46 \pm 0.04$  (Zhang et al., 2018), indicating a 1.1-fold difference.

### 2.3.3 Evaluation of the BMCL<sub>05</sub> for prediction of a safe comparator exposure level

#### 2.3.3.1 PBK model development and validation

In order to evaluate the use of the *in vitro* BMCL<sub>05</sub> values to define a safe level of exposure to the comparator compounds, the values of DIM and BIC were translated to the *in vivo* urinary excretion and external dose level, respectively, *via* PBK model

facilitated reverse dosimetry enabling QIVIVE. The PBK model used for DIM was developed and validated previously by Dent et al. (2019). The PBK model for BIC was developed in the present study. To enable evaluation of this PBK model for BIC, **Figure 2.3** reports the PBK-model predicted and literature reported time-dependent plasma concentrations after a single oral dose of 50 mg BIC (**Figure 2.3A**) and a repeated oral dose of 10 mg/day BIC (**Figure 2.3B**) in humans. From this comparison it appears that the model predicts the dose-dependent plasma concentration of BIC well with a 1.3- to 1.6-fold difference between the reported and predicted  $C_{\max}$  values of BIC.

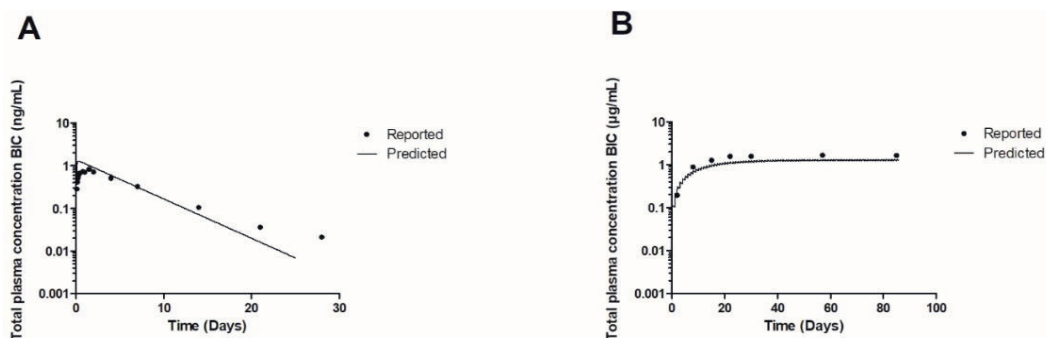


**Figure 2.3.** PBK model predicted (lines) and reported (individual data points represented as the average values as reported in literature) for the time-dependent plasma concentration after **A.** a single oral dose of 50 mg BIC in humans (experimental data from Mckillop et al., 1993), and **B.** repeated oral doses of 10 mg/day BIC in humans (experimental data from Tyrrell et al., 1998).

### 2.3.3.2 Sensitivity analysis

For further evaluation of the PBK models, a sensitivity analysis was performed at a dose of 50 mg for DIM and of 10 mg/day for BIC. **Figure 2.4** presents the parameters with a  $SC > 0.1$  or  $< -0.1$  representing the PBK model parameters that are most influential on the PBK model output for  $C_{\max}$  and the AUC of DIM or BIC. The DIM PBK model prediction of the  $C_{\max}$  appears to be sensitive to the permeability, Log D,  $f_{ub \text{ in vivo}}$ , and  $R_{b2p}$ , and the prediction of the AUC is sensitive to these latter three. The BIC PBK model prediction of  $C_{\max}$  is sensitive to Log D,  $CL_{\text{hep}}$ , and  $f_{ub \text{ in vivo}}$  whereas the prediction of the AUC is sensitive to only LogD and  $f_{ub \text{ in vivo}}$ . The remaining parameters had an SC within -0.1 and 0.1.

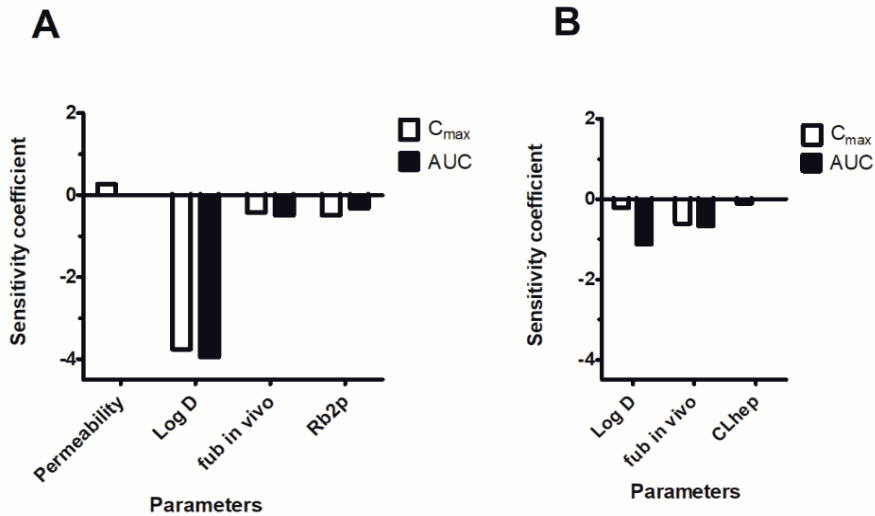


**Figure 2.4.** Sensitivity analysis of the parameters of the PBK model of **A.** DIM and **B.** BIC predicting the  $C_{max}$  (open bars) and AUC (closed bars) following an oral dose of 50 mg DIM or an oral dose of 10 mg/day BIC, respectively. Parameters with a SC > 0.1 or < -0.1 are plotted. Permeability = intestinal permeability. Log D = distribution coefficient.  $f_{ub \text{ in vivo}}$  = fraction unbound *in vivo*.  $R_{b2p}$  = blood: plasma ratio.  $CL_{hep}$  = hepatic clearance. Only parameters with a SC > 0.1 or < -0.1 are presented.

### 2.3.3.3 PBK modelling-based QIVIVE

To enable PBK modelling-based QIVIVE, first the nominal  $BMCL_{05}$  values from the concentration-response curves obtained in the AR-CALUX assay were converted to the nominal  $C_{max}$  values of DIM and BIC correcting for differences in protein binding in the *in vitro* and *in vivo* situation using Eq. (2). Next, the PBK models defined were used to translate the nominal  $C_{max}$  values of DIM and BIC to the corresponding urinary excretion and external dose level, respectively, that could be compared to potential human exposure scenarios. The nominal  $C_{max}$  values thus obtained amounted to 71 nM and 0.43 nM for DIM and BIC respectively, and the urinary excretion and external dose level resulting in these  $C_{max}$  values amounted to 0.64 mg DIM and 1.4  $\mu$ g/day BIC, respectively. This urinary excretion level of DIM is 84- to 533-fold higher than the urinary excretion level resulting from consumption of 50 g Brussels sprouts which was estimated to amount to  $1.2 \times 10^{-3}$  to  $7.6 \times 10^{-3}$  mg DIM (Dent et al., 2019). For BIC the dose level is approximately 4 orders of magnitude lower than the therapeutic dose of 25 mg/day used for treatment of hirsutism (Müderris et al., 2002) and 50 mg/day used in treatment of prostate cancer (B.C. Cancer Agency, 2001).

### 2.3.4 Definition of the EAR values

The  $EAR_{\text{comparator}}$  of DIM and BIC calculated based on the AR-CALUX were  $4.04 \times 10^{-3}$  and  $1.51 \times 10^{-3}$ , respectively. The  $EAR_{\text{test}}$  values of exposure scenarios to the putative anti-androgenic test compounds as reported by Dent et al. (2019) were corrected for protein binding and are summarized in Supplementary material S2.2.

### 2.3.5 DCR values based on the different comparator exposure scenarios

Using the EAR values obtained, the DCR values were calculated for the different putative anti-antagonist exposure scenarios using the newly defined EAR comparator values for DIM (**Figure 2.5C**) and BIC (**Figure 2.5D**). **Figure 2.5** also presents, for comparison, the DCR values as shown previously using 50 g Brussels sprouts as the comparator without correction for differences in protein binding (**Figure 2.5A**) (Dent et al., 2019) or with correction for differences in protein binding (**Figure 2.5B**). Using the EAR based on the exposure to DIM *via* consumption of 50 g Brussels sprouts as the comparator scenario, either without (**Figure 2.5A**) or with correction for differences in protein binding (**Figure 2.5B**), resulted in DCRs  $> 1$  for all test compounds, indicating that all the exposure scenarios evaluated present a higher chance to result in *in vivo* anti-antagonistic effects than the intake of 50 g Brussels sprouts for which this effect is absent. Comparison of the data in **Figure 2.5A** and **B** reveals that the effect of the correction for the difference in protein binding in the *in vitro* and *in vivo* situation is limited, resulting in 0.9- to 7.6-fold higher DCR values upon correction for differences in protein binding with the highest increase observed for compounds with relative high  $f_{\text{ub}}$  values. The DCRs calculated using the newly defined AR-CALUX based  $EAR_{\text{comparator}}$  values for DIM (**Figure 2.5C**) and BIC (**Figure 2.5D**) were less conservative. To further evaluate the validity of these comparator values, the predictions made for the test compounds were compared to actual knowledge on the anti-androgenicity of the respective exposure scenarios (**Table 2.2**). To this end in **Figure 2.5**, the DCRs of test compounds where no *in vivo* anti-androgenic effects are expected at the corresponding exposure scenario (**Table 2.2**) are presented as green symbols. The DCRs of test compounds where *in vivo* anti-androgenic effects are expected or where this is unknown at the corresponding exposure scenario (**Table 2.2**) are presented as red and purple symbols, respectively. Given that in **Figure 2.5C** and **D** all exposure scenarios that have DCR values  $\leq 1$  relate to exposures that are known to not result in anti-androgenic activity, supports the use of the newly defined  $EAR_{\text{comparator}}$  values as points

of departure to define safe levels of exposure. There are even two of the test scenarios of DDE where no *in vivo* anti-androgenic effects were observed with DCR values > 1.

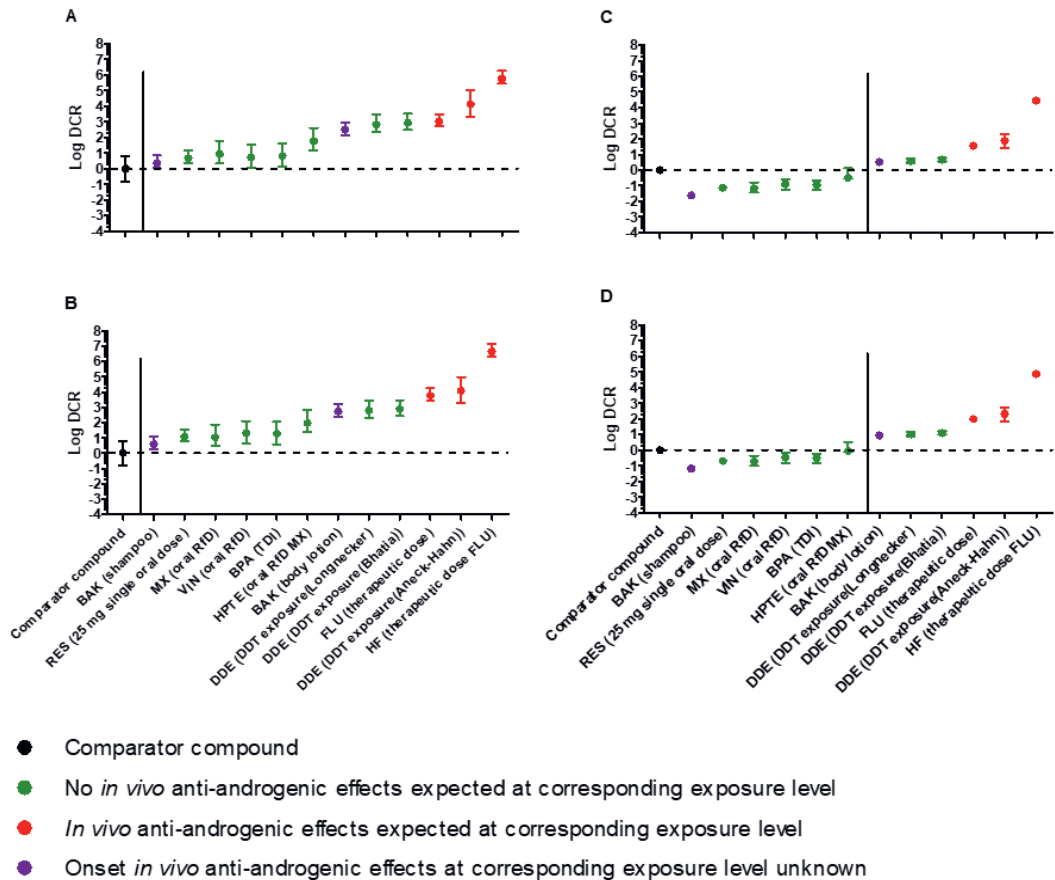


**Figure 2.5.** The DCRs of the series of exposure scenarios to anti-androgenic test compounds (Table 2.2) based on different  $EAR_{\text{comparator}}$  values including **A.** the  $EAR_{\text{comparator}}$  for DIM intake from 50 g Brussels sprouts without correction for differences in protein binding as reported by Dent et al. (2019) calculated using an  $EAR_{\text{comparator}}$  of  $3.51 \times 10^{-4}$  at the mean and  $1.16 \times 10^{-4}$  and  $7.43 \times 10^{-4}$  at the 5th and 95th percentile, **B.** the  $EAR_{\text{comparator}}$  for DIM intake from 50 g Brussels sprouts with correction for differences in protein binding, calculated using an  $EAR_{\text{comparator}}$  of  $2.55 \times 10^{-5}$  at the mean and  $8.43 \times 10^{-6}$  and  $5.39 \times 10^{-5}$  at the 5th and 95th percentile **C.** the  $EAR_{\text{comparator}}$  for DIM based on AR-CALUX data of  $4.04 \times 10^{-3}$ , and **D.** the  $EAR_{\text{comparator}}$  for BIC based on AR-CALUX data of  $1.51 \times 10^{-3}$ . The comparator DCRs are represented as black symbols and by definition equal to 1 (log DCR = 0). The DCRs of test compounds where no *in vivo* anti-androgenic effects are expected at the corresponding exposure scenario (Table 2.2) are presented as green symbols and the DCRs of test compounds

where *in vivo* anti-androgenic effects are expected or where this is unknown at the corresponding exposure scenario (**Table 2.2**) are presented as red and purple symbols, respectively. The dotted horizontal line marks the DCR of 1 (log DCR = 0). The vertical lines separate the exposure scenarios with  $DCR \leq 1$  from those with  $DCR > 1$ .

## 2.4 Discussion

In the DCR approach, the EAR of an exposure scenario to a test compound under study ( $EAR_{test}$ ) is compared to the EAR of a safe human exposure to a comparator compound ( $EAR_{comparator}$ ). A DCR cut-off value of 1 is then used to evaluate the safety of the respective test compound exposure. This DCR approach was introduced for the evaluation of anti-androgenic effects by Dent et al. (2019) using the EAR for DIM resulting from consumption of 50 g Brussels sprouts as the comparator. However, when using this  $EAR_{comparator}$  the DCR of all test compounds, even the ones for exposures known to be safe, were above 1, which indicates that use of this  $EAR_{comparator}$  may be overprotective. Therefore in the present study, alternative  $EAR_{comparator}$  values were defined. The  $EAR_{comparator}$  value of DIM was redefined and an additional  $EAR_{comparator}$  was defined using the anti-androgenic drug BIC. Using BIC as a comparator compound implies that formally the term dietary comparator should be reconsidered but we preferred to maintain current terminology. To develop an NGRA compliant method to define the new  $EAR_{comparator}$  values, the values were determined using the  $BMCL_{05}$  and  $IC_{50}$  for anti-androgenicity obtained in the *in vitro* AR-CALUX assay as the surrogate endpoints to define safe and effective *in vivo* plasma concentrations, respectively. Evaluation of the adequacy of the EAR values thus obtained was based on PBK modelling-based translation of the  $BMCL_{05}$  values to *in vivo* relevant biomarker levels and on the comparison of the DCR values obtained for exposures to test compounds with the actual knowledge on the anti-androgenicity of the respective exposure scenarios. In contrast to the  $EAR_{comparator}$  based on intake of 50 g Brussels sprouts, with the newly defined  $EAR_{comparator}$  values, test compound exposure scenarios with DCR values  $\leq 1$  were all negative for *in vivo* AR antagonist mediated responses. All scenarios known to induce *in vivo* anti-androgenic effects had DCR values  $> 1$ , indicating the method did not result in false negatives among the scenarios tested. There were even two of the test scenarios of DDE known to be without *in vivo* anti-androgenic activity with DCR values  $> 1$  which represent false positives. This result indicates that even the newly defined  $EAR_{comparator}$  values seem to be conservative.

Conversion of the AR-CALUX derived  $BMCL_{05}$  for the safe level of endogenous exposure to DIM and BIC to the corresponding *in vivo* levels *via* PBK modelling-based QIVIVE resulted in a predicted urinary excretion level of 0.64 mg DIM and a safe dose level of



1.4 µg/day BIC. This urinary excretion level of DIM is 84- to 533-fold higher than the urinary excretion level resulting from consumption of 50 g Brussels sprouts which was estimated to amount to  $1.2 \times 10^{-3}$  to  $7.6 \times 10^{-3}$  mg DIM in urine (Dent et al., 2019). The reason to compare with urinary excretion levels was because DIM is not consumed with Brussels sprouts as such but has to be formed from indol-3-carbinol, with the corresponding external dose which would result in this urinary excretion of DIM being influenced by high variance in the processing and pharmacokinetics of indol-3-carbinol following in the intake of Brussels sprouts (Barba et al., 2016; Fujioka et al., 2014; Thomson et al., 2016). However, comparison of the urinary DIM levels corresponding to the established safe plasma levels to the urinary DIM levels resulting from intake of 50 g of Brussels sprouts, indicates that the new comparator exposure scenario for DIM is far less conservative than the one based on the intake of only 50 g Brussels sprouts. The modelled safe external dose of BIC is 4 orders of magnitude lower than the therapeutic dose of 25 mg/day in hirsutism (Müderris et al., 2002) and 50 mg/day in prostate cancer (B.C. Cancer Agency, 2001) corroborating the adequacy of this exposure scenario and the AR-CALUX based method used to define this safe  $EAR_{\text{comparator}}$ .

The  $EAR_{\text{comparator}}$  and DCR values defined in the present study based on the *in vitro* AR-CALUX assay also included a correction for differences in protein binding in the *in vitro* and *in vivo* situation. The capability of chemicals to bind to proteins present in the surrounding medium influences their availability for the biological target and the corresponding potency (Gülden et al., 2002). Therefore, the free concentration of a chemical is considered to be a more appropriate dose metric than the nominal concentration. This correction appeared to influence the  $EAR$  values to the largest extent for compounds with relatively high  $f_{\text{ub}}$  values, for which the differences between the  $f_{\text{ub}}$  *in vivo* and  $f_{\text{ub}}$  *in vitro* were most substantial. The comparison of the DCR values obtained using the newly defined  $EAR_{\text{comparator}}$  values with actual knowledge on the anti-androgenicity resulting from the exposure scenarios of the test compounds (**Figure 2.5C and D**), provides further support for using the AR-CALUX based  $BMCL_{05}$  and  $IC_{50}$  to define the  $EAR_{\text{comparator}}$  value. All together the results of the present study using newly defined  $EAR_{\text{comparator}}$  values further validate the DCR approach as an animal free *in silico/in vitro* 3R compliant method in NGRA.

### Declaration of Competing Interest

The authors declare that they have no known competing financial interests or personal relationships that could have appeared to influence the work reported in this paper.

## **Acknowledgment**

The authors would like to express their gratitude towards the people at BioDetection Systems (BDS, Amsterdam, the Netherlands) for their contribution to defining the AR-CALUX concentration-response data for BIC and Beate Nicol (Unilever) for her helpful discussions valuable to this work.

## Supplementary materials S2.1. BMC Analysis

The benchmark concentration (BMC) analysis of DIM and BIC was performed based on the *in vitro* concentration-response data reported by Dent et al., (2019) and kindly provided by BioDetection Systems (BDS, Amsterdam the Netherlands), respectively, using BMDS3.1 software (U.S. EPA). The benchmark response (BMR) was defined as a 5% extra response (BMR<sub>05</sub>). The BMC<sub>05</sub> and its upper (BMCU<sub>05</sub>) and lower (BMCL<sub>05</sub>) 95% confidence interval were also determined. The model was accepted when the fitted model had a p-value > 0.05, indicating support for a concentration-response.

### Supplementary material S2.1.1 BMC modelling of *in vitro* concentration-response data of DIM

**Supplementary Table S2.1.1.1.** Input values of the *in vitro* concentration-response data of DIM (Dent et al., 2019).

Concentration ( $\mu\text{M}$ )	n	100 - % Relative induction <sup>1</sup>	Standard deviation
0.003	3	7.6	11.8
0.01	3	7.1	11.1
0.03	3	7.1	13.3
0.1	3	8.9	9.5
0.3	3	22.3	7.1
1	3	47.6	6.9
10	3	98.9	1.9

<sup>1</sup> As reported in **Figure 2.2**

**Supplementary Table S2.1.1.2.** BMC analysis of the *in vitro* concentration-response data of DIM (Dent et al., 2019). BMC<sub>05</sub> and BMCL<sub>05</sub> values were obtained using BMDS software version 3.1, at a BMC of 5% extra risk and default settings.

Model	BMC ( $\mu\text{M}$ )	BMCL ( $\mu\text{M}$ )	BMCU ( $\mu\text{M}$ )	Test 4 P-Value	AIC	Accepted
Exponential 2 (CV - normal)	0.25	0.19	0.35	<0.0001	178.94	No

Exponential 3 (CV - normal)	0.25	0.19	Infinity	<0.0001	178.94	No
Exponential 4 (CV - normal)	7.12E-03	5.13E-03	0.01	0.98	154.18	Yes, recommended
Exponential 5 (CV - normal)	8.94E-03	5.13E-03	0.07	0.93	156.15	Yes
Hill (CV - normal)	1.32E-02	4.15E-03	0.08	0.95	156.05	Yes
Polynomial Degree 6 (CV - normal)	7.69E-02	5.88E-02	0.15	3.52E-04	174.61	Yes
Polynomial Degree 5 (CV - normal)	7.69E-02	5.88E-02	0.15	3.52E-04	174.61	Yes
Polynomial Degree 4 (CV - normal)	7.69E-02	5.88E-02	0.15	3.52E-04	174.61	Yes
Polynomial Degree 3 (CV - normal)	7.69E-02	5.88E-02	0.15	3.52E-04	174.61	Yes
Polynomial Degree 2 (CV - normal)	7.69E-02	5.88E-02	0.15	3.52E-04	174.61	Yes
Power (CV - normal)	7.69E-02	5.88E-02	0.19	3.52E-04	174.61	Yes
Linear (CV - normal)	7.69E-02	5.88E-02	0.11	3.52E-04	174.61	Yes

### Supplementary material S2.1.2 BMC modelling of *in vitro* concentration-response data of BIC

**Supplementary Table S2.1.2.1.** Input values of the *in vitro* concentration-response data of BIC (BDS, Amsterdam, the Netherlands).

Concentration ( $\mu\text{M}$ )	n	100 - % Relative induction <sup>1</sup>	Standard deviation
0.001	3	5.7	3.4
0.003	3	13.6	5.4
0.01	3	21.5	3.6
0.03	3	38.4	6.3
0.1	3	62.4	7.6
0.3	3	88.0	0.7
1	3	96.4	0.1
3	3	98.0	0.1

<sup>1</sup> As reported in **Figure 2.2**

**Supplementary Table S2.1.2.2.** BMC analysis of the *in vitro* concentration-response data of BIC (BDS, Amsterdam, the Netherlands).  $\text{BMC}_{05}$  and  $\text{BMCL}_{05}$  values obtained using the BMDS software version 3.1, a BMC of 5% extra risk and default settings.

Model	BMC ( $\mu\text{M}$ )	BMCL ( $\mu\text{M}$ )	BMCU ( $\mu\text{M}$ )	Test 4 P-Value	AIC	Accepted
Exponential 2 (CV - normal)	0.11	0.08	0.17	<0.0001	234.50	No
Exponential 3 (CV - normal)	0.11	0.08	0.33	<0.0001	234.50	No
Exponential 4 (CV - normal)	6.91E-04	5.50E-04	9.06E-04	<0.0001	167.80	No
Exponential 5 (CV - normal)	6.91E-04	5.50E-04	1.16E-03	<0.0001	167.80	No
Hill (CV - normal)	1.35E-04	1.03E-04	3.53E-04	0.23	143.97	Yes
Polynomial Degree 6 (CV - normal)	0.05	0.04	0.11	<0.0001	231.52	No
Polynomial Degree 5 (CV - normal)	0.05	0.04	0.11	<0.0001	231.52	No

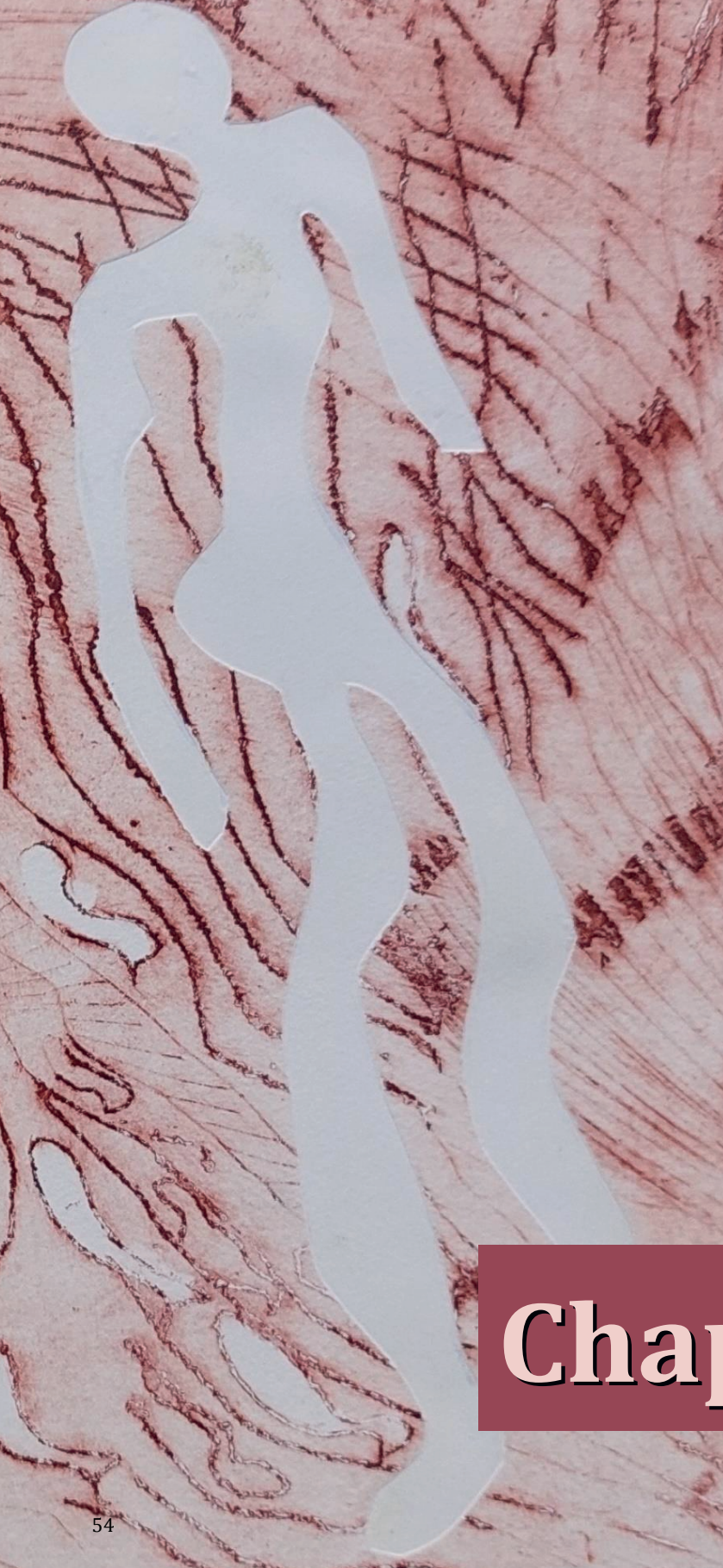
Polynomial Degree 4 (CV - normal)	0.05	0.04	0.11	<0.0001	231.52	No
Polynomial Degree 3 (CV - normal)	0.05	0.04	0.11	<0.0001	231.52	No
Polynomial Degree 2 (CV - normal)	0.05	0.04	0.11	<0.0001	231.52	No
Power (CV - normal)	0.05	0.04	0.11	<0.0001	231.52	No
Linear (CV - normal)	0.05	0.04	0.14	<0.0001	231.52	No

### Supplementary material S2.2. $EAR_{\text{comparator}}$ and $EAR_{\text{test}}$ values

**Supplementary Table S2.2.** The  $EAR$  values of the exposure scenarios to the comparator and test compounds as calculated in this work. Note that for some compounds no distribution of the data were available since no biomarker distribution and thus no distribution of the nominal internal concentration upon defined external dose level was reported (Dent et al., 2019).

Compound	$EAR$ (5 <sup>th</sup> or 25 <sup>th</sup> percentile)	$EAR$ (mean)	$EAR$ (95 <sup>th</sup> or 75 <sup>th</sup> percentile)
<b>DIM</b> (AR-CALUX based) (50 g Brussels sprouts; this work)	$8.43 \times 10^{-6}$	$4.04 \times 10^{-3}$ $2.55 \times 10^{-5}$	$5.39 \times 10^{-5}$
<b>BIC</b> (AR-CALUX based)		$1.51 \times 10^{-3}$	
<b>BAK</b> (shampoo) (body lotion)		$9.80 \times 10^{-5}$ $1.34 \times 10^{-2}$	
<b>RES</b> (25 mg single oral dose)		$3.06 \times 10^{-4}$	
<b>VIN</b> (oral RfD)	$2.32 \times 10^{-4}$	$5.12 \times 10^{-4}$	$1.06 \times 10^{-3}$

<b>BPA (TDI)</b>	2.12 x 10 <sup>-4</sup>	4.69 x 10 <sup>-4</sup>	9.44 x 10 <sup>-4</sup>
<b>MX (oral RfD MX)</b>	1.52 x 10 <sup>-4</sup>	2.79 x 10 <sup>-4</sup>	6.44 x 10 <sup>-4</sup>
<b>HPTE (oral RfD MX)</b>	1.24 x 10 <sup>-3</sup>	2.27 x 10 <sup>-3</sup>	5.32 x 10 <sup>-3</sup>
<b>3,3-DDE</b> (DDT exposure (Longnecker)) (DDT exposure (Bhatia)) (DDT exposure (Aneck-Hahn))	1.08 x 10 <sup>-2</sup> 1.44 x 10 <sup>-2</sup> 0.10	1.54 x 10 <sup>-2</sup> 1.93 x 10 <sup>-2</sup> 0.31	2.37 x 10 <sup>-2</sup> 2.55 x 10 <sup>-2</sup> 0.81
<b>FLU (therapeutic dose FLU)</b>		0.15	
<b>HF (therapeutic dose FLU)</b>		114.78	



# Chapter 3



## **Chapter 3. Next generation risk assessment of human exposure to estrogens using safe comparator compound values based on *in vitro* bioactivity assays**

Tessa C. A. van Tongeren, Si Wang, Paul L. Carmichael, Ivonne M. C. M. Rietjens, Hequn Li

Published in *Archives of Toxicology* (2023), 97(6):1547-75

## Abstract

In next generation risk assessment (NGRA), the Dietary Comparator Ratio (DCR) can be used to assess the safety of chemical exposures to humans in a 3R compliant approach. The DCR compares the Exposure Activity Ratio (EAR) for exposure to a compound of interest ( $EAR_{\text{test}}$ ) to the EAR for an established safe exposure level to a comparator compound ( $EAR_{\text{comparator}}$ ), acting by the same mode of action. It can be concluded that the exposure to a test compound is safe at a corresponding  $DCR \leq 1$ . In this study, genistein (GEN) was selected as a comparator compound by comparison of reported safe internal exposures to GEN to its  $BMCL_{05}$ , as no effect level, the latter determined in the *in vitro* estrogenic MCF7/Bos proliferation, T47D ER-CALUX, and U2OS ER $\alpha$ -CALUX assay. The  $EAR_{\text{comparator}}$  was defined using the  $BMCL_{05}$  and  $EC_{50}$  values from the 3 *in vitro* assays and subsequently used to calculate the DCRs for exposures to 14 test compounds, predicting the (absence of) estrogenicity. The predictions were evaluated by comparison to reported *in vivo* estrogenicity in humans for these exposures. The results obtained support in the DCR approach as an important animal-free new approach methodology (NAM) in NGRA and show how *in vitro* assays can be used to define DCR values.

**Key words:** Risk assessment · 3R compliant method · Estrogen receptor · Dietary comparator · *In vitro/in silico* approaches

### 3.1 Introduction

The use of animal testing for toxicological risk assessment is under debate because of ethical, economic, and legislative issues, and their adequacy to accurately represent the human situation. In contrast, in next generation risk assessment (NGRA), *in silico* and *in vitro* approaches are used to assure human safety (Becker et al., 2015; Dent et al., 2019). The Dietary Comparator Ratio (DCR) is an NGRA compliant tool (Becker et al., 2015) which compares the Exposure Activity Ratio (EAR) for exposure to a compound of interest ( $EAR_{\text{test}}$ ) to the EAR for an established safe level of human exposure to a comparator compound ( $EAR_{\text{comparator}}$ ), acting by the same mode of action. In the EAR, the unbound internal concentration of a compound at a defined exposure level is divided by its *in silico* or *in vitro* derived half maximum effective concentration ( $EC_{50}$ ) (Becker et al., 2015). A  $DCR \leq 1$  for the compound of interest, calculated as the ratio  $EAR_{\text{test}}/EAR_{\text{comparator}}$ , indicates that the respective exposure scenario will be safe.

Proof of principle for the DCR approach (evaluating the safety of exposure scenarios to estrogenic and anti-androgenic compounds) was originally reported by Becker et al. (2015) and Dent et al. (2019). Becker et al. (2015) defined the  $EAR_{\text{comparator}}$  based on reported human exposures to the phytoestrogen (isoflavone) genistein (GEN, **Figure 3.1**), mostly found in soybeans (Elsenbrand, 2007), from different diets. In this study it was indicated that these dietary exposure levels were considered conservative and health protective in humans. Results obtained indicated that 6 out of the 30 exposure scenarios to several test compounds had a  $DCR > 1$  and the authors concluded that these exposures should be prioritized for safety assessment (Becker et al., 2015). However, no evaluation against information on corresponding *in vivo* estrogenic activity at these exposure scenarios was made to further affirm this prioritization. Dent et al. (2019) defined the  $EAR_{\text{comparator}}$  for anti-androgenic effects based on diindolylmethane (DIM) from the intake of 50 g Brussels sprouts with a history of safe use. Whilst protective, this comparator exposure scenario appeared to be overly conservative since all exposure scenarios to the test compounds had a  $DCR > 1$ , including exposures with supportive data on the absence of corresponding *in vivo* anti-androgenic effects in humans. Previously, we reported a newly defined  $EAR_{\text{comparator}}$  based on safe levels of exposure to anti-androgens which was solely based on *in vitro* data. It was proven that this  $EAR_{\text{comparator}}$  was adequately protective for evaluating the safety of exposure scenarios to anti-androgenic compounds in the DCR approach (van Tongeren et al., 2021).

The aim of the current study was to define and use new  $EAR_{\text{comparator}}$  values based on safe levels of exposure to estrogens solely based on *in vitro* data to evaluate human

exposures to estrogens. These newly defined  $EAR_{\text{comparator}}$  values were based on the *in vitro* MCF-7/Bos proliferation assay, T47D estrogen receptor (ER)-CALUX assay, and U2OS ER $\alpha$ -CALUX assay using GEN as comparator compound. A series of biologically relevant exposure scenarios to 14 compounds constituting endogenous hormones, phthalates, ethyl paraben, pesticides, bisphenol A, phytoestrogens, the mycotoxin zearalenone, and drugs with information regarding accompanying *in vivo* estrogenic activity were included, generating  $EAR_{\text{test}}$  values for exposure scenarios that were known to be positive or negative for estrogenic effects, or in some cases still unknown. This enabled evaluation of the corresponding DCR values obtained when using the newly defined  $EAR_{\text{comparator}}$  values.

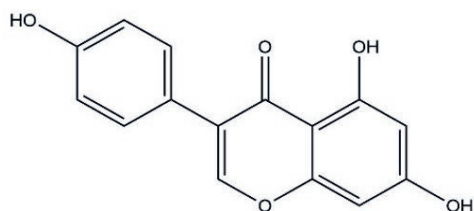


**Figure 3.1.** Structure formula of genistein (GEN).

## 3.2 Methods

### Workflow of the DCR approach

The DCR approach was executed following multiple steps which are depicted in the workflow (**Figure 3.2**).

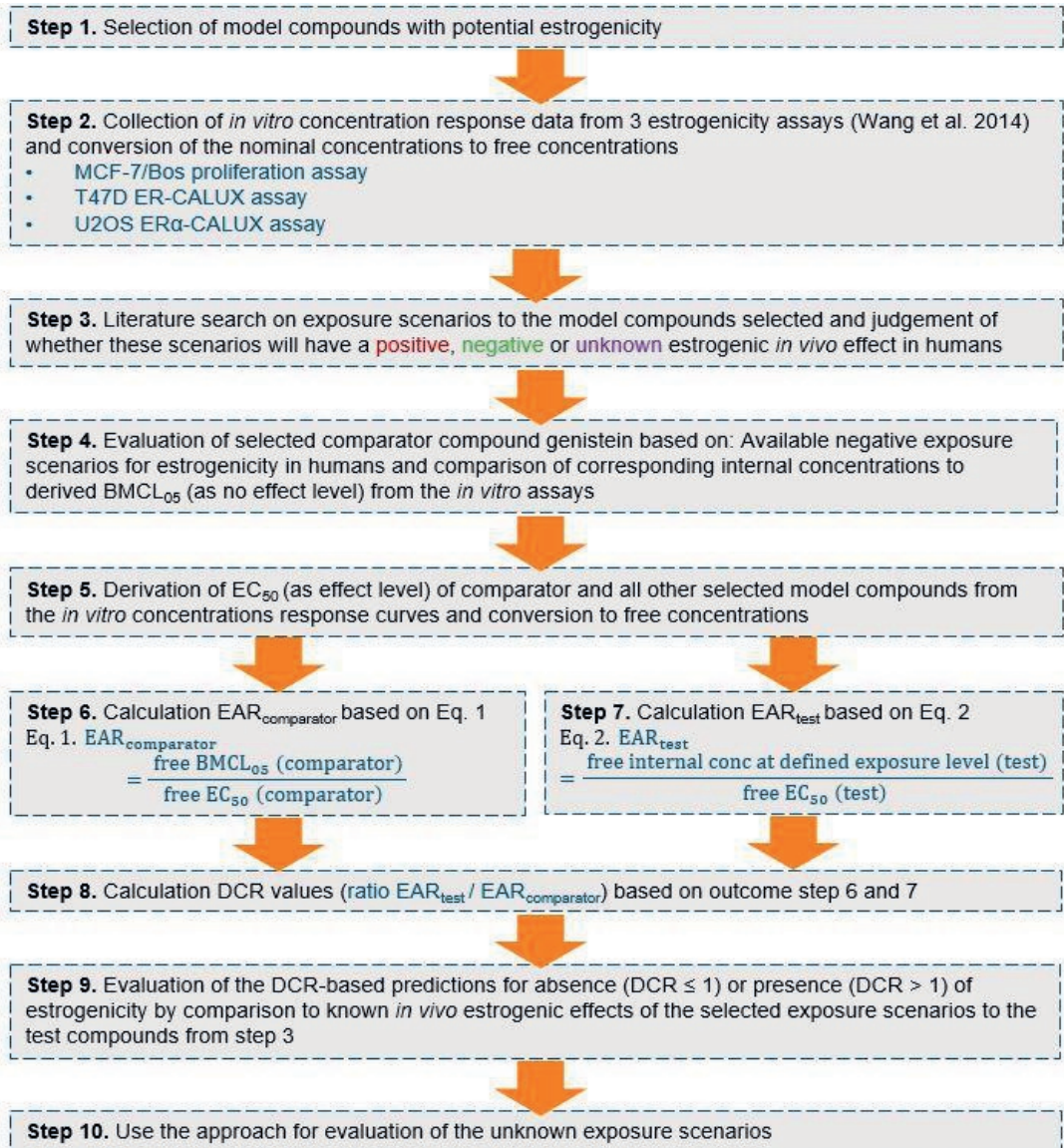


**Figure 3.2.** Schematic scheme of the workflow used in the present study executing the DCR approach to evaluate exposure scenarios to (putative) estrogenic compounds using data from *in vitro* bioassays.

### 3.2.1 Step 1: Selection of model compounds with potential estrogenicity.

Compounds that were active in the *in vitro* estrogenic MCF-7/Bos proliferation assay, T47D ER-CALUX assay, or U2OS ER $\alpha$ -CALUX assay were selected as model compounds. For these compounds *in vitro* concentration-response data and *in vivo* estrogenicity data for selected exposure regimens in humans were collected in Step 2 and 3, respectively. From these compounds a comparator compound was selected in Step 4.

### 3.2.2 Step 2: Collection of *in vitro* concentration-response data from 3 estrogenicity assays.

The concentration-response data of the selected model compounds in the *in vitro* estrogenic MCF-7/Bos proliferation assay, T47D ER-CALUX assay, or U2OS ER $\alpha$ -CALUX assay were derived from Wang et al. (2014). In short, the human breast cancer estrogenic-sensitive MCF-7 cells were exposed to concentration ranges of the compounds for 6 days in the MCF-7/Bos proliferation assay. The number of cells was measured with the Burton diphenylamine assay, quantifying the amount of DNA per well. In the CALUX assays, the human breast carcinoma T47D cells endogenously expressing the ER $\alpha$  and ER $\beta$  and the human osteosarcoma U2OS cells transfected with the ER $\alpha$  were exposed to increasing concentrations of the compounds for 24 h whereafter the luciferase reporter gene activity as the fold ER induction was measured. The concentrations were converted to the free concentrations using the fraction unbound *in vitro* ( $f_{ub \text{ in vitro}}$ ) since only the free unbound form is assumed to induce toxicity. This  $f_{ub \text{ in vitro}}$  and also the fraction unbound *in vivo* ( $f_{ub \text{ in vivo}}$ ) of the model compounds were determined as described by van Tongeren et al. (2021). In short, the  $f_{ub \text{ in vivo}}$  values were calculated using the ADMET predictor™ version 9.6 (Simulation Plus Inc.). The  $f_{ub \text{ in vitro}}$  at the 5% protein content present in the *in vitro* media (Wang et al., 2014) was linear extrapolated based on an  $f_{ub \text{ in vitro}} = 1.0$  at 0% protein and the  $f_{ub \text{ in vivo}}$  values at an 8% protein content in human plasma (Mescher 2009; Mathew et al. 2020). In line with literature data, it was assumed that the protein content and fraction unbound are linearly related (Gülden et al., 2002).

### 3.2.3 Step 3: Literature search on exposure scenarios to the model compounds selected and judgement of whether these scenarios will have a positive, negative or unknown estrogenic *in vivo* effect in humans.

Human exposure scenarios to the model compounds were gathered from literature to be evaluated in the DCR approach and provided information regarding the *in vivo* estrogenicity in humans to evaluate the DCR-based predictions. The compounds at the respective dose levels were reported to be positive or negative for *in vivo* estrogenicity in humans. When information on the *in vivo* estrogenicity was not reported, a comparison of the corresponding intake level of the test compound to safe reference dose values was made to judge whether the exposure would be positive or negative for *in vivo* estrogenicity. When no intake levels but only internal exposure levels were reported, it was assumed that at the corresponding external exposure levels the occurrence of *in vivo* estrogenic effects was unknown. The online database PubMed was used for the literature search. The key words included the compound name AND human AND internal/plasma/*in vivo* AND exposure/levels/concentrations, the compound name AND human dietary intake, the compound name AND human clinical trial/study, or the compound name AND human pharmacokinetic/biomonitoring blood concentrations upon exposure to the model compound in humans were included. Serum concentrations were assumed to be equal to plasma concentrations. Blood concentrations were transformed to corresponding plasma concentrations using the ADMET predictor™ predicted blood to plasma ratio ( $R_{b2p}$ ). Furthermore, the units of the reported internal concentrations were transformed to  $\mu\text{M}$  using the molecular weight of the respective compound and the concentrations were transformed to the corresponding free concentrations using the ADMET predictor™ predicted  $f_{ub}$  *in vivo*.

### 3.2.4 Step 4: Evaluation of the selected comparator compound genistein based on available negative exposure scenarios and comparison of corresponding internal concentrations to derived $\text{BMCL}_{05}$ (no effect level) values from the *in vitro* assays.

GEN was selected as the comparator compound based on available negative exposure scenarios for estrogenicity in humans (Becker et al., 2015) (Supplementary material S3.1) and comparison of the corresponding free internal levels to the derived free  $\text{BMCL}_{05}$  values as no effect levels from the *in vitro* assays. This comparison was to confirm that the free  $\text{BMCL}_{05}$  values are below the free plasma concentrations at the

selected safe exposure scenarios for the comparator compound genistein and thus will not induce an estrogenic effect.

*3.2.4.1 Step 4a: Derivation of free internal concentrations corresponding to negative exposure scenarios for the comparator compound.*

The reported human internal plasma or serum concentrations of GEN resulting from a Western diet, an Asian diet, or GEN supplements (Becker et al., 2015) (Supplementary material S3.1), were considered to be conservative and not associated with any adverse health effects in humans. A Western diet is an animal sourced diet with an overall high fat and sugar intake and a lower vegetable, fruit, legumes, whole cereals, raw foods, and fibers intake (Adlercreutz, 1998; Rizzello et al., 2019). Western dietary intake of GEN amounts to 0.003–0.01 mg/kg body weight (bw)/day (Aguilar et al. 2015; “Risk Assessment for Peri- and Post-Menopausal Women Taking Food Supplements Containing Isolated Isoflavones,” 2015). An Asian diet is a plant sourced diet with a high intake of soy and soy based products (Elsenbrand, 2007) leading to a GEN intake of 0.21–0.71 mg/kg bw/day (Rietjens et al., 2013). Supplementary intake of GEN amounts to 0.43–13 mg/kg bw/day (Aguilar et al. 2015 (“Risk Assessment for Peri- and Post-Menopausal Women Taking Food Supplements Containing Isolated Isoflavones,” 2015). Only plasma levels of unconjugated GEN were used for comparison since the unconjugated form of GEN is known to be active (Hosoda et al., 2011). When the internal concentrations of GEN were reported in the conjugated + unconjugated form, correction with a factor 0.003 was made to obtain the internal concentrations of unconjugated GEN since 0.3% of GEN is reported to exist in the unconjugated form in plasma (Becker et al., 2015).

*3.2.4.2 Step 4b: Derivation of the free BCML<sub>05</sub> for the comparator compound as no effect level from the 3 in vitro assays.*

To derive the no effect level of GEN, a benchmark dose analysis was performed of the *in vitro* concentration-response data of the 3 *in vitro* estrogenicity assays to obtain the BMC causing a 5% increase in response compared to the control (BMC<sub>05</sub>) and the upper (BMCU<sub>05</sub>) and lower (BMCL<sub>05</sub>) bound of its 95% confidence interval (Hardy et al., 2017). The derived BMCL<sub>05</sub> values reflect the concentrations where no biologically significant ER-mediated effects occur since the BMCL<sub>05</sub> resembles a no observed adverse effect level (Hardy et al., 2017) and thus are considered as the safe internal exposure levels, which can be used to set the EAR<sub>comparator</sub>. The BMC analysis was performed using the BMDS3.2.1 software (U.S. EPA). All models (Exponential, Hill, Power, Linear and



Polynomial) were fitted for continuous data for a BMR type Hybrid model-extra risk with normal distribution and constant variance. Acceptance criteria for a dose-response was indicated with a p value > 0.01, and a BMDU<sub>05</sub>: BMDL<sub>05</sub> ratio (precision factor) below 3 while the lowest AIC was used to select the preferred model (US Environmental Protection Agency 2012; Hardy et al., 2017).

#### 3.2.4.3 Step 4c. Comparison of the free internal concentrations of the non-estrogenic exposures to the comparator to its free BCML<sub>05</sub>.

The derived free *in vitro* BMCL<sub>05</sub> values of GEN were used as surrogate for the free internal concentrations and considered equal to the free *in vivo* BMCL<sub>05</sub>. This enables comparison to the free internal concentrations of the non-estrogenic exposure scenarios to GEN to evaluate whether the BMCL<sub>05</sub> can indeed be considered to reflect a safe exposure scenario so that it can be used to define the EAR<sub>comparator</sub>.

#### 3.2.5 Step 5: Derivation of EC<sub>50</sub> values (as effect levels) from the *in vitro* concentration-response curves and conversion to free concentrations.

The EC<sub>50</sub> values from the concentration-response data of the 3 *in vitro* estrogenicity assays (Wang et al., 2014), were converted to free EC<sub>50</sub> values to be used as the effect levels of the comparator and test compounds. The free EC<sub>50</sub> of GEN was used to calculate the EAR<sub>comparator</sub> in Step 6 whereas those of all other selected model compounds were used to calculate the EAR<sub>test</sub> in Step 7.

#### 3.2.6 Step 6: Calculation of the EAR<sub>comparator</sub> values.

With the free BMCL<sub>05</sub> and free EC<sub>50</sub> values of the comparator compound GEN derived from the *in vitro* estrogenic MCF-7/Bos proliferation assay, T47D ER-CALUX assay, and U2OS ER $\alpha$ -CALUX assay, the EAR<sub>comparator</sub> values were calculated following Eq. 1.

$$\text{Eq. 1} \quad \text{EAR}_{\text{comparator}} = \frac{\text{free BMCL}_{05} (\text{comparator})}{\text{free EC}_{50} (\text{comparator})}$$

The free BMCL<sub>05</sub> and free EC<sub>50</sub> values of GEN were derived from the *in vitro* MCF-7/Bos proliferation assay, T47D ER-CALUX assay, or U2OS ER $\alpha$ -CALUX assay (Wang et al., 2014), transforming the nominal concentrations to free concentration using the  $f_{\text{ub}}$  in

*vitro*. The free *in vitro* BMCL<sub>05</sub> was considered equal to the free *in vivo* BMCL<sub>05</sub> and represents an internal no effect level. It is also of interest to note that the EAR<sub>comparator</sub> remains unaffected by the correction for protein binding since the correction will affect the nominator and denominator of Eq. 1 in the same way.

### 3.2.7 Step 7: Calculation of EAR<sub>test</sub> values.

With the derived free internal concentrations at the respective exposure scenarios from literature of the 14 test compounds and their free EC<sub>50</sub> values derived from the 3 *in vitro* estrogenicity assays, the EAR<sub>test</sub> values were calculated using Eq. 2.

$$\text{Eq. 2} \quad \text{EAR}_{\text{test}} = \frac{\text{free internal concentration at defined exposure level (test)}}{\text{free EC}_{50} \text{ (test)}}$$

The free internal concentration at a defined exposure level of the test compounds was derived from literature reported human *in vivo* data, which often also included its variability presented as percentiles, range or standard deviation. The corresponding lowest, mean, and highest reported free internal concentrations of the exposure scenarios were selected for this evaluation and the corresponding EAR<sub>test</sub> values were calculated. This resulted in corresponding lowest, mean, and highest EAR<sub>test</sub> values. When no distribution was reported, no variability was included resulting in one corresponding EAR<sub>test</sub> value for the respective exposure scenario. Reported nominal concentrations were transformed to free concentrations using the  $f_{\text{ub } in \text{ vivo}}$ . The free EC<sub>50</sub> values were calculated based on the EC<sub>50</sub> values derived from the concentration-response curves in the MCF-7/Bos proliferation assay, T47D ER-CALUX assay, or U2OS ER $\alpha$ -CALUX assay (Wang et al., 2014), transforming the nominal concentrations to free concentration using the  $f_{\text{ub } in \text{ vitro}}$ .

### 3.2.8 Step 8: Calculation of DCR values.

With the obtained EAR<sub>comparator</sub> and EAR<sub>test</sub> values, the DCR values were calculated using Eq. 3, generating the DCR values of the test compounds based on each of the 3 *in vitro* estrogenicity assays using GEN as comparator compound.

$$\text{Eq. 3} \quad \text{DCR} = \frac{\text{EAR}_{\text{test}}}{\text{EAR}_{\text{comparator}}}$$

Lowest, mean, and highest DCR values were obtained whenever it was possible in Step 7 to derive from the exposure data of the test compounds lowest, mean, and highest  $EAR_{\text{test}}$  values. The highest, or when not available the mean, DCR value was used to make a conservative DCR-based safety decision of the respective exposure scenario to the test compound. A  $DCR \leq 1$  indicates that the corresponding exposure scenario to the test compound will unlikely induce estrogenicity whereas a  $DCR > 1$  indicates the opposite.

### Step 9: Evaluation of the DCR-based predictions of the selected exposure scenarios.

To evaluate the DCR outcomes, a comparison was made between the obtained DCR values and actual knowledge on the *in vivo* estrogenic effects at the corresponding exposure scenario for the test compounds in humans as taken from literature in Step 3. When the exposure scenario was reported to be negative or positive for estrogenicity, a  $DCR \leq 1$  or  $> 1$  is expected, respectively.

#### 3.2.9 Step 10: Use the approach for evaluation of the unknown exposure scenarios.

After evaluation of the DCR-based predictions of the exposures being negative or positive for estrogenicity, DCR-based predictions were made to evaluate the safety of the exposure scenarios to the test compounds for which it was unknown whether or not they would result in *in vivo* estrogenicity in humans.

## 3.3 Results

### 3.3.1 Step 1: Selection of model compounds with potential estrogenicity.

15 compounds including endogenous hormones, phthalates, ethyl paraben, pesticides, bisphenol A, phytoestrogens, the mycotoxin zearalenone, and drugs were active in the *in vitro* estrogenic MCF-7/Bos proliferation assay, T47D ER-CALUX assay, or U2OS ER $\alpha$ -CALUX assay and were included as model compounds (**Table 3.1**).

**Table 3.1.** The 15 model compounds selected in this study that were observed to have estrogenic activity in the MCF-7/Bos proliferation assay, T47D ER-CALUX assay, or U2OS ER $\alpha$ -CALUX assay (Wang et al., 2014).

Compound group	Test compounds
Endogenous hormones	17 $\beta$ -Estradiol (E2) Testosterone (T)
Phthalates	Butylbenzyl phthalate (BBzP) Di-n-butyl phthalate (DBP)
Paraben	Ethyl paraben (EP)
Pesticides	Kepone (KEP) o,p'-Dichlorodiphenyltrichloroethane (DDT)
Bisphenol	Bisphenol A (BPA)
Phytoestrogens	Genistein (GEN) Coumestrol (COU) Apigenin (API)
Mycotoxin	Zearalenone (ZEA)
Drugs	17 $\alpha$ -Ethinyl estradiol (EE) Diethylstilbesterol (DES) Tamoxifen (TAM)

### 3.3.2 Step 2: Collection of *in vitro* concentration-response data from 3 estrogenicity assays.

The *in vitro* concentration-response data of the selected model compounds from the MCF-7/Bos proliferation assay, T47D ER-CALUX assay, and U2OS ER $\alpha$ -CALUX assay were taken as reported by Wang et al. (2014). The concentrations were converted to free concentrations using the  $f_{ub}$  *in vitro*. The  $f_{ub}$  *in vitro* and  $f_{ub}$  *in vivo* values of the model compounds are listed in **Table 3.2**. The  $f_{ub}$  *in vivo* values were predicted with the ADMET predictor™. The  $f_{ub}$  *in vitro* values at a 5% protein content in the *in vitro* media were linear extrapolated based on the  $f_{ub}$  *in vivo* at an 8% human plasma protein content, setting the  $f_{ub}$  at 1.0 in the absence of protein (van Tongeren et al., 2021).

**Table 3.2.** The ADMET predictor™ predicted  $f_{ub}$  *in vivo* values and the linear extrapolated  $f_{ub}$  *in vitro* values of the model compounds.

Compound	$f_{ub}$ <i>in vivo</i>	$f_{ub}$ <i>in vitro</i>
GEN	0.07	0.42
E2	0.08	0.42
T	0.16	0.48
BBzP	0.04	0.40
DBP	0.06	0.41
EP	0.20	0.50
O,p'-DDT	0.03	0.39
KEP	0.08	0.43
BPA	0.09	0.43
API	0.06	0.41
COU	0.08	0.43
ZEA	0.07	0.42
EE	0.05	0.41
TAM	0.04	0.40
DES	0.04	0.40

### 3.3.3 Step 3: Literature search on exposure scenarios to the model compounds selected and judgement of whether these scenarios will have a positive, negative or unknown estrogenic *in vivo* effect in humans.

Literature reported exposure scenarios for the 15 model compounds with information regarding accompanying *in vivo* estrogenic effects in humans were collected. 21 Reports on exposures to GEN were available which were indicated to be conservative and health protective in humans (Becker et al., 2015) (Supplementary material S3.1) and thus considered negative for *in vivo* estrogenicity. For the remaining compounds, the reported internal concentrations and corresponding free internal concentrations of the corresponding exposure scenarios are compiled in **Table 3.3**. In **Table 3.4**, the evaluation of the likely occurrence of *in vivo* estrogenic effects at the exposure scenarios for these model compounds is summarized. This evaluation was based on reports of *in vivo* estrogenic effects at the dose levels applied or comparison of the reported intake

levels to safe reference values like acceptable daily intakes (ADIs). The outcomes were used as the basis to label the exposure as positive or negative for *in vivo* estrogenicity. Based on the information on the exposure scenarios and the (clinical) data on accompanying *in vivo* estrogenic effects, 7 of the 41 evaluated exposure scenarios were labelled to be negative and 8 to be positive for *in vivo* estrogenicity (**Table 3.4**). From comparison of reported exposure levels to safe reference values for the model compounds, 8 of the 41 evaluated exposure scenarios were indicated to be negative and 7 to be positive for *in vivo* estrogenicity. For 11 exposure scenarios the corresponding *in vivo* estrogenicity was not reported, no dose levels were provided or no safe reference levels were available and therefore the *in vivo* estrogenic effects induced by the corresponding exposures was listed as unknown (**Table 3.4**).

**Table 3.3.** Literature reported exposure scenarios to the model compounds with the corresponding nominal internal concentrations and the transformed free plasma concentrations, using the  $R_{b2p}$  and  $f_{ub \text{ in vivo}}$ .

Compound	Exposure scenario(s)	Reference	Plasma serum, or blood concentrations reported	Nominal internal concentrations ( $\mu\text{M}$ ) <sup>1,2,3</sup>			$R_{b2p}$	$f_{ub \text{ in vivo}}$	Free internal plasma concentrations ( $\mu\text{M}$ )		
				Lowest	Mean	Highest			Lowest	Mean	Highest
E2	Female levels	Mayo Clinic Staff (2022a)	Plasma	5.51E-05	1.28E-03	0.08	0.08	4.18E-06	9.76E-05		
E2	Male levels	Mayo Clinic Staff (2022a)	Plasma	3.67E-05	1.47E-04			2.79E-06	1.12E-05		
T	Female levels	Mayo Clinic Staff (2022b)	Plasma	2.77E-06	2.08E-05	0.16	0.16	4.44E-07	3.33E-06		
T	Male levels	Mayo Clinic Staff (2022b)	Plasma	8.32E-05	3.29E-04			1.33E-05	5.27E-05		
BBzP	BBzP exposure biomonitoring 2-3 weeks after delivery in 36 Swedish women	(Högberg et al., 2008)	Blood	1.99E-04	1.16E-03	0.80	0.04	8.05E-06	4.67E-05	2.26E-04	
DBP	DBP exposure biomonitoring 2-3 weeks after delivery in 36 Swedish women	(Högberg et al., 2008)	Blood	9.34E-05	5.34E-03	0.81	0.06	5.49E-06	3.13E-04	2.38E-03	
EP	EP exposure biomonitoring in 60 healthy Danish young men	(Frederiksen et al., 2011)	Serum	2.65E-03	1.25E-01		0.20	5.19E-04	2.45E-02		

EP	EP exposure biomonitoring in 58 fertile male patients of the Centre of Assisted Reproduction Pronatal, Prague	(Kolarova Sosvorova et al., 2017)	Plasma		2.17E-03					4.24E-04	
EP	EP exposure biomonitoring in 150 healthy Malaysians	(Wiraagni et al., 2020)	Plasma		2.41E-03	5.72E-03				4.71E-04	1.12E-03
KEP	Affected workers Life Science Product Company, KEP production plant, Hopewell, USA (a)	(Cannon et al., 1978)	Blood	1.25E-02	3.50	1.63E+01	1.47	0.08	1.03E-03	2.89E-01	1.35
KEP	Unaffected workers Life Science Product Company, KEP production plant, Hopewell, USA (b)	(Cannon et al., 1978)	Blood	4.15E-03	8.31E-01	5.68			3.43E-04	6.85E-02	4.68E-01
KEP	Family members workers Life Science Product Company (c)	(Cannon et al., 1978)	Blood	4.15E-03	1.38E-01	5.40E-01			3.43E-04	1.14E-02	4.45E-02
KEP	Workers from another KEP production plant (Allied Chemical Corporation) (d)	(Cannon et al., 1978)	Blood	3.18E-03	8.31E-02	6.23E-01			2.63E-04	6.85E-03	5.14E-02
KEP			Blood			4.29E-02					





KEP	Occupational exposure nonagricultural sectors, Guadeloupe	(Multigner et al., 2006, 2008, 2016)	Blood	4.29E-03	1.16E-02	6.45E-02			3.54E-04	9.59E-04	5.32E-03
KEP	Estimated intake unpolluted area 1.9 (0.1 - 20.6) µg/day	(Guldner et al., 2010)	Blood		1.14E-03					9.37E-05	
KEP	Estimated intake polluted area 6.6 (1.0 -22.2) µg/day	(Guldner et al., 2010)	Blood		1.41E-03					1.16E-04	
KEP	Consumption contaminated foodstuffs	(Kadhel et al., 2014)	Plasma	3.67E-04	7.95E-04	4.02E-02			3.03E-05	6.56E-05	3.31E-03
KEP	Consumption contaminated foodstuffs	(Emeville et al., 2015)	Plasma	3.47E-04	8.56E-04	9.42E-02			2.86E-05	7.06E-05	7.77E-03
o,p'-DDT	Occupational exposure to 26 workers spraying DDT Brazil	(Minelli & Ribeiro, 1996)	Serum	1.43E-03		9.58E-03		0.03	3.63E-05		2.44E-04
o,p'-DDT	Environmental exposure to 193 children from polluted area Brazil	(Freire et al., 2013)	Serum	7.54E-04	2.38E-03	4.48E-03			1.92E-05	6.06E-05	1.14E-04
o,p'-DDT	Environmental exposure to 575 mothers from prospective birth cohort in the US	(Kezios et al., 2013)	Serum	2.04E-05	8.76E-04	9.09E-03			5.18E-07	2.23E-05	2.31E-04
BPA	TDI	(Dent et al., 2019; Wetmore et al., 2015)	Plasma	1.55E-03	3.43E-03	6.91E-03			1.37E-04	3.02E-04	6.09E-04

COU	Biomonitoring of 246 healthy Chinese originating from two rural villages and two urban neighbourhoods	(Liu et al., 2018)	Plasma	8.58E-03	1.01E-02	1.12E-02	0.08	6.87E-04	8.06E-04	8.96E-04
API	Single oral dose 17.77 ± 4.19 mg in 11 Healthy subjects	(Meyer et al., 2006)	Plasma	4.61E-02	1.27E-01	1.92E01	0.06	2.80E-03	7.69E-03	1.17E-02
API	Regular diet of 41 men from a cross-sectional study	(Bolarinwa & Linseisen, 2005)	Plasma	7.40E-03	9.30E-03	5.25E-02		4.49E-04	5.65E-04	3.19E-03
ZEA	Calculated dietary intake 0.039 and 0.076 µg/kg/day in 260 healthy rural residents in China	(Fan et al., 2019)	Plasma	1.98E-04	4.93E-04	1.31E-03	0.07	1.39E-05	3.34E-05	8.90E-05
EE	Single oral dose 0.03 mg EE + 0.15 mg desogestrel to 24 healthy Indian females	(Nair et al., 2018)	Plasma	3.07E-04	3.12E-04	3.38E-04	0.05	1.66E-05	1.69E-05	1.82E-05
EE	Single oral dose 0.06 mg EE + 4 mg chlormadinone acetate to 20 healthy Caucasian females	(Bonn et al., 2009)	Plasma	2.80E-04	4.22E-04	5.63E-04		1.51E-05	2.28E-05	3.04E-05
DES	Single oral dose 2 mg to 12 healthy Chinese males	(H. Zhang et al., 2014)	Plasma	7.08E-03	1.12E-02	1.53E-02	0.04	6.54E-04	8.12E-04	9.71E-04

TAM	Single oral dose of 20 mg TAM to female early-stage breast cancer patients, in poor metabolizers	(Madlensky et al., 2011)	Serum	2.13E-01	3.83E-01	5.53E-01	0.04	8.97E-03	1.61E-02	2.33E-02
TAM	Single oral dose of 20 mg TAM female early-stage breast cancer patients, in intermediate metabolizers	(Madlensky et al., 2011)	Serum	1.94E-01	3.85E-01	5.75E-01		8.16E-03	1.62E-02	2.42E-02
TAM	Single oral dose of 20 mg TAM female early-stage breast cancer patients, in ultrarapid metabolizers	(Madlensky et al., 2011)	Serum	2.29E-01	3.86E-01	5.43E-01		9.62E-03	1.62E-02	2.28E-02

<sup>1</sup> Serum concentration were assumed to be equal to plasma concentrations.

<sup>2</sup> Nominal internal blood concentrations were transformed to plasma concentration using the ADMET predicted blood to plasma ratio ( $R_{b2p}$ ) of the respective compound.

<sup>3</sup> The units of the reported concentrations were transformed to the concentrations in  $\mu\text{M}$  using the molecular weight of the respective compound.

**Table 3.4.** Evaluation of the exposure scenarios to the model compounds to be positive, negative or unknown for *in vivo* estrogenicity.

Compound	Exposure scenario(s)	Reference	Corresponding <i>in vivo</i> estrogenic effects at exposure scenario reported	Safe reference level compound	<i>In vivo</i> estrogenicity at exposure scenario expected	Reasoning
E2	Female levels	Mayo Clinic Staff (2022a)	Endogenous levels estradiol		Yes	Endogenous estrogen
E2	Male levels	Mayo Clinic Staff (2022a)	Endogenous levels estradiol		Yes	Endogenous estrogen
T	Female levels	Mayo Clinic Staff (2022b)	Endogenous levels testosterone		No	Endogenous androgen
T	Male levels	Mayo Clinic Staff (2022b)	Endogenous levels testosterone		No	Endogenous androgen
BBzP	BBzP exposure biomonitoring 2-3 weeks after delivery in 36 Swedish women	(Högberg et al., 2008)	No information reported	TDI = 0.5 mg/kg <sup>1</sup>	Unknown	No intake levels of the exposure scenario were quantified, disabling comparison to the safe reference dose
DBP	DBP exposure biomonitoring 2-3 weeks after delivery in 36 Swedish women	(Högberg et al., 2008)	No information reported	TDI = 0.01 mg/kg <sup>1</sup>	Unknown	No intake levels of the exposure scenario were quantified, disabling comparison to the safe reference dose

EP	EP exposure biomonitoring in 60 healthy Danish young men	(Frederiksen et al., 2011)	No information reported	Group ADI with methyl paraben and their sodium salts = 0 - 10 mg/kg bw <sup>2</sup>	Unknown	No intake levels of the exposure scenario were quantified, disabling comparison to the safe reference dose
EP	EP exposure biomonitoring in 58 fertile male patients of the Centre of Assisted Reproduction Pronatal, Prague	(Kolatorova Sosvorova et al., 2017)	No information reported		Unknown	No intake levels of the exposure scenario were quantified, disabling comparison to the safe reference dose
EP	EP exposure biomonitoring in 150 healthy Malaysians	(Wirraagni et al., 2020)	No information reported		Unknown	No intake levels of the exposure scenario were quantified, disabling comparison to the safe reference dose
KEP	Affected workers Life Science Product Company, KEP production plant, Hopewell, USA (a)	(Cannon et al., 1978)	Aside from some reports on toxic effects in the testis, no conclusion on onset of estrogenic effects in the subjects was given	ADI = 0.5 µg/kg bw <sup>3</sup>	Yes	No intake levels of the exposure scenario were quantified, disabling comparison to the ADI or ARfD. Assuming a male population of the subjects, comparison to the NOEL in blood indicates that <i>in vivo</i> estrogenic effects may be expected

KEP	Unaffected workers Life Science Product Company, KEP production plant, Hopewell, USA (b)	(Cannon et al., 1978)	No information reported	ARfD = 10 µg/kg bw <sup>3</sup>	Yes	No intake levels of the exposure scenario were quantified, disabling comparison to the ADI or ARfD. Assuming a male population of the subjects, comparison to the NOEL in blood indicates that <i>in vivo</i> estrogenic effects may be expected
KEP	Family members workers Life Science Product Company (c)	(Cannon et al., 1978)	No information reported	NOEL in men based on a clinically relevant decrease in sperm count = 0.1-0.5 mg/L = 0.2-1.0 µM in blood <sup>4</sup>	Yes	No intake levels of the exposure scenario were quantified, disabling comparison to the ADI or ARfD. Assuming a male population of the subjects, comparison to the NOEL in blood indicates that <i>in vivo</i> estrogenic effects may be expected
KEP	Workers from another KEP production plant (Allied Chemical Corporation) (d)	(Cannon et al., 1978)	No information reported	Using the R <sub>b2p</sub> of 1.47 the NOEL in plasma (assumed to be equal as in serum) = 0.14 - 0.68 µM	Yes	No intake levels of the exposure scenario were quantified, disabling comparison to the ADI or ARfD. Assuming a male population of the subjects, comparison to the NOEL in blood indicates that <i>in vivo</i> estrogenic effects may be expected

KEP	Neighbourhood workers (e)	(Cannon et al., 1978)	No information reported		No	No intake levels of the exposure scenario were quantified, disabling comparison to the ADI or ARfD. Assuming a male population of the subjects, comparison to the NOEL in blood indicates that no <i>in vivo</i> estrogenic effects are expected
KEP	Workers of a sewage treatment plant receiving effluents from the plant (f)	(Cannon et al., 1978)	No information reported		No	No intake levels of the exposure scenario were quantified, disabling comparison to the ADI or ARfD. Assuming a male population of the subjects, comparison to the NOEL in blood indicates that no <i>in vivo</i> estrogenic effects are expected
KEP	Cab driver (g)	(Cannon et al., 1978)	No information reported		No	No intake levels of the exposure scenario were quantified, disabling comparison to the ADI or ARfD. Assuming a male population of the subjects, comparison to the NOEL in blood indicates that no <i>in vivo</i> estrogenic effects are expected



KEP	Truck driver (h)	(Cannon et al., 1978)	No information reported		No	No intake levels of the exposure scenario were quantified, disabling comparison to the ADI or ARfD. Assuming a male population of the subjects, comparison to the NOEL in blood indicates that no <i>in vivo</i> estrogenic effects are expected
KEP	Hopewell residents (i)	(Cannon et al., 1978)	No information reported		No	No intake levels of the exposure scenario were quantified, disabling comparison to the ADI or ARfD. Assuming a male population of the subjects, comparison to the NOEL in blood indicates that no <i>in vivo</i> estrogenic effects are expected

KEP	Occupational exposure, chemical plant workers, last day exposure	(Adir et al., 1978)	No information reported		Yes	No intake levels of the exposure scenario were quantified, disabling comparison to the ADI or ARfD. Assuming a male population of the subjects, comparison to the transformed NOEL in serum indicates that <i>in vivo</i> estrogenic effects may be expected
KEP	Occupational exposure, chemical plant workers, after 6-7 m	(Adir et al., 1978)	No information reported		Yes	No intake levels of the exposure scenario were quantified, disabling comparison to the ADI or ARfD. Assuming a male population of the subjects, comparison to the transformed NOEL in serum indicates that <i>in vivo</i> estrogenic effects may be expected

KEP	General population within one mile radius chemical plant	(Adir et al., 1978)	No information reported	No	No intake levels of the exposure scenario were quantified, disabling comparison to the ADI or ARfD. Assuming a male population of the subjects, comparison to the transformed NOEL in serum indicates that no <i>in vivo</i> estrogenic effects are expected
KEP	Occupational exposure banana agriculture, Guadeloupe	(Multigner et al., 2006, 2008, 2016)	No significant difference in sperm and hormone characteristics were found	No	It was reported that no corresponding <i>in vivo</i> estrogenic effects at exposure scenario occurred
KEP	Occupational exposure nonagricultural sectors, Guadeloupe	Multigner et al. 2006, 2008, 2016	No significant difference in sperm and hormone characteristics were found	No	It was reported that no corresponding <i>in vivo</i> estrogenic effects at exposure scenario occurred
KEP	Estimated intake unpolluted area 1.9 (0.1 - 20.6) µg/day	(Guldner et al., 2010)	No information reported	No	Estimated intake levels were below the ADI and ARfD
KEP	Estimated intake polluted area 6.6 (1.0 - 22.2) µg/day	(Guldner et al., 2010)	No information reported	No	Estimated intake levels were below the ADI and ARfD

KEP	Consumption contaminated foodstuffs	(Kadhel et al., 2014)	Maternal plasma levels of > 0.52 ng/mL KEP were related to changes in the length of gestation and risk of preterm birth		Yes	At the highest reported maternal plasma concentrations it was reported that corresponding <i>in vivo</i> estrogenic effects occurred
KEP	Consumption contaminated foodstuffs	(Eneville et al., 2015)	No information reported		No	Exposure in the control subjects in a case-control study on the relationship of prostate cancer
<i>o,p'</i> -DDT	Occupational exposure to 26 workers spraying DDT Brazil	(Minelli & Ribeiro, 1996)	No information reported	ADI = 0.01 mg/kg <sup>5</sup>	Unknown	No intake levels of the exposure scenario were quantified, disabling comparison to the safe reference dose
<i>o,p'</i> -DDT	Environmental exposure to 193 children from polluted area Brazil	(Freire et al., 2013)	No information reported		Unknown	No intake levels of the exposure scenario were quantified, disabling comparison to the safe reference dose
<i>o,p'</i> -DDT	Environmental exposure to 575 mothers from prospective birth cohort in the US	(Kezios et al., 2013)	No information reported		Unknown	No intake levels of the exposure scenario were quantified, disabling comparison to the safe reference dose

BPA	TDI	(Dent et al., 2019; Wetmore et al., 2015)	No information reported	TDI = 4 µg/kg bw/d <sup>6</sup>	No	Exposure scenario at the TDI so no <i>in vivo</i> estrogenic effects expected
COU	Biomonitoring of 246 healthy Chinese originating from two rural villages and two urban neighbourhoods	(Liu et al., 2018)	No information reported		Unknown	No safe reference dose is available and no intake levels of the exposure scenario were quantified
API	Single oral dose 17.77 ± 4.19 mg in 11 Healthy subjects	(Meyer et al., 2006)	No information reported		Unknown	No safe reference dose is available to compare reported intake levels
API	Regular diet of 41 men from a cross-sectional study	(Bolarinwa & Linseisen, 2005)	No information reported		Unknown	No safe reference dose is available and no intake levels reported
ZEA	Calculated dietary intake 0.039 and 0.076 µg/kg/day in 260 healthy rural residents in China	(Fan et al., 2019)	No information reported	TDI = 0.25 µg/kg bw/d <sup>7</sup>	No	Calculated dietary intake was below the TDI
EE	Single oral dose 0.03 mg EE + 0.15 mg desogestrel to 24 healthy Indian females	(Nair et al., 2018)	Therapeutic dose		Yes	Exposure scenarios embody the therapeutic use of EE
EE	Single oral dose 0.06 mg EE + 4 mg chlormadinone acetate to 20 healthy Caucasian females	(Bonn et al., 2009)	Therapeutic dose		Yes	Exposure scenarios embody the therapeutic use of EE
DES	Single oral dose 2 mg to 12 healthy Chinese males	(H. Zhang et al., 2014)	Therapeutic dose		Yes	Exposure scenarios embody the therapeutic use of DES

TAM	Single oral dose of 20 mg TAM to female early-stage breast cancer patients, in poor metabolizers	(Madlensky et al., 2011)	Therapeutic dose	Yes	Exposure scenarios embody the therapeutic use of TAM
TAM	Single oral dose of 20 mg TAM female early-stage breast cancer patients, in intermediate metabolizers	(Madlensky et al., 2011)	Therapeutic dose	Yes	Exposure scenarios embody the therapeutic use of TAM
TAM	Single oral dose of 20 mg TAM female early-stage breast cancer patients, in ultrarapid metabolizers	(Madlensky et al., 2011)	Therapeutic dose	Yes	Exposure scenarios embody the therapeutic use of TAM

<sup>1</sup> Silano et al. (2019)

<sup>2</sup> Anton et al. (2004)

<sup>3</sup> French Agency for Food, Environmental and Occupational Health and Safety (ANSES) (2018a, 2018b, 2019)

<sup>4</sup> Guzelian (1992)

<sup>5</sup> Joint Food Agricultural Organization/World Health Organization Meeting on Pesticide Residues (JMPR) (2000)

<sup>6</sup> Bolognesi et al. (2015)

<sup>7</sup> Alexander et al. (2011)

TDI = Tolerable daily intake. ADI = Acceptable daily intake. ARfD = Acute reference dose. NOEL = No observed effect level

### 3.3.4 Step 4: Evaluation of the selected comparator compound genistein based on available negative exposure scenarios and comparison of corresponding internal concentrations to derived BMCL<sub>05</sub> (no effect level) values from the *in vitro* assays.

GEN was selected as comparator compound based on the large amount of available data on exposures that result in negative outcomes for *in vivo* estrogenicity in humans, such as the exposures resulting from dietary intake levels which are indicated to be conservative and health protective in humans, and correspond to a Western diet, an Asian diet, or GEN supplements (Becker et al., 2015) (Supplementary material S3.1). The results of the benchmark dose modelling to derive the BMCL<sub>05</sub> values are presented in Supplementary material S3.2 and the derived nominal and transformed free *in vitro* BMCL<sub>05</sub> values of GEN (considered equal to safe free *in vivo* BMCL<sub>05</sub> values) are compiled in **Table 3.5**. The free *in vivo* BMCL<sub>05</sub> values were compared to the free human internal concentrations of GEN transformed from the literature reported nominal concentrations at the reported exposures using the  $f_{ub\ in\ vivo}$  (**Figure 3.3**). The free internal concentrations resulting from a western diet ranged from  $3.36 \times 10^{-6} \pm 2.00 \times 10^{-6}$   $\mu\text{M}$  (Grace et al., 2004) to  $2.76 \times 10^{-3} \pm 1.60 \times 10^{-3}$   $\mu\text{M}$  (Busby et al., 2002), indicating orders of magnitude variation, although all concentrations were substantially lower than the free BMCL<sub>05</sub> values derived from the *in vitro* assays. GEN intake reported from an Asian diet resulted in free internal concentrations ranging from  $2.76 \times 10^{-5} \pm 0.30 \times 10^{-5}$   $\mu\text{M}$  (Ritchie et al., 2004) to  $1.26 \times 10^{-4} \pm 0.99 \times 10^{-4}$   $\mu\text{M}$  (Yuan et al., 2012), showing less variance, with still all values being below the free BMCL<sub>05</sub> values derived from the *in vitro* assays (**Figure 3.3**). Supplement intake resulted in reported free internal GEN concentrations ranging from  $2.68 \times 10^{-5} \pm 0.39 \times 10^{-5}$   $\mu\text{M}$  (Setchell et al., 2003) to  $1.89 \times 10^{-2} \pm 1.16 \times 10^{-2}$   $\mu\text{M}$  (Busby et al., 2002), showing variance due to the different intake levels of GEN when using different supplements at different dosing regimens. The highest internal concentration was reported from supplement intake of GEN by Busby et al. (2002) and was 13- to 34-fold higher than the free *in vivo* BMCL<sub>05</sub> values of GEN. However, because the study also reported that there were no estrogenic effects observed in the 30 male volunteers studied it can be concluded that these results further support that also the exposure to the comparator GEN that results in an internal free concentration equal to the *in vitro* free BMCL<sub>05</sub> can be considered safe and is adequate to calculate the EAR<sub>comparator</sub> in the DCR approach.

**Table 3.5.** Nominal and transformed free EC<sub>50</sub> and BMCL<sub>05</sub> values, using the  $f_{ub}$  *in vitro*, of comparator compound GEN based on the *in vitro* MCF-7/Bos proliferation assay, T47D ER-CALUX assay, or U2OS ER $\alpha$ -CALUX assay and the corresponding EAR<sub>comparator</sub> values calculated using Eq. 1.

Assay	Nominal EC <sub>50</sub> ( $\mu$ M)	Nominal <i>in vitro</i> BMCL <sub>05</sub> ( $\mu$ M)	$f_{ub}$ <i>in vitro</i> (comparator)	Free EC <sub>50</sub> ( $\mu$ M)	Free <i>in vitro</i> BMCL <sub>05</sub> ( $\mu$ M) = Free <i>in vivo</i> BMCL <sub>05</sub> ( $\mu$ M)	EAR <sub>comparator</sub>
MCF-7/BOS proliferation	4.60E-02	3.48E-03	0.42	0.02	1.46E-03	7.59E-02
T47D ER-CALUX	0.13	3.29E-03		0.05	1.38E-03	2.53E-02
U2OS ER $\alpha$ -CALUX	6.80E-02	1.34E-03		0.03	5.60E-04	1.97E-02

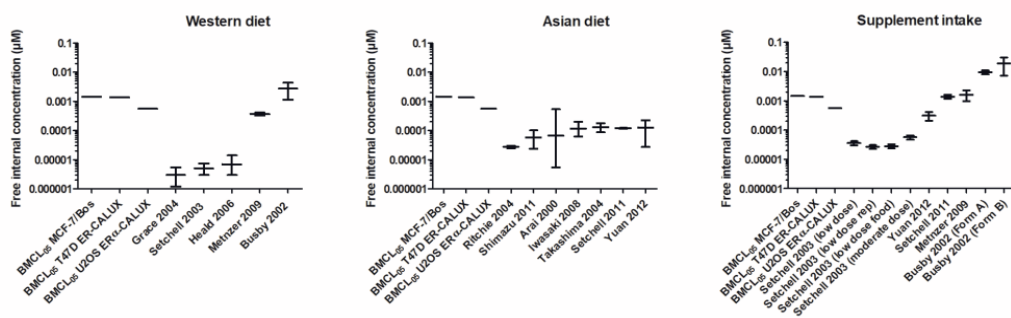


**Figure 3.3.** Comparison of the free *in vivo* BMCL<sub>05</sub> values based on the MCF-7/Bos proliferation assay, T47D ER-CALUX assay, or U2OS ER $\alpha$ -CALUX assay (first 3 bars in each graph) and literature reported free *in vivo* internal concentrations of GEN, including the variability, following a Western diet, an Asian diet, or supplement intake in humans as derived from the respective references.



### 3.3.5 Step 5: Derivation of EC<sub>50</sub> values (as effect levels) from the *in vitro* concentration-response curves and conversion to free concentrations.

The free EC<sub>50</sub> values as effect level of the compounds were derived from the concentration-response curves obtained in the MCF-7/Bos proliferation assay, T47D ER-CALUX assay, and U2OS ER $\alpha$ -CALUX assay (Wang et al., 2014), transforming the nominal concentrations to the free concentrations using the  $f_{ub \text{ in vitro}}$  (**Table 3.6**). Note that testosterone had no response in the T47D ER-CALUX assay.

### 3.3.6 Step 6: Calculation of the EAR<sub>comparator</sub> values.

With free BMCL<sub>05</sub> and free EC<sub>50</sub> values of GEN derived from data from the MCF-7/Bos proliferation assay, T47D ER-CALUX assay, and U2OS ER $\alpha$ -CALUX assay (Step 5), the EAR<sub>comparator</sub> values were calculated using Eq. 1 and are listed in **Table 3.5**. The EAR<sub>comparator</sub> values derived from the 3 assays increased in the order U2OS ER $\alpha$ -CALUX assay < T47D ER-CALUX assay < MCF-7/Bos proliferation assay.

### 3.3.7 Step 7: Calculation of EAR<sub>test</sub> values.

Using the free internal concentrations at the respective exposure scenario of the model compounds and their free EC<sub>50</sub> values (**Table 3.6**) derived from the data from the 3 *in vitro* estrogenicity assays, the EAR<sub>test</sub> values were calculated following Eq. 2 and are compiled in **Table 3.7**. When information on the variability of the exposure was available, the corresponding lowest, mean, and highest EAR<sub>test</sub> value was calculated.

**Table 3.6.** EC<sub>50</sub> values of the test compounds derived from the MCF-7/Bos proliferation assay, T47D ER-CALUX assay, and U2OS ER $\alpha$ -CALUX assay. The nominal EC<sub>50</sub> values as taken from Wang et al. (2014) were transformed to the free EC<sub>50</sub> values using the  $f_{ub}$  *in vitro*.

Compound	Nominal EC <sub>50</sub> ( $\mu$ M)			$f_{ub}$ <i>in vitro</i> (test)	Free EC <sub>50</sub> ( $\mu$ M)		
	MCF-7/BOS proliferation	T47D ER-CALUX	U2OS ER $\alpha$ -CALUX		MCF-7/BOS proliferation	T47D ER-CALUX	U2OS ER $\alpha$ -CALUX
E2	2.00E-05	5.00E-06	8.60E-06	0.42	8.45E-06	2.11E-06	3.63E-06
T	2.10		8.50E-01	0.48	1.00		4.04E-01
BBzP	2.00	5.70	1.00E+01	0.40	8.00E-01	2.28	4.00
DBP	3.00	1.70E+01	1.90E+01	0.41	1.24	7.00	7.82
EP	1.40E+01	5.50	4.20E+01	0.50	6.96	2.74	2.09E0+1
KEP	4.90E+01	6.70E-01	8.50E-01	0.43	2.09E-01	2.86E-01	3.63E-01
o,p'-DDT	3.80E-01	4.10E-01	7.20E-01	0.39	1.49E-01	1.60E-01	2.80E-01
BPA	3.60E-01	7.70E-01	2.20E-01	0.43	1.55E-01	3.31E-01	9.46E-02
COU	1.30E-02	5.20E-03	4.40E-02	0.43	5.53E-03	2.21E-03	1.87E-02
API	6.20E-01	4.10E-01	5.80E-01	0.41	2.56E-01	1.69E-01	2.40E-01
ZEA	1.50E-04	2.30E-04	4.20E-04	0.42	6.26E-05	9.60E-05	1.75E-04
EE	9.70E-06	2.70E-06	5.60E-06	0.41	3.96E-06	1.10E-06	2.29E-06
DES	3.80E-05	1.80E-05	8.10E-05	0.40	1.52E-05	7.18E-06	3.23E-05
TAM	4.10E-03	1.50E-02	2.10E-02	0.40	1.65E-03	6.02E-03	8.43E-03

**Table 3.7.** EAR<sub>test</sub> values of the test compounds based on the MCF-7/Bos proliferation assay, T47D ER-CALUX assay, and U2OS ER $\alpha$ -CALUX assay calculated using Eq. 2.

Compound	Exposure scenario(s)	Reference	EAR <sub>test</sub> MCF-7/BOS proliferation			EAR <sub>test</sub> T47D ER-CALUX			EAR <sub>test</sub> U2OS ER $\alpha$ -CALUX		
			Lowest	Mean	Highest	Lowest	Mean	Highest	Lowest	Mean	Highest
E2	Female levels	Mayo Clinic Staff (2022a)		4.95E-01	1.16E+01		1.98	4.62E+01		1.15	2.69E+01
E2	Male levels	Mayo Clinic Staff (2022a)		3.30E-01	1.32		1.32	5.28		7.68E-01	3.07
T	Female levels	Mayo Clinic Staff (2022b)		4.45E-07	3.34E-06					1.10E-06	8.25E-06
T	Male levels	Mayo Clinic Staff (2022b)		1.34E-05	5.29E-05					3.30E-05	1.31E-04
BBzP	BBzP exposure biomonitoring 2-3 weeks after delivery	(Högberget al., 2008)	1.01E-05	5.84E-05	2.82E-04	3.53E-06	2.05E-05	9.89E-05	2.01E-06	1.17E-05	5.63E-05
DBP	DBP exposure biomonitoring 2-3 weeks after delivery	(Högberget al., 2008)	4.44E-06	2.54E-04	1.92E-03	7.84E-07	4.48E-05	3.40E-04	7.01E-07	4.01E-05	3.04E-04
EP	EP exposure biomonitoring	(Frederiksen et al., 2011)	7.45E-05		3.52E-03	1.90E-04		8.96E-03	2.48E-05		1.17E-03
EP	EP exposure biomonitoring	(Kolatorova Sosvorova et al., 2017)		6.09E-05			1.55E-04			2.03E-05	





KEP	Occupational exposure banana agriculture, Guadeloupe	(Multigner et al., 2006, 2008, 2016)	1.80E-03	5.85E-03	5.71E-02	1.32E-03	4.28E-03	4.18E-02	1.04E-03	3.37E-03	3.29E-02
KEP	Occupational exposure nonagricultural sectors, Guadeloupe	Multigner et al. 2006, 2008, 2016	1.69E-03	4.59E-03	2.55E-02	1.24E-03	3.36E-03	1.86E-02	9.77E-04	2.65E-03	1.47E-02
KEP	Estimated intake unpolluted area 1.9 (0.1 - 20.6) µg/day	(Guldner et al., 2010)		4.48E-04			3.28E-04			2.58E-04	
KEP	Estimated intake polluted area 6.6 (1.0 - 22.2) µg/day	(Guldner et al., 2010)		5.57E-04			4.08E-04			3.21E-04	
KEP	Consumption contaminated foodstuffs	(Kadhel et al., 2014)	1.45E-04	3.14E-04	1.58E-02	1.06E-04	2.29E-04	1.16E-02	8.35E-05	1.81E-04	9.13E-03
KEP	Consumption contaminated foodstuffs	(Emeville et al., 2015)	1.37E-04	3.38E-04	3.96E-02	1.00E-04	2.47E-04	2.89E-02	7.88E-05	1.95E-04	2.28E-02
o,p'-DDT	Occupational exposure spraying DDT Brazil	(Minelli & Ribeiro, 1996)	3.38E-04		2.27E-03	3.13E-04		2.10E-03	1.78E-04		1.20E-03
o,p'-DDT	Environmental exposure from polluted area Brazil	(Freire et al., 2013)	1.79E-04	5.65E-04	1.06E-03	1.66E-04	5.23E-04	9.84E-04	9.43E-05	2.98E-04	5.61E-04

o,p'-DDT	Environmental exposure US	(Kezios et al., 2013)	4.83E-06	2.08E-04	2.15E-03	4.47E-06	1.92E-04	2.00E-03	2.55E-06	1.10E-04	1.14E-03
BPA	TDI	(Dent et al., 2019; Wetmore et al., 2015)	8.82E-04	1.95E-03	3.93E-03	4.12E-04	9.13E-04	1.84E-03	1.44E-03	3.19E-03	6.43E-03
COU	Biomonitoring	(Liu et al., 2018)	1.24E-01	1.46E-01	1.62E-01	3.11E-01	3.65E-01	4.05E-01	3.67E-02	4.31E-02	4.79E-02
API	Single oral dose 17.77 ± 4.19 mg	(Meyer et al., 2006)	3.53E-02	3.00E-02	4.56E-02	3.53E-02	4.54E-02	6.89E-02	3.53E-02	3.21E-02	4.87E-02
API	Regular diet	(Bolarinwa & Linseisen, 2005)	2.07E-02	2.21E-03	1.24E-02	2.07E-02	3.33E-03	1.88E-02	2.07E-02	2.36E-03	1.33E-02
ZEA	Calculated dietary intake 39 and 76 ng/kg/day, mean and max resp	(Fan et al., 2019)	1.97E-01	5.34E-01	1.42	1.29E-01	3.48E-01	9.27E-01	7.04E-02	1.91E-01	5.08E-01
EE	Single oral dose 0.03 mg EE + 0.15 mg desogestrel	(Nair et al., 2018)	4.18	4.25	4.60	1.50E+01	1.53E+01	1.65E+01	7.23	7.37	7.97
EE	Single oral dose 0.06 mg EE + 4 mg chlormadinone acetate	(Bonn et al., 2009)	3.82	5.74	7.66	1.37E+01	2.06E+01	2.75E+01	6.61	9.94	1.33E+01
DES	Single oral dose 2 mg	(H. Zhang et al., 2014)	1.80E+01	2.85E+01	3.89E+01	3.81E+01	6.01E+01	8.22E+01	8.47	1.34E+01	1.83E+01
TAM	Single oral dose of 20 mg	(Madlensky et al., 2011)	5.45	9.79	1.41E+01	1.49	2.68	3.86	1.06	1.91	2.76

TAM	TAM, in poor metabolizers	(Madlensky et al., 2011)	4.96	9.83	1.47E+01	1.36	2.69	4.02	9.69E-01	1.92	2.87
TAM	Single oral dose of 20 mg TAM, in intermediate metabolizers	(Madlensky et al., 2011)	5.85	9.87	1.39E+01	1.60	2.70	3.80	1.14	1.93	2.71
	Single oral dose of 20 mg TAM, in ultrarapid metabolizers										

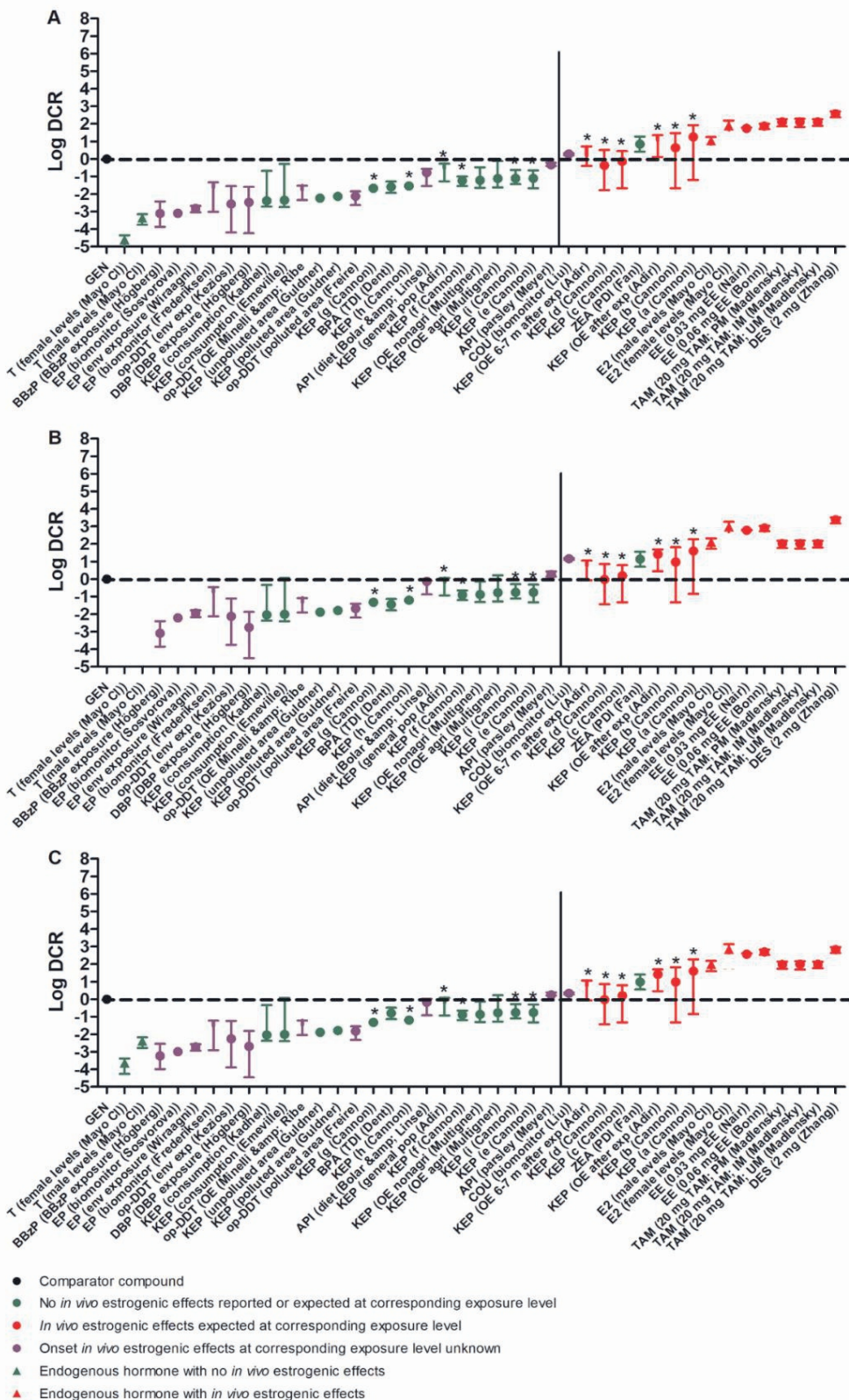


### 3.3.8 Step 8: Calculation of DCR values.

With the established  $EAR_{test}$  values for the multiple exposure scenarios for the selected model compounds (**Table 3.7**) and the *in vitro*-based  $EAR_{comparator}$  values of GEN (**Table 3.5**), the DCR values were calculated using Eq. 3 using data from the MCF-7/Bos proliferation assay (**Figure 3.4A**), T47D ER-CALUX assay (**Figure 3.4B**), and U2OS ER $\alpha$ -CALUX assay (**Figure 3.4C**). Comparison of the results presented in **Figure 3.4A-C** reveals that the exposure scenarios with a DCR value  $\leq 1$  are the same when based on the 3 *in vitro* estrogenic activity assays and the corresponding *in vitro*-based  $EAR_{comparator}$  values of GEN, and this also holds true for the exposure scenarios with a DCR value  $> 1$ . The derived DCR values were relatively lower when based on the MCF-7/Bos proliferation assay (**Figure 3.4A**). The  $EAR_{comparator}$  from this assay was highest compared to the other *in vitro* assays (**Table 3.5**) which indicates that the corresponding DCR values from the MCF-7/Bos proliferation assay appear least conservative so that on the basis of this assay it is more likely to conclude an exposure is safe.

### 3.3.9 Step 9: Evaluation of the DCR-based predictions of the selected exposure scenarios to the test compounds.

To evaluate the calculated DCR values, a comparison was made to actual knowledge on the corresponding *in vivo* estrogenic effects at the respective exposure levels (**Table 3.4**), also including endogenous hormone levels of androgen T and estrogen E2 in males and females. Indeed, the male and female levels of T (green triangles) and E2 (red triangles) had DCR values of respectively 1 indicating they are negative and positive for inducing *in vivo* estrogenicity. In adult males, E2 regulates efferent duct and prostate functioning and the flow of sperm from testis to the epididymis, thus playing a role in male fertility and reproductive functioning (Hess & Cooke, 2018). All exposure scenarios which were expected based on existing knowledge to be positive for *in vivo* estrogenic effects (red circles) had a DCR  $> 1$ . There was one false positive value that related to the evaluated exposure scenario for ZEA (Fan et al., 2019) wherefrom no *in vivo* estrogenic effects are expected but still resulted in a DCR  $> 1$ . All exposures which were negative for *in vivo* estrogenicity (green circles) had a DCR  $\leq 1$ .



\* The exposed populations reported by Cannon et al. (1978) and Adir et al. (1978) were assumed to be male

**Figure 3.4.** The DCRs of a series of exposures to 14 model compounds including endogenous hormones, phthalates, ethyl paraben, pesticides, bisphenol A, phytoestrogens, the mycotoxin zearalenone, and drugs with information regarding accompanying *in vivo* estrogenic effects calculated using  $EAR_{\text{comparator}}$  values of GEN (**Table 3.5**) based on A. the MCF-7/Bos proliferation assay, B the T47D ER-CALUX assay, and C the U2OS ER $\alpha$ -CALUX assay. The mean DCR values are presented as symbols and, when information on the variability was available, the lowest and highest DCR values as the lowest and highest whiskers, respectively. The DCRs of comparator GEN are represented as black circles and by definition equal to 1 (log DCR = 0). The DCRs of model compound exposure scenarios where no *in vivo* estrogenic effects are expected (see **Table 3.4**) are presented as green circles. The DCRs of test compound exposure scenarios for which *in vivo* estrogenic effects are expected (see **Table 3.4**) are presented as red circles. The DCRs of test compound scenarios for which the *in vivo* estrogenic effects are unknown (see **Table 3.4**) are presented as purple circles. The DCRs for the endogenous hormone levels of testosterone and estradiol are presented as green and red triangles, respectively. The dotted horizontal lines display the DCR of 1 (log DCR = 0) whereas the solid vertical lines separate the exposures with mean DCR values  $\leq 1$  from those with mean DCR values  $> 1$ . See **Table 3.1** for compound abbreviations.

### 3.3.9.1 Step 9a: Evaluation of exposures to ZEA.

A further analysis of the false positive result for the exposure scenario of ZEA (Fan et al., 2019) was performed. The corresponding DCR values were  $> 1$ , which suggests that there would be a risk for *in vivo* estrogenicity at this exposure. At the reported internal exposures, Fan et al. (2019) calculated a probable daily intake (PDI) of  $3.9 \times 10^{-2}$  -  $7.6 \times 10^{-2}$   $\mu\text{g}/\text{kg}$  bw/day which is 3.2- to 6.4-fold lower than the tolerable daily intake (TDI) of ZEA of 0.25  $\mu\text{g}/\text{kg}$  bw/day established based on the no observed effect level (NOEL) for estrogenic effects of ZEA and its metabolites on the ovary, uterus, and vulva in pigs (Alexander et al. 2011). Based on this result this exposure scenario was expected to not result in estrogenicity, indicating that the positive DCR based prediction or this scenario to be apparently false. However, this PDI reported by Fan et al. (2019) was calculated using simple kinetics and may not provide an adequate estimation of the corresponding external dose levels that correspond with the reported plasma concentrations of ZEA. Using physiologically based kinetic (PBK) modelling, we aimed to obtain a more accurate dose prediction of ZEA at the reported plasma concentrations of Fan et al. (2019). To this purpose, the PBK model describing ZEA kinetics in humans developed and validated by Mendez-Catala et al. (2021) (PBK model code available in the Supplementary data of (Mendez-Catala et al., 2021)) was used to predict the

external dose levels of ZEA at the internal exposure reported by Fan et al. (2019), using Berkeley Madonna 10.4.2 (UC Berkeley, CA, USA) with the Rosenbrock's algorithm for stiff systems. The PBK model of ZEA includes the metabolic transformation and kinetics of the more estrogenic active metabolite  $\alpha$ -zearalenol ( $\alpha$ -ZEL). The nominal plasma concentrations of ZEA ( $1.98 \times 10^{-4}$  -  $0.13 \times 10^{-4}$   $\mu\text{M}$ ) were transformed using the ADMET predicted  $R_{b2p}$  of ZEA (0.89) to the corresponding nominal blood concentrations ( $1.76 \times 10^{-4}$  -  $0.12 \times 10^{-4}$   $\mu\text{M}$ ). Next, the corresponding doses of ZEA that would be required to reach these nominal blood concentrations were predicted using the PBK model. The predicted doses amounted to 335 – 2200  $\mu\text{g}/\text{kg}$  bw/day and appear 3 to 4 orders of magnitude higher than the calculated PDI of Fan et al. (2019). These dose levels are also higher than the TDI of ZEA indicating that this exposure to ZEA can be expected to result in estrogenicity. This indicates the DCR values being  $>1$  would be in line with what would be expected indicating the data point for ZEA to be a real positive. It is of interest to note that Mendez-Catala et al. (2021) used the PBK model to predict the free plasma concentrations of ZEA at its TDI and at the estimated daily intake (EDI) ranging from  $2.40 \times 10^{-3}$  to  $29 \times 10^{-2}$   $\mu\text{g}/\text{kg}$  bw/day (Alexander et al. 2011). The predicted free plasma concentration at the TDI amounted to  $1.88 \times 10^{-8}$   $\mu\text{M}$  and at the EDI to  $9.00 \times 10^{-9}$  -  $9.00 \times 10^{-11}$   $\mu\text{M}$  (Mendez-Catala et al., 2021). Thus, the plasma concentrations reported by Fan et al. (2019) appear 6 orders of magnitude higher than these predicted plasma concentrations at the TDI also indicating that the exposure scenario reported by Fan et al. (2019) represents a scenario that would likely test positive for estrogenicity. To further illustrate thus by the DCR approach, these free plasma concentrations resulting from exposure at the EDI or TDI were used to calculate the corresponding  $\text{EAR}_{\text{test}}$  (Supplementary material S3.3) and DCR values using GEN as comparator compound. The DCRs at the EDI and TDI of ZEA were indeed the exposure scenario of Fan et al. (2019) now coloured red instead of green is also presented in **Figure 3.5**.

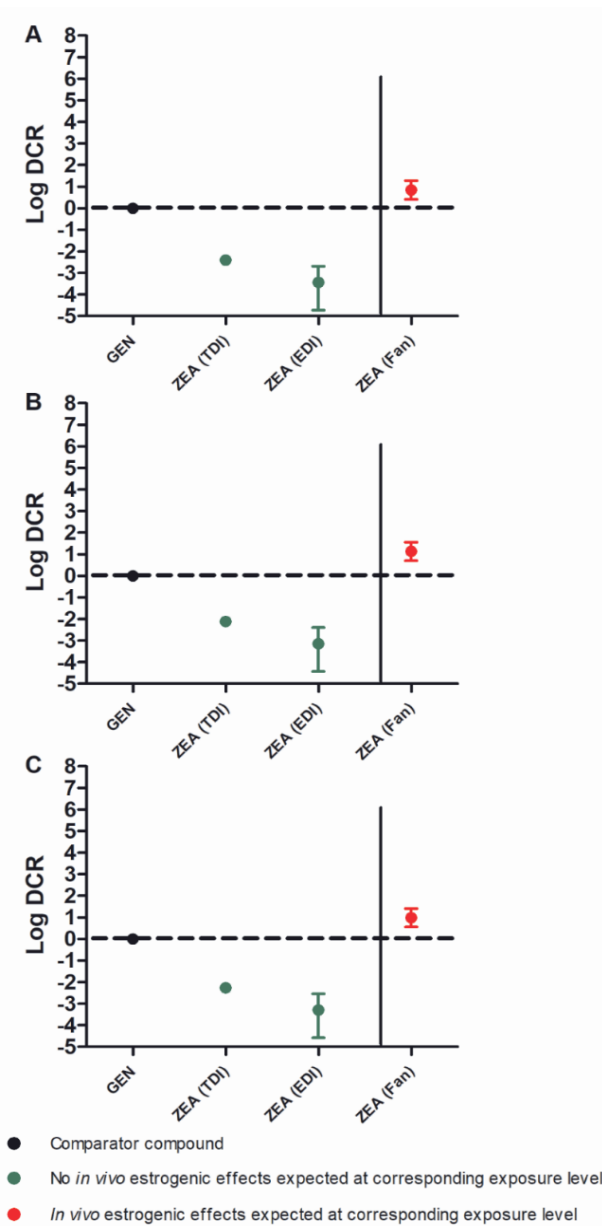


**Figure 3.5.** The DCRs of the TDI, EDI and the reported exposure scenario (Fan et al. 2019) of ZEA calculated using  $EAR_{\text{comparator}}$  values of GEN (Table 3.5) based on **A** the MCF-7/Bos proliferation assay, **B** the T47D ER-CALUX assay, and **C** the U2OS ER $\alpha$ -CALUX assay. The mean DCR values are presented as circles and, when information on the variability was available, the lowest and highest DCR values as the lowest and highest whiskers, respectively. The DCRs of comparator GEN are represented as black circles and by definition equal to 1 ( $\log \text{DCR} = 0$ ). The DCRs of the exposure scenarios to

ZEA where no *in vivo* estrogenic effects are expected are presented as green circles. The DCRs of exposure scenarios to ZEA for which *in vivo* estrogenic effects are expected are presented as red circles. The dotted horizontal lines display the DCR of 1 ( $\log \text{DCR} = 0$ ) whereas the solid vertical lines separate the exposures with mean DCR values  $\leq 1$  from those with mean DCR values  $> 1$ .

### 3.3.10 Step 10: Use the approach for evaluation of the unknown exposure scenarios.

With the DCR-based predictions being evaluated, the use of the DCR approach for the safety evaluation of putative estrogenic exposures was supported and enabled the evaluation of the 11 exposure scenarios for which the corresponding *in vivo* estrogenic effects were unknown (purple circles) (**Figure 3.4**). 10 out of these 11 exposure scenarios had a  $\text{DCR} \leq 1$  and 1 had a  $\text{DCR} > 1$ , indicating to be negative and positive for *in vivo* estrogenicity, respectively.

## 3.4 Discussion

In the DCR approach, the EAR of an exposure scenario to a test compound ( $\text{EAR}_{\text{test}}$ ) is compared to the EAR of safe human exposure to a comparator compound ( $\text{EAR}_{\text{comparator}}$ ). A DCR value  $\leq 1$  indicates that the evaluated exposure to the test compound is expected to be safe. Van Tongeren et al. (2021) used an *in vitro*-based definition of the  $\text{EAR}_{\text{comparator}}$  with the  $\text{BMCL}_{05}$  as safe level of exposure to comparator compounds to evaluate putative anti-androgenic test compounds based on the AR-CALUX assay. The results obtained indicated that this NGRA strategy might be of use to also evaluate other biological endpoints for which *in vitro* bioassay results are available. In the current work, this DCR approach with *in vitro* assay-based EAR values was further developed using an *in vitro*-based  $\text{EAR}_{\text{comparator}}$  value defined for GEN to evaluate 41 human estrogenic exposure scenarios to 14 model compounds including endogenous hormones, phthalates, ethyl paraben, pesticides, bisphenol A, phytoestrogens, the mycotoxin zearalenone, and drugs. The *in vitro* data were derived from concentration-response curves obtained in the estrogenic *in vitro* MCF-7/Bos proliferation assay, T47D ER-CALUX assay, or U2OS ER $\alpha$ -CALUX assay (Wang et al., 2014). The DCRs of the 41 exposure scenarios for the 14 test compounds were calculated taking into account differences in *in vitro* and *in vivo* protein binding. The calculated DCR values of the test compounds were evaluated against actual knowledge on the corresponding occurrence of *in vivo* estrogenic effects at the respective level of exposure.

GEN was selected as the comparator compound because of (i) the wide range of available data on exposures that were reported to test negative for *in vivo* estrogenicity in humans and (ii) comparison of the free *in vitro* BMCL<sub>05</sub> values to the reported free plasma concentrations at these non-estrogenic exposure levels. The fact that at the highest internal concentrations reported from supplement intake of GEN (Busby et al., 2002) no estrogenic effects were observed in the 30 male volunteers studied and that these concentrations were 13- to 34-fold higher than the free *in vitro* BMCL<sub>05</sub> values of GEN (**Figure 3.3**), provides additional support for the conclusion that exposure to the comparator GEN that results in an internal free concentration equal to the *in vitro* free BMCL<sub>05</sub> can be considered safe and is adequate to calculate the EAR<sub>comparator</sub> in the DCR approach. The large variation of the internal concentrations of GEN resulting from the different diets and within the different diets indicates that using human clinical or biomonitoring studies of GEN to define a safe level of exposure may leave substantial uncertainty. Furthermore, conflicting data on estrogenic (beneficial or adverse) effects are reported following GEN exposure. It is suggested that the effects can be dependent on, among others, sex, menstrual phase, and health status (Hargreaves et al., 1999; Khan et al., 2012; Niculescu et al., 2007; Petrakis et al., 1996; Van Der Velpen et al., 2014). Using reported internal concentrations of GEN to set the EAR<sub>comparator</sub> values may therefore not be adequate. However, using *in vitro*-based BMCL<sub>05</sub> values as an alternative safe level of exposure provides a more consistent way to set an adequate and safe EAR<sub>comparator</sub>. Thus, this novel *in vitro*-based EAR<sub>comparator</sub> approach can be applied for endpoints for which a corresponding *in vitro* bioactivity assay is available, enabling the use of the DCR approach for many additional endpoints.

The use of this novel safe *in vitro*-based EAR<sub>comparator</sub> in the DCR approach resulted in the correct prediction of the occurrence of *in vivo* estrogenic activity of the exposure scenarios for the various model compounds (**Figure 3.4**), without the occurrence of false negatives, and, after reconsideration of the data for ZEA also without false positives. This further highlights that data from *in vitro* bioactivity assays are suitable for use in the DCR approach to evaluate the estrogenicity of compounds. The U2OS ER $\alpha$ -CALUX assay seems to provide the most conservative approach for setting DCR values for estrogenic exposure scenarios, generating relatively higher DCR values for the different exposure scenarios and thus being more likely to predict *in vivo* estrogenicity, than the approaches based on the T47D ER-CALUX assay and MCF-7/Bos proliferation assay. The MCF-7/Bos proliferation assay seemed the least conservative generating relatively lower DCR values for estrogenic exposure scenarios so that evaluation by this approach is less likely to predicted *in vivo* estrogenicity, thus easier suggesting a scenario to be safe. For all 3 approaches there was initially one false positive DCR outcome (**Figure 3.4**), namely for the exposure to ZEA at a level below the established TDI (Fan et al., 2019). The reported PDIs of ZEA at the reported internal exposure levels

evaluated in this scenario were lower than the TDI of ZEA of 0.25  $\mu\text{g}/\text{kg}$  bw/day established based on the NOEL for estrogenic effects of ZEA and its metabolites on the ovary, uterus, and vulva in pigs (Alexander et al. 2011). However, this PDI was calculated using only kinetic parameters for urinary excretion and is thus a rough estimation rather than an exact assessment. Using a PBK model describing the ADME of ZEA in humans (Mendez-Catala et al., 2021) provided a more accurate prediction of the external dose. The PBK model-based prediction of the external doses at the internal exposure levels reported by Fan et al. (2019) were 3 to 4 orders of magnitude higher than the TDI of ZEA and the calculated PDIs of Fan et al. (2019). This indicates that these PBK model based calculations show that at the reported exposure there is a risk of *in vivo* estrogenicity and that the corresponding DCR values were thus correctly predicted by the DCR approach to be  $> 1$ . To further evaluate the DCR-based predictions of exposure to ZEA, the DCR at the EDI and TDI were calculated and were indeed  $< 1$  (**Figure 3.5**). The DCR-based safety decisions on the KEP exposure scenarios reported by Cannon et al. (1978) and Adir et al. (1978) were predicted based on the assumption of a male populations, which enabled comparison to the NOEL set in men based on a clinically relevant decrease in sperm count (Guzelian, 1992). The DCR outcomes thus confirm that the assumption made was adequate.

The DCR predictions being validated enabled the safety estimation of the 11 exposure scenarios to model compounds for which it was unknown as to whether they would result in *in vivo* estrogenicity in humans (**Figure 3.4**). Of these 11 exposure scenarios, 10 had a  $\text{DCR} \leq 1$  and 1 had a  $\text{DCR} > 1$  and are thus expected to be negative and positive for *in vivo* estrogenicity, respectively.

To cover variability,  $\text{EAR}_{\text{test}}$  values of the test compounds used for the DCR analysis included, when available, lowest, mean, and highest  $\text{EAR}_{\text{test}}$  values calculated using lowest, mean, and highest internal dose levels of the exposure scenarios. The DCR obtained with the highest, or when not available the mean  $\text{EAR}_{\text{test}}$  values, was used to make a conservative safety decision on the exposure scenario to the respective test compound. As already stated, this approach correctly predicted the *in vivo* estrogenicity (**Figure 3.4**). In this work, a cut-off of  $\text{DCR} \leq 1$  was used to estimate the estrogenicity of the studied exposure scenarios to the test compounds because the  $\text{BMCL}_{05}$  value reflecting an internal dose level without estrogenicity for the comparator compound GEN was considered safe and adequate to be used in the DCR approach. However, in future work, it can be considered whether in defining a cut-off for the DCR also uncertainty has to be taken into account, choosing a value lower than 1 for the cut-off since this will result in an even more conservative DCR-based safety decision.



When applying the NGRA approach based on *in vitro* studies it is important to note that the *in vitro* bioactivity assays that can be used in the DCR approach rarely capture toxicokinetics, such as metabolism, as in the human body (Coecke et al., 2006). BBzP, DBP, o,p'-DDT, ZEA, and TAM are known to be converted to more bioactive metabolites which will contribute to the *in vivo* estrogenicity of the respective parent compound. When using the three *in vitro* bioactivity assays in the DCR approach, this contribution to the estrogenicity may not be captured so that the observed *in vitro* toxicity of a parent compound may underestimate the toxicity in the human body. This issue can be overcome by using PBK models describing the kinetics of a parent compound and its respective relevant metabolites in humans enabling the prediction of the corresponding combined internal concentrations in parent compound equivalents (Mendez-Catala et al., 2021; van Tongeren et al., 2022; Q. Wang et al., 2020). Furthermore, co-incubation with liver S9 fraction in the *in vitro* bioactivity assays (Mollergues et al., 2017) offers the opportunity to evaluate whether a compound will be converted to hepatic metabolites and whether they would be more potent to the corresponding biological target. Such strategies could be implemented in the DCR approach to overcome this limitation.

When exposure to a novel chemical is to be evaluated for estrogenic effects by the DCR approach, one may choose to use the most conservative assay, in this case the U2OS ER $\alpha$ -CALUX assay, instead of all three assays to reduce the labour intensity and use of resources. The endpoints of gene expression in the CALUX assays which are more upstream in the adverse outcome pathway (Legler et al., 1999; Sonneveld et al., 2005; van der Burg, Winter, Weimer, et al., 2010), may be more sensitive, and this may explain the more conservative evaluation compared to the DCR approach based on the more functional endpoint of estrogen-induced proliferation of the cells measured in the MCF/7-Bos proliferation assay (Soto et al., 1995). Furthermore, one may also choose to use the assay which is the least time consuming, which in this case are the CALUX assays with only a 24 h exposure time compared to the 6 days exposure time in the MCF/7-Bos proliferation assay. The results of the present study revealed that in principle all 3 bioassays resulted in similar outcomes. This is related to the fact that when using a less sensitive bioassay not only the EC<sub>50</sub> values of the test compounds will be higher but also the EC<sub>50</sub> value of the comparator will be higher, i.e., the relative potency of the compound is similar in all 3 bioassays, resulting in lower EAR<sub>test</sub> and EAR<sub>comparator</sub> values and thus comparable DCR values.

The present study focusing on estrogenicity and a previous study focusing on anti-androgenicity (van Tongeren et al., 2022) showed that the DCR approach can offer a relatively quick analysis on the safety of a defined exposure scenario regarding

biological endpoints of which corresponding *in vitro* bioactivity assays are available. In NGRA, a tiered workflow could be followed when an exposure to a (novel) compound is to be evaluated. For instance, with *in silico* tools like the molecular initiating events (MIE) ATLAS, a prediction can be made if a chemical has affinity to bind and thus interact with a biological target based on its molecular structure (Allen et al., 2018). When a perturbation on a certain biological endpoint is expected, the use of an *in vitro* bioactivity assay covering this endpoint and using an adequate  $EAR_{\text{comparator}}$  will enable the determination of the corresponding DCR. When the DCR is  $\leq 1$ , it can be suggested that the studied exposure scenario for the compound of interest does not raise a safety concern whereas when the DCR is  $> 1$ , this test compound should be prioritized for further testing. To conclude, the DCR approach was further developed using multiple *in vitro* bioactivity assays for estrogenicity as the biological endpoint as 3R compliant NAM in NGRA to evaluate the safety of estrogenic exposures in humans.

### **Funding**

This work was supported by Unilever (United Kingdom).

### **Disclosure**

The current affiliation at time of publication of Si Wang is PepsiCo International, Beaumont Park, 4 Leycroft Road, Leicester LE4 1ET, UK.

**Supplementary material S3.1. Negative exposure scenarios to GEN**

**Supplementary Table S3.1.** The reported nominal and transformed free internal concentrations of GEN, using the  $f_{ub \text{ in vivo}}$ , following intake of different diets which are indicated to be conservative and health protective in humans.

Reference	Diet	Exposure scenario(s)	Plasma, serum, or blood concentrations reported	Nominal internal concentrations ( $\mu\text{M}$ ) <sup>1,2</sup>	$F_{ub}$ <i>in vivo</i>	Free internal plasma concentrations ( $\mu\text{M}$ )
(Busby et al., 2002)	Western diet	Isoflavone intake of < 10 mg/d	Plasma	3.80E-02 $\pm$ 22E-02 (mean $\pm$ SD)	0.07	2.76E-03 $\pm$ 1.60E-03
(Metzner et al., 2009)	Western diet	A 14 day prohibition of soy foods and their derivatives prior to the study	Plasma	5.10E-03 $\pm$ 6.00E-04 (mean $\pm$ SEM)		3.70E-04 $\pm$ 4.35E-05
(Grace et al., 2004)	Western diet	EPIC-Norfolk following information from a 7 day dietary diary	Serum	4.64E-05 $\pm$ 3.00E-05 (mean $\pm$ SD)		3.36E-06 $\pm$ 2.18E-06
(Heald et al., 2006)	Western diet	Control men from a case-control study of prostate cancer	Serum	1.00E-04 (median) (4.00E-05 - 1.40E-04 (IQR))		7.25E-06 (2.90E-06 - 1.02E-05)
(Setchell et al., 2003)	Western diet	Consumption a soy-deficient diet for 1 months prior	Serum	1.10E-05 $\pm$ 3.00E-06 (mean $\pm$ SEM)		7.98E-07 $\pm$ 2.18E-07
(Yuan et al., 2012)	Asian diet	Polyphenol-free diet for 10 days prior to the study	Plasma	1.74E-03 $\pm$ 1.36E-03 (mean $\pm$ SD)		1.26E-04 $\pm$ 9.86E-05
(Setchell et al., 2011)	Asian diet	Consumption of 250 mL soy milk 2 per day for 3.5 day, equivalent to 19 mg GEN per day	Plasma	1.65E-03 $\pm$ 4.60E-05 (mean $\pm$ SD)		1.20E-04 $\pm$ 3.34E-06
(Arai et al., 2000)	Asian diet	Estimated dietary intake of 30.1 mg/day	Plasma	9.23E-04 (median) (7.60E-05 - 7.40E-03 (range))		6.69E-05 (5.51E-06 - 5.37E-04)

(Iwasaki et al., 2008)	Asian diet	Calculated GEN intake of 21.7 (16.8-26.1) mg/d from dietary assessment with a food frequency questionnaire	Plasma	1.60E-03 (median) (8.70E-04 - 2.80E-03 (IQR))	1.16E-04 (6.31E-05 - 2.03E-04)
(Shimazu et al., 2011)	Asian diet	Calculated GEN intake (not specified) from dietary assessment with a food frequency questionnaire	Plasma	8.00E-04 (median) (3.30E-04 - 1.40E-03 (IQR))	5.80E-05 (2.39E-05 - 1.02E-04)
(Takashima et al., 2004)	Asian diet	Calculated GEN intake of 22.9 ± 15.9 mg/d from hospital diet	Serum	1.20E-03 ± 1.26E-03 (mean ± SEM)	8.70E-05 ± 9.14E-05
(Ritchie et al., 2004)	Asian diet	A specific diet was followed over a 24 h recording period	Plasma	3.80E-04 ± 3.80E-05 (mean ± SD)	2.76E-05 ± 2.76E-06
(Busby et al., 2002), Formulation A	Supplement intake	Single oral dose of 8 mg/kg bw of a 90% GEN formulation	Plasma	0.13 ± 0.02 (mean ± SD)	9.50E-03 ± 1.52E-03
(Busby et al., 2002), Formulation B	Supplement intake	Single oral dose of 8 mg/kg bw of a 45% GEN formulation	Plasma	0.26 ± 0.16 (mean ± SD)	1.89E-02 ± 1.16E-02
(Metzner et al., 2009)	Supplement intake	Repeated dose of 30 mg GEN per day for 7 days	Plasma	2.24E-02 ± 9.00E-03 (mean ± SEM)	1.62E-03 ± 6.53E-04
(Yuan et al., 2012)	Supplement intake	4 mg GEN twice per day for 7 days	Plasma	4.31E-03 ± 1.44E-03 (mean ± SD)	3.13E-04 ± 1.04E-04

(Setchell et al., 2003) (low dose)	Supplement intake	A single dose of 0.4 mg/kg bw	Serum	4.95E-04 ± 8.10E-05 (mean ± SEM)	3.59E-05 ± 5.87E-06
(Setchell et al., 2003) (low dose repeat)	Supplement intake	Twice a dose of 0.4 mg/kg bw	Serum	3.69E-04 ± 5.40E-05 (mean ± SEM)	2.68E-05 ± 3.92E-06
(Setchell et al., 2003) (low dose after food)	Supplement intake	A single dose of 0.4 mg/kg bw and another low dose after 1 week of daily soymilk consumption containing 50 mg natural isoflavones	Serum	3.87E-04 ± 6.30E-05 (mean ± SEM)	2.81E-05 ± 4.57E-06
(Setchell et al., 2003) (moderate dose)	Supplement intake	A single dose of 0.8 mg/kg	Serum	7.83E-04 ± 1.26E-04 (mean ± SEM)	5.68E-05 ± 9.14E-06
(Setchell et al., 2011)	Supplement intake	A single oral dose of 50 mg GEN	Plasma	1.92E-02 ± 2.96E-03 (mean ± SEM)	1.39E-03 ± 2.15E-04

<sup>1</sup> As derived from Becker et al. (2015).

<sup>2</sup> Serum concentration were assumed to be equal to plasma concentrations.

## Supplementary material S3.2. BMC analysis

The benchmark concentration (BMC) analysis of GEN was performed based on the *in vitro* concentration-response data reported by Wang et al. (2014), using BMDS3.2.1 software (U.S. EPA). The benchmark response (BMR) was defined as a 5% extra response (BMR<sub>05</sub>). The BMC<sub>05</sub> and its upper (BMCU<sub>05</sub>) and lower (BMCL<sub>05</sub>) 95% confidence interval were also determined. The model was accepted when the fitted model had a p-value > 0.01, a BMDU<sub>05</sub>: BMDL<sub>05</sub> ratio (precision factor) below 3, or the lowest AIC, indicating support for a concentration-response.

### Supplementary material S3.2.1 BMC modelling of *in vitro* concentration-response data of GEN in the MCF-7/Bos proliferation assay

**Supplementary Table S3.2.1.1.** Input values of the *in vitro* concentration-response data of GEN in the MCF-7/Bos proliferation assay (Wang et al., 2014).

Concentration (µM)	n	Response	SEM
0.006	3	0.05	0.02
0.02	3	0.17	0.02
0.06	3	0.35	0.02
0.2	3	0.55	0.04
0.6	3	0.64	0.02
2	3	0.63	0.08
6	3	0.54	0.06

**Supplementary Table S3.2.1.2.** BMC analysis of the *in vitro* concentration-response data of GEN in the MCF-7/Bos proliferation assay (Wang et al., 2014). BMC<sub>05</sub> and BMCL<sub>05</sub> values were obtained using BMDS software version 3.2.1, at a BMC of 5% extra risk, BMR type Hybrid model-extra risk with normal distribution and constant variance.

Model	BMC (µM)	BMCL (µM)	BMCU (µM)	Test 4 P-Value	AIC	Accepted
<u>Exponentia</u> <u>l 2 (CV -</u> <u>normal)</u>	4.31	2.66	33.91	<0.0001	- 1.24	No

<u>Exponential 3 (CV - normal)</u>	4.31	2.66	33.91	<0.0001	- 1.24	No
<u>Exponential 4 (CV - normal)</u>	0.06	0.05	0.10	<0.0001	- 26.06	No
<u>Exponential 5 (CV - normal)</u>	0.06	0.05	0.12	<0.0001	- 26.06	No
<u>Hill (CV - normal)</u>	0.01	3.48E-03	0.02	0.01	- 57.35	Yes
<u>Polynomial Degree 6 (CV - normal)</u>	3.42	1.87	19.43	<0.0001	- 1.86	No
<u>Polynomial Degree 5 (CV - normal)</u>	3.42	1.87	19.43	<0.0001	- 1.86	No
<u>Polynomial Degree 4 (CV - normal)</u>	3.42	1.87	19.43	<0.0001	- 1.86	No
<u>Polynomial Degree 3 (CV - normal)</u>	3.42	1.87	19.43	<0.0001	- 1.86	No
<u>Polynomial Degree 2 (CV - normal)</u>	3.42	1.87	19.43	<0.0001	- 1.86	No
<u>Power (CV - normal)</u>	3.42	1.87	19.43	<0.0001	- 1.86	No
<u>Linear (CV - normal)</u>	3.42	1.87	19.43	<0.0001	- 1.86	Yes

**Supplementary material S3.2.2 BMC modelling of *in vitro* concentration-response data of GEN in the T47D ER-CALUX assay**

**Supplementary Table S3.2.2.1.** Input values of the *in vitro* concentration-response data of GEN in the T47D ER-CALUX assay (Wang et al., 2014).



Concentration ( $\mu\text{M}$ )	n	Response	SEM
0.0003	3	-10.00	6.25
0.001	3	-15.37	4.91
0.003	3	-9.58	2.01
0.01	3	6.47	1.79
0.03	3	67.17	0.89
0.1	3	107.11	9.15
0.3	3	129.64	6.03
1	3	210.20	6.70

**Supplementary Table S2.2.2.** BMC analysis of the *in vitro* concentration-response data of GEN in the T47D ER-CALUX assay (Wang et al. 2014).  $\text{BMC}_{05}$  and  $\text{BMCL}_{05}$  values were obtained using BMDS software version 3.2.1, at a BMC of 5% extra risk, BMR type Hybrid model-extra risk with normal distribution and constant variance.

Model	BMC ( $\mu\text{M}$ )	BMCL ( $\mu\text{M}$ )	BMCU ( $\mu\text{M}$ )	Test 4 P-Value	AIC	Accepted
<u>Exponential 2 (CV - normal)</u>	-9999	0.00	Infinity	<0.0001	292.43	No
<u>Exponential 3 (CV - normal)</u>	-9999	0.00	Infinity	<0.0001	294.43	No
<u>Exponential 4 (CV - normal)</u>	-9999	0.00	Infinity	<0.0001	294.43	No
<u>Exponential 5 (CV - normal)</u>	-9999	0.00	Infinity	<0.0001	296.43	No
<u>Hill (CV - normal)</u>	4.88E-03	3.29E-03	7.98E-03	<0.0001	208.38	Yes
<u>Polynomial Degree 6 (CV - normal)</u>	0.14	0.11	0.21	<0.0001	249.67	No
<u>Polynomial Degree 5 (CV - normal)</u>	0.14	0.11	0.21	<0.0001	249.67	No

<u>Polynomial Degree 4 (CV - normal)</u>	0.14	0.11	0.21	<0.0001	249.67	No
<u>Polynomial Degree 3 (CV - normal)</u>	0.14	0.11	0.21	<0.0001	249.67	No
<u>Polynomial Degree 2 (CV - normal)</u>	0.14	0.11	0.21	<0.0001	249.67	No
<u>Power (CV - normal)</u>	0.14	0.11	0.21	<0.0001	249.67	No
<u>Linear (CV - normal)</u>	0.14	0.11	0.20	<0.0001	253.51	Yes

**Supplementary material S3.2.3 BMC modelling of *in vitro* concentration-response data of GEN in the U2OS ER $\alpha$ -CALUX assay**

**Supplementary Table S3.2.3.1.** Input values of the *in vitro* concentration-response data of GEN in the U2OS ER $\alpha$ -CALUX assay (Wang et al., 2014).

Concentration ( $\mu$ M)	n	Response	SEM
0.0003	3	-12.10	0.00
0.001	3	-9.73	0.00
0.003	3	-0.75	6.13
0.01	3	34.64	19.10
0.03	3	90.08	23.35
0.1	3	102.83	4.25
0.3	3	108.74	16.98
1	3	170.78	24.53

**Supplementary Table S3.2.3.2.** BMC analysis of the *in vitro* concentration-response data of GEN in the U2OS ER $\alpha$ -CALUX assay (Wang et al., 2014). BMC<sub>05</sub> and BMCL<sub>05</sub> values were obtained using BMDS software version 3.2.1, at a BMC of 5% extra risk, BMR type Hybrid model-extra risk with normal distribution and constant variance.

<b>Model</b>	<b>BMC (<math>\mu\text{M}</math>)</b>	<b>BMCL (<math>\mu\text{M}</math>)</b>	<b>BMCU (<math>\mu\text{M}</math>)</b>	<b>Test 4 P-Value</b>	<b>AIC</b>	<b>Accepted</b>
<u>Exponential 2 (CV - normal)</u>	-9999	0	Infinity	<0.0001	287.18	No
<u>Exponential 3 (CV - normal)</u>	-9999	0	Infinity	<0.0001	289.18	No
<u>Exponential 4 (CV - normal)</u>	-9999	0	Infinity	<0.0001	289.18	No
<u>Exponential 5 (CV - normal)</u>	-9999	0	Infinity	<0.0001	291.18	No
<u>Hill (CV - normal)</u>	2.34E-03	1.34E-03	4.83E-03	0.0005	219.11	Yes
<u>Polynomial Degree 6 (CV - normal)</u>	0.20	0.15	0.34	<0.0001	251.79	No
<u>Polynomial Degree 5 (CV - normal)</u>	0.20	0.15	0.34	<0.0001	251.79	No
<u>Polynomial Degree 4 (CV - normal)</u>	0.20	0.15	0.34	<0.0001	251.79	No
<u>Polynomial Degree 3 (CV - normal)</u>	0.20	0.15	0.34	<0.0001	251.79	No
<u>Polynomial Degree 2 (CV - normal)</u>	0.20	0.15	0.34	<0.0001	251.79	No
<u>Power (CV - normal)</u>	0.20	0.15	0.33	<0.0001	251.79	No
<u>Linear (CV - normal)</u>	0.19	0.15	0.29	<0.0001	259.52	Yes



## Supplementary material S3.3. Evaluation of exposures to ZEA

**Supplementary Table S3.3.** The  $EAR_{test}$  values at the EDI and TDI of ZEA compounds based on the MCF-7/Bos proliferation assay, T47D ER-CALUX assay, and U2OS ER $\alpha$ -CALUX assay calculated using Eq. 2.

Compound	Exposure scenario (s)	Reference	$EAR_{test}$ MCF-7/BOS proliferation			$EAR_{test}$ T47D ER-CALUX			$EAR_{test}$ U2OS ER $\alpha$ -CALUX			
			Lowest	Mean	Highest	Lowest	Mean	Highest	Lowest	Mean	Highest	
ZEA	TDI	Alexander et al. (2011)		3.00E-04			1.96E-04			1.07E-04		
ZEA	EDI	Alexander et al. (2011)	1.44E-06	2.78E-05	1.57E-04	9.38E-07	1.81E-05	1.02E-04	5.14E-07	9.94E-06	5.60E-05	



# Chapter 4

## **Chapter 4. Next generation risk assessment of the anti-androgen flutamide including the contribution of its active metabolite hydroxyflutamide**

Tessa C. A. van Tongeren, Paul L. Carmichael, Ivonne M. C. M. Rietjens, Hequn Li

Published in *Frontiers in Toxicology* (2022), 4: 881235

## Abstract

In next generation risk assessment (NGRA), non-animal approaches are used to quantify the chemical concentrations required to trigger bioactivity responses, in order to assure safe levels of human exposure. A limitation of many *in vitro* bioactivity assays, which are used in an NGRA context as new approach methodologies (NAMs), is that toxicokinetics, including biotransformation, are not adequately captured. The present study aimed to include, as a proof of principle, the bioactivity of the metabolite hydroxyflutamide (HF) in an NGRA approach to evaluate the safety of the anti-androgen flutamide (FLU), using the ARCALUX assay to derive the NAM point of departure (PoD). The NGRA approach applied also included PBK modelling-facilitated quantitative *in vitro* to *in vivo* extrapolation (QIVIVE). The PBK model describing FLU and HF kinetics in humans was developed using GastroPlus™ and validated against human pharmacokinetic data. PBK model-facilitated QIVIVE was performed to translate the *in vitro* AR-CALUX derived concentration-response data to a corresponding *in vivo* dose-response curve for the anti-androgenicity of FLU, excluding and including the activity of HF (-HF and +HF, respectively). The *in vivo* benchmark dose 5% lower confidence limits (BMDL<sub>05</sub>) derived from the predicted *in vivo* dose-response curves for FLU, revealed a 440-fold lower BMDL<sub>05</sub> when taking the bioactivity of HF into account. Subsequent comparison of the predicted BMDL<sub>05</sub> values to the human therapeutic doses and historical animal derived PoDs, revealed that PBK modelling-facilitated QIVIVE that includes the bioactivity of the active metabolite is protective and provides a more appropriate PoD to assure human safety *via* NGRA, whereas excluding this would potentially result in an underestimation of the risk of FLU exposure in humans.

**Key words:** Risk assessment · 3R compliant method · PBK modelling · anti-androgens · *In vitro/in silico* approaches



## 4.1 Introduction

Many toxicologists have long aimed to replace, reduce, and refine (3Rs) the use of animals for experimentation (Russell & Burch, 1959) in assuring safe levels of human exposure to chemicals. The use of new approach methodologies (NAMs) in next generation risk assessment (NGRA) has become a solution to this goal (US Environmental Protection Agency, 2018). In this context, *in vitro* cell-based assays have been developed and used to quantify toxicodynamic responses of chemicals to predict the potential corresponding *in vivo* responses (P. Carmichael et al., 2009; NRC, 2007) or to define a safe (protective) level of exposure to a chemical agent or ingredient (Baltazar et al., 2020). Ongoing developments seek to translate the *in vitro* responses to the corresponding *in vivo* responses in humans or to determine the ideal battery of NAMs to define safe exposure levels in humans, without aiming to predict levels of expected animal pathology. One particular limitation of simple *in vitro* cell-based systems, however, is that they are rarely able to replicate the toxicokinetics of a compound, as seen in the *in vivo* situation and therefore the exact pattern of exposure at the biological target site (Coecke et al., 2006; Hartung, 2018; Jacobs et al., 2008; Mazzoleni et al., 2009). Metabolic biotransformation, for instance, can result in bioactivation or detoxication of compounds and thus change their potency at their biological target in the human body (Coecke et al., 2006; Gu & Manautou, 2012; Jacobs et al., 2008).

The present study aimed to include, as a proof of principle, the bioactivity of the metabolite hydroxyflutamide (HF, **Figure 4.1**) in an NGRA approach to evaluate the safety of the pharmaceutical anti-androgen flutamide (FLU, **Figure 4.1**) based on a point of departure (PoD) derived from the validated *in vitro* androgen receptor (AR)-CALUX assay (Sonneveld et al., 2005; van der Burg, Winter, Man, et al., 2010). The approach applied included physiologically based kinetic (PBK) modelling-facilitated quantitative *in vitro* to *in vivo* extrapolation (QIVIVE). PBK modelling enables the *in silico* simulation of the absorption, distribution, metabolism and excretion of chemicals in the human body based on physiological, physicochemical, and kinetic parameters. This allows the prediction and subsequent interpretation of concentrations of a parent compound and its relevant metabolites for a certain time-point, route of administration, and dose in specific target organs. Thus, PBK modelling is a useful tool in the translation of *in vitro* concentration-response data to *in vivo* dose-response data (H. Li et al., 2021; Rietjens et al., 2011; Zhang et al., 2018).

In this study, FLU was selected as model compound. FLU is a nonsteroidal anti-androgen used in the treatment for prostate cancer or hirsutism and metabolised to its more anti-androgenic active metabolite HF (**Figure 4.1**) (Calaf et al., 2007; McLeod,

1993; Radwanski et al., 1989; Schulz et al., 1988; Shet et al., 1997). FLU is selected as model compound since it is a well characterized chemical with high human and historical animal data availability to validate the approach. This approach however may also be used to evaluate not just pharmaceutical agents but also other chemicals such as cosmetics, pesticides, and other environmental agents. The hydroxylation of FLU occurs predominantly in the liver and is catalysed by cytochrome P450 (CYP) enzymes. CYP1A2 is the major enzyme responsible for the conversion but CYP1A1, CYP1B1, and CYP3A4 are also involved (Shet et al., 1997; Tevell et al., 2006); Kang et al., 2008). Besides its conversion to HF, FLU is hepatically converted to other metabolites, but no anti-androgenic activity has been reported for these compounds (Shet et al., 1997; Tevell et al., 2006; Kang et al., 2008). Upon its formation, HF is conjugated by hepatic enzymes and excreted in urine (Shet et al., 1997; Tevell et al., 2006; Kostrubsky et al., 2007; Kang et al., 2008). The anti-androgenicity of FLU can be quantified in the AR-CALUX assay (Sonneveld et al., 2005; van der Burg et al., 2010). Given the bioactivity of HF, it is likely that the FLU-dependent anti-androgenic response in humans is to be incompletely predicted if based solely on the results of the *in vitro* AR-CALUX assay, as this metabolism does not occur under the *in vitro* assay conditions. Therefore, the contribution of the bioactivity of HF was included in the PBK modelling-facilitated QIVIVE of the anti-androgenic activity of FLU based on the *in vitro* AR-CALUX assay in order to derive a more *in vivo* relevant PoD. The Michaelis-Menten kinetic parameters for the hydroxylation of FLU to HF and the hepatic clearance ( $CL_{int}$ ) of FLU were obtained following incubations with microsomes from human liver. The  $CL_{int}$  of HF was determined following incubation with the human hepatoma HepaRG cell line (Aninat et al., 2006; Gripon et al., 2002). The PBK model describing FLU and HF kinetics in humans was then developed using GastroPlus™ and validated against human *in vivo* pharmacokinetic data. PBK modelling-facilitated QIVIVE was performed to translate the *in vitro* AR-CALUX derived concentration-response curve for FLU to the corresponding dose-response curves for the anti-androgenicity of FLU, either excluding or including the anti-androgenic activity of HF (-HF and +HF, respectively). Benchmark dose (BMD) analysis of the derived dose-response curves was performed to obtain the *in vivo* benchmark dose 5% lower confidence limits (BMDL<sub>05</sub>) as PoDs for comparison to human therapeutic doses and historical animal derived PoDs of FLU (Calaf et al., 2007; Schellhammer et al., 1998; Zacharia, 2017) to evaluate the use of the NGRA approach to define safe levels of human exposure to FLU.

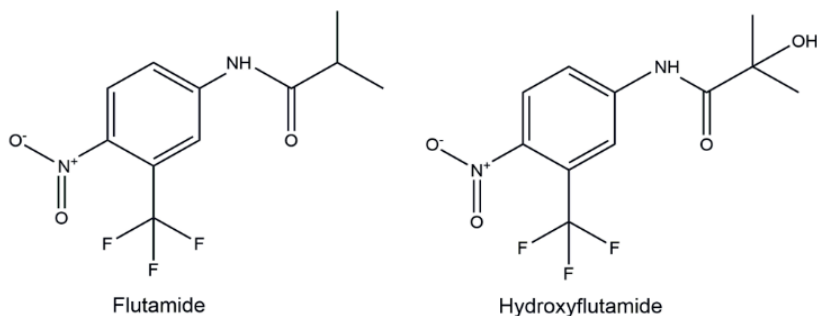


**Figure 4.1.** Structure formulas of flutamide and hydroxyflutamide.

## 4.2 Materials and methods

### 4.2.1 Materials

DHT (CAS no. 521-18-6), FLU (CAS no. 13311-84-7), HF (CAS no. 52806-53-8), tributyltin acetate (TBTa, Cas no. 56-36-0), reduced nicotinamide adenine dinucleotide phosphate (NADPH), alamethicin, magnesium chloride ( $\text{MgCl}_2$ ), sodium phosphate, sodium chloride, human insulin, hydrocortisone 21- hemisuccinate (HCC), and glutamine were purchased from Sigma-Aldrich Chemie B.V. (Zwijndrecht, Netherlands). Penicillin-streptomycin solution was purchased from Invitrogen (Breda, Netherlands). Phosphate-buffered saline (PBS), trypsin EDTA (trypsin (0.025%)/EDTA (0.01%)), Dulbecco's modified Eagle's Medium/Ham's nutrient mixture F12 (DMEM/F12), Phenol Red Free DMEM/F-12, fetal calf serum (FCS), dextran-coated charcoal-treated (DCC) FCS, non-essential amino acids (NEAAs), geneticin (G-418), Williams' E medium (WEM), Phenol Red Free WEM was purchased from Gibco (Paisley, United Kingdom). Dimethyl sulfoxide (DMSO) was purchased from Acros Organics (Geel, Belgium). Low salt buffer (LSB) consisted of 10 mM Tris (Invitrogen), 2 mM dithiothreitol (DTT) (Duchefa Biochemie bv, Haarlem, Netherlands), and 2 mM 1, 2-diaminocyclohexane triacetic acid monohydrate (CDTA) (Fluka, Munich, Germany). The flashmix consisted of 20 mM tricine (Jansen chemica, Landsmeer, Netherlands), 1.07 mM  $(\text{MgCO}_3)_4\text{Mg}(\text{OH})_2 \cdot 5\text{H}_2\text{O}$  (Sigma-Aldrich, 99% purity), 2.67 mM magnesium sulphate ( $\text{MgSO}_4$ ) (Ridel de Haën, Landsmeer, Netherlands), 0.1 mM ethylenedinitrilotetraacetic acid disodium salt dihydrate (Titriplex III; Merck, Amsterdam, Netherlands), 2 mM DTT (Duchefa Biochemie), 0.47 mM D-luciferin (Duchefa Biochemie), and 5 mM adenosine-5' -triphosphate (ATP, Boehringer, Alkmaar, Netherlands). Acetonitrile (ACN) was purchased from Biosolve (Valkenswaard, Netherlands).

## 4.2.2 Methods

Performing the PBK modelling-facilitated QIVIVE of FLU without and with the contribution of HF bioactivity (-HF and +HF, respectively), the following steps were defined:

1. Determination of *in vitro* concentration-response data of FLU and HF in the AR-CALUX assay.
2. PBK model development describing FLU and HF kinetics in humans.
3. Sensitivity analysis and PBK model validation with population simulation.
4. PBK modelling-facilitated QIVIVE translating the *in vitro* concentration-response data to *in vivo* dose-response data, -HF and +HF.
5. BMD analysis of the predicted dose-response data and comparison to relevant *in vivo* doses.

### 4.2.2.1 *Determination of in vitro Concentration-Response Data of FLU and HF in the AR-CALUX Assay*

#### 4.2.2.1.1 Cell culture

Cells from the stably transfected human osteosarcoma (U2OS) cell line expressing the human AR (BioDetection Systems (BDS), Amsterdam, Netherlands) were maintained in DMEM/F-12 supplemented with 10% FCS, 1% NEAAs, 10 units/mL penicillin, 10 µg/mL streptomycin, and 0.2 mg/mL G-418 in an incubator (37°C, 5% CO<sub>2</sub>, 100% humidity). The cells were routinely subcultured when reaching 85–95% confluency (i.e., every 3–4 days) using trypsin-EDTA.

#### 4.2.2.1.2 AR-CALUX assay

The AR-CALUX assay used to obtain the concentration-response curves of FLU and HF was performed as described previously (Sonneveld et al., 2005; van der Burg et al., 2010). Briefly, the AR-CALUX U2OS cells were plated in white, clear-bottomed 96-well plates at a density of  $1 \times 10^5$  cells/mL in a volume of 100 µL/well assay medium consisting of Phenol Red Free DMEM/F-12 supplemented with 5% DCC-FCS, 1%

NEAAs, 10 units/mL penicillin, and 10 µg/mL streptomycin. The outer wells were left empty to be loaded with 200 µL PBS to prevent evaporation of the assay medium. The cells were plated for 24 h in an incubator (37°C, 5% CO<sub>2</sub>, 100% humidity) after which 100 µL of the assay medium was refreshed and the cells were placed again for 24 h in an incubator (37°C, 5% CO<sub>2</sub>, 100% humidity). Next, the assay medium was aspirated and the cells in each well were exposed for 24 h in an incubator (37°C, 5% CO<sub>2</sub>, 100% humidity) to 100 µL assay medium containing the assigned concentration of the corresponding compound, the exposure medium. A concentration range of DHT (0.01–100 nM) (added from 1,000 times concentrated stock solutions in DMSO, prepared in 2 mL exposure medium), the vehicle control (0.1% DMSO) and the cytotoxicity control (10 µM TBT) were tested in triplicates in the agonism assay. A concentration range of FLU (0.03–300 µM) or HF (0.001–30 µM) (added from 2000 times concentrated stock solutions in DMSO, prepared in 2 mL exposure medium), the vehicle control (0.1% DMSO) and the cytotoxicity control (10 µM TBT) were all tested in triplicates in the antagonism assay. In the antagonism assay, the assay medium was supplemented with the EC<sub>50</sub> (1 nM) of the agonist DHT (added from a 2000 times concentrated stock solution in DMSO, prepared in the 2 mL exposure medium). After the exposure medium was aspirated, the cells were washed with 100 µL PBS in MilliQ water (1:1) and lysed with 30 µL LSB. After a 30 min arrest on ice, plates were stored overnight in –80° C. Luminescence was measured using the GloMax 96 Microplate luminometer (Promega Benelux, Leiden, Netherlands) wherein 100 µL flash mix containing ATP and luciferin was automatically added to each well. Cytotoxicity was measured using cytotox CALUX cells (U2OS cell line expressing a constitutive active luciferase reporter gene [BDS, Amsterdam, Netherlands (Van der Linden et al., 2014)], following the same protocol. The data presented are from three independent studies executed in technical triplicates.

#### 4.2.2.1.3 Data analysis

Antagonism was defined as a > 20% decrease in the relative induction of the DHT induced response at a non-cytotoxic concentration of FLU or HF in the AR-CALUX cells. The test concentrations tested in the cytotox CALUX cells were similar to those tested in the AR-CALUX assay and considered as cytotoxic when the relative induction of the test condition decreased more than 15% compared to the solvent control set at 100%. For these samples the observed reduction in luminescence was considered not to be due to antagonism and excluded from the analysis. The IC<sub>50</sub> values of FLU and HF were modelled with a nonlinear regression of log (inhibitor) vs. response (four parameters) model using GraphPad Prism 5 (GraphPad, San Diego, United States). A statistical comparison was made between the concentration-response curves of FLU and HF to

check whether they are parallel. This was achieved with the option “Do the best fit values of selected parameters differ between data sets” of the nonlinear regression of log (inhibitor) vs. response (four parameters) model of GraphPad Prism 5.

#### 4.2.2.2 PBK Model Development Describing FLU and HF Kinetics in Humans

The PBK model describing FLU and HF kinetics upon FLU exposure in humans was developed using the commercially available software GastroPlus™ version 9.8 (Simulation Plus Inc., Lancaster, CA, United States). The built-in Population Estimates for Age-Related (PEAR) Physiology™ module was used to parameterize for different human physiologies for model development and validation based on available human *in vivo* pharmacokinetic data reported from literature (Doser et al., 1997; Radwanski et al., 1989) to constantly match the target population. In GastroPlus, the options are to parameterize for a population of Americans, Japanese, or Chinese. To resemble a Caucasian population used in Radwanski et al. (1989) and Doser et al. (1997), the PBK model was parameterized for an American population. The chemical-specific parameters were collected from literature, PubChem databases (Kim et al., 2016), or predicted from chemical structure with the built-in ADMET Predictor™ version 9.6 (Simulation Plus Inc., Lancaster, CA) (**Table 4.1**).

The effective permeability ( $p_{\text{eff}}$ ) of FLU was simulated from the Caco-2 value, derived from the *in vitro* colorectal adenocarcinoma cell intestinal permeability assay (Van Breemen & Li, 2005), reported by Zuo et al. (2000) using the built-in conversion equation based on the Absorption Systems Caco-2 calibration (ABSCa). The distribution of FLU and HF into tissues was assumed to be perfusion limited and the tissue: plasma partition coefficients ( $K_{\text{ps}}$ ) were calculated with the Lucakova method (GastroPlus; Rodgers et al., 2005, Rodgers and Rowland, 2006).

**Table 4.1.** Input parameters of the PBK model describing FLU and HF kinetics in humans. MW = molecular weight. LogP = partition coefficient. pKa = dissociation constant.  $P_{\text{eff}}$  = effective permeability.  $f_{\text{ub in vivo}}$  = fraction unbound *in vivo*.  $R_{\text{b2p}}$  = blood:plasma ratio.

Parameters	FLU	HF
MW (g/mol)	276.22 <sup>a</sup>	292.21 <sup>a</sup>
LogP	3.35 <sup>a</sup>	2.70 <sup>a</sup>
Solubility at 25 ° C (mg/mL)	5.7*10 <sup>-3</sup> <sup>b</sup>	0.16 <sup>c</sup>
pKa	Acid 10.54 <sup>b</sup> Base 0.83 <sup>b</sup>	Acid 0.84 <sup>b</sup>
$P_{\text{eff}}$ (x 10 <sup>-4</sup> cm/s)	5.25 <sup>d</sup>	
$f_{\text{ub in vivo}}$	0.20 <sup>b</sup>	0.32 <sup>b</sup>
$R_{\text{b2p}}$	0.83 <sup>b</sup>	0.84 <sup>b</sup>

<sup>a</sup> Kim et al. (2016)

<sup>b</sup> ADMET predictor™

<sup>c</sup> Wishart et al. (2007)

<sup>d</sup> Zuo et al. (2000)

#### 4.2.2.2.1 *In vitro* Incubations of FLU and HF to Derive Kinetic Parameters

##### 4.2.2.2.1.1 HLM incubations

To obtain the Michaelis-Menten parameters for the hepatic hydroxylation of FLU to HF, FLU was incubated with human liver microsomes (HLM), pooled from 50 donors, male and female (M0317, Sigma–Aldrich Chemie B.V. Zwijndrecht, Netherlands) adapting the method described by Kang et al. (2008). Prior to the kinetic study, the incubation time and HLM concentration were optimized (data not shown) to determine the conditions where the metabolite formation was linear with time and the amount of HLM. FLU (1–50  $\mu\text{M}$  final concentration added from 100 times concentrated stock solutions in DMSO) was incubated for 15 min in a water bath (37° C) in a reaction mixture consisting of 0.1 M potassium phosphate (pH 7.4), 0.8 mg/mL HLM, 1 mM NADPH, and 5 mM  $\text{MgCl}_2$  in a final volume of 200  $\mu\text{L}$ . Reaction mixtures wherein the volume of NADPH was replaced by an equal volume of potassium phosphate (pH 7.4) served as blanks. Prior to adding the substrate to the reaction mixtures, the mixtures were pre-incubated for 1 min in a water bath (37°C). Likewise, 1  $\mu\text{M}$  FLU was incubated over time (0–30 min) in the same reaction mixtures to obtain the  $\text{CL}_{\text{int}}$  of FLU. The reactions were terminated by addition of 100  $\mu\text{L}$  cold acetonitrile (ACN) followed by a 30 min arrest on ice. After centrifugation

(4°C) for 10 min at  $15,000 \times g$  (CT 15RE, Hitachi Koki Co., Ltd.), 100  $\mu\text{L}$  supernatant was collected for LC-MS/MS analysis for HF or FLU quantification, respectively. The data presented are from three independent studies executed in technical duplicates.

#### 4.2.2.2.1.2 HepaRG cell culture

To  $CL_{\text{int}}$  of HF was obtained using the hepatoma HepaRG cell line (undifferentiated HepaRG cells were purchased from Biopredic International, HPR101, p12 Rennes, France), since no clearance was observed in HLM or human S9 incubations (data not shown). In light of the scope of this work, the incubations were performed with HepaRG cells differentiated *in vitro* to hepatocyte- and cholangiocyte-like cells (1:1) (Aninat et al., 2006; Gripon et al., 2002). To this end, cryopreserved undifferentiated HepaRG cells were thawed and grown in T75 flasks in culture medium consisting of WEM supplemented with 10% FCS, 100 units/mL penicillin, 100  $\mu\text{g}/\text{ml}$  streptomycin, 2 mM glutamine, 50  $\mu\text{M}$  HCC, and 5  $\mu\text{g}/\text{mL}$  human insulin for approximate 2 weeks and placed in an incubator (37°C, 5%  $\text{CO}_2$ , 100% humidity). The culture medium was refreshed every 2–3 days until 80–90% confluency was reached. Then, the cells were plated at a density of  $2 \times 10^5$  cells/well in 6 well plates in a volume of 2 mL in culture medium and placed in an incubator (37°C, 5%  $\text{CO}_2$ , 100% humidity). The culture medium was refreshed every 2–3 days until 80–90% confluency was reached before initiating the differentiation of the cells. At day 1 of the differentiation, the culture medium was supplemented with 1.7% DMSO. After two days, the culture medium was supplemented with 2% DMSO (differentiation medium) which was refreshed every 2–3 days until day 14 at which HepaRG cells are known to be fully differentiated (Aninat et al., 2006; Gripon et al., 2002).

#### 4.2.2.2.1.3 HepaRG cell incubations

The differentiated HepaRGs were washed 2 times with assay medium consisting of Phenol Red Free WEM supplemented with 100 units/mL penicillin, 100  $\mu\text{g}/\text{ml}$  streptomycin, 2 mM glutamine, 50  $\mu\text{M}$  HCC, and 5  $\mu\text{g}/\text{mL}$  human insulin. Next, HepaRG cells were exposed to 2 mL assay medium consisting of 0.1  $\mu\text{M}$  HF (final concentration added from a 1,000 times concentrated stock solution in DMSO) or the vehicle control (0.1% DMSO) in triplicate and incubated for 0, 2, 4, 6, and 24 h. After each timepoint, 100  $\mu\text{L}$  supernatant was transferred to vials for LC-MS/MS analysis. A similar experiment was conducted in sync using cell free plates to serve as blanks. After the 24 h timepoint, the cells of each well were washed 2 times with 1 ml PBS and once with 0.5 mL trypsin-EDTA. After 2–3 min, the cells were resuspended with 2 mL assay medium and collected in Eppendorf tubes for cell counting using a Cellometer® (Nexcelom



Bioscience, Lawrence, MA, United States). The data presented are from two independent studies.

#### 4.2.2.2.1.4 Quantification of FLU and HF using LC-MS/MS

The detection and quantification of FLU and HF in the supernatant following the incubations were performed using a Shimadzu LCMS-8045 mass spectrometer (Kyoto, Japan), operating under negative electrospray ionization (ESI) conditions. Chromatographic separation was performed on a Kinetic® 1.7  $\mu\text{m}$  C18 100 Å column (50  $\times$  2.1 mm) (Phenomenex, Torrance, CA, United States). The column and autosampler temperature were set at 40° C and 5°C, respectively. The injection volume was 1  $\mu\text{L}$  at a flow rate of 0.3 mL/min. The mobile phase A consisted of MilliQ water with 0.1% (v/v) formic acid. Mobile phase B was ACN with 0.1% (v/v) formic acid. The following gradient was used: 0–7 min linear increase from 0% B to 100% B, 7–8 min 100% B, 8–9 min back to initial conditions of 0% B. Subsequently, the column was re-equilibrated for 4 min at 0% B before the next injection. The acquisition parameters of FLU and HF are summarized in Supplementary Material S4.1.

#### 4.2.2.2.1.5 Calculation of Kinetic Parameters of FLU and HF

Michaelis-Menten equation (Eq. 1) was used to calculate the  $V_{\text{max}}$  and  $K_{\text{m}}$  of the hydroxylation of FLU to HF by HLM.

$$\text{Eq. 1} \quad v = \frac{V_{\text{max}} * [S]}{(K_{\text{m}} + [S])}$$

In this equation  $v$  represents the reaction rate expressed in nmol/min/mg microsomal protein,  $V_{\text{max}}$  the apparent maximum rate in nmol/min/mg microsomal protein,  $S$  the substrate concentration in  $\mu\text{M}$ , and  $K_{\text{m}}$  the Michaelis-Menten constant in  $\mu\text{M}$ . The calculation was executed with GraphPad Prism 5 (GraphPad, San Diego, United States). To determine the  $CL_{\text{int}}$  of FLU, a depletion curve of the measured concentrations over time following the incubation with HLM was constructed by plotting the  $\ln(C_{\text{compound}}/C_{\text{blank}})$  versus time. The elimination rate constant  $k$  ( $\text{min}^{-1}$ ) is obtained from the slope of the linear part of this depletion curve.  $C_{\text{compound}}$  and  $C_{\text{blank}}$  are the remaining concentration of the compounds after the incubation in the incubation samples or the corresponding blanks, respectively. Next the  $CL_{\text{int}}$  value of FLU (expressed in  $\mu\text{L}/\text{min}/\text{mg}$  microsomal protein) was calculated following Eq. 2.

$$\text{Eq. 2} \quad \text{CL}_{\text{int}} = k * \frac{V}{P (\text{HLM})}$$

In this formula  $k$  represents the elimination rate constant ( $\text{min}^{-1}$ ),  $V$  presents the incubation volume ( $\mu\text{L}$ ) and  $P$  (HLM) the amount of microsomes (mg microsomal protein) in the incubation mixture. The  $V_{\text{max}}$  and  $\text{CL}_{\text{int}}$  following HLM incubations with FLU were scaled to whole human liver assuming an HLM protein concentration of 34 mg/g liver and a liver weight of 1.58 kg (females) or 1.84 kg (males) (GastroPlus suggested default values). To determine the  $\text{CL}_{\text{int}}$  of HF a depletion curve was constructed of the measured concentrations over time following the HepaRG incubations. The  $\text{CL}_{\text{int}}$  of HF (expressed in  $\mu\text{L}/\text{min}/\text{million cells}$ ) was calculated following Eq. 3.

$$\text{Eq. 3} \quad \text{CL}_{\text{int}} = k * \frac{V}{P (\text{cell})}$$

In this equation  $k$  represents the elimination rate constant ( $\text{min}^{-1}$ ),  $V$  presents the incubation volume ( $\mu\text{L}$ ) and  $P$  (cell) represents the cell amount per well expressed per million liver cells. The  $\text{CL}_{\text{int}}$  was scaled to whole human liver based on hepatocyte scaling factors (Punt et al., 2019) embodying 120 million hepatocytes/g liver and a liver weight of 1.58 kg (females) or 1.84 kg (males). It was assumed that the scaling factor expressed per million hepatocytes would be valid to translate the  $\text{CL}_{\text{int}}$  for the HepaRG liver cells to the whole liver, an assumption supported by the fact that the metabolic capacity of HepaRGs has been frequently reported to resemble that of human primary (Gripon et al., 2002; Punt et al., 2019; Zanelli et al., 2012).

The PBK model was parameterized for a fasted 30 year old female with a body weight of 75.57 kg to consistently match *in vivo* pharmacokinetic data reported from females by Doser et al. (1997). Simulations were carried out and the  $V_{\text{max}}$  of FLU hydroxylation to HF was further optimized by visual examination until the prediction of the time-dependent plasma concentrations of FLU and HF consistently matched the *in vivo* pharmacokinetic data (Doser et al., 1997) to confirm the model development.

#### 4.2.2.3 Sensitivity Analysis and PBK Model Validation With Population Simulation

##### 4.2.2.3.1 Sensitivity Analysis

A sensitivity analysis was performed to indicate which parameters are most influential on the prediction of the maximum plasma concentration ( $C_{\text{max}}$ ) and area under the concentration time curve (AUC) of FLU and HF upon an oral dose regimen of 250 mg

FLU at the first day and 250 mg three times a day through day 2–8, later denoted as the repeated dose model (Radwanski et al., 1989). The PBK model was parameterized for a 30 year old American male with a body weight of 70 kg, to estimate a standard human (Brown et al., 1997), and the sensitivity analysis was executed with the built-in parameter sensitivity analysis (PSA) mode of GastroPlus. The sensitivity coefficients (SCs) for the  $C_{\max}$  and AUC of FLU and HF were calculated as the % change in model outcome divided by the % change in parameter value (Eq. 4).

$$\text{Eq. 4} \quad \text{SC} = \frac{\% \text{ change in model outcome}}{\% \text{ change in parameter value}}$$

The % change in parameter value was set at 5% for one parameter at a time (Zhang Q. et al., 2018; Moxon et al., 2020). Parameters with a SC > 0.1 or < -0.1 were considered to be influential on the prediction of the  $C_{\max}$  and AUC of FLU and HF (Zhang et al., 2018).

#### 4.2.2.3.2 PBK Model Validation With Population Simulation

Next, the developed PBK model describing FLU and HF kinetics in humans upon FLU exposure was parameterized for a 66 year old male with a body weight of 89 kg for validation of the predictions by the repeated dose model, an oral dose regimen of 250 mg FLU at the first day and 250 mg three times a day through day 2–8, against reported data following repeated exposure (Radwanski et al., 1989). Population simulation of the repeated dose model in humans was carried out using the GastroPlus built-in population simulator, based on the Monte Carlo method, to obtain the distribution in the predicted time-dependent plasma concentrations of the FLU and HF over a healthy American population. Default distributions of the Population Estimates for Age Related Physiology (PEAR) were used for an American population of 100 healthy American (with 50: 50 ratio of male: female) of 20–80 years old with a body weight of 50–110 kg. The number of iterations was set at 300 and simulation time at 288 h to reach the  $C_{\max}$  values. The PBK model is defined valid when the predicted FLU and HF kinetics in humans are within the acceptance criteria predicting the  $C_{\max}$  values within a 2-fold difference of the corresponding literature reported  $C_{\max}$  values (Jones et al., 2015).

#### 4.2.2.4 *PBK Modelling-Facilitated QIVIVE Translating the In vitro Concentration-Response Data to In vivo Dose-Response Data, – and +HF*

PBK modelling-facilitated QIVIVE was performed to translate the *in vitro* AR-CALUX derived concentration-response curve of FLU to the corresponding *in vivo* dose-

response curves, either without or with taking the effect of HF into account (-HF and +HF). The PBK model was parameterized for a 30 year old American male with a body weight of 70 kg to estimate a standard human (Brown et al., 1997). Simulations were carried out with the repeated dose model with a simulation time of 288 h in order to reach steady state of the  $C_{max}$ . In the QIVIVE, it is assumed that the free *in vitro* effect concentrations are equal to the free *in vivo*  $C_{max}$ .

#### 4.2.2.4.1 2.2.4.1 QIVIVE -HF

Performing the QIVIVE -HF, the nominal concentrations of FLU from the *in vitro* AR-CALUX assay were corrected for *in vitro* protein binding to obtain the free *in vitro* concentrations, following Eq. 5.

$$\text{Eq. 5} \quad \text{free } in \text{ vitro concentration FLU} = \text{nominal } in \text{ vitro concentration FLU} * f_{ub \text{ in vitro, FLU}}$$

The nominal *in vitro* concentrations of FLU were derived from the AR-CALUX assay and the  $f_{ub \text{ in vitro, FLU}}$  represents the fraction unbound in the medium used in the AR-CALUX assay amounting to 0.50 for FLU (van Tongeren et al., 2021). Next, the free *in vitro* concentrations of FLU were assumed equal to the free  $C_{max}$  values of FLU at steady state. Using the developed PBK model, the FLU doses were simulated that are required to reach the corresponding free  $C_{max}$  values at steady state, generating the dose-response curve for the anti-androgenic activity of FLU -HF.

#### 4.2.2.4.2 QIVIVE +HF

Performing the QIVIVE of the *in vitro* AR-CALUX derived concentration-response curve to generate a dose-response curve for the anti-androgenic effect of FLU taking the activity of HF into account, a toxic equivalency factor (TEF) approach (Zhao et al., 2021) was included in the PBK model to predict the combined free  $C_{max}$  values of FLU and HF expressed in FLU equivalents (Eq. 6).

Eq. 6

$$\text{Combined free } C_{max} \text{ of FLU and HF expressed in FLU equivalents} = C_{max, \text{FLU}} * f_{ub \text{ in vivo, FLU}} * \text{TEF}_{\text{FLU}} + C_{max, \text{HF}} * f_{ub \text{ in vivo, HF}} * \text{TEF}_{\text{HF}}$$

The  $C_{\max}$ , FLU and  $C_{\max}$ , HF are the maximum plasma concentration of FLU and HF, respectively. The  $f_{ub}$  *in vivo*, FLU and the  $f_{ub}$  *in vivo*, HF are the fraction unbound *in vivo* of FLU and HF (**Table 4.1**). The  $TEF_{FLU}$  and  $TEF_{HF}$  correspond to the toxic equivalency factor of FLU and HF, respectively. The  $TEF_{FLU}$  was equalized to 1.0 whereas  $TEF_{HF}$  was calculated following Eq. 7.

$$\text{Eq. 7} \quad TEF_{HF} = \frac{IC_{50} \text{ FLU}}{IC_{50} \text{ HF}}$$

To use this TEF approach, 3 criteria need to be met (Zhao et al., 2021). First, FLU and HF act *via* the same mode of action. Second, the concentration-response curves in the AR-CALUX assay of FLU and HF are parallel. Third, the toxicity of FLU and HF in the AR-CALUX assay is additive. If the data are compliant to these criteria, QIVIVE +HF is performed. The free *in vitro* concentrations of FLU obtained from the *in vitro* AR-CALUX assay were then set equal to the combined free  $C_{\max}$  of FLU and HF expressed in FLU equivalents in the PBK model. Next, the FLU doses that are required to obtain the corresponding combined free  $C_{\max}$  of FLU and HF expressed in FLU equivalents were simulated using the PBK model. This generates the dose-response curve of the anti-androgenic activity of FLU +HF.

#### 4.2.2.5 BMD Analysis of the Predicted Dose-Response Data and Comparison to Relevant *In vivo* Doses

BMD analysis was performed for the predicted dose-responses of FLU – and +HF to define the  $BMDL_{05}$ , and the upper bound of the 95% confidence interval of the benchmark dose at a 5% extra response compared to the background ( $BMDU_{05}$ ) values using the BMDS3.2.1 software (US EPA). When the  $BMDU_{05}$ :  $BMDL_{05}$  ratio (precision factor) was below 3 and the p-value > 0.05, support for a dose-response was indicated and the  $BMDL_{05}$  value was accepted (US Environmental Protection Agency, 2012; European Food Safety Authority et al., 2017). The  $BMDL_{05}$  values were then compared to the therapeutic dose of 250 mg FLU 3 times per day for the treatment of prostate cancer (Schellhammer et al., 1998) and 125 mg FLU per day for the treatment of hirsutism (Calaf et al., 2007). Furthermore, a comparison was made with PoDs defined for FLU exposure. To this end, a literature search was conducted to collect available. So include a PODs to FLU exposure from animal studies. Then it was checked whether these studies comply with the most up to date evaluation and assessment criteria of the current testing guidelines and whether the same conclusion in terms of the reference values could be made. Only the no observed adverse effect level (NOAEL) values obtained from the studies that met these criteria (Zacharia, 2017) were used for

comparison, following the OECD protocol 407 for a 28 days toxicity study in rats incorporating the Hershberger bioassay (OECD, 2008), the OECD protocol 441 for the Hershberger bioassay in rats (OECD, 2009), or the OECD protocol 421 for the Reproduction/Developmental Toxicity Screening Test (OECD, 2016).

## 4.3 Results

### 4.3.1 Determination of *in vitro* Concentration-Response Data of FLU and HF in the AR-CALUX Assay

The *in vitro* concentration-response curves for the anti-androgenic activity of FLU and HF in the AR-CALUX assay are depicted in **Figure 4.2**. The nominal  $IC_{50}$  values of FLU and HF equalled 1.14 and 0.05  $\mu\text{M}$ , respectively. The statistical comparison between the concentration-response curves of FLU and HF confirmed that they run parallel with a hillslope of  $-1.247$  and  $-1.354$ , respectively (p value = 0.6985).

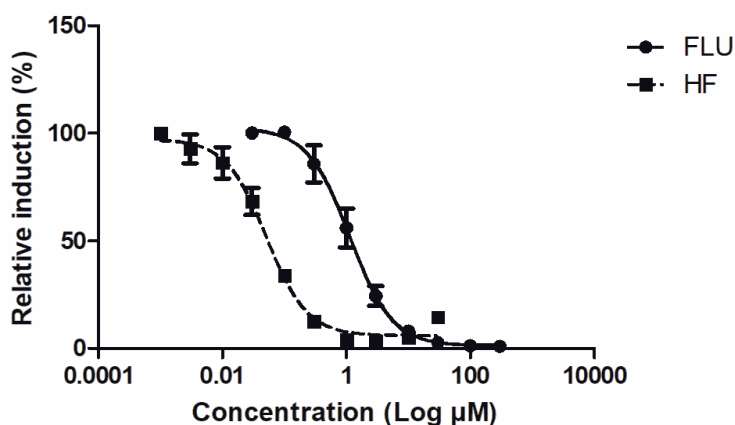


**Figure 4.2.** The concentration-dependent antagonistic activity of FLU (solid line and circles) and HF (dashed line and squares), on the DHT-mediated luciferase induction in the U2OS AR-CALUX reporter gene assay. The symbols present the mean  $\pm$  SD values of 3 independent studies.

### 4.3.2 PBK Model Development Describing FLU and HF Kinetics in Humans

To enable PBK modelling-facilitated QIVIVE of the anti-androgenic response of FLU, - and +HF, a PBK model was developed describing FLU and HF kinetics in humans. Parameters describing hepatic metabolism of FLU and HF were determined *in vitro*.

#### 4.3.2.1 *In vitro* Incubations of FLU and HF to Derive Kinetic Parameters

The kinetic parameters for the hepatic hydroxylation of FLU to HF were obtained by incubation of FLU with pooled HLM. **Figure 4.3** shows the Michaelis-Menten kinetics of FLU conversion to HF. The corresponding  $V_{max}$  and  $K_m$  values and the HLM incubation derived  $CL_{int}$  value of FLU are summarized in **Table 4.2**. The  $V_{max}$  was further optimized by visual examination until the prediction of the time-dependent plasma concentrations of FLU and HF consistently matched the *in vivo* pharmacokinetic data (Doser et al., 1997) (**Figure 4.5A**). The  $CL_{int}$  value of HF was obtained following incubations with HepaRGs (**Table 4.2**). The cell count after 24 h of HF incubation with HepaRGs revealed 0.61 million cells/incubation and this value was used to calculate the  $CL_{int}$  of HF. All kinetic values were scaled to whole human liver in the PBK model as described in the Materials and methods section.

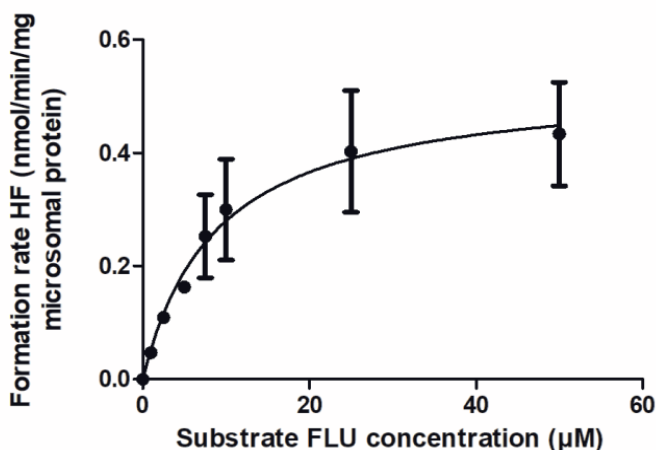


**Figure 4.3.** CYP-mediated formation rate of HF following HLM incubations with FLU. The symbols present the mean  $\pm$  SEM values of 3 independent studies.

**Table 4.2.** Kinetic parameters of hepatic metabolism of FLU and HF.

Kinetic parameter	Value <i>in vitro</i>
$V_{\max}$ FLU to HF	$0.53 \pm 0.08$ nmol/min/mg protein
Optimized $V_{\max}$ FLU to HF <sup>a</sup>	0.27 nmol/min/mg protein
$K_m$ FLU to HF	$8.85 \pm 3.64$ $\mu$ M
$CL_{\text{int}}$ FLU	$116.63 \pm 15.61$ $\mu$ L/min/mg protein
$CL_{\text{int}}$ HF	$10.18 \pm 0.50$ $\mu$ L/min/million cells

<sup>a</sup> Optimized value by visual examination until the prediction of the time-dependent plasma concentrations of FLU and HF consistently matched the *in vivo* pharmacokinetic data (Doser et al., 1997) (**Figure 4.5A**).

### 4.3.3 Sensitivity Analysis and PBK Model Validation With Population Simulation

#### 4.3.3.1 Sensitivity Analysis

The PBK model was parameterized for a 30 year old American male with a body weight of 70 kg to estimate a standard human (Brown et al., 1997) and the sensitivity analysis was conducted on the repeated dose model for evaluation. **Figure 4.4** depicts the SCs of parameters as identified being most influential ( $SC > 0.1$  or  $< -0.1$ ) on the model outcomes for  $C_{\max}$  and the AUC of FLU and HF. The PBK model prediction of the  $C_{\max}$  of FLU is sensitive to the solubility, permeability, LogD,  $f_{\text{ub } in vivo}$ , and  $CL_{\text{hep}}$  of FLU, the  $V_{\max}$  and  $K_m$ , and the  $f_{\text{ub } in vivo}$  and  $CL_{\text{hep}}$  of HF. The prediction of the AUC of FLU is sensitive to the LogD,  $f_{\text{ub } in vivo}$ , and  $CL_{\text{hep}}$  of FLU, and the  $V_{\max}$  and  $K_m$ . Influential parameters on the prediction of the  $C_{\max}$  and AUC of HF are the  $CL_{\text{hep}}$  of FLU, the  $V_{\max}$  and  $K_m$ , and the  $f_{\text{ub } in vivo}$  and  $CL_{\text{hep}}$  of HF.



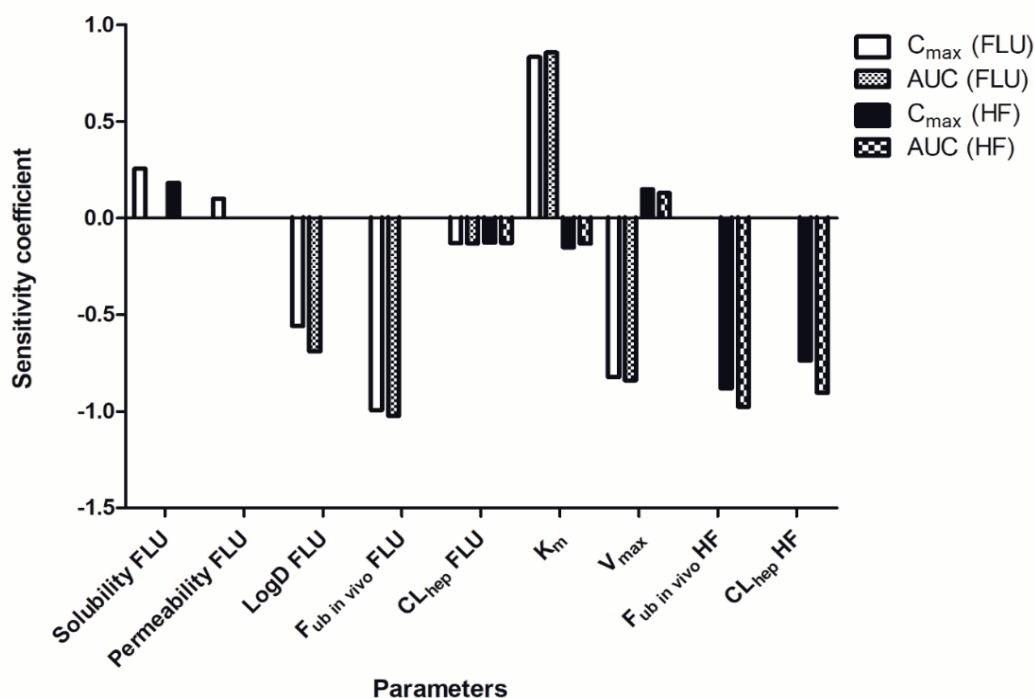


**Figure 4.4.** Sensitivity analysis of the parameters of the PBK model describing FLU and HF kinetics in humans by the repeated dose model. Only parameters with a SC > 0.1 or < -0.1 for predicting the  $C_{max}$  and AUC of FLU and HF are presented. Permeability = intestinal permeability. LogD = distribution coefficient.  $f_{ub}$  *in vivo* = fraction unbound *in vivo*.  $CL_{hep}$  = hepatic clearance.  $V_{max}$  =  $V_{max}$  of FLU conversion to HF.  $K_m$  =  $K_m$  of FLU conversion to HF.

#### 4.3.3.2 PBK Model Validation With Population Simulation

To further evaluate the developed PBK model describing FLU and HF kinetics in humans with the optimized  $V_{max}$  value of FLU conversion to HF, model predictions were compared with reported human *in vivo* pharmacokinetic data (Radwanski et al., 1989; Doser et al., 1997). **Figure 4.5A** shows the predicted and literature reported time-dependent total plasma concentrations of FLU and HF following a single oral dose of 250 mg FLU. **Figures 4.5B, C** show the predicted and literature reported time-dependent total plasma concentrations following the repeated dose model, including the distribution of the predictions over a healthy American population. Comparison indicates that the PBK model predicts the time-dependent total plasma concentrations of FLU and HF within the acceptance criteria, i.e., predicting the  $C_{max}$  values within a 2-fold difference of the corresponding literature reported  $C_{max}$  values (Jones et al., 2015).

Furthermore, the distribution of the predicted plasma concentrations of FLU and HF following the repeated dose model in a healthy American population was quantified by dividing the 95th percentile by the geometric mean amounting to 1.22  $\mu\text{g}/\text{mL}$  and 1.37  $\mu\text{g}/\text{mL}$  and of FLU and HF respectively. Additionally, the coefficient of variation (CV) which compares the standard deviation to the mean of predicted time-dependent total plasma concentrations was calculated amounting to 13% and 23% for FLU and HF, respectively. This indicates there is a somewhat wider distribution of the HF plasma concentrations in the PBK model predictions than of the FLU concentrations.

#### 4.3.4 PBK Modelling-Facilitated QIVIVE Translating the *in vitro* Concentration-Response Data to *in vivo* Dose-Response Data, – and +HF

This work is compliant to the three criteria set since, firstly, FLU and HF both inhibit the AR (**Figure 4.2**). Secondly, the concentration-response curves of FLU and HF in the AR-CALUX are parallel. Thirdly, the toxicity of FLU and HF in the AR-CALUX are additive (Supplementary Material S4.2).

##### 4.3.4.1 QIVIVE –and +HF

The free *in vitro* concentrations of FLU were obtained by correcting for protein binding. These were set equal to the free  $C_{\text{max}}$  of FLU or the combined free  $C_{\text{max}}$  of FLU and HF expressed in FLU equivalents, the  $\text{TEF}_{\text{FLU}}$  being set at 1 and the  $\text{TEF}_{\text{HF}}$  calculated as 23 (Eq. 7). Using the developed PBK model, the corresponding FLU doses to reach those  $C_{\text{max}}$  values were predicted. **Figure 4.6** shows the predicted *in vivo* dose-response curve for the anti-androgenic effects following FLU exposure in humans, –HF and +HF. A clear left-shift in the predicted dose-dependent anti-androgenic effect of FLU is observed, indicating that FLU appears to be more potent once the formation and activity of HF is taken into account.

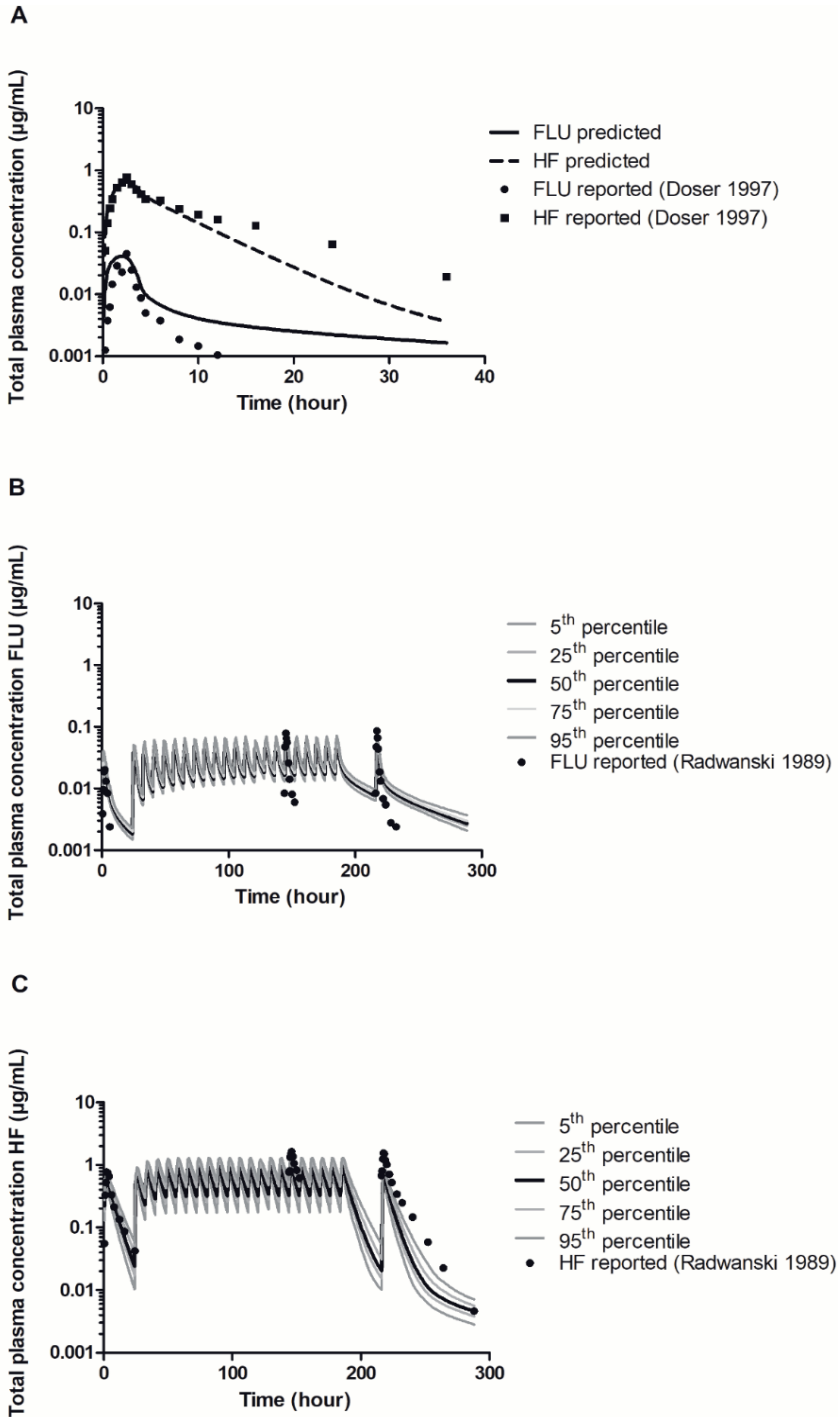


**Figure 4.5.** A. PBK model predicted (line and dashed line) and reported (circles and squares) time-dependent total plasma concentrations of FLU and HF following a single oral dose of 250 mg FLU (experimental data from Doser et al., 1997) in humans for

model development. Prediction was obtained after optimization of the  $V_{\max}$  against reported data (Doser et al., 1997). **B** and **C**. PBK model predicted and reported (circles) time-dependent total plasma concentrations of FLU and HF, respectively, following an oral dose regimen of 250 mg FLU at the first day and 250 mg three times a day through day 2–8 (repeated dose model) (experimental data from Radwanski et al., 1989) for model validation, including the distribution of the predictions among an American healthy population. The 5th and 95th percentiles and the 25th and 75th percentiles of the predictions are presented as dark grey and light grey lines, respectively, the 50th percentile presented by the black lines.

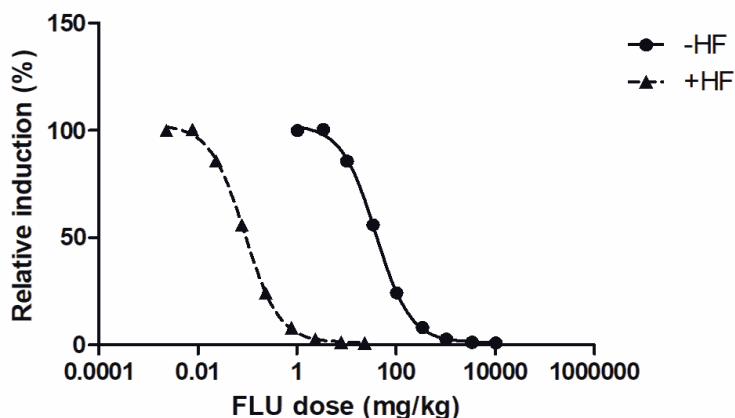


**Figure 4.6.** The PBK modelling-facilitated QIVIVE predicted *in vivo* dose-dependent anti-androgenic effects following FLU exposure –HF (solid line and triangles) and +HF (dashed line and squares) in humans.

#### 4.3.5 BMD Analysis of the Predicted Dose-Response Data and Comparison to Relevant *in vivo* Doses

To evaluate the predicted dose-dependent anti-androgenic effects of FLU, – and +HF, BMD analysis was performed (Supplementary Material S4.3). The predicted  $BMDL_{05}$  of the anti-androgenic effects of FLU –HF and +HF amounted to 3.08 mg/kg and 0.007 mg/kg, respectively. This indicates that when including the activity of HF in the PBK model, QIVIVE of the *in vitro* anti-androgenic response of FLU results in a  $BMDL_{05}$  value that is 440-fold lower compared to the value obtained when the activity of HF is excluded. Such a difference can be expected given that HF was 23 times more potent in the *in vitro* AR-CALUX assay and has an approximately 20 times higher plasma peak

concentrations than FLU following FLU exposure in humans due to the rapid hydroxylation of FLU to HF (Doser et al., 1997). In **Figure 4.7**, the BMDL<sub>05</sub> values obtained for FLU were compared to the therapeutic dose of FLU for the treatment of prostate cancer or hirsutism and the NOAELs of FLU derived from historical 28 days repeated dose toxicity studies in rats (**Figure 4.7**) (Schellhammer et al., 1997; Toyoda et al., 2000; Yamada et al., 2000; Freyberger et al., 2003; Kunitatsu et al., 2004; Rouquié et al., 2009; Ludwig et al., 2011; Calaf et al., 2017; Zacharia, 2017). The PBK model-facilitated QIVIVE of the *in vitro* anti-androgenicity of FLU -HF results in a BMDL<sub>05</sub> comparable to the therapeutic doses of FLU, indicating that this may not be protective in humans given that at the therapeutic doses of FLU anti-androgenic effects are expected and that in reality HF will also contribute. This is corroborated by the fact that the PBK modelling-facilitated QIVIVE of the *in vitro* anti-androgenicity of FLU +HF results in a BMDL<sub>05</sub> value substantially (i.e., 2 to 3 orders of magnitude) lower than the therapeutic dose levels. This BMDL<sub>05</sub> value is also 35-fold lower than the lowest reported NOAEL from a historical 28 days *in vivo* study in rats (Toyoda et al., 2000). Together, this could suggest that a PoD based on this BMDL<sub>05</sub> for FLU +HF would be health protective in humans for *in vivo* anti-androgenic responses, whereas a PoD based on the BMDL<sub>05</sub> for FLU -HF would potentially underestimate the risk given that it is comparable to the therapeutic dose and higher than the historical animal derived NOAELs of FLU.

## 4.4 Discussion

In NGRA, safe levels of human chemical exposures are assured *via in vitro* and *in silico* approaches, without the use of animal testing. However, using *in vitro* bioactivity assays to quantify the chemical-dependent response might not always represent the corresponding *in vivo* response in the human body, since in the *in vitro* bioassay effects of toxicokinetics, such as biotransformation, are generally not included. In this work, we aimed to include the contribution of the bioactivity of HF in the PBK modelling-facilitated QIVIVE of the anti-androgenic activity of FLU using the *in vitro* AR-CALUX assay in order to set the PoD for safety assessment.

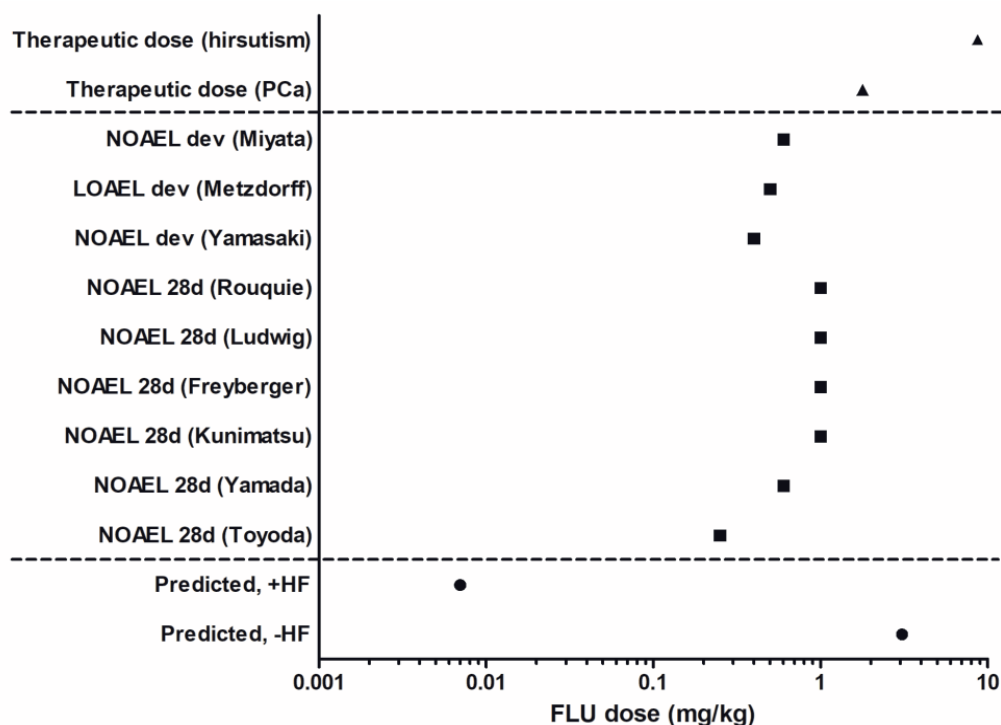


**Figure 4.7.** Comparison of the predicted BMDL<sub>05</sub> of FLU -HF and +HF (circles), therapeutic active doses of FLU (triangles, Schellhammer et al., 1997; Calaf et al., 2017), and historical animal derived NOAELs of FLU (squares, Toyoda et al., 2000; Yamada et al., 2000; Freyberger et al., 2003; Kunimatsu et al., 2004; Rouquié et al., 2009; Ludwig et al., 2011; Zacharia, 2017).

The parameters of the hepatic metabolism of FLU and HF in the PBK model development were determined *in vitro*. It is worth noting that large interindividual variation has been observed in protein content and metabolic activities in microsomes from human liver samples (Zhang et al., 2015) plus, microsomal incubations are prone to inter-laboratory variation (Chiba et al., 2009). The HLM derived  $V_{\max}$  of FLU hydroxylation to HF amounting to  $0.53 \pm 0.08$  nmol/min/mg protein was approximately 3-fold higher than the corresponding literature reported value amounting to  $0.16 \pm 0.07$  nmol/min/mg protein (Goda et al., 2006). The derived  $K_m$  of  $8.85 \pm 3.64$   $\mu\text{M}$  was in concordance with the reported values derived from supersomes expressing CYP1A2 amounting to  $18 \pm 7.50$   $\mu\text{M}$  (Rochat et al., 2001) and from purified fusion protein containing CYP1A2 amounting to  $6 \pm 0.50$   $\mu\text{M}$  (Shet et al., 1997). Based on the sensitivity analysis, the  $V_{\max}$  of FLU appeared to be influential on both FLU and HF kinetics. Given these results, the  $V_{\max}$  of FLU was further optimized against the *in*

*in vivo* data of Doser et al. (1997), resulting in an optimized  $V_{\max}$  of 0.27 nmol/min/mg protein, a value intermediate between our value and that previously reported in the literature (Goda et al., 2006). This resulted in an adequate PBK model able to predict the time-dependent plasma concentrations of FLU and HF in human following repeated exposure to FLU (**Figures 4.5B, C**) (Radwanski et al., 1989). The PBK model developed describing FLU and HF kinetics in humans was also considered adequate to perform the QIVIVE of the *in vitro* anti-androgenic response of FLU.

Chemicals may bind to constituents in the surrounding medium which influences their availability for the biological target and the corresponding potency (Gülden et al., 2002). Therefore, the free concentration of a chemical is considered to be a more appropriate dose metric than the nominal concentration. It was assumed that proteins present in the media were of major influence on the free concentrations of FLU and HF. Therefore, the QIVIVE was based on the free concentrations of the FLU and HF in the *in vitro* medium and *in vivo* plasma which were obtained by correction for protein binding.

Ideally, for evaluation purposes, the  $BMDL_{05}$  derived from PBK modelling-facilitated QIVIVE of FLU -/+HF could be compared to non-anti-androgen active levels of FLU exposure in a healthy population. However, such data were not available so the  $BMDL_{05}$  was compared to the therapeutic active doses of FLU for treating prostate cancer or hirsutism based on its anti-androgenic effect (Calaf et al., 2007; Schellhammer et al., 1998). The  $BMDL_{05}$  from QIVIVE of FLU -HF appeared to be 440-fold higher than the  $BMDL_{05}$  obtained for FLU +HF which takes the activity of HF into account. The predicted  $BMDL_{05}$  value for FLU +HF is 35-fold lower than the lowest reported NOAEL from a historical 28 days *in vivo* study in rats (Toyoda et al., 2000), indicating it is likely to be protective of health in humans, especially after taking potential uncertainty factors (UFs), such as an UF for interindividual variation, into account. Not taking the HF contribution into account would result in a  $BMDL_{05}$  and thus a PoD that appears not to be sufficiently conservative. This highlights the importance of the contribution of HF to the *in vivo* anti-androgenic activity of FLU and of including the toxicokinetics and toxicodynamics of an active metabolite in the *in vitro* to *in vivo* extrapolation to derive PoDs.

The observation that the  $BMDL_{05}$  value resulting from QIVIVE for FLU +HF is 35-fold lower than the lowest reported animal-based PoD, the NOAEL from a historical 28 days repeat dose toxicity study in rats reported by Toyoda et al. (2000), might be due to kinetic species differences. Although CYP1A2 is the main enzyme responsible for the conversion of FLU to HF in both rat and humans (Chang et al., 2000; Shet et al., 1997), the rat liver microsomal (RLM) incubation derived *in vitro*  $V_{\max}$  of FLU hydroxylation to

HF amounting to  $0.063 \pm 0.008$  nmol/min/mg protein (Chang et al., 2000) appears to be 4-fold lower than the HLM derived and optimized *in vitro*  $V_{\max}$  for FLU hydroxylation to HF of 0.27 nmol/min/mg protein obtained in this work. Furthermore, the rat S9 derived *in vitro*  $CL_{\text{int}}$  of FLU of 4.6  $\mu\text{L}/\text{min}/\text{mg}$  protein (Fabian et al., 2019) is over 400-fold lower than the in this work HLM derived *in vitro*  $CL_{\text{int}}$  of FLU of  $116.63 \pm 15.61$   $\mu\text{L}/\text{min}/\text{mg}$  protein. The slower metabolic rate for conversion of FLU to HF and the slower overall clearance of FLU in rats can be expected to result in a species difference in the *in vivo* toxicity following FLU exposure because it would result in potentially higher steady state plasma levels of the active HF metabolite at equal dose levels in human than in rats, resulting in anti-androgenic effects in human at potentially lower dose levels of FLU. Thus, HF levels in humans are suspected to be higher compared to rats at similar exposure levels and bioavailability. This could explain why the predicted PoD of FLU is lower than the animal derived PoD obtained from literature. Indeed, when in the human PBK model the  $V_{\max}$  was exchanged for the RLM derived  $V_{\max}$ , the derived  $\text{BMDL}_{05}$  from the QIVIVE of FLU +HF amounted to 0.014 mg/kg. This  $\text{BMDL}_{05}$  is only 17-fold lower than the lowest reported animal-based PoD (Toyoda et al., 2000), illustrating that the differences in kinetics between rat and humans accounts for a substantial part of the difference between the predicted PoD for human and the animal derived PoD of FLU. Since the aim of NGRA is not to predict animal-based PoDs but to protect human health, the QIVIVE of FLU +HF is supportive of the NGRA strategy to assure human safety.

The observation that *in vitro* derived PoDs can be lower than animal derived PoDs was also reported in a study of Paul Friedman et al. (2020). In this study, 89% of *in vitro* derived PoDs were lower than the traditional animal derived PoDs for different compounds and endpoints. An explanation of this difference stated that an *in vitro* bioactivity assay measures disruption at a molecular level whereas the animal-based PoDs reflect disruption at tissue or organ level (Paul Friedman et al., 2020). Similarly, in our study, the *in vitro* derived PoD was based on chemical induced disturbances in AR-dependent transcriptional activity which was compared to animal derived PoDs based on chemical induced disturbances on body or organ weight. This may further explain the 35-fold difference between the *in vitro*- and animal-based PoDs. Consequently, the PoD from the *in vitro* AR-CALUX assay is more conservative when used in a risk assessment relative to animal-based PoDs, so that a decision based on the *in vitro* derived PoD can be considered health protective for humans.

Using *in vitro* derived PoDs instead of animal derived PoDs for toxicological risk assessment would necessitate a re-evaluation of the use of UFs (Kramer et al., 2021). The use of the UF for interspecies differences could be eliminated since the *in vitro*



derived PoDs are based on human cell lines and human data. However, a different UF could be included to cover the uncertainties in NGRA being based on *in silico* and *in vitro* data, while an UF for interindividual differences in both kinetics and dynamics should also be considered. Contrary, Baltazar et al. (2020) reported *in vitro* derived PoDs which were at least as protective as corresponding animal-based PoDs, indicating the NGRA may not need the use of UFs. PBK modelling predicting chemical levels in different human populations including sensitive groups such as children and pregnant women could further help in the estimation of an adequate UF for these interindividual differences in kinetics when using an *in vitro* derived PoD in NGRA.

The 440-fold lower BMDL<sub>05</sub> value from QIVIVE of FLU +HF as compared to the BMDL<sub>05</sub> value from QIVIVE of FLU -HF reveals that HF substantially contributes to the anti-androgenic response following FLU exposure. Comparison of this 440-fold difference to the TEF<sub>HF</sub> being 23 further highlights that in addition to a difference in toxicodynamics of the metabolite and the parent compound also differences in their kinetics contribute to the difference in the overall BMDL<sub>05</sub> -HF and +HF. Thus, including PBK modelling in QIVIVE to also capture the contribution in toxicokinetics of the metabolite appears essential to set an adequate PoD. FLU is designed as a prodrug for HF and therefore it could be expected upfront that including HF in the PBK modelling-facilitated QIVIVE of FLU has a substantial effect. However, also for different types of chemicals, for which this information may be unknown, this approach will provide quantitative insights into the contribution of metabolites to both toxicokinetics and toxicodynamics following exposure to the parent compound.

In conclusion, the combined *in vitro* PBK modelling-facilitated QIVIVE provides a NAM to characterise the role of metabolism to the metabolite HF in the *in vivo* anti-androgenic responses of FLU. This presents a strategy to include toxicodynamics and toxicokinetics of relevant metabolites when defining *in vitro* derived PoDs in the NGRA evaluation of a parent compound.

## Funding

This work was funded *via* a grant from Unilever (United Kingdom) to Wageningen University and Research (WUR, Netherlands) for the PhD project of TvT.

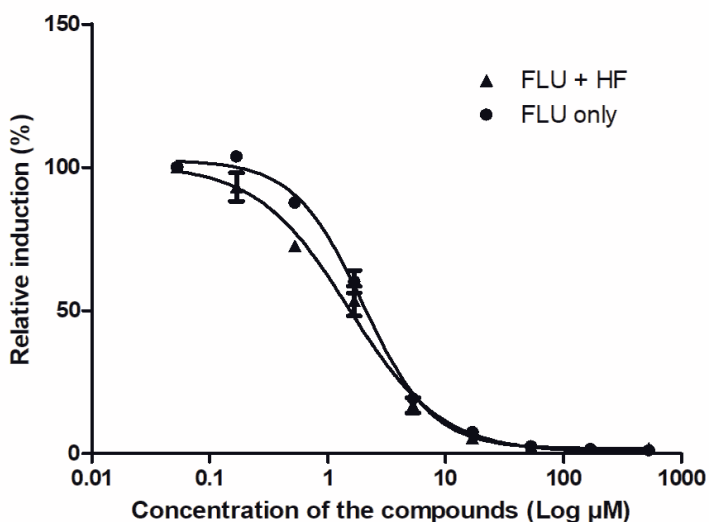
## **Acknowledgements**

The authors would like to express their many thanks to Matthew Dent (Unilever) for his discussions valuable to this work.

**Supplementary material S4.1**

LC-MS/MS acquisition parameters.

Compound	Precursor ion (m/z)	Product ion (m/z)	Collision energy (V)	Retention time (min)
FLU	275.25	202.1	24	7.38
		205.1	22	
		186.1	32	
HF	291.25	205.00	20	6.87
		175.05	31	
		155.05	38	

**Supplementary material S4.2**

**Supplementary Figure S4.1.2.** The concentration-dependent antagonistic activity of FLU only (solid line and circles) and an equipotent mixture of FLU + HF (solid line and triangles) on the DHT-mediated luciferase induction in the U2OS AR-CALUX reporter gene assay. The symbols present the mean  $\pm$  SD values of 3 independent studies. The activity obtained in the presence of 1 nM DHT was set at 100%. The IC<sub>50</sub> values of FLU only and the equipotent mixture of FLU +HF were calculated as 1.51 and 1.98  $\mu$ M, respectively.

### Supplementary material S4.3

The BMD analysis of the predicted anti-androgenic response of FLU – and +HF was performed using BMDS3.2.1 software (U.S. EPA). The benchmark response (BMR) was defined as a 5% extra response (BMR<sub>05</sub>). The BMC<sub>05</sub> and its upper (BMCU<sub>05</sub>) and lower (BMCL<sub>05</sub>) 95% confidence interval were also determined. The model was accepted when the fitted model had a p-value > 0.05, a BMDU<sub>05</sub>: BMDL<sub>05</sub> ratio (precision factor) below 3, or the lowest AIC, indicating support for a concentration-response.

**Supplementary material S4.3.1.** BMD modelling of the predicted anti-androgenic response of FLU -HF

**Supplementary Table S4.3.1.1.** Input values of the predicted dose-response data of FLU -HF.

Dose (mg/kg)	n	response	SD
1.03	3.00	100.00	0.00
3.42	3.00	100.47	3.61
10.27	3.00	85.84	14.98
34.25	3.00	56.06	15.64
102.74	3.00	24.46	8.03
342.47	3.00	8.18	4.42
1027.40	3.00	2.78	1.37

**Supplementary Table S4.3.1.2.** BMD analysis of the predicted dose-response data of FLU –HF. BMD<sub>05</sub>, BMDL<sub>05</sub>, and BMDU<sub>05</sub> values were obtained using BMDS software version 3.2.1, at a BMD of 5% extra risk, BMR type Relative Deviation with normal distribution and constant variance.

Model	BMD (mg/kg)	BMDL (mg/kg)	BMDU (mg/kg)	Test 4 P-Value	AIC	Accepted
Exponential 2 (CV - normal)	0.066	0.000	0.079	<0.0001	251.490	No
Exponential 3 (CV - normal)	0.066	0.000	0.079	<0.0001	251.490	No

Exponential 4 (CV - normal)	0.066	0.000	0.079	<0.0001	251.490	No
Exponential 5 (CV - normal)	0.066	0.000	0.079	<0.0001	251.490	No
Hill (CV - normal)	0.008	0.007	0.010	0.985	188.287	Yes
Polynomial Degree 6 (CV - normal)	0.914	0.677	2.935	<0.0001	275.764	No
Polynomial Degree 5 (CV - normal)	0.914	0.677	2.935	<0.0001	275.764	No
Polynomial Degree 4 (CV - normal)	0.914	0.677	2.935	<0.0001	275.764	No
Polynomial Degree 3 (CV - normal)	0.914	0.677	2.934	<0.0001	275.764	No
Polynomial Degree 2 (CV - normal)	0.914	0.677	2.935	<0.0001	275.764	No
Power (CV - normal)	0.914	0.612	2.935	<0.0001	275.764	No
Linear (CV - normal)	0.914	0.612	2.935	<0.0001	275.764	Yes

### Supplementary material S4.3.2. BMD modelling of the predicted anti-androgenic response of FLU +HF

Supplementary Table S4.3.2.1. Input values of the predicted dose-response data of FLU +HF.

Dose (mg/kg)	n	response	SD
0.002	3.00	100.00	0.00
0.008	3.00	100.47	3.61

0.02	3.00	85.84	14.98
0.08	3.00	56.06	15.64
0.23	3.00	24.46	8.03
0.78	3.00	8.18	4.42
2.33	3.00	2.78	1.37

**Supplementary Table S4.3.2.2.** BMD analysis of the predicted dose-response data of FLU +HF. BMD<sub>05</sub>, BMDL<sub>05</sub>, and BMDU<sub>05</sub> values were obtained using BMDS software version 3.2.1, at a BMD of 5% extra risk, BMR type Relative Deviation with normal distribution and constant variance.

Model	BMD (mg/kg)	BMDL (mg/kg)	BMDU (mg/kg)	Test 4 P-Value	AIC	Accepted
Exponential 2 (CV - normal)	8.81	6.95	12.17	<0.0001	251.49	No
Exponential 3 (CV - normal)	8.81	6.95	22.50	<0.0001	251.49	No
Exponential 4 (CV - normal)	8.81	6.95	12.17	<0.0001	251.49	No
Exponential 5 (CV - normal)	8.81	6.95	22.50	<0.0001	251.49	No
Hill (CV - normal)	0.39	0.11	1.20	0.98	188.29	Yes
Polynomial Degree 6 (CV - normal)	269.25	170.66	1032.61	<0.0001	275.76	No
Polynomial Degree 5 (CV - normal)	269.25	170.90	1032.74	<0.0001	275.76	No
Polynomial Degree 4 (CV - normal)	269.25	170.73	1032.61	<0.0001	275.76	No
Polynomial Degree	269.25	170.73	1032.61	<0.0001	275.76	No

3 (CV - normal)						
Polynomial Degree 2 (CV - normal)	269.25	170.67	1032.61	<0.0001	275.76	No
Power (CV - normal)	269.25	170.67	1032.61	<0.0001	275.76	No
Linear (CV - normal)	269.25	170.66	1032.61	<0.0001	275.76	Yes



# Chapter 5



## **Chapter 5. A two-chamber co-culture system with human liver and reporter cells for evaluating androgenic responses**

Tessa C.A. van Tongeren, Susan J. Hall, Samantha J. Madnick, Blanche C. Ip, Paul L. Carmichael, Hequn Li, Wei Chen, Lori A. Breitweiser, Heather Pence, David M. Ames, Andrew J. Bowling, Kamin J. Johnson, Richard Cubberley, Bruce Sherf, Jeffrey R. Morgan, Kim Boekelheide

Submitted

## Abstract

Considerable progress has been made to develop New Approach Methodologies (NAMs) like *in vitro* bioactivity assays to quantify toxicodynamic responses of chemicals for toxicological safety assessments without animal experimentation. However, under normal assay conditions, toxicokinetics including hepatic metabolic transformation of chemicals are rarely captured in these *in vitro* models and consequently the *in vitro* derived response may not fully reflect the potential human *in vivo* toxicity. Here, a two-chamber co-culture system with human liver and reporter cells was used to measure the androgenic response of testosterone (T) and 5 $\alpha$ -dihydrotestosterone (DHT) in the absence and presence of hepatic biotransformation. Differentiated HepaRG human liver cells were seeded in the outer ring-shaped trough of an agarose hydrogel, forming 3D HepaRG microtissues that exhibit active hepatic metabolism, which were separated from the androgen receptor (AR) reporter gene target cells in the central chamber of the two-chamber co-culture system. The presence of 3D HepaRG microtissues significantly reduced the DHT and T induced AR response in the two-chamber co-culture system with human liver and AR-CALUX or AR-INDIGO reporter cells. LC-MS/MS analysis revealed androstenedione formation following T incubation with the 3D HepaRG microtissues. Thus, the observed change in T- and DHT- mediated AR response in the presence of 3D HepaRG microtissues reflects the hepatic inactivation of the parent compounds, known to occur by similar metabolic inactivation pathways, demonstrating that this two-chamber co-culture system with integrated hepatic biotransformation will contribute to the hazard identification of compounds with (unknown) metabolites affecting the corresponding bioactivity.

**Key words:** toxicity testing · 3D HepaRG microtissues · AR-CALUX · AR-INDIGO · *in vitro* testing

## 5.1 Introduction

In next generation risk assessment (NGRA), new approach methodologies (NAMs) are developed and used to replace, reduce, and refine (3Rs) the use of animals for experimentation (Russell & Burch, 1959) to assure safety of chemical exposure in humans (US EPA, 2018). NAMs include *in vitro* bioactivity assays to quantify toxicodynamic responses of chemicals in cell lines. From these concentration-responses the *in vitro* derived point of departure (PoD) can be defined to set safe exposure levels of the respective chemicals (Baltazar et al., 2020; P. Carmichael et al., 2009; P. L. Carmichael et al., 2022; Middleton et al., 2022). However, a single *in vitro* cell line that represents a target tissue seldom captures the toxicokinetics of compounds of that tissue as in a complex *in vivo* environment where hepatic metabolism can transform compounds to more or less active metabolites, due to the lack of expression of hepatic enzymes. Consequently, the role of potential (in)active metabolites is not captured in the quantified *in vitro* response of the parent compound and thus may only partially reflect the pattern of toxicity at the biological target *in vivo* (Coecke et al., 2006; Gu & Manautou, 2012; OECD DRP 97, 2008). For example, our understanding of the testosterone (T)- and 5 $\alpha$ -dihydrotestosterone (DHT)-mediated androgen receptor (AR) response measured in an *in vitro* reporter gene assay is incomplete without considering that T is hepatically activated to DHT and, *via* another pathway, T and DHT are inactivated. The AR response is essential in the development and maintenance of the male reproductive system (Marcoccia et al., 2017; Schiffer et al., 2018) and thus its correct *in vitro* characterization is of importance when using NAMs to study compounds with (putative) androgenic effects.

DHT is the more AR bioactive metabolite of T that is formed by conversion of T by 5 $\alpha$ -reductase (SRD5A1) (**Figure 5.1**). The inactivation pathway in the liver includes the oxidation of T to the less AR active 6 $\beta$ -hydroxy testosterone (6 $\beta$ OHT) predominantly by the cytochrome P450 Family 3 Member A4 (CYP3A4) (Hashimoto et al., 2016; Usmani & Tang, 2004) and oxidation of T to the less AR active androstenedione (AD) by mainly 17 $\beta$ -hydroxysteroid dehydrogenase 2 (HSD17B2) (Hilborn et al., 2017; Suzuki et al., 2000; Wilson & LeBlanc, 2000). Conjugation of DHT and T is catalysed mainly by UDP-glucuronosyltransferase Family 2 Member B17 (UGT2B17) and the compounds are predominantly excreted as T- and DHT-glucuronide (TG and DHTG) in urine (Bhatt et al., 2018; C. Y. Li et al., 2019; Schiffer et al., 2018; Usmani & Tang, 2004; H. Zhang et al., 2018). Thus, quantifying the androgenic response of T or DHT with an *in vitro* androgen receptor (AR) reporter gene assay does not provide a complete understanding of the response at the *in vivo* target site since, in the absence of metabolism, activating and inactivating reactions do not occur.

Hepatic biotransformation of compounds *in vitro* can be measured by incubation with primary human hepatocytes (PHHs), which are considered the gold standard *in vitro* liver model due to the functional preservation of metabolism, uptake and excretion, and receptor signalling pathways as they are obtained from the human liver (Jackson et al., 2016; Stanley & Wolf, 2022). However, PHHs have significant limitations for use in *in vitro* studies, including availability of human liver samples, large inter-donor variations in enzyme levels, and a limited *in vitro* half-life for expression of their differentiated functionality (Ramaiahgari et al., 2017). A more stable *in vitro* alternative to measure biotransformation is provided by the immortalized human hepatocellular carcinoma derived (HepaRG) cell line, which can be differentiated *in vitro* to hepatocyte- and cholangiocyte-like cells (Aninat et al., 2006; Gripon et al., 2002). Three dimensional (3D) HepaRG microtissues have prolonged and more stable liver functionality compared to 2D HepaRGs, including physiological phase I and phase II enzyme levels and activities, a biliary excretion system, and hepatic zonation characteristics under different medium conditions (Gunness et al., 2013; Jackson et al., 2016; Leite et al., 2012; Ramaiahgari et al., 2017; Ip et al. submitted). 3D HepaRG microtissue formation can be achieved by culturing the cells in a non-adhesive agarose mold system which creates a stable microenvironment with free and efficient chemical diffusion throughout the system (Ip et al., submitted).

The aim of this study was to develop an *in vitro* two-chamber co-culture system with human liver and reporter cells to capture the steroidal T- or DHT-mediated AR response in the absence or presence of hepatic biotransformation. An agarose mold system was developed (Ip et al., submitted) allowing 3D HepaRG microtissues to be formed and cultured in a separate space around the AR reporter gene target tissue within a single well. The selected reporter gene assays were the validated *in vitro* androgen receptor (AR)-CALUX reporter assay (Chemically Activated LUCiferase gene eXpression) assay (Sonneveld et al., 2005; van der Burg, Winter, Man, et al., 2010) and the human AR-INDIGO reporter gene assay (INDIGO Biosciences, Inc., State Collage, PA, USA).

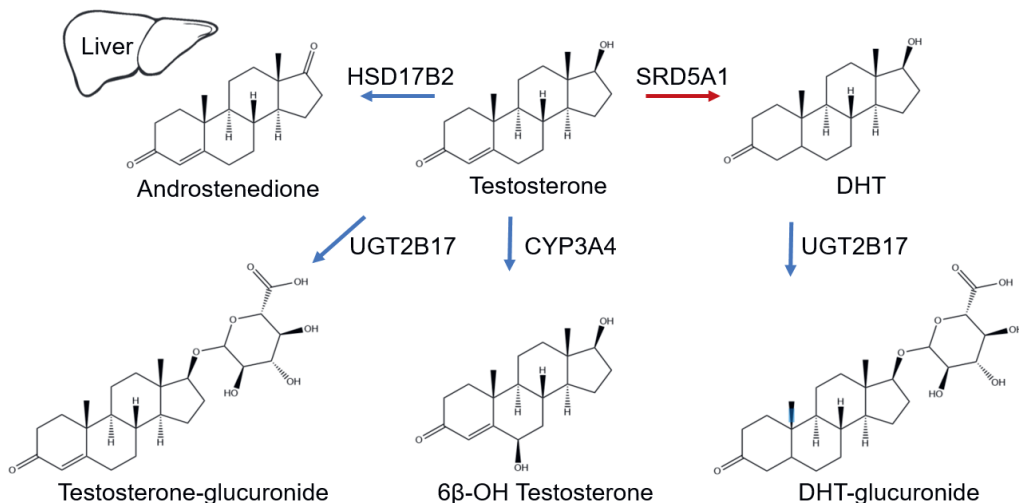


**Figure 5.1.** Simplified metabolic pathway of testosterone and dihydrotestosterone (DHT) biotransformation in the liver. The predominant activating (red) and inactivating (blue) conversions are depicted: SRD5A1 = 5 $\alpha$ -reductase type 1, HSD17B2 = 17 $\beta$ -hydroxysteroid dehydrogenase 2, SRD5A1 = 5 $\alpha$ -reductase type 1, GT2B17 = UDP glucuronosyltransferase Family 2 Member B17, CYP3A4 = Cytochrome P450 Family 3 Member A4.

## 5.2 Material and methods

### 5.2.1 Materials

Dulbecco's modified Eagle's Medium/Ham's nutrient mixture F12 (DMEM/F12, 10565-018), GlutaMax (35050061), penicillin/streptomycin (15140-122), MEM (100 $\times$ ) non-essential amino acids (NEAAs, 11140035), Geneticin (G418, 10131035), phosphate buffered saline (PBS, 14190), trypsin EDTA (trypsin (0.025%)/EDTA (0.01%), 15400-054), UltraPure agarose (BP160-500), phenol red free Williams' E medium (A12176-01), dimethyl sulfoxide (DMSO, BPP321-100), trypan blue (T10282), Triton (X100), and LIVE/DEAD™ Viability/Cytotoxicity Kit, for mammalian cells (L3224) were purchased from ThermoFisher (Fisher Scientific, Waltham, MA, USA). Testosterone (CAS no. 58-22-0, T1500), DHT (CAS no. 521-18-6, A8380), human insulin (I9278), and hydrocortisone (HC, H088) were purchased from Sigma (MilliporeSigma, Burlington, MA, USA). Charcoal dextran stripped fetal bovine serum (CDS-FBS, 100-119) was purchased from GeminiBio (West Sacramento, CA, USA). MHTAP HepaRG supplement was purchased from Lonza (Basel, Switzerland). Lysis mix (Cat no: 26) and Illuminate mix (Cat no: 35) were purchased from BioDetection Systems (BDS, Amsterdam, The

Netherlands). Cell recovery medium (CRM) was donated by INDIGO Biosciences Inc. (State College, USA). 96-square well plates (50305829) were purchased from Ibidi (Gräfelfing, Germany). LoBind Protein tubes (0030108442) were purchased from Eppendorf (Hamburg, Germany). The materials used for the mRNA analysis, immunohistochemical analysis, and LC-MS/MS analysis are listed by Ip et al. (submitted).

## 5.2.2 Methods

### 5.2.2.1 *Fabrication of two-chamber co-culture system in 96-well plate platform*

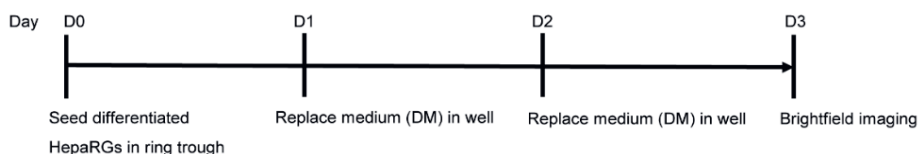
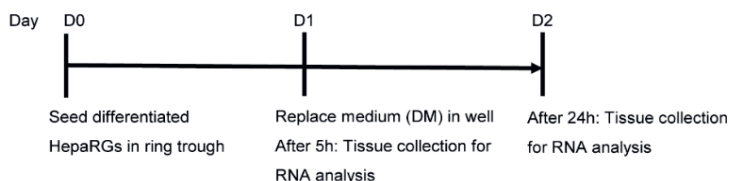
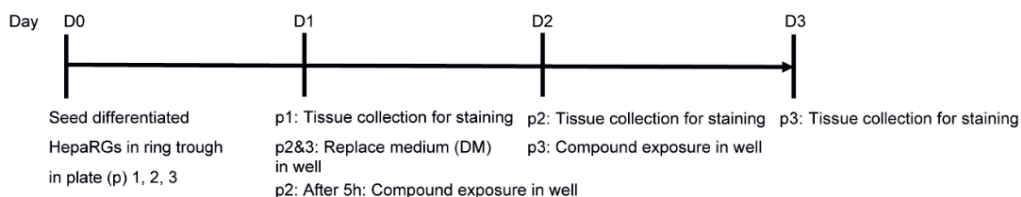
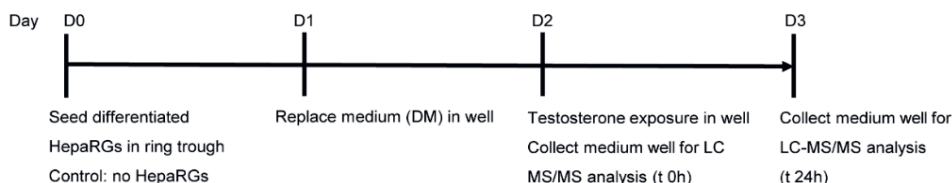
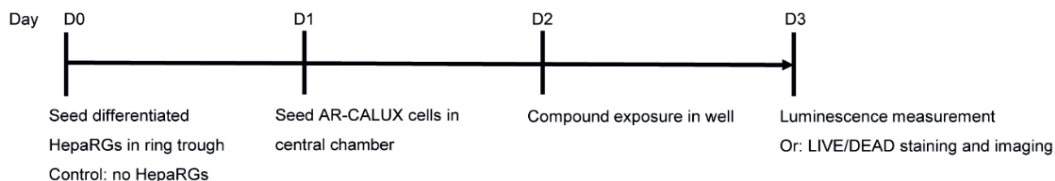
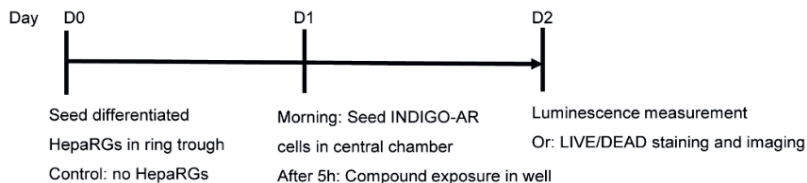
The two-chamber co-culture system using agarose hydrogels was fabricated as described by Ip et al. (submitted). In short, a stainless steel mold was designed using computer-assisted design (CAD) (Solidworks, Concord, MA) and consisted of a base platform with pegs of a circular ring and a central peg as a cylinder that touches the bottom of the well plate, designed to fit within one well of a 96-square well plate (Ibidi Gräfelfing, Germany). To make the agarose hydrogel-based two-chamber system in the wells, each well was filled with 135  $\mu$ L sterile molten agarose in sterile PBS (2% w/v) whereafter the heated stainless steel mold was placed inverted into the plate. After the agarose solidified, the stainless steel mold was removed, leaving an agarose hydrogel with an outer ring-shaped trough (human liver tissue chamber) with a circular central chamber at the bottom of the plate (AR reporter gene assay chamber). Wells were equilibrated with sterile PBS with 1% penicillin/streptomycin and stored at 4°C until the plates are ready to be used. The plates were prepared for experimentation by equilibrating 3 times every 2 h with 200  $\mu$ L base medium consisting of serum-free Williams' E medium supplemented with 1% GlutaMax and 1% penicillin/streptomycin, and placed in an incubator (37°C, 5% CO<sub>2</sub>, 100% humidity). The wells around the periphery of the plates devoid of the agarose hydrogels were filled with sterile PBS with 1% penicillin/streptomycin to prevent evaporation of the inner wells.

### 5.2.2.2 *Differentiation of HepaRG cells*

HepaRG cells were expanded and differentiated according to the supplier's protocol (BioPredic International, HPR101, Rennes, France; proprietary method). Differentiated cells (6.5 million cells per vial) were frozen by placing the cells overnight at -80°C with Mr. Frosty™ Freezing Containers (5100-0001) and then stored in liquid nitrogen.

### 5.2.2.3 3D HepaRG microtissue formation and characterization

The experimental procedure of 3D HepaRG microtissue formation and characterization is depicted in **Figure 5.2A**. On day 0 (D0), differentiated HepaRG cells were thawed in 4.5 mL base medium supplemented with MHTAP HepaRG (MHTAP medium), centrifuged at  $500 \times g$  for 3 min (Avanti J-14 Centrifuge, Beckman Coulter), reconstituted in MHTAP medium after which live cells were counted with the Nageotte Counting Chambers (Hawksley, United Kingdom). Serum-free medium was aspirated from the wells with agarose hydrogels and the differentiated HepaRGs were seeded at a density of 50000 cells in a volume of 25  $\mu$ L MHTAP medium per well in the outer ring-shaped trough of the agarose two-chamber system, the central chamber was left empty. Note that all pipetting steps using the system were executed slowly to avoid cells drifting to the other compartment. After a 20 min settlement of the cells, 150  $\mu$ L of MHTAP medium was added to the wells, filling up both the outer ring-shaped trough and central chamber with medium and topping them off. Plates were incubated (37°C, 5% CO<sub>2</sub>, 100% humidity) on an orbital rotator (36 rpm, Orbi-Shaker™ CO<sub>2</sub>, Benchmark Scientific, Sayreville, NJ) overnight, wherein the HepaRGs formed 3D HepaRG microtissues. For HepaRG microtissue characterization, on day 1 (D1) after visual examination of the microtissues, 140  $\mu$ L medium was replaced with 140  $\mu$ L differentiation medium (DM), maintaining differentiation, consisting of base medium supplemented with 10% CDS-FBS, 5  $\mu$ g/mL human insulin, and 0.5% DMSO. On day 2 (D2), 100  $\mu$ L DM was refreshed and on day 3 (D3), and on D3 brightfield images were obtained with the Perkin Elmer Opera Phenix taking images every 30  $\mu$ m with a 5x air objective to generate stitched maximum projection images using the Perkin Elmer Harmony software (Harmony 4.9; Perkin Elmer).

**A. 3D HepaRG microtissue characterization****B. Gene expression analysis****C. Immunohistochemical analysis of CYP3A4****D. Kinetic study Testosterone****E. Two-chamber liver-AR-CALUX co-culture (and LIVE/DEAD staining)****F. Two-chamber liver-AR-INDIGO co-culture (and LIVE/DEAD staining)**

**Figure 5.2.** Timelines of the experimental procedures of **A.** Characterizing the 3D HepaRG microtissues, **B.** Gene expression analysis, **C.** Immunohistochemical analysis of CYP3A4, **D.** Performing the kinetic study incubating T with 3D HepaRG microtissues for 24 h, and performing the two-chamber co-culture system with human liver and AR-CALUX (**E**) or AR-INDIGO (**F**) cells to obtain concentration-dependent T- and DHT-



mediated luciferase induction in the AR reporter gene assays in the absence or presence of hepatic metabolism, including performing the LIVE/DEAD staining of the U2OS AR-CALUX or CV-1 AR-INDIGO cells.

#### 5.2.2.4 *Gene expression analysis*

For gene expression analysis (**Figure 5.2B**), at D0 differentiated HepaRGs were seeded and on D1 the MHTAP media was replaced with DM as described above. After 5 and 24 h following the medium change to DM (at D1 and D2, respectively), the plate containing the HepaRG microtissues was placed on ice and the microtissues were collected for RNA extraction. The medium was aspirated and the wells were washed three times with ice-cold PBS and tissues from the outer ring were transferred into 1.5 mL Eppendorf tubes with a wide bore pipet tip. Tissues were then centrifuged at 600 x *g* at 4°C for 10 min (Avanti J-14 Centrifuge, Beckman Coulter). The supernatant was removed and tubes were frozen in liquid nitrogen. Tissues were stored at -80°C until analysis for the gene expression of CYP1A2, CYP2B6, CYP3A4, and UGT2B17. From the frozen HepaRG microtissues, RNA was extracted as described by Ip et al. (submitted). For the analysis, probes for genes of interest (GOI) were included: CYP1A1 (Hs01054796\_g1), CYP1A2 (Hs00167927\_m1), CYP2B6 (Hs04183483\_g1), CYP2C9 (Hs04260376\_m1), CYP3A4 (Hs00604506\_m1), and UGT2B17 (Hs07293020\_g1); the housekeeping gene Actb (Hs01060665\_g1) was used for normalization of gene expression.

#### 5.2.2.5 *Immunohistochemical analysis of CYP3A4 in 3D HepaRG microtissues*

For immunohistochemical analysis of CYP3A4 in HepaRG microtissues (**Figure 5.2C**), at D0 differentiated HepaRGs were seeded in MHTAP in plate (p) 1, 2, and 3. After 24h on D1, the tissues of p1 were immunostained for CYP3A4 (Abcam, ab124921) as described by Ip et al. (submitted). Also on D1, the MHTAP media in p2 and 3 was replaced with DM as described above. After 5h at D1, the HepaRG microtissues in p2 were exposed to 10 nM T or 3 nM DHT in DM for 24 h. The compounds were diluted in DM from 1,000 times concentrated stock solutions in DMSO. Since the total volume in the well including the agarose is 285  $\mu$ L, the compound concentrations were corrected for this extra dilution and added from the stock solutions 2.85 times more concentrated, leaving a dilution factor of 350.88 (1000/2.85) and the targeted final concentration of T and DHT in 0.29% DMSO. Exposing the cells, 100  $\mu$ L DM was replaced with 100  $\mu$ L of DM spiked with 10 nM T or 3 nM DHT in 0.29% DMSO, or DM spiked with the vehicle control (0.29% DMSO). On D2, the medium was removed from the wells in p2 and the tissues were immunostained for CYP3A4. Similar, the microtissues in p3 were exposed at D2 to 10 nM T or 3 nM DHT in DM or vehicle control (0.29% DMSO) as described

above. After 24 h at D3, the medium was removed from the wells in p2 and the tissues were immunostained for CYP3A4.

#### 5.2.2.6 *Kinetic study of T in differentiated 3D HepaRG microtissues*

To study the 3D HepaRG microtissue-mediated metabolism of T, the microtissues were incubated with T over time (**Figure 5.2D**). On D0, differentiated HepaRGs were thawed and seeded as described above in the outer ring-shaped trough. In control wells, no HepaRGs were seeded and the outer ring-shaped troughs were filled with 175  $\mu$ L MHTAP medium, leaving wells with and without (w/o) 3D HepaRG microtissues. On D1 after visual examination of the microtissues, 140  $\mu$ L medium was replaced with 140  $\mu$ L DM. On D2, the HepaRG microtissues were exposed to 0, 30 or 100 nM T in DM (final concentration in 0.29% DMSO) for 0 or 24 h (n=5). After the assigned exposure time, the supernatant was collected in LoBind Eppendorf Tubes (Eppendorf, Hamburg, Germany) and stored at -80°C prior to LC-MS/MS analysis.

##### 5.2.2.6.1 Quantification of T and metabolites using LC-MS/MS

Prior to the LC-MS/MS quantification of T and metabolite concentrations in media samples, 50  $\mu$ L of sample and 150  $\mu$ L of working internal standard (deuterated analogues of each analyte, specified below) were mixed and centrifuged (5 mins at 3000rpm) prior to LC-MS analysis. The detection and quantification of T, AD, 6 $\beta$ OHT, and DHT in the supernatant following HepaRG microtissue incubation of T were accomplished using a Waters Xevo TQ-XS mass spectrometer, operating under positive electrospray ionization mode, connected to a Waters Acquity UPLC system. Chromatographic separation was performed using a Waters Acquity BEH C18 (50 x 2.1 mm, 1.7  $\mu$ m particle size) column. The column and autosampler temperature were set at 40°C and 5°C, respectively. The injection volume was 5  $\mu$ L at a flow rate of 0.5 mL/min. The mobile phase A consisted of MilliQ water with 0.1% (v/v) formic acid and mobile phase B of ACN. The gradient was set at 10% B for 0.3 min, followed by a linear increase to 100% B from 0.3 – 1.5 min, 100% B from 1.5 – 1.8 min, a linear decrease to 10% B from 1.8 – 2.0 min, and re-equilibration from 2.0 - 2.5 min at 10% B. The acquisition parameters of T, AD, 6 $\beta$ OHT, and DHT are summarized in Supplementary Material S5.1. Calibration standards of T and AD were prepared as 0.25 – 50 nM in DM and for DHT and 6 $\beta$ OHT as 1.25 – 50 nM in DM. Working internal standards consisted of 10 nM <sup>13</sup>C<sub>3</sub>-T, D<sub>3</sub>-DHT and D<sub>3</sub>-6 $\beta$ OHT in ACN, <sup>13</sup>C<sub>3</sub>-T was also used as internal standard for AD. For the quantification of the T and metabolite concentrations, a calibration graph of the analyte peak area / internal standard peak area was constructed and a 1/x<sup>2</sup> weighting applied.

### 5.2.2.7 Cell culture AR-CALUX

Cells from the stably transfected human osteosarcoma (U2OS) cell line expressing the human AR (BioDetection Systems (BDS), Amsterdam, the Netherlands) were maintained in DMEM/F-12 supplemented with 10% FCS, 1% NEAAs, 10 units/mL penicillin, 10 µg/mL streptomycin, and 0.2 mg/mL G418 in an incubator (37°C, 5% CO<sub>2</sub>, 100% humidity). The cells were routinely subcultured when reaching 85–95% confluency (*i.e.* every 3 to 4 days) using trypsin-EDTA (Sonneveld et al., 2005; van der Burg et al., 2010).

### 5.2.2.8 Two-chamber co-culture system with human liver and AR-CALUX cells

To determine the androgenic response of DHT and T from the AR-CALUX assay in the absence or presence of hepatic biotransformation, a two-chamber co-culture system with human liver and AR-CALUX cells was developed. **Figure 5.2E** summarizes the experimental procedure. At D0, differentiated HepaRGs were thawed and seeded in the outer ring-shaped trough of the agarose mold as described above. Control wells w/o HepaRGs in the outer ring-shaped trough were loaded with 175 µL MHTAP medium. On D1, 3D HepaRG microtissues were visually examined by microscopy. 140 µL medium was carefully removed from each well, removing the media from both chambers whereafter the central chambers were further aspirated. 8000 U2OS AR-CALUX cells were seeded in the central chamber of the agarose two-chamber system in a volume of 15 µL DM. After 5-10 min, 140 µL of DM was slowly added to each well, filling up and topping off both compartments, and plates were incubated (37°C, 5% CO<sub>2</sub>, 100% humidity). Thus, AR-CALUX cells were loaded in the central chamber of the wells w/o and with 3D HepaRG microtissues in the outer ring-shaped trough. On D2, the cells were exposed to a concentration range of DHT or T. 100 µL medium was replaced with 100 µL of DM spiked with T or DHT to result in a final concentration of 1-30 nM in 0.29% DMSO, or DM spiked with the vehicle control (0.29% DMSO) for 24 h. After the assigned exposure time at D3, the medium was aspirated from each well, removing the medium from both compartments. The agarose hydrogels were removed using a pipet tip leaving only the AR-CALUX cells on the bottom of the plate. The cells were washed with 150 µL of 1:1 PBS:nanopore water solution and lysed with 30 µL lysis mix. The plates were placed for at least 30 min on a plate shaker (300 rpm) until cells were lysed after which luminescence was measured using the Synergy H1 Hybrid Multimode (H1MM) Microplate Reader (BioTek® Instruments, Inc. Vermont, USA) wherein 100 µL Illuminate mix was automatically added to each well. The data presented are from three independent studies executed in technical triplicates.

### 5.2.2.9 *AR-INDIGO cells*

Proprietary CryoMite™ preserved cells from the human AR transfected African green monkey kidney-isolated CV-1 cell line (NR3C4, INDIGO Biosciences Inc., State College, United States) were stored in the -80°C at a density of 1.5 million cells/mL per vial in a volume of 0.6 mL.

### 5.2.2.10 *Two-chamber co-culture system with human liver and AR-INDIGO cells*

To determine the androgenic response of DHT and T from the AR INDIGO assay in the presence of hepatic metabolism, a two-chamber co-culture system with human liver and AR-INDIGO cells was developed (**Figure 5.2F**). At D0, the seeding of the differentiated HepaRG cells in the outer ring-shaped trough of the two-chamber co-culture system was executed as aforementioned. The outer ring-shaped troughs of control wells w/o HepaRG were loaded with 175 µL MHTAP medium. On D1, 140 µL medium was slowly subtracted from each well, removing the media from both chambers whereafter the central chamber of each well was further aspirated. The human AR-INDIGO cells were taken from the -80°C and rapidly thawed by adding 6.4 mL pre-heated (37°C) CRM to the vial and placed in a water bath (37°C). After 5-10 min, the cells were centrifuged at 500 x *g* for 3 min (Avanti J-14 Centrifuge, Beckman Coulter). The supernatant was removed and the cells were resuspended in 1.5 mL CRM. From this cell suspension, 15 µL was slowly added to the central chamber of each well of the agarose two-chamber system, seeding approximately 9000 cells per well. After 5-10 min, 140 µL of DM was slowly added to each well, filling up both compartments, and plates were incubated (37°C, 5% CO<sub>2</sub>, 100% humidity). 5 h after seeding of AR-INDIGO cells, 100 µL medium was removed from the wells and the cells were exposed to 100 µL T or DHT spiked DM at a final concentration of DHT of 0.01-1 nM in 0.29% DMSO, or vehicle control-spiked DM (0.29% DMSO) for 24 h. After the exposure time, at D2, the medium from each well was aspirated, removing medium from both compartments, and the agarose hydrogels were removed using a pipet tip, leaving only the AR-INDIGO cells on the bottom of the plate. The cells were lysed and luciferase detection was induced and measured. 100 µL of Luciferase Detection Reagent (LDR) consisting of Detection Buffer and Detection Substrate (1:1) was added to each well and plates were rested at room temperature for at least 5 min, avoiding shaking. When the cells were lysed, luminescence was measured using the Synergy H1 Hybrid Multimode (H1MM) Microplate Reader. The data are presented from three independent studies executed in technical triplicates.

### 5.2.2.11 Data analysis

JMP Pro software (JMP®, Version 16. SAS Institute Inc., Cary, NC) was used for statistical analysis. The mean and SD are presented with N = 9 for the compound concentrations and N = 18 for the vehicle control. The equal variance and normality of the data were tested with the Shapiro-Wilk test. Next, the effect of the presence of 3D HepaRG microtissues on the AR reporter gene response at each exposed DHT and T concentration was evaluated using the student's *t*-test, Welch's test or Median test. Statistical significance was set at  $P \leq 0.05$ .

### 5.2.2.12 LIVE/DEAD staining of U2OS and CV-1 cells in the central chamber of the two-chamber co-culture system

To evaluate the viability of the U2OS (AR-CALUX; **Figure 5.2E**) and the CV-1 (AR-INDIGO; **Figure 5.2F**) cells in the central chamber, a LIVE/DEAD staining (Invitrogen Corp., Carlsbad, United States) was performed following the same exposure protocol as used for the respective co-culture. Cells were exposed to the varying DHT and T concentrations, and to 0.10% triton in ultrapure water serving as positive control for 24 h for U2OS cells and 10 min for CV-1 cells. The different 0.10% Triton exposure times of the different cells was required for an effective staining. Medium was aspirated and the agarose hydrogels were removed using a pipet tip. Cells were washed 2 times with PBS. U2OS cells were treated with 100  $\mu$ L of LIVE/DEAD reagent consisting of 1  $\mu$ M ethidium homodimer (EthD-1) and 0.5  $\mu$ M calcein acetoxymethylester (AM) in PBS. CV-1 cells were treated with 100  $\mu$ L of LIVE/DEAD reagent consisting of 10  $\mu$ M EthD-1 and 0.5  $\mu$ M calcein AM in PBS. The cells were incubated for 2 h. Live cells are stained by intracellular esterase activity converting calcein AM to the green fluorescent calcein. Dead cells are stained by EthD-1 that enters the cells with disrupted membranes and bind nucleic acids which intensifies its red fluorescence, whereas the membrane of live cells protects from EthD-1 entrance. Fluorescent images of live and dead cells were obtained at ex/em 494/517 nm and ex/em 528/617 nm, respectively. For the dead cells, a nuclear count was performed.

## 5.3 Results

### 5.3.1 Fabrication of two-chamber co-culture system in 96-well plate platform

The two-chamber co-culture system in a 96 square well plate format was fabricated to assess the androgenic response of DHT and T in the absence and presence of HepaRG microtissues (**Figure 5.3**). In each well of the 96-well plate, the 2% agarose hydrogel was molded into an outer ring-shaped trough to house the 3D human HepaRG microtissues, and a circular central chamber where the AR reporter gene assay cells were cultured as a 2D monolayer of cells on the bottom of the plate.

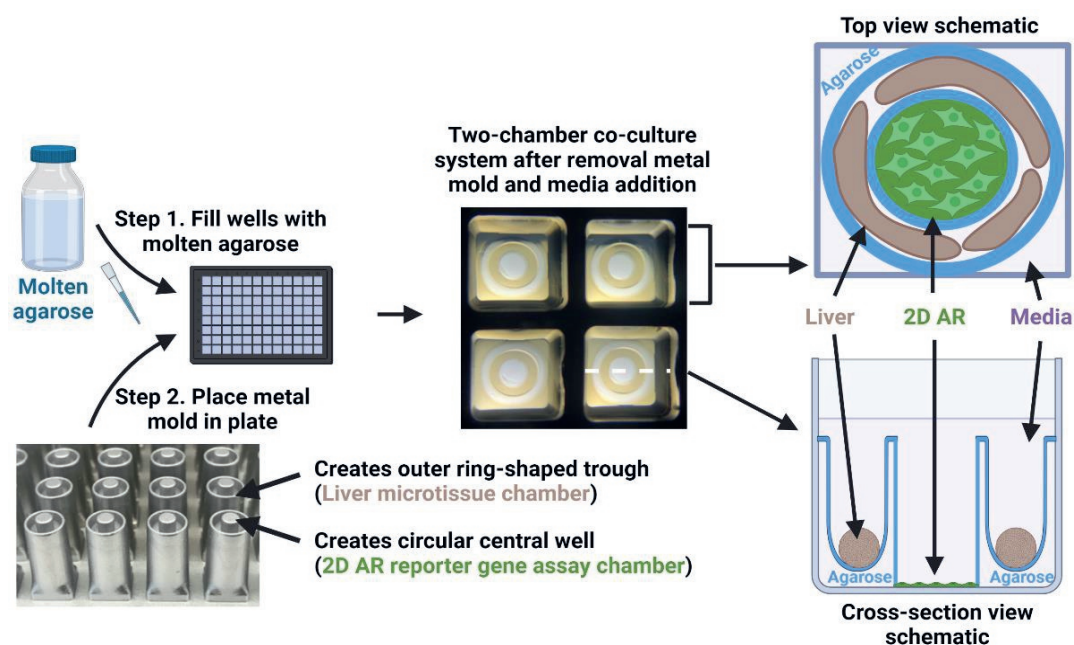


**Figure 5.3.** Schematic representation of the development of the two-chamber co-culture system in 96 square well plate format. In Step 1 molten 2% agarose hydrogel is added to the wells of the plate and in Step 2 the metal mold is inverted in the plate until the agarose hardens. After removal of the metal mold and addition of media, the outer ring-shaped trough is used as the 3D human liver tissue chamber and the circular central chamber is the 2D AR reporter gene assay chamber with cells adherent to the bottom of the plate (adapted from Ip et al., submitted). Media is added placing the pipet tip in the corner of each well, filling and topping off both chambers with media, also allowing diffusion *via* the agarose. The right panel displays a schematic top and cross-sectional view of the agarose mold with liver and AR tissue in a well.

### 5.3.2 3D HepaRG microtissue and AR reporter cell formation and characterization

Interference of medium components on the AR response was evaluated resulting in the removal of hydrocortisone (HC) from the DM culture medium (Supplementary data S5.2). For characterization purposes, 50000 differentiated HepaRG cells (Ip et al., submitted) were seeded in the outer ring-shaped trough at D0 and at D1 U2OS AR-CALUX cells were seeded in the central chamber. At D3, live cell brightfield images were taken. As shown in **Figure 5.4**, both cell types were successfully imaged at different planes using confocal microscopy. At D3 the HepaRG microtissues were formed throughout the outer ring-shaped trough and the U2OS AR-CALUX cells formed a 2D monolayer on the bottom of the plate.

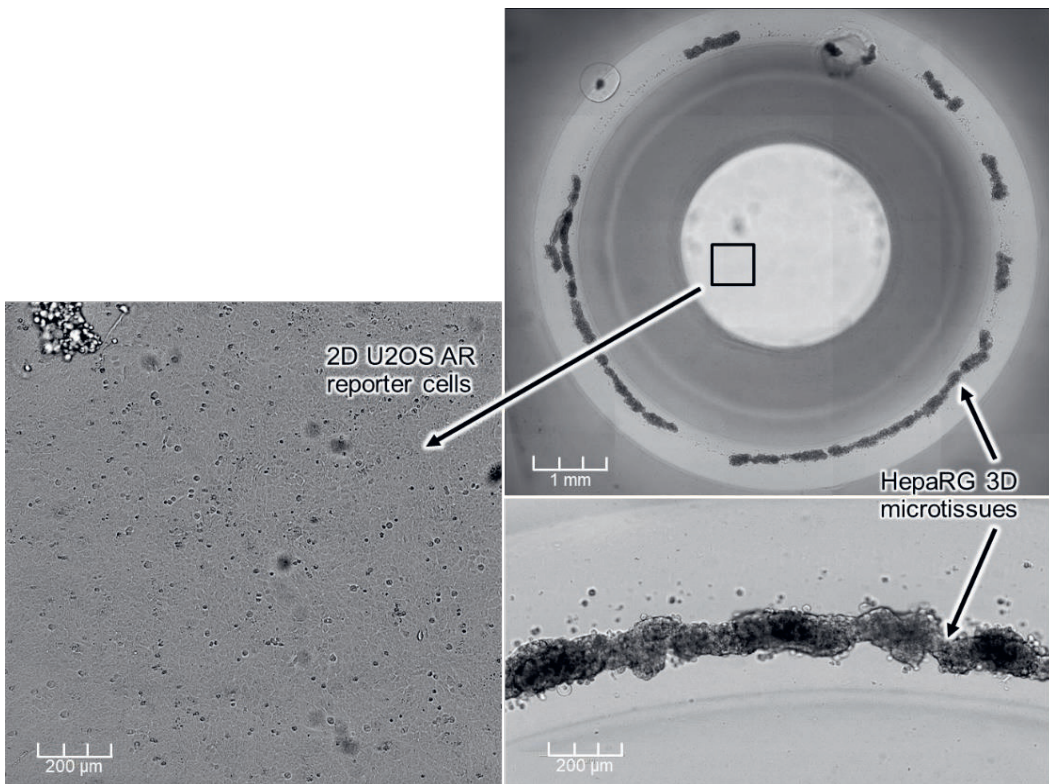


**Figure 5.4.** Live cell brightfield images of 50000 differentiated HepaRG cells forming 3D microtissues during culture in the outer ring-shaped trough and 8000 2D U2OS AR reporter cells in the central chamber of the two-chamber system at D3.

### 5.3.3 Gene expression analysis in HepaRG microtissues

For further characterization of the HepaRG microtissues, the gene expression of CYP1A1, CYP1A2, CYP2B6, CYP2C9, CYP3A4, and UGT2B17 at D1 (for microtissues grown in MHTAP medium) and D2 (when grown in DM) was compared to the corresponding expression in HepaRG microtissues at D1 (grown in MTHAP medium), switching to DM supplemented with HC at D2 and growing the microtissues in this media to D3, where the gene expression was measured at D3 (Ip et al., submitted) (**Figure 5.5**). HepaRG microtissues grown in DM with HC show a time-dependent increase of gene expression of all evaluated enzymes from D1 to D3 (**Figure 5.5A**), while expression levels of the enzymes in HepaRG microtissues did not change when switching to DM without HC at D2 (**Figure 5.5B**).

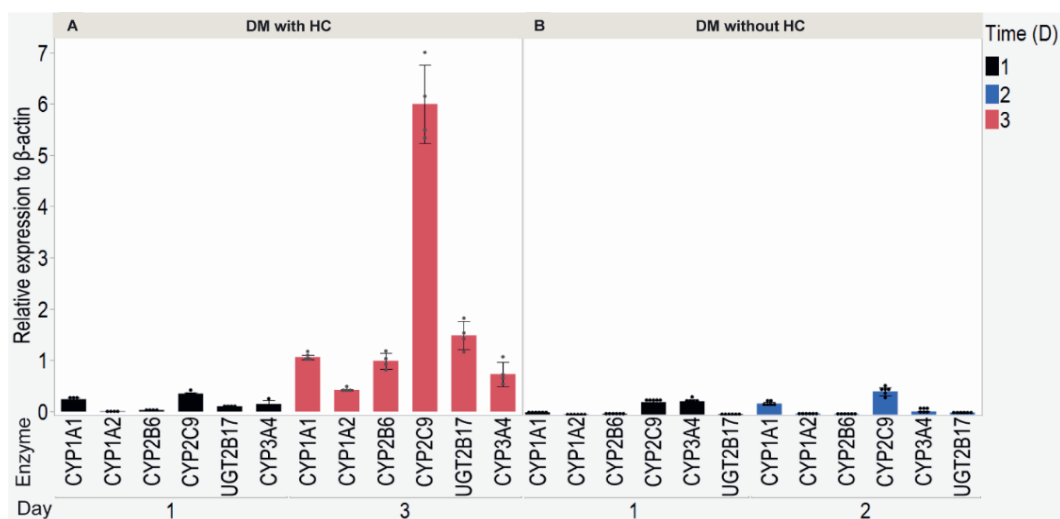


**Figure 5.5.** mRNA expression of CYP1A1, CYP1A2, CYP2B6, CYP2C9, CYP3A4, and UGT2B17 relative to  $\beta$ -actin in **A.** 3D HepaRG microtissues at D1 and 3 grown in DM supplemented with HC (Ip et al., submitted), no analysis was made at D2, and in **B.** HepaRG microtissues at D1 and 2 grown in DM without HC, no analysis was made at D3. The HepaRG microtissues were switched to DM with or without HC at D2.

### 5.3.4 Immunohistochemical analysis of CYP3A4 in 3D HepaRG microtissues

Since the mRNA expression levels of the studied enzymes were low in the 3D HepaRG microtissues grown in DM (**Figure 5.5B**), it was researched what the protein



expression levels were, selecting CYP3A4 for immunohistochemical analysis (**Figure 5.6**) as this protein is involved in the inactivation pathway of T and DHT. Also, a comparison was made to the immunohistochemical analysis of CYP3A4 in 3D HepaRG microtissues grown for 6 or 10 days in DM supplemented with HC (Ip et al., submitted). Results indicate that qualitatively, there is a similar proportion of cells of the 3D HepaRG microtissues expressing CYP3A4, independent of maturation time or compound exposure. It is also demonstrated that even though CYP3A4 mRNA levels were low in 3D HepaRG microtissues grown in DM (**Figure 5.5**), not supplementing the DM with HC did not affect the overall appearance in the proportion of cells expressing CYP3A4 from D1 to D3.

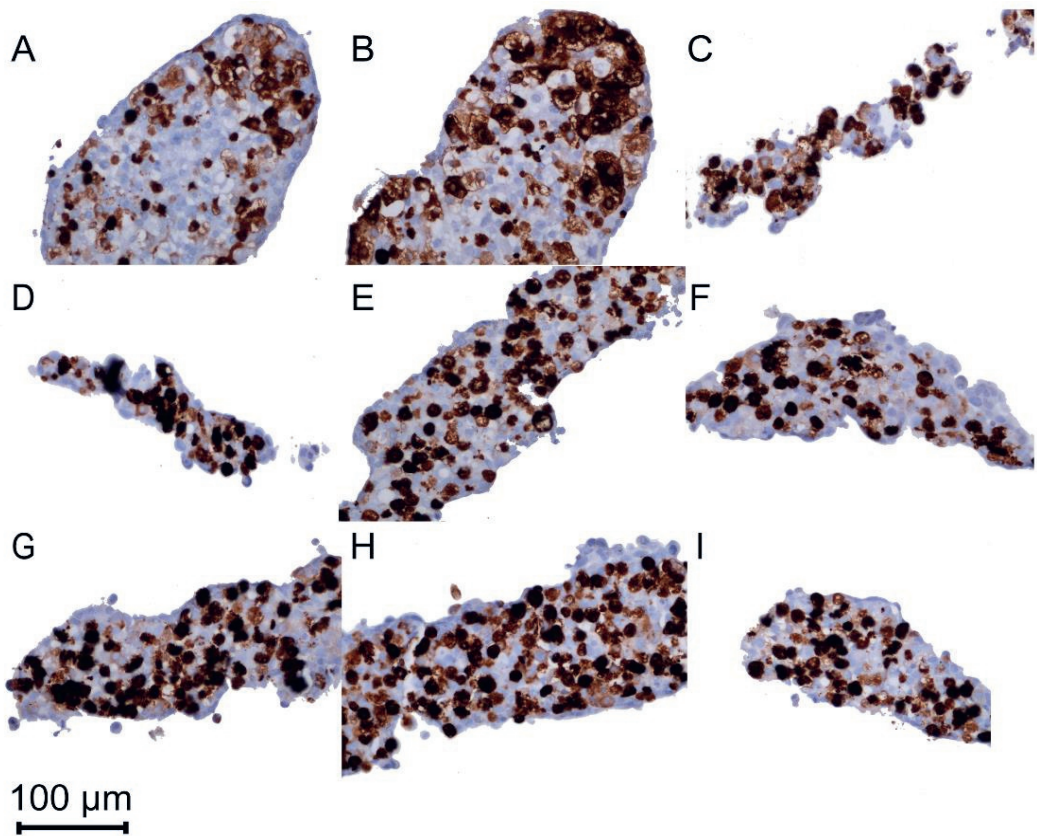


**Figure 5.6.** Immunohistochemical analysis of CYP3A4 in 3D HepaRG microtissues grown in DM supplemented with HC for 6 days (**A**) or 10 days (**B**) (Ip et al. submitted). Immunohistochemical analysis of CYP3A4 in 3D HepaRG microtissues grown in MHTAP for 1 day (**C**), or exposed to vehicle control (0.29% DMSO) in DM for 24h at D2 (**D**) or D3 (**E**), 3 nM DHT in DM for 24 h at D2 (**F**) or D3 (**G**), or 10 nM T in DM for 24 h at D2 (**H**) or D3 (**I**).

### 5.3.5 Kinetic study of T in differentiated 3D HepaRG microtissues

The concentrations of T and its metabolites AD, 6 $\beta$ OHT, and DHT following incubation of 0, 30 or 100 nM T in HepaRG microtissues for 24 h were measured using LC-MS/MS (**Table 5.1**). The recovery of the detection of the compounds was sufficient with minor adsorption (data not shown), indicating the adequacy of the LC-MS/MS method to detect the parent compound at t 0h. After 24 h in the absence of HepaRG microtissues,  $24.08 \pm 0.76$  and  $72.60 \pm 5.31$  nM T were detected following incubation of 30 and 100 nM T, respectively, which decreased in the presence of HepaRG microtissues to  $6.42 \pm 0.37$  and  $24.37 \pm 5.69$  nM T, respectively. This decrease in T was accompanied by its conversion to AD producing  $11.88 \pm 0.81$  and  $37.09 \pm 4.03$  nM AD, respectively. This result complements prior work where AD was the major metabolite formed in *in vitro* incubations of T with human liver cells was also observed by Zhang et al. (2018), where T was incubated with human hepatocytes for 60 min. 6 $\beta$ OHT and DHT were not detected when HepaRG microtissues were exposed to these concentrations of T, likely because the amounts formed resulted in concentrations that fell below the limit of detection (LOD) of 1.25 nM. Nevertheless, the formation of 6 $\beta$ OHT was observed when HepaRG microtissues were exposed to 200  $\mu$ M of T for 2 h (Ip et al., submitted).

**Table 5.1.** LC-MS/MS measured T and AD concentrations following incubation of 0, 30 or 100 nM T w/o and with HepaRG microtissues for 0 and 24 h. Data are depicted as mean  $\pm$  SD (n=5). 6 $\beta$ OHT and DHT were detected <LOD.

T incubated (nM)	w/o or with HepaRG microtissues	Incubation time (h)	Measured concentration T (nM)	Measured concentration AD (nM)
0	w/o HepaRG	24	<0.25	<0.25
0	HepaRG	24	<0.25	<0.25
30	w/o HepaRG	24	$24.08 \pm 0.76$	<0.25
30	HepaRG	24	$6.42 \pm 0.37$	$11.88 \pm 0.81$
100	w/o HepaRG	24	$72.60 \pm 5.31$	<0.25
100	HepaRG	24	$24.37 \pm 5.69$	$37.09 \pm 4.03$

### 5.3.6 Two-chamber co-culture system with human liver and AR reporter cells

The two-chamber co-culture system with human liver and reporter cells was fabricated to investigate the AR-mediated response of the reporter cells towards DHT and T in the absence or presence of human hepatic biotransformation by the 3D HepaRG microtissues. **Figure 5.7** shows the *in vitro* concentration-dependent response of DHT and T in the AR-CALUX assay in the absence and presence of 3D HepaRG microtissues. A significant difference in AR-response in the absence and presence of HepaRG microtissues was observed at 1 and 3 nM DHT and 3 and 10 nM T. **Figure 5.8** shows the *in vitro* concentration-dependent response of DHT and T in the AR-INDIGO assay in the absence and presence of the 3D HepaRG microtissues. A significant difference in AR-response in the absence and presence of HepaRG microtissues can be seen at 0.01 to 0.3 nM DHT and at 0.1 and 0.3 nM T.

The INDIGO reporter cells were more sensitive in exhibiting an AR response already showing a response at concentrations as low as 0.01 nM DHT or T compared to the CALUX reporter cells that displayed AR-induction from 1 nM DHT or T onwards. The INDIGO reporter cells generated however lower luciferase signal intensity (**Figure 5.8**) compared to the CALUX reporter cells (**Figure 5.7**).

The U2OS CALUX and CV-1 INDIGO reporter cells were viable in the co-culture system over time and the presence of 3D HepaRG microtissue did not affect viability (Supplementary Materials S5.3). Furthermore, increasing DHT or T concentrations and the presence of 3D HepaRG microtissue did not alter the AR response of the INDIGO reporter cells constitutively expressing the luciferase vector in the central chamber of the co-culture system (Supplementary Materials S5.4). These data demonstrate that the loss in AR response in the presence of HepaRG microtissues is not due to loss of AR target tissues or loss in AR reporter functionality of the target tissues.

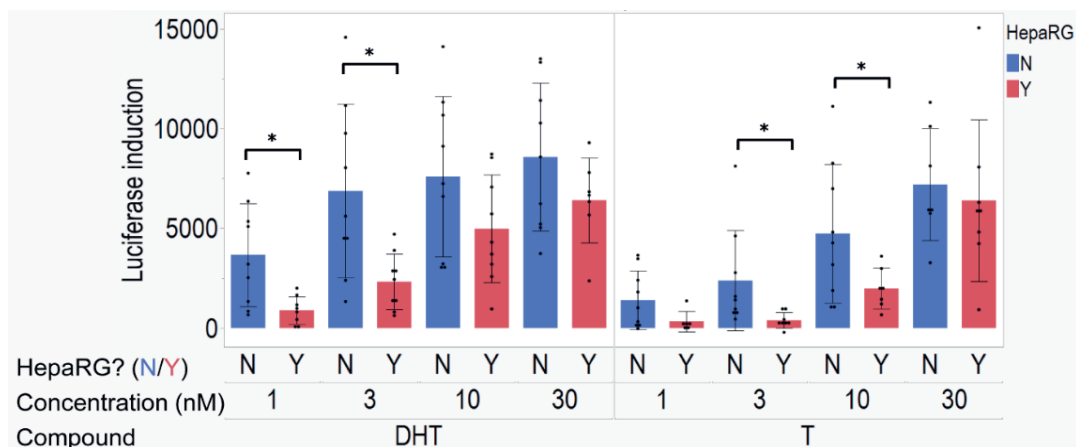


**Figure 5.7.** The concentration-dependent activity of DHT and T in the U2OS AR-CALUX reporter gene assay in the absence (blue bars (N)) and presence (red bars (Y)) of HepaRG microtissues using the two-chamber co-culture system with human liver and reporter cells. Data are depicted as mean  $\pm$  SD and individual datapoints are depicted as filled circles in the graphs. Student's *t*-test, Welch's test or Median test were used to assess statistical significance between the responses observed in the absence and presence of HepaRG microtissues,  $p \leq 0.05$  (\*).

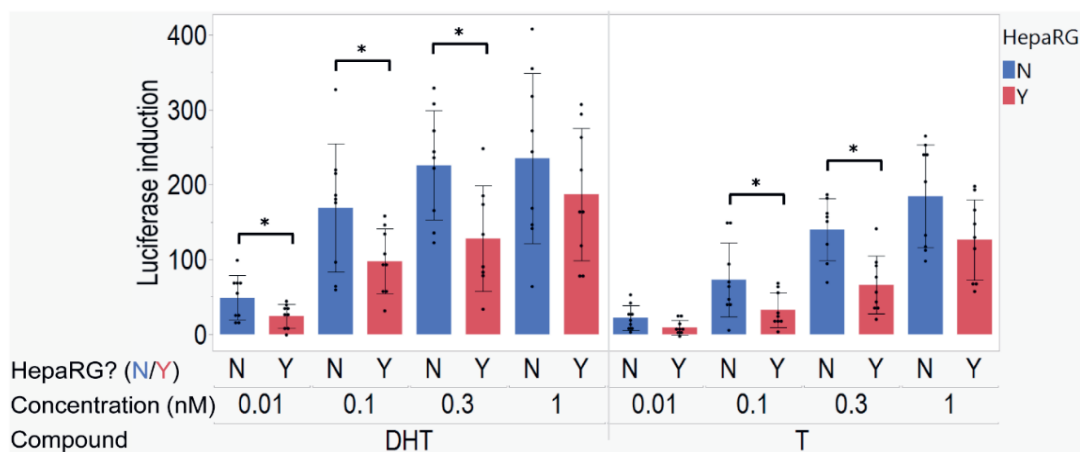


**Figure 5.8.** The concentration-dependent activity of DHT and T in the CV-1 AR-INDIGO reporter gene assay in the absence (blue bars (N)) and presence (red bars (Y)) of HepaRG microtissues using the two-chamber co-culture system with human liver and reporter cells. Data are depicted as mean  $\pm$  SD and individual datapoints are depicted as filled circles in the graphs. Student's *t*-test, Welch's test or Median test were used to

assess statistical significance between the responses observed in the absence and presence of HepaRG microtissues,  $p \leq 0.05$  (\*).

## 5.4 Discussion

In NGRA, *in vitro* bioactivity assays can be used to quantify toxicodynamic responses of chemicals and to derive the NAM point of departure (PoD) for the safety assessment of chemical exposure in humans. However, under single cell culture conditions, processes such as hepatic biotransformation are rarely captured and, thus, the *in vitro* derived toxicodynamic response of the parent compound may not completely capture the pattern of toxicity in the human body (Coecke et al., 2006; Gu & Manautou, 2012; OECD DRP 97, 2008). In this study, an *in vitro* two-chamber co-culture system with human liver and reporter cells was fabricated to capture the T- or DHT-mediated AR response in the absence or presence of hepatic biotransformation. For this purpose, an agarose hydrogel system was developed (Ip et al., submitted) allowing 3D HepaRG microtissues to be formed and cultured in a separate space around the AR reporter gene target cells (**Figure 5.3**). The agarose hydrogel separates the 2 different cell lines into separate compartments within the same well of a 96-well plate, allowing the free diffusion of chemicals throughout the system.

Many of the limitations of high interindividual variability and less stable enzyme activities using PHHs or subcellular fractions like human liver S9 or microsomes and dedifferentiation using 2D HepaRGs as *in vitro* liver metabolism systems can be overcome by using 3D HepaRG microtissues. 3D HepaRG microtissues have prolonged and robust liver characteristics such as phase I and phase II metabolism enzyme expression, biliary excretion, and zonation characteristics as in the human liver (Gunness et al., 2013; Jackson et al., 2016; Leite et al., 2012; Ramaiahgari et al., 2017; Ip et al. submitted), making them suitable as a physiologically relevant human *in vitro* liver model to measure the hepatic biotransformation of compounds. Another advantage of using 3D HepaRG microtissues to capture biotransformation in an *in vitro* bioactivity assay is that it utilizes human liver cells and exhibit the chemical permeability through the cell membrane, thus reflecting metabolism in a more human relevant manner as opposed to co-incubation with S9/microsomes (Mollergues et al., 2017; Sumida et al., 2001; van Vugt-Lussenburg et al., 2018).

The capability of the 3D HepaRG microtissues to metabolize T and DHT was assessed by looking at relevant gene expression profiles, protein expression and metabolite formation. The enzymes involved in the hepatic inactivation of DHT and T are mainly

CYP3A4, HSD17B2, and UGT2B17 forming 6 $\beta$ OHT, AD, TG, and DHTG which are reduced in AR activity or inactivate metabolites (Bhatt et al., 2018; Hashimoto et al., 2016; C. Y. Li et al., 2019; Schiffer et al., 2018; Usmani & Tang, 2004; H. Zhang et al., 2018). The relative CYP enzyme mRNA expression levels in the 3D HepaRG microtissues grown in DM for 2 days (**Figure 5.5B**) were CYP2C9 > CYP1A1 > CYP3A4, CYP1A2, CYP2B6, and UGT2B17 which is a discrepancy with the relative CYP enzyme mRNA expression levels in the *in vivo* human liver where the CYP3A4 level is the highest followed by CYP2C9 (Pelkonen et al., 2008). However, whilst gene expression of CYP3A4 in 3D HepaRG microtissues grown in DM at D2 was low, CYP3A4 immuno-staining revealed that CYP3A4 protein was present (**Figure 5.6**), and 3D HepaRG microtissues metabolized T to AD, demonstrating their metabolic activities. The mRNA expression levels in the 3D HepaRG microtissues grown in DM (without HC) for 2 days were lower compared to the corresponding levels measured in 3D HepaRG microtissues grown in DM with HC for 3 days, as reported by Ip et al. (submitted) (**Figure 5.5A**). HC thus may be suggested to have an important role in maintaining metabolizing enzyme gene expression in 3D HepaRG microtissues.

Following incubation of 30 and 100 nM T for 24h in 3D HepaRG microtissues, 6 $\beta$ OHT and DHT were not detected (<LOD of 1.25 nM). Ip et al. (submitted) incubated 200  $\mu$ M T for 2 h with 3D HepaRG microtissues with an initial seeding density of 50000 cells and matured for 10 days in medium with HC and reported the formation of 0.07 nM 6 $\beta$ OHT/cell, in the presence of HC. Comparing to the companion paper, there were differences in i) the T concentration of 200  $\mu$ M being 3 orders of magnitude higher than 100 nM, ii) the presence of HC in the DM, and iii) 3D HepaRG microtissue maturation for 10 days, where it was shown that enzyme gene expression further increased compared to D3, suggesting higher enzyme levels of the 3D HepaRG microtissues of this work at D3 grown in DM without HC. This offers a reasonable explanation for why 6 $\beta$ OHT production was below the LOD of 1.25 nM in this work.

Nevertheless, the metabolism of T and DHT of the 3D HepaRG microtissues in our two-chamber co-culture system translated to a reduction in AR activation in two independent AR-reporter systems, the AR-CALUX and the AR-INDIGO. Since the AR reporter gene assays are highly sensitive measuring the T- and DHT-mediated AR response, the compound concentrations used to detect the corresponding AR response was lower than the concentration of T that was used in the kinetic study. This indicates that the metabolic capacity of the 3D HepaRG microtissues, even when resulting in metabolite amounts below the LOD of the LC-MS/MS, is still high enough to convert a substantial part of the parent compounds to inactivated metabolites. Our cell viability data (supplementary material S5.3) further support the notion that the decline in AR

response is the reflection of HepaRG-mediated metabolism of T and DHT, and not due to cell death of the AR reporter cells. The AR-CALUX versus the AR-INDIGO in the two-chamber liver co-culture system had different concentration-dependent sensitivity in measuring significant alterations in androgen response in the absence and presence of 3D HepaRG microtissues (**Figure 5.7** and **5.8**). This observed T and DHT concentration-dependent difference in potential for induction of androgen activity could be due to the sensitivity and dynamic ranges of the two AR-transfected cell lines, as well as the different experimental protocol of the two systems. That the INDIGO system produced lower luciferase signal intensity could be due to the fact that, although both INDIGO and CALUX systems use cell lines transfected with the human AR, the mechanism of the luciferase reporter construct to induce the reporter gene differs (Sonneveld et al., 2005; INDIGO Biosciences, Inc., State Collage, PA, USA). The shorter experimental time and less processing steps of the INDIGO as compared to the CALUX assay may lend itself to having less variability.

While complicated, the chemically-induced *in vitro* AR response derived in the presence of 3D HepaRG microtissues is more informative and *in vivo* relevant than the derived AR response in the absence of liver-mediated biotransformation, thus allowing the determination of more informed and physiologically relevant NAM PoDs to set safe exposure levels in humans than when this is absent. Following physiologically based kinetic (PBK) modelling-based quantitative *in vitro* to *in vivo* extrapolation (QIVIVE) (Fabian et al., 2019; Louisse et al., 2017; Punt et al., 2019; Rietjens et al., 2011; Wetmore et al., 2015; Yoon et al., 2012), the *in vitro* concentration-responses of T and DHT in the presence of hepatic biotransformation can be transformed to the corresponding dose-responses for the androgenic effects in humans, to set the PoD. Another method to reflect hepatic biotransformation and thus the contribution of relevant metabolites to the *in vivo* bioactivity of the parent compound is using a toxic equivalency factor (TEF) approach in PBK modelling-based (QIVIVE) of the parent compound (van Tongeren et al., 2022). Other advantages of the two-chamber co-culture system with human liver and reporter cells is its applicability as a high-throughput screening tool of (anti)androgenic compounds, giving insight into both toxicokinetics and toxicodynamics. Integrating reporter and metabolism systems into the toxicological screening of androgens would help identify compounds that are (in)activated early on, without using animal experimentation.

Performing the two-chamber co-culture system has some requirements and limitations. First, preliminary optimization studies were required to test the function of the target assay under the two-chamber co-culture conditions, including viability over time (Supplementary Materials S5.3), functionality (Supplementary Materials S5.4) in

the presence of the 3D HepaRG microtissues, appropriate media conditions (Supplementary Materials S5.2), and the optimal reporter cell number. Replicate variability in the observed AR responses (**Figure 5.7** and **5.8**) was likely due to the many required pipetting steps, an issue that could be addressed with robotics. Finally, the two-chamber co-culture system using 2 cell types may not fully recapitulate the biotransformation mechanisms observed in the human body. For instance, the ratio between HepaRG cells and CALUX or INDIGO reporter gene cells in the two-chamber co-culture system is 6.25 and 5.55, respectively, which may not be indicative of the ratio between hepatic tissue mediating DHT and T inactivation and androgen responsive tissues in the body.

In conclusion, this two-chamber co-culture system with human liver and reporter cells will allow the rapid *in vitro* determination of toxicodynamic responses in the presence of hepatic biotransformation, and contribute to the hazard identification of compounds with (unknown) metabolites affecting the corresponding bioactivity.

### **Funding statement**

This work was funded by the Center for Alternatives to Animals in Testing at Brown, and by Unilever (United Kingdom) as part of Unilever's ongoing effort to develop new ways of assuring consumer safety and *via* a grant from Unilever to Wageningen University and Research (WUR, The Netherlands) for the PhD project of T.C.A. van Tongeren. The Genomics Core Facility has received partial support from the National Institutes of Health (NIGMS grant Number P30GM103410, NCRR grant Numbers P30RR031153, P20RR018728 and S10RR02763), National Science Foundation (EPSCoR grant No 0554548), Lifespan Rhode Island Hospital, Brown University's Division of Biology and Medicine and Provost's office.

### **Conflict of interest**

The authors declare that the research was conducted in the absence of any commercial or financial relationships that could be construed as a potential conflict of interest. J.R. Morgan has an equity interest in Microtissues, Inc and in XM Therapeutics, Inc. These relationships have been reviewed and are managed by Brown University in accordance with its conflict of interest policies. B.C. Ip, S.J. Hall, J.R. Morgan, and K. Boekelheide are joint inventors of the provisional patent that describe the invention of the multi-compartment device described in this manuscript.



## **Acknowledgement**

The authors would like to express their gratitude to Ivonne M.C.M. Rietjens (Wageningen University and Research) for her technical advice and valuable comments contributing to this work. The authors would also like to express their gratitude having carried out work at the Genomics Core Facility at Brown University. A special thanks to the teams at Brown, Unilever, Indigo, and Corteva for stimulating discussions and technical advice, and to Donna McGraw Weiss '89 and Jason Weiss for their generous gift.

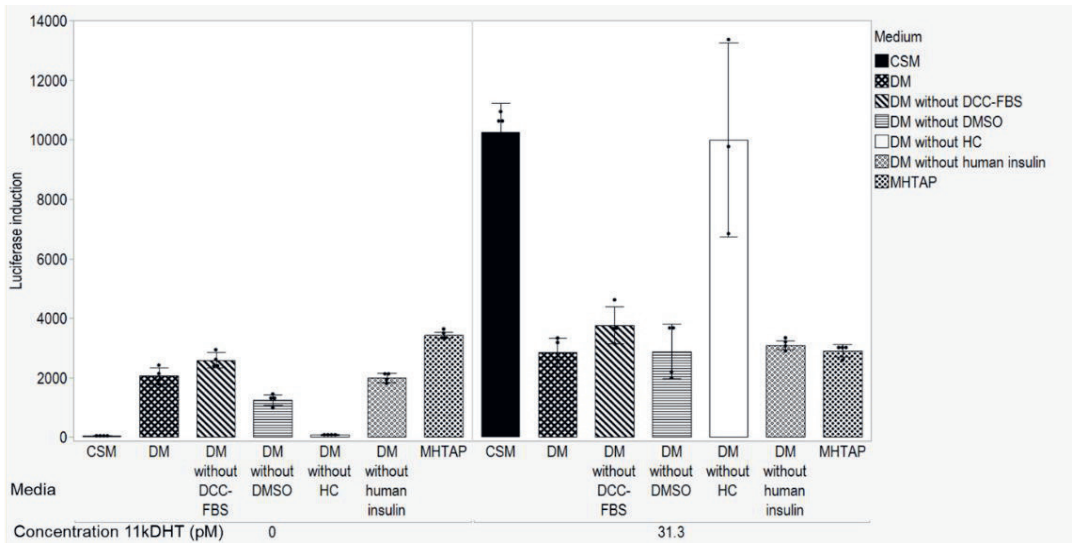
### Supplementary materials S5.1. LC-MS/MS acquisition parameters

Compound	Precursor ion (m/z)	Product ion (m/z)	Collision energy (V)	Retention time (min)
T	289.1000	97.1000	22	1.87
<sup>13</sup> C3-T	292.1597	100.1260	22	1.87
DHT	291.1600	255.2100	16	1.97
DHT-d <sub>3</sub>	294.2000	258.2000	16	1.97
6βOHT	305.1000	269.2100	14	1.58
6βOHT-d <sub>3</sub>	308.1000	272.2000	16	1.58
AD	287.10	97.0700	18	1.92

### Supplementary materials S5.2. Co-culture medium optimization

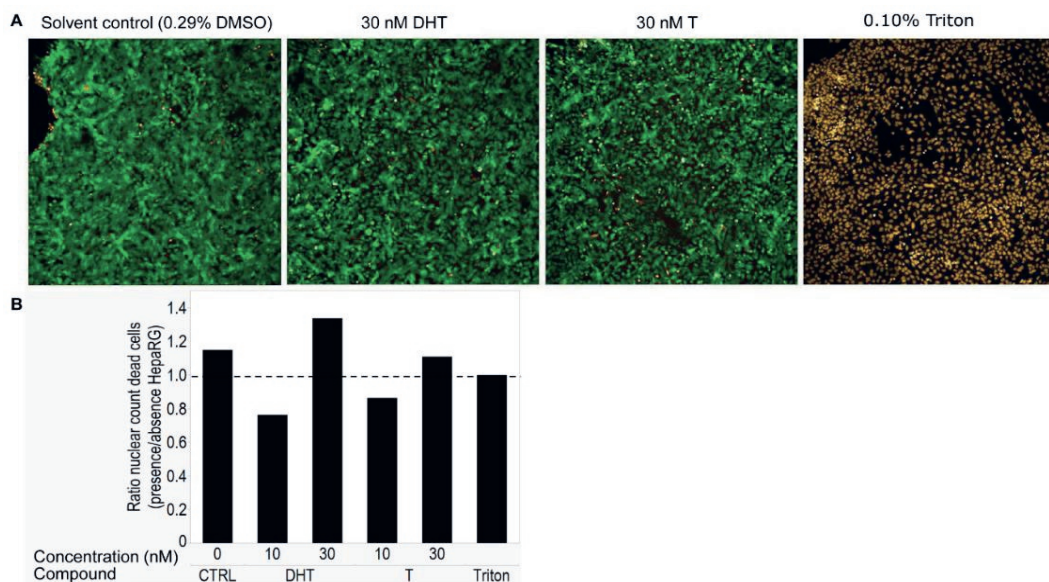
The 3D HepaRG microtissues were formed in MHTAP and differentiation medium (DM) consisting of base medium supplemented with 10% CDS-FBS, 5 µg/mL insulin, and 0.5% DMSO. In the co-culture system, the HepaRG and reporter gene cells resided in the same medium. Therefore, it was evaluated whether the components in the DM affected the reporter gene cells. Performing the standard AR-CALUX assay, the U2OS cells appeared to be fully functional when grown in DM (data not shown). However, the AR-INDIGO cells showed a lower signal and a high background response when the standard assay was grown using DM. Therefore, a standard AR-INDIGO assay was performed using 11-keto-DHT (11kDHT) as a model compound since this is the reference compound used in the standard INDIGO assay. 11kDHT has similar AR activity as DHT (Schiffer et al., 2018). The standard compound screening medium (CRM), MHTAP, full DM, and removing 1 component from the DM in each separate conditions, and the MHTAP medium to identify components affecting 11kDHT-mediated AR response was evaluated (Supplementary Fig. S5.2).

Comparing the background response at 0 nM 11kDHT using DM or DM without HC, removing HC from the DM decreased the background response. Removing HC from the DM increased the AR response at 31.3 pM 11kDHT. To synchronize methodologies using both reporter gene assays, HC was removed from the DM in the AR-CALUX and AR-INDIGO co-cultures.

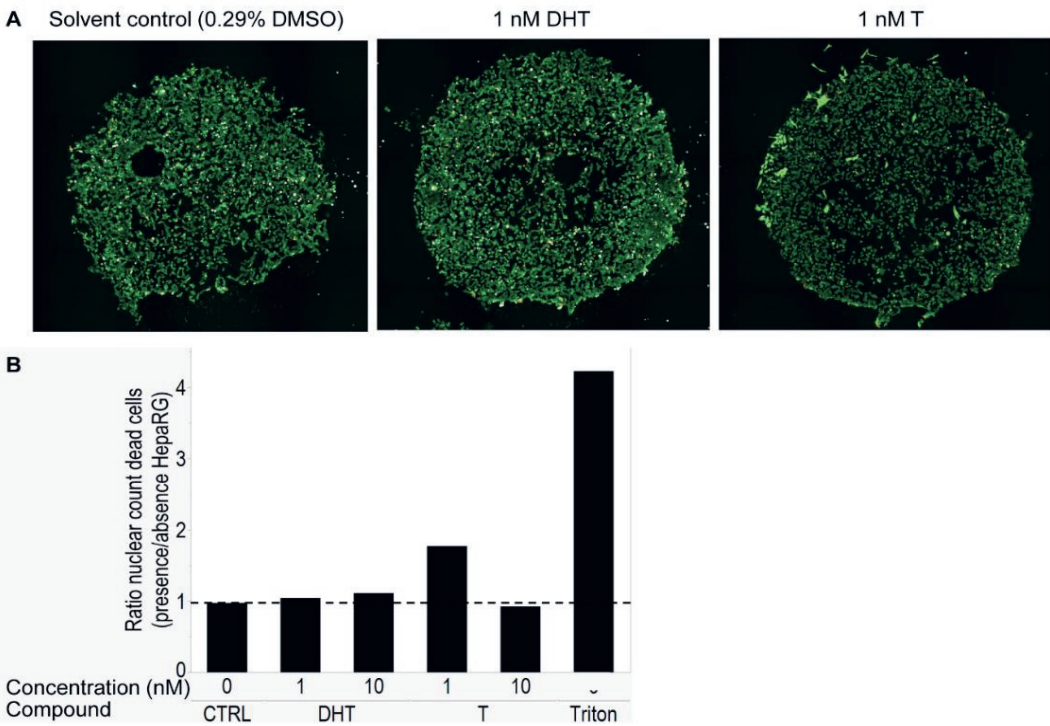


**Supplementary Figure S5.2.** 11kDHT-mediated AR response in the standard INDIGO assay using different types of media. CSM = compound screening medium. DM = differentiation medium. Data are depicted as mean  $\pm$  SD and individual datapoints are depicted as the rounds in the graphs.

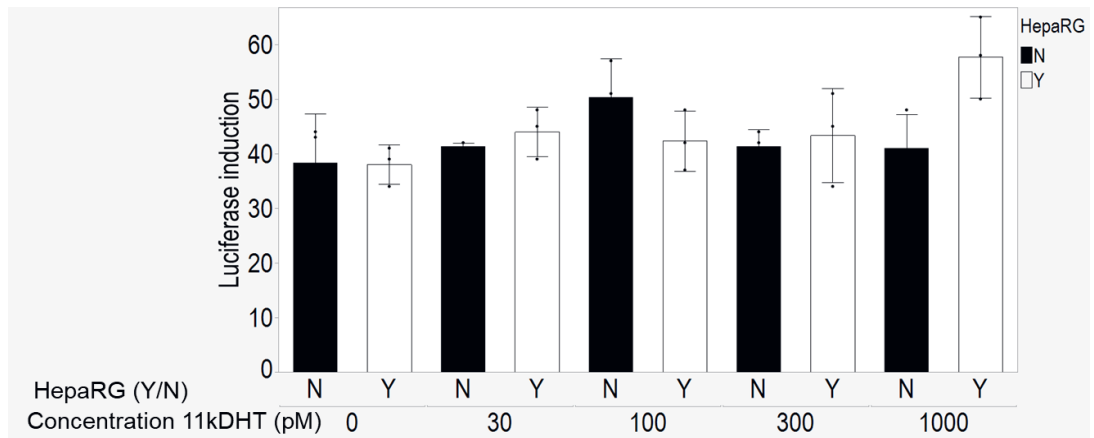
### Supplementary Materials S5.3. LIVE/DEAD staining of U2OS and CV-1 cells in the central chamber of the two-chamber co-culture system



**Supplementary Fig. S5.3.1** LIVE/DEAD staining of AR-CALUX cells in the central chamber at day 3 in the two-chamber co-culture system with 3D HepaRG microtissues in the outer ring-shaped trough. **A.** Calcein AM (green)- and EthD-1 (red)-stained U2OS cells exposed to solvent control (DMSO), 10 or 30 DHT or T or 0.10% triton. Live cells are stained by intracellular esterase activity converting calcein AM to the green fluorescent calcein. Dead cells are stained by EthD-1 that enters the cells with disrupted membranes and bind nucleic acids which intensifies its red fluorescence whereas the membrane of live protects from EthD-1 entrance. **B.** Ratio of the nuclear count of dead U2OS cells in the presence/absence of 3D HepaRG microtissues in the co-culture system exposed to 0, 10 or 30 nM T or DHT or 0.10% Triton.

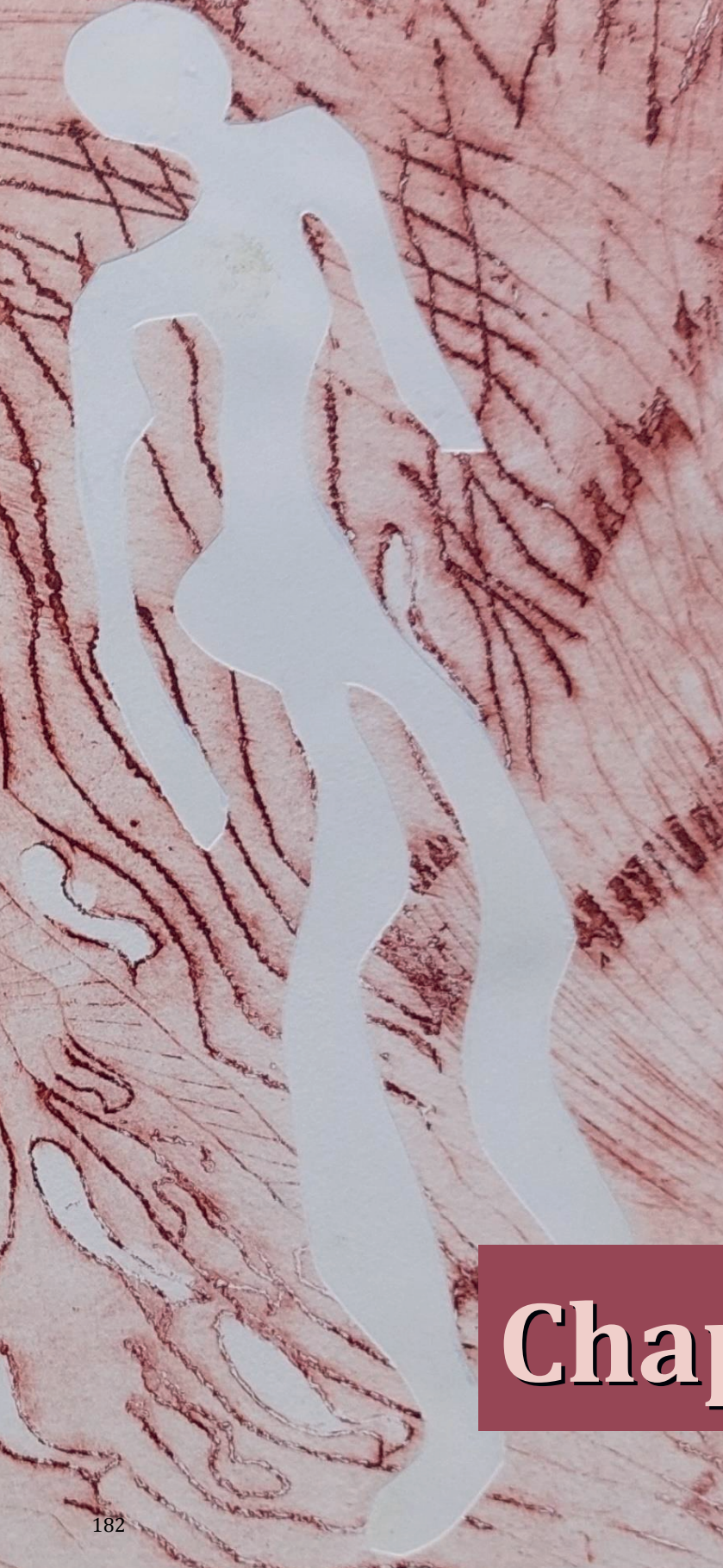


**Supplementary Fig. S5.3.2** LIVE/DEAD staining of AR-INDIGO cells in the central chamber at day 2 in the two-chamber co-culture system with 3D HepaRG microtissues in the outer ring-shaped trough. **A.** Calcein AM (green)- and EthD-1 (red)-stained CV-1 cells exposed to solvent control (DMSO), 1 or 10 nM T or DHT or 0.10% triton. Live cells are stained by intracellular esterase activity converting calcein AM to the green fluorescent calcein. Dead cells are stained by EthD-1 that enters the cells with disrupted membranes and bind nucleic acids which intensifies its red fluorescence whereas the membrane of live protects from EthD-1 entrance. **B.** Ratio of the nuclear count of dead CV-1 cells in the presence/absence of 3D HepaRG microtissues in the co-culture system exposed to 0, 1 or 10 nM T or DHT or 0.10% Triton.

**Supplementary Materials S5.4. Two-chamber liver-Constitutively LUC-INDIGO co-culture**

**Supplementary Fig. S5.4.** The concentration-dependent agonistic activity of 11kDHT (0-1000 pM) in INDIGO cells constitutively expressing luciferase in the absence (black bars (N)) and presence (white bars (Y)) of 3D HepaRG microtissues. Data are depicted as mean  $\pm$  SD.





# Chapter 6



## Chapter 6. General discussion

### 6.1 Main findings

Toxicological risk and safety assessment is often still based on animal toxicity studies to define safe levels of human exposure. However, the use of animal-based testing strategies is disputed because of ethical, economic, and legislative issues, and also because the human body may not adequately be reflected by experimental animals. Next Generation Risk Assessment (NGRA) aims to not predict animal pathology but to assure human safety based on human data and *in vitro* and *in silico* approaches. The aim of this thesis was to perform NGRA to define human relevant safe levels of chemical exposure, by integrating *in vitro-in silico* approaches for compounds with (anti)androgenic and estrogenic effects.

*In vitro* bioactivity assays cannot directly be used in risk assessment to set human safe exposure levels because cells *in vitro* do not represent all aspects of an intact body. For example, under normal assay conditions, the absorption, distribution, metabolism, and excretion (ADME) characteristics occurring in the human body are seldomly captured. In **Chapter 2** and **3** of this thesis, the so-called Dietary Comparator Ratio (DCR) was presented that could serve as an NGRA tool that uses *in vitro* concentration-response data and physiologically based kinetic (PBK) modelling to define internal exposure levels in the safety assessment of chemical exposure scenarios. In the DCR, the Exposure Activity Ratio (EAR) for the compound of interest is compared to the EAR of an established safe level of human exposure to a comparator compound with the same mode of action. A  $DCR \leq 1$  indicates that the respective exposure to the compound under study is safe. In **Chapter 2**, the aim was to define adequate and safe comparator compound exposures for evaluation of anti-androgenic effects. The anti-androgen 3,3-diindolylmethane (DIM), from cruciferous vegetables, and the anti-androgenic drug bicalutamide (BIC) were selected as comparator compounds and their  $EAR_{\text{comparator}}$  values were defined solely based on the *in vitro* 95% lower confidence limit of the benchmark concentration (BMC) causing 5% extra response above background level ( $BMCL_{05}$ ) and  $IC_{50}$  values from the AR-CALUX assay. The adequacy of the new comparator EAR values to reflect safe exposure levels was evaluated and confirmed by comparison of predicted DCR values for a series of exposure scenarios for androgens with known biological outcome. Thus, comparison was made of the generated DCRs of literature reported exposure scenarios for a series of test compounds with actual knowledge of the resulting (absence) of *in vivo* anti-androgenicity. The DCR values for test compound exposure scenarios which were reported to be positive for *in vivo* anti-androgenicity all were predicted to be  $> 1$  with no false negatives whereas negative *in*

*in vivo* anti-androgenic exposure scenarios had DCR values  $\leq 1$ , with 2 false positives out of the 10 exposure scenarios with known biological outcome that were evaluated. This supports the adequacy of the *in vitro*-based comparator EARs to be used in a DCR-based NGRA for anti-androgens. This outcome enabled the safety evaluation of 2 exposure scenarios to the anti-androgen bakuchiol for which data on the *in vivo* anti-androgenic effects were unknown in an animal free *in silico*-*in vitro* 3R compliant way. One of these scenarios was predicted to not result in anti-androgenicity (DCR  $< 1$ ) and one to result in anti-androgenicity (DCR  $> 1$ ).

In another NGRA study described in **Chapter 3**, the DCR approach was used to estimate the safety of human exposures to estrogenic compounds. Genistein (GEN), from soy, was selected as comparator compound based on the comparison of reported safe internal exposures to GEN at its BMCL<sub>05</sub> as an assumed safe internal concentration. The BMCL<sub>05</sub> and the EC<sub>50</sub> as effect level of GEN were derived from the *in vitro* estrogenic MCF7/Bos proliferation, T47D ER-CALUX, and U2OS ER $\alpha$ -CALUX assay to set the EAR<sub>comparator</sub>. 41 Exposure scenarios to 14 test compounds were included for which the EAR<sub>test</sub> values were calculated based on data from the *in vitro* estrogenicity assays and literature reporter internal exposure levels. The DCR values, calculated using the EAR<sub>comparator</sub> values of GEN and the EAR values of the test compounds, were used to predict the (absence of) estrogenicity. The results obtained revealed that the DCR predictions for each exposure scenario were similar based on all 3 *in vitro* assays. The DCR outcomes were assessed by comparing the predictions to actual knowledge of *in vivo* estrogenicity in humans upon the tested exposure scenarios, revealing the correct prediction of the (absence) of *in vivo* estrogenicity in humans for all 30 exposure scenarios for which actual data on biological outcome of the exposure were available. The results obtained thus allowed the safety assessment of the 11 exposures for which the outcome of *in vivo* estrogenicity was unknown. This evaluation revealed that 1 exposure scenario resulted in a DCR  $> 1$ , indicating that exposure may result in estrogenic effects in humans whereas for the other 10 exposure scenarios with a DCR  $\leq 1$  no *in vivo* estrogenicity is expected. The results of this work further supported the DCR approach as an important animal-free tool in NGRA and also the use of *in vitro* bioassay data to define the EAR<sub>comparator</sub> and EAR<sub>test</sub> values.

Exposure scenarios evaluated in **Chapter 2** and **3** related to compounds that were themselves anti-androgenic or estrogenic, without a need for bioactivation, or to compounds that are converted to more bioactive metabolites which contribute to the *in vivo* bioactivity. This hepatic biotransformation and the resulting potential bioactivation or detoxification is seldomly captured in *in vitro* bioactivity assays. This implies that for compounds that are bioactivated or detoxified by metabolic conversion

the quantified *in vitro* responses may not fully represent the chemical-dependent toxic potency at the *in vivo* target site. In this thesis, two approaches were presented to include biotransformation in an NGRA context using *in vitro* bioactivity assays and *in silico* tools. In **Chapter 4**, a proof of principle was presented where the bioactivity of the metabolite hydroxyflutamide (HF) was included in an NGRA approach to evaluate the safety of the parent anti-androgen flutamide (FLU). To this purpose, a PBK model describing FLU and HF kinetics in humans was developed to enable PBK modelling-facilitated quantitative *in vitro* to *in vivo* extrapolation (QIVIVE) taking the contribution of the active metabolite HF into account. In the QIVIVE, the *in vitro* concentration-response data derived from the AR-CALUX assay for FLU were translated to the corresponding *in vivo* dose-response curves for the anti-androgenicity of FLU, either excluding or including the activity of HF (-HF and +HF, respectively), the latter using a toxic equivalency factor (TEF) approach. From these dose-response curves, the BMDL<sub>05</sub> values were determined as points of departure (PoD) for further safety assessment. From the predicted *in vivo* dose-response curve of FLU including the bioactivity of HF, a 440-fold lower BMDL<sub>05</sub> value was derived compared to the BMDL<sub>05</sub> for FLU derived excluding the bioactivity of its metabolite HF. To estimate to what extent these derived BMDL<sub>05</sub> values of FLU -/+HF would reflect a safe level of human exposure, a comparison was made to human therapeutic, and thus anti-androgenic active, doses and literature reported animal derived PoDs of FLU. Results obtained indicated that the BMDL<sub>05</sub> obtained by the PBK modelling-facilitated QIVIVE of FLU -HF is comparable to the therapeutic doses of FLU for the treatment of hirsutism and prostate cancer while the BMDL<sub>05</sub> obtained by the PBK modelling-facilitated QIVIVE of FLU +HF was 35-fold lower than the lowest reported animal derived PoD of FLU. Together these results indicate that inclusion of the anti-androgenicity of the metabolite will result in a PoD that is likely to be protective of health in humans whereas exclusion will result in a PoD that is too high and thus in an underestimation of the risk of FLU exposure. This corroborates that an NGRA-compliant strategy should include both toxicodynamics and toxicokinetics of relevant metabolites in setting the PoD of a parent compound.

In **Chapter 5**, another strategy to take metabolism into account in NGRA was presented based on a new *in vitro* technology enabling co-cultivation of metabolically competent cells and reporter gene cells to identify the influence of hepatic metabolism on the *in vitro* response of a compound. To this purpose, a two-chamber co-culture system with human liver and reporter cells was applied to measure the androgenic response of testosterone (T)- and 5 $\alpha$ -dihydrotestosterone (DHT), which are known to be metabolically inactivated, in the absence and presence of hepatic biotransformation. In the outer ring-shaped trough of an agarose hydrogel, differentiated human liver HepaRG cells were seeded to form 3D HepaRG microtissues, and these were separated by the agarose hydrogel from the central chamber of the two-chamber co-culture

system where AR reporter gene target cells were seeded. The 3D HepaRG microtissues were metabolically competent for inactivation of T, and thus also DHT following a similar inactivation pathway, which translated in the two-chamber co-culture system into the reduction in T- and DHT-mediated AR activation in the presence of the microtissues for two independent AR-reporter systems, the AR-CALUX and the AR-INDIGO. Thus, the observed reduction in the DHT- and T-mediated AR response in the presence of 3D HepaRG microtissues reflects the hepatic inactivation of the parent compounds. The two-chamber co-culture system can thus be used as a tool to assess whether hepatic biotransformation to (unknown) metabolites affects the bioactivity of a parent compound.

## **6.2 General discussion, future perspectives and conclusion**

In this thesis NGRA strategies were applied and evaluated aiming at novel methods to assure human safety based on human data and *in vitro* and *in silico* approaches. In the following sections the methods used as well as the results obtained are discussed in some more detail, followed by proposed future perspectives and the conclusion.

## **6.3 Use of *in vitro* bioactivity assays as New approach methodologies (NAMs)**

In the last decades considerable progress has been made in the development of *in vitro* bioactivity assays to be used as new approach methodologies (NAMs) to identify and quantify, amongst others, androgenic or estrogenic responses. This resulted in bioactivity assays such as the AR- or ER-CALUX assay which are based on the human osteosarcoma (U2OS) cell line (Sonneveld et al., 2005; van der Burg et al., 2010). The main advantages of human-based *in vitro* bioactivity assays compared to animal tests are that they do not use animals and are designed to mimic human biology. Furthermore, advantages are their time, resource, and cost effectiveness, making them suitable for high-throughput use, providing more controlled experimental conditions and control over external factors affecting the assay, resulting in lower variability and higher reproducibility (Kaur & Dufour, 2012; NRC, 2007; Paul Friedman et al., 2020; Sonneveld et al., 2005). Disadvantages of using human cell-based *in vitro* bioactivity assays include the use of genetically manipulated cancer cells, such as the U2OS cells which form the basis of the CALUX assays and that they are engineered to display a reporter gene response and stripped from some of their other cellular biological

pathways (Sonneveld et al., 2005). Furthermore, being derived from cancerous tissues, like the U2OS cell line being derived from an osteosarcoma, cell lines may genetically and phenotypically deviate from different healthy target tissues that are ER or AR responsive. They may thus not fully represent the biology of those target tissues as observed in the human body (Kaur & Dufour, 2012) or reflect the genetic variability in cells over the human population but are rather designed to specifically study a molecular initiating event (MIE). To add, the sensitivity of the reporter gene assay used to quantify the *in vitro* response is dependent on not only the used cell line, but also on the reporter gene construct inserted in the cell, and the experimental setup as illustrated in **Chapter 5** where the AR-CALUX (U2OS cells) and AR-INDIGO (CV-1 cells) showed different AR-induction sensitivities. Furthermore, additional important disadvantages of using cell-based *in vitro* bioactivity assays as NAMs are that a cell does not represent a whole intact body, that a cell line lacks a functional immune system (Kaur & Dufour, 2012), and that the absorption, distribution, metabolism, and excretion (ADME) characteristics of a chemical, as well as interactions between different cells, tissues, and extracellular matrix occurring in the human body are rarely captured under normal assay conditions (Coecke et al., 2006; Kaur & Dufour, 2012; OECD DRP 97, 2008). From an NGRA perspective, the derived *in vitro* concentration-responses cannot directly be used in the safety assessment of chemical exposure to humans since dose-responses are required to set the PoD. In the present thesis, the DCR approach was presented to overcome this issue as it can be used to directly relate the derived *in vitro* effect concentration to the internal exposure level of a chemical of interest, where a safety estimation is made using a relevant comparator compound (**Chapter 2** and **3**). In this, internal exposure level kinetics and other factors affecting the internal dose level of a chemical are taken into account.

## 6.4 Advantages, limitations, and recommendations of and for the dietary comparator ratio (DCR) approach

The unique feature of the DCR approach is that it integrates *in vitro* bioactivity data of a compound under study with exposure data to that compound to estimate whether that exposure scenario is safe in humans. In this thesis, the DCR approach was used to estimate the safety of (putative) anti-androgenic (**Chapter 2**) and estrogenic (**Chapter 3**) exposures in humans. From the results obtained it appeared that for the future and broader use of the DCR approach as useful and reliable tool for human safety assessment, several factors need to be considered to a further extent which will be discussed in the following sections, including i) the selection of the comparator

compound and the (dis)advantages of the *in vitro*-based comparator EAR, ii) the quantitative interpretation of the DCR, iii) whether the DCR approach can elucidate the mode of action, iv) the use of the DCR approach for other *in vivo* endpoints with available *in vitro* bioactivity assays, v) limitations of the DCR approach, and vi) recommendations for future use of the DCR approach.

i) The selection of the comparator compound and (dis)advantages of its *in vitro*-based EAR

The selection of a comparator compound in the DCR approach should be based on the following criteria: i) the compound operates by the same mode of action as the compound(s) under study, ii) negative exposure scenarios for the biological activity of the selected compound in humans should be available, and iii) the internal concentrations at the negative exposure scenarios should be available. Suitable comparator compounds are thus in most cases well studied compounds like therapeutic agents or common diary constituents which are extensively characterized and thus have good data availability. In the present thesis it was shown that for the comparator compound the  $BMCL_{05}$  values derived from an *in vitro* concentration-response curve in a relevant bioactivity assay can be used as a surrogate for the internal safe level of exposure. When using a  $BMCL_{05}$  value it is important to keep in mind that modelling the  $BMCL_{05}$  value is dependent on the quality of the data and thus on the number of consecutive concentrations tested, sample size, variance within and between samples (Hardy et al., 2017) and that estimates at low concentrations may be subjective to uncertainty. However, evaluating the  $BMCL_{05}$  values of the comparator compounds used in this thesis to internal concentrations of negative exposure scenarios confirmed their adequacy to reflect no effect levels. Importantly, the fact that using the  $BMCL_{05}$  to set the *in vitro*-based  $EAR_{\text{comparator}}$  resulted in the correct DCR-based predictions of *in vivo* bioactivity in humans and produced no false negative DCR outcomes further validates the approach (**Chapter 2 and 3**). The approach appeared to provide a less conservative but more realistic and useful  $EAR_{\text{comparator}}$  than what was obtained by using historical safe exposure data to for instance DIM from the intake of 50 grams of Brussels sprouts which resulted in a large number of false positives reflected by the DCR-based prediction of *in vivo* anti-androgenicity in humans of exposure scenarios which were actually reported to be inactive for the onset of anti-androgenicity (Dent et al., 2019). The  $EAR_{\text{comparator}}$  based on the intake of DIM from 50 grams of Brussels sprouts thus appeared overly conservative and this highlights the importance of a well-defined safe comparator exposure level. The use of the  $BMCL_{05}$  from an *in vitro* bioactivity assay to define an  $EAR_{\text{comparator}}$  widens the possibilities and criteria for selection of comparator

compounds and use of the DCR approach, also for other endpoints for which *in vitro* bioassay are available.

## ii) A quantitative interpretation of the DCR

Besides the advantage of the relatively quick and cost- and recourse-efficient procedure of the DCR-based safety assessment of exposure scenarios, the DCR outcomes may also be subject to a quantitative interpretation. The higher the DCR value, the higher the *in vivo* activity and thus the severity of related health effects associated with the respective exposure scenario to the chemical of interest is expected to be. This is further supported by the fact that using therapeutic active doses as positive exposure scenarios resulted in high DCR values amounting to values up to 76063 (**Chapter 2**). This indicates that an exposure scenario with a higher predicted DCR value would likely be more effective to induce the respective *in vivo* activity than an exposure scenario with a lower predicted DCR value. However, for all exposure scenarios with a DCR > 1, the onset of *in vivo* bioactivity cannot be excluded and should be prioritized for further safety assessment.

## iii) Whether the DCR approach can elucidate the mode of action

In this thesis, the DCR approach was used to assess exposures to anti-androgens (**Chapter 2**) and estrogens (**Chapter 3**). However, compounds can be both anti-androgenic and estrogenic *in vitro* with anti-androgens resulting in estrogen-like effects. Therefore in this discussion chapter a DCR-based evaluation of the exposure scenarios was made for both endpoints for some selected compounds that have both anti-androgenic and estrogenic potential. In **Chapter 3**, a DCR-based safety assessment for the *in vivo* estrogenic effects of reported exposures to BBzP and o.p'-DDT (Freire et al., 2013; Högberg et al., 2008; Kezios et al., 2013; Minelli & Ribeiro, 1996), being active in the *in vitro* estrogenicity assays (Wang et al., 2014), was made. The resulting DCR values of the exposure scenarios to BBzP and o.p'-DDT were < 1 indicating these exposures would be unlikely to result in *in vivo* estrogenicity in humans. However, BBzP and o.p'-DDT were also found to have antagonistic activity in the *in vitro* AR-CALUX assay with IC<sub>50</sub> values of 0.62 ± 0.13 and 1 µM, respectively (Krüger et al., 2008; Sonneveld et al., 2005). Thus, to further illustrate that the DCR approach can elucidate a mode of action, the reported exposure scenarios to BBzP and o.p'-DDT were also evaluated by the DCR approach for anti-androgenicity using the EAR<sub>comparator</sub> values of DIM and BIC and the AR-CALUX assay (**Chapter 2**) (Freire et al., 2013; Högberg et al., 2008; Kezios et al., 2013; Minelli & Ribeiro, 1996).

For this purpose, first the AR-CALUX derived IC<sub>50</sub> values were transformed to the free IC<sub>50</sub> values using the  $f_{ub \text{ in vitro}}$  and with the reported free internal concentrations (**Table 3.3, Chapter 3**), the EAR<sub>test</sub> values were calculated following **Eq. 2, Chapter 3**. Using the EAR<sub>comparator</sub> values of DIM and BIC based on the AR-CALUX assay amounting to  $4.04 \times 10^{-3}$  and  $1.51 \times 10^{-3}$  (**Chapter 2**) the DCR values for the anti-androgenic safety assessment of the exposures to BBzP and o.p'-DDT were calculated following **Eq. 3, Chapter 2 and 3 (Figure 6.1)**. All exposure scenarios resulted in a DCR value < 1 and are thus suggested to not result in *in vivo* anti-androgenicity. Thus also based on the DCR outcomes for anti-androgenicity, the exposures are unlikely to result in estrogenic effects in humans *via* an anti-androgenic mode of action. Interestingly, the DCR values derived for anti-androgenicity were relatively higher than for estrogenicity, which could indicate that the DCR approach may turn out to be able to establish the critical effect and/or mode of action upon a chemical exposure. Clearly this would provide an interesting topic for future research.



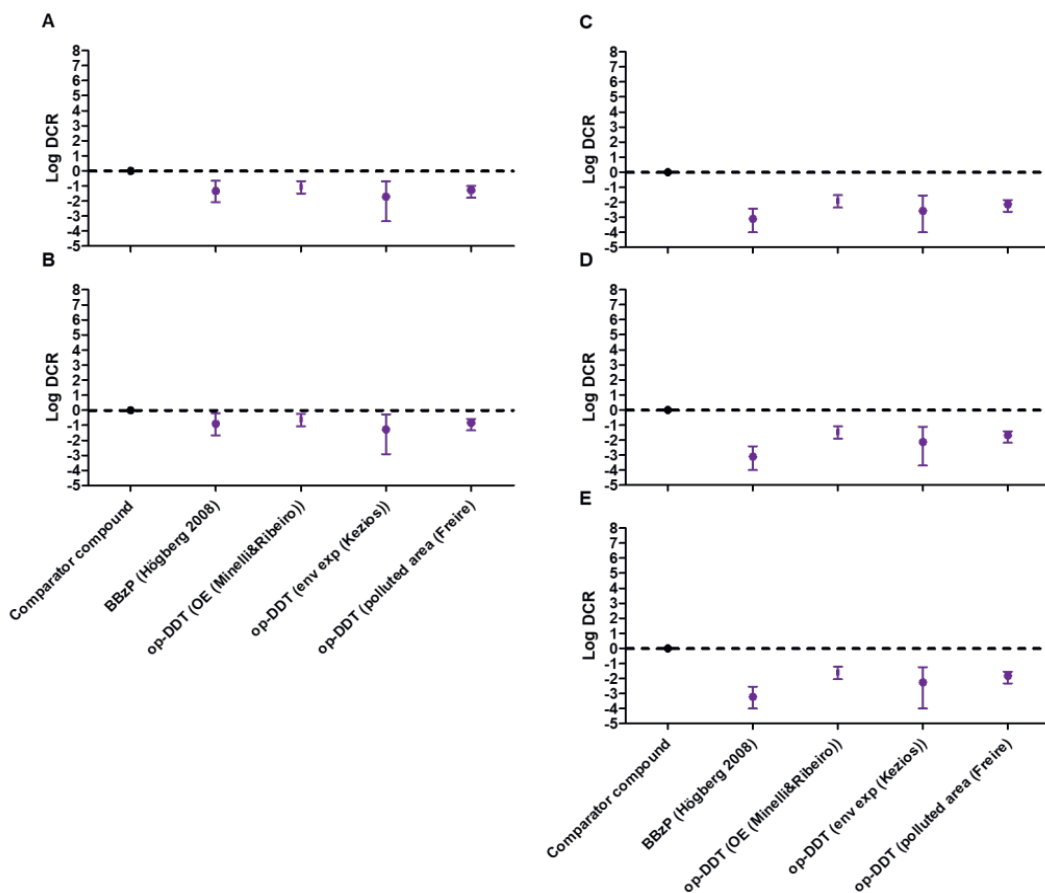


**Figure 6.1.** The DCRs of the exposure scenarios to BBzP and o.p'-DDT based on **A.** the  $EAR_{\text{comparator}}$  of DIM from the AR-CALUX assay and **B.** the  $EAR_{\text{comparator}}$  of BIC from the AR-CALUX assay. The comparator DCRs, equal to 1 ( $\log \text{DCR} = 0$ ), are represented as black. The DCRs for the exposure scenarios to BBzP and o.p'-DDT (**Table 3.3, Chapter 3**) for which data on *in vivo* anti-androgenicity are not available are highlighted as purple symbols. The dotted horizontal lines mark the DCR of 1 ( $\log \text{DCR} = 0$ ). For comparison the results obtained in **Chapter 3** for the estrogenicity using comparator compound GEN of these exposure scenarios are presented in **C** based on the MCF-7/Bos proliferation assay, **D** the T47D ER-CALUX assay, and **E** the U2OS ER $\alpha$ -CALUX assay.

iv) The use of the DCR approach for other *in vivo* endpoints with available *in vitro* bioactivity assays

Another advantage of the DCR approach that uses the  $BMCL_{05}$  to establish the  $EAR_{\text{comparator}}$ , is that it can be used for the chemical safety assessment for other *in vivo* endpoint besides anti-androgenicity and estrogenicity, provided that *in vitro* bioactivity assay(s) that cover the respective molecular initiating event (MIE) are available. This bioactivity assay is then used to derive *in vitro* concentration-response data and subsequently the  $EC_{50}$  or  $IC_{50}$  as effect levels for the model compounds and the  $BMCL_{05}$  as no effect level for the comparator compound(s). For the endpoints evaluated in this thesis, anti-androgenicity and estrogenicity, the MIE of AR or ER binding has been well defined and is covered in the respective CALUX assays. A broad range of other CALUX reporter gene assays is available that cover receptor binding MIEs, like the progesterone receptor (PR)-CALUX assay to quantify progestin activity (Sonneveld et al., 2011), which could be used in a DCR approach to evaluate progestins. Other examples which can be implemented in the DCR approach are *in vitro* bioactivity data from ToxTracker (Thakkar et al., 2023) to assess *in vivo* genotoxicity or from the embryonic stem cell test (EST) (Genschow et al., 2002, 2004) to assess *in vivo* developmental toxicity in humans, demonstrating the broad applicability domain of the DCR approach.

v) Limitations of the DCR approach

It is also important to consider that an *in vitro* bioactivity assay must be available that not only captures the MIE of an *in vivo* endpoint and *vice versa*, but that the *in vitro* bioactivity must also capture the mechanism of toxicity in the human body following the respective MIE. This is a limitation for application of the DCR approach for the full range of potential adverse effects relevant in human safety assessment, This is because not every MIE has been elucidated for every *in vivo* endpoint in and thus an *in vitro* bioactivity assay cannot always be selected. In this case, first the MIE and preferably the whole adverse outcome pathway (AOP) of the compound known to cause the respective *in vivo* critical effect might be elucidated. To this purpose, the *in silico* prediction can be employed to determine a chemical its affinity to certain receptors, which could be related to the *in vivo* endpoint using, for instance, the MIE ATLAS (Allen et al., 2018). This could potentially lead to the identification of a corresponding *in vitro* bioassay. It can also be the case that the measured *in vitro* bioactivity has no clear *in vivo* toxicological outcome in humans, so that validation and thus use of the DCR approach becomes challenging since this hampers the characterization of whether a defined

exposure to a compound active in the bioassay would result in a positive or negative *in vivo* effect in humans. Note that also negative *in vivo* exposure data are helpful to evaluate the *in vitro* derived  $BMCL_{05}$  of the comparator compound(s). The information regarding positive or negative exposure scenarios is necessary to evaluate the corresponding DCR outcomes which will, when successful, allow an accurate DCR-based safety assessment of the exposure(s) to compounds which were active in the respective *in vitro* bioactivity assay but wherefrom it is unknown whether the tested exposure is to result in *in vivo* activity.

An example where the DCR approach was discontinued was for the safety assessment of chemicals that were predicted to perturb the nuclear liver X receptor (LXR). To see whether the DCR approach could be used to evaluate human safety for exposures to chemicals perturbing the LXR, it was first investigated what *in vivo* consequences LXR activation or inactivation would have on human physiology. The  $LXR\alpha$  is expressed in metabolically active tissues like the liver and  $LXR\beta$  is expressed ubiquitous (Bilotta et al., 2020). Both receptors have a wide range of functions and are activated by endogenous oxidized cholesterol metabolites resulting in, among others, effects on cholesterol and lipid metabolism and homeostasis, immune function, and anti-proliferative effects in cancer cells (Fessler, 2018; Jarvis et al., 2019; Nilsson et al., 2007; She et al., 2022). Polyunsaturated fatty acids (PUFAs) from the diet antagonise the LXR, which is suggested to affect cholesterol and lipid metabolism and homeostasis upon exposure (Bedi et al., 2017). However, following perturbed agonism or antagonism of the  $LXR\alpha$  or  $LXR\beta$ , no clear and direct pattern adversely affecting human physiology is yet described, and consequently the effect on human health remains inconclusive. Although *in vitro* LXR bioactivity assays are available such as the LXR-CALUX assay (Escher et al., 2022), the DCR approach for LXR perturbation in human safety assessment is hampered since no clear *in vivo* endpoint can be defined and it is thus unclear whether exposure to putative LXR (ant)agonists would result in a negative or positive biological effect in humans.

## vi) Recommendations for the DCR approach

The developments in the DCR approach described in this thesis include the use of the *in vitro*  $BMCL_{05}$  to define the EAR of the comparator compound. This implies that in essence every compound, not just dietary compounds, can be a comparator compound provided the *in vitro* concentration-response curve is available to model the  $BMCL_{05}$ . Another observation is that the  $EAR_{\text{comparator}}$  is no longer an EAR but rather a NAR (No Activity Ratio) since it compares the benchmark concentration as no effect

concentration to the effect concentration. All this calls for reformulation of the term Dietary Comparator Ratio to for instance the No activity Comparator Ratio (NCR).

Another remark is that it is of interest to note is that using the  $BMCL_{05}$  as the no effect level in the DCR approach could also support an additional methodology in the safety assessment of chemical exposures, where the internal exposures resulting from a specified dose of the test compounds can directly be compared to their own  $BMCL_{05}$  value. This ratio could be called for example the No activity Exposure Ratio (NER), and does no longer relate the  $EAR_{test}$  to an  $EAR_{comparator}$ . To see whether this NER approach would be less or more conservative than the DCR approach, the anti-androgenic exposure scenarios from **Chapter 2** were also evaluated based on such a NER approach. To this purpose, the nominal  $BMCL_{05}$  value of each test compound was derived from the concentration-response curve in the AR-CALUX assay and converted to the free  $BMCL_{05}$  using the  $f_{ub}$  *in vitro* (**Table 2.3, Chapter 2**). Next, the free internal concentrations at the defined external dose level of each test compound (**Chapter 2**) were divided by the free  $BMCL_{05}$  values of the compound of interest to derive the NER values. **Figure 6.2A** presents the NER values thus obtained for using the same colour code for the knowledge on the actual anti-androgenic nature of the evaluated exposure scenarios as presented in **Figure 2.5** of **Chapter 2** which is also included in **Figure 6.2** for comparison. Interestingly, when a cut-off of a safe exposure scenario at a  $NER \leq 1$  is applied, the NER-based safety estimation results in the same predictions as a DCR-based safety estimation using for example AR-CALUX based  $EAR_{comparator}$  of DIM (**Chapter 2**) (**Figure 6.2B**), except for the safety evaluation of the exposure to BAK from body lotion. For this latter exposure scenario, for which the actual outcome with respect to anti-androgenicity is unknown (purple colour code) the NER-based safety evaluation appears less conservative suggesting that it will not result in *in vivo* anti-androgenicity whereas a DCR-based safety evaluation suggests that *in vivo* anti-androgenic effects in humans cannot be excluded. Therefore, the NER approach can be used as an additional NGRA-compliant approach when the concentration-response data of the compound under study is adequate for the BMC analysis. However, having an adequate  $EAR_{comparator}$ , the DCR approach appears a more conservative approach for an adequate safety estimation.

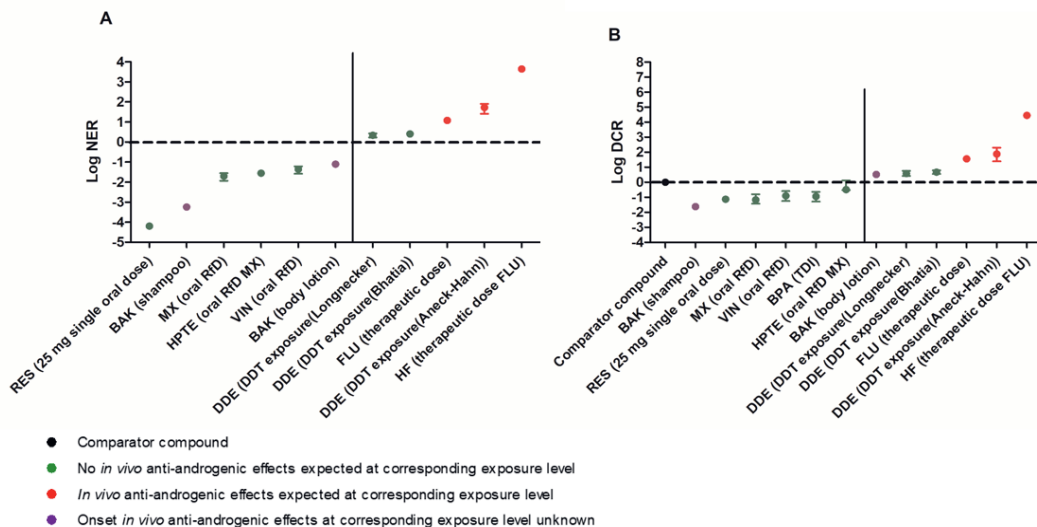


**Figure 6.2.** **A.** The NERs of the series of exposure scenarios to anti-androgenic compounds (Table 2.2, Chapter 2). **B.** The DCRs of the series of exposure scenarios to anti-androgenic compounds based on the  $EAR_{\text{comparator}}$  for DIM based on AR-CALUX data (Chapter 2). The comparator DCR is represented as black symbols and by definition equal to 1 ( $\log \text{DCR} = 0$ ). The NERs and DCRs of test compounds where no *in vivo* anti-androgenic effects are expected at the corresponding exposure scenario (Table 2.2, Chapter 2) are presented as green symbols and the NERs and DCRs of test compounds where *in vivo* anti-androgenic effects are expected or where this is unknown at the corresponding exposure scenario (Table 2.2, Chapter 2) are presented as red and purple symbols, respectively. The dotted horizontal line marks the NER or DCR of 1 ( $\log \text{NER}$  or  $\text{DCR} = 0$ ). The vertical lines separate the exposure scenarios with NER or  $\text{DCR} \leq 1$  from those with NER or  $\text{DCR} > 1$ .

## 6.5 PBK modelling to integrate NAM *in vitro* data in NGRA

The DCR approach relates *in vitro* bioactivity data to exposure data in an NGRA compliant way. It uses the internal concentrations of compounds to calculate the  $EAR$  values. When these data are not available, the internal concentrations can be predicted upon a given external dose with PBK modelling. However, PBK modelling can also be used as an NGRA compliant strategy to use *in vitro* concentration-responses in the safety assessment of chemical exposure to humans, translating the *in vitro* bioactivity data to the *in vivo* dose-response in QIVIVE to set the PoD without using animal data.

Also for this approach, the *in vitro* bioactivity assay must cover the *in vivo* endpoint for which the toxicological response will be predicted in humans, as in this thesis where PBK modelling-facilitated QIVIVE based on AR-CALUX assays was used to predict *in vivo* anti-androgenicity of DIM, BIC, and FLU. Based on the results obtained, some considerations of PBK modelling-facilitated QIVIVE but also of using PBK models to predict internal concentrations in the DCR approach as an NGRA-compliant and effective tool, can be identified and are discussed in the next sections, including i) the PBK modelling software used, ii) the use of a compound specific or generic PBK model, iii) PBK model validation when no human *in vivo* pharmacokinetic (PK) data are available, and iv) QIVIVE with single or multiple dosing.

### i) PBK modelling software

Many different computational software packages are available for PBK modelling. They can be divided in license-based or open source packages. The advantages of license-based PBK model software are that they are actively developed to include the newest innovations and techniques, and technical support and training modules are available. Further advantages are the built-in libraries containing parameters for different human physiologies, enabling the parameterization of a PBK model for specific populations, drug-specific ADME parameters and built-in modules for simulating different routes of administration for different compound formulations, e.g. capsule or tablet. These software modules are thoroughly validated favouring regulatory acceptance. License-based software is often non-programmatic with an intuitive and user-friendly graphical interface. However this can also be a disadvantage because the model code is not made available and the functioning of the model becomes a black box disabling the insight on the specific model equations and standard parameters (Loizou et al., 2008), making it difficult to understand how the model operates. Other disadvantages are the expensive license-fees hampering their broad availability and use, and technical complexity leading to required user expertise (Sager et al., 2015). Examples of license-based non-programmatic software packages are GastroPlus™ (Simulation Plus Inc., Lancaster, CA, United States) used in **Chapter 2** and **4** and SimCyp® (Certara, Princeton, NJ, United States). Berkeley Madonna (UC Berkeley, CA, USA) is license-based programmatic software, which allows insight in the underlying model code with the potential to modify the code according to the users requirements and thus provides a platform for technical developments (Bessemers et al., 2014; Paini et al., 2019). Most programmatic software packages are however open source. The advantages of open source PBK model software, besides the just mentioned benefits of being programmatic, is that they are freely accessible to everyone. Disadvantages are however that the user needs programming skills and that the models are not actively maintained (Paini et al., 2019)

and therefore may not use the latest techniques or received adequate quality control and potentially have incomplete functionality. Examples of open source software packages include the High-Throughput Toxicokinetics (httk)-R package (Pearce et al., 2017), IndusChemFate (Cefic LRI, Brussels, Belgium), MEGEN-RVis (Loizou & Hogg, 2011), and PK-sim (Open Systems Pharmacology Suite (OSPS)) which can be freely downloaded as an R package.

Making use of the different software packages hampers PBK model compatibility across the research field. Open source software with transparent model codes and parameter libraries will improve the interpretability of the PBK model predictions and the acceptance by regulatory agencies. This is also highlighted in the guidance document Good Modelling Practises (GMP) (Loizou et al., 2008), describing the requirements in PBK model development, characterization, documentation, and evaluation.

## ii) A compound specific or generic PBK model in NGRA

The PBK models developed in **Chapter 2** and **4** were compound specific models with a high level of detail describing the chemical kinetics in human physiology. Input parameters were specifically determined or predicted and thus the ADME characteristics of the compounds were accurately reflected in the model. The development of such compound specific PBK models is thus dependent on mechanistic understanding of the compound its kinetics in the body. The models are thoroughly evaluated and validated, aiming at predictions within a factor of 2 compared to *in vivo* data (Jones et al., 2015; WHO et al., 2005), which validates them for safety assessment purposes in NGRA. The development of such compound specific PBK models is labour intensive given that often many of especially the kinetic parameters for uptake and metabolism need to be experimentally determined in suitable *in vitro* bioassays. To increase the efficiency in developing PBK models and enable their use for higher throughput of compounds in NGRA, efforts are also directed at creating so-called generic PBK models. A generic PBK model uses only limited input parameters and thus reflects more general ADME characteristics. For chemicals with limited data available, this type of PBK model can be favoured to a compound specific model using fewer parameters for a first, quicker, estimation of the kinetics (Najjar et al., 2022 (Paini et al., 2021; Testai et al., 2021)). It has been suggested that the predictions of a generic PBK model must fall within a factor of 3 to the human *in vivo* PK data in the model evaluation (Jones et al., 2015; WHO et al., 2005). Although use of a generic model, once developed and validated, is more time and resource efficient, the model predictions may still need validation and thus the utility and validity of generic PBK models in the safety assessment of chemical exposure in humans may still be hampered by the absence of

available human *in vivo* PK data. Therefore a generic PBK model may be used at lower tier predictions of for instance the intestinal absorption of a compound, but a compound specific PBK model is necessary for higher tier predictions required in the safety decisions in NGRA, based on for example plasma or tissue levels of a compound.

iii) PBK model validation when no human *in vivo* pharmacokinetic (PK) data are available

Thus, the adequacy of the PBK model predictions must be evaluated against human *in vivo* PK data to confirm the validity of the model. The PBK models developed for BIC (**Chapter 2**) and FLU (**Chapter 4**) and the PBK model for DIM developed by Dent et al. (2019) predicted the respective human *in vivo* PK data within a factor of 2. However, for many (novel) chemicals, human *in vivo* PK data may be lacking, hampering PBK model validation. Recent attention directed at finding other ways to validate PBK models led to a guidance document on Good *in vitro* Method Practices (GIVIMP). The document focusses on increasing the quality of deriving the parameter values from *in vitro* assays as input for PBK models and thus reducing the uncertainty of those parameters (OECD, 2018a). This may consequently lead to reduced uncertainty in the PBK model predictions and possibly less dependency on validation against human *in vivo* PK data. Furthermore, read across approaches like QSARs may be considered for the PBK model development of chemicals lacking human PK data (Paini et al., 2021; Wambaugh et al., 2015) Najjar et al., 2022), whereby the human PK data of chemical(s) with a similar structure and thus potentially comparable kinetic characteristics are used for validation of the PBK model predictions of the target chemical. This highlights the need for an open source PK database for good availability for human *in vivo* PK data of compounds (Testai et al., 2021) Najjar et al., 2022) which could be used in the read across based validation of PBK models for novel compounds.

iv) QIVIVE with single or multiple dosing

With a developed and validated PBK model, QIVIVE can thus be implemented to translate *in vitro* concentration-response data to *in vivo* dose-response data. In **Chapter 2**, the QIVIVE of DIM and BIC was performed and in **Chapter 4** the QIVIVE of FLU, all translating the AR-CALUX derived *in vitro* concentration-response data to corresponding *in vivo* dose-response data of the compounds. The AR-CALUX assay covers a 24 h exposure time and is used to predict the respective *in vivo* response following exposure to a single dose or multiple doses of the compound in humans. It depends on the kinetics of a chemical whether QIVIVE has to be based on single or



multiple dosing. For chemicals for which the toxicity is dependent on the peak concentration ( $C_{\max}$ ) and the plasma/blood levels are cleared and the toxic effect is repaired within 24h, using the  $C_{\max}$  after a single dose is adequate for QIVIVE predicting single as well as repeated exposure. However, when the toxic effect is not repaired after 24 h or when a compound accumulates in the body following multiple dosing, the steady state of the  $C_{\max}$  after multiple dosing should be used in QIVIVE to predict the dose-response following repeated exposure in humans, as demonstrated in **Chapter 2** and **4**.

## 6.6 The free unbound compound concentration as appropriate dose metric in the DCR approach and QIVIVE

The nominal compound concentration is often used as the dose metric in both *in vitro* and *in vivo* studies. However, this appears not to be the appropriate dose metric since only the free unbound concentration of a compound will exert toxicity and thus the free concentration is considered a more suitable dose metric. The determination of the free unbound concentration of a compound in the *in vitro* and *in vivo* situation is a topic for considerable debate in toxicology. In this thesis, it was assumed that correcting for only differences in *in vitro* and *in vivo* protein binding provides an adequate free concentration as dose metric in the DCR approach (**Chapter 2** and **3**) and for QIVIVE (**Chapter 4**). However, compounds bind not only to proteins but also to lipids, plastic, other compounds, and surfaces or matrix components all with different affinity. Furthermore in *in vitro* model systems compounds may distribute over, for instance, the liquid and air phase also affecting the free bioavailable concentration. The free concentration of a chemical *in vitro* is thus dependent on the experimental setup whereas the free concentration *in vivo* is dependent on for example tissue type and its blood flow. For these reasons, only correcting for protein binding could be expected to have limitations. However, at the present state of the art, there are many examples (Gilbert-Sandoval et al., 2020; Shi et al., 2020; D. Wang et al., 2021; Q. Wang et al., 2022) where correction for only protein binding was proven to be sufficient for an adequate extrapolation of *in vitro* to *in vivo* concentrations, as also corroborated by the results from **Chapter 2** and **4** in this thesis. It is an ongoing effort to find and validate methods to measure the free unbound concentration of a compound in its surroundings. Some *in vitro* approaches are available to measure the protein unbound fraction like the rapid equilibrium dialysis (RED) assay (van Liempd et al., 2011). Also, *in silico* tools are available to predict the protein unbound fraction *in vivo* like the ADMET™ predictor that can predict parameter values based on QSARs, and was used in this thesis. From the predicted fraction unbound *in vivo*, the protein fraction unbound *in vitro* can be

extrapolated assuming 100% of the chemical to be in the free form in the absence of added serum in the bioassay (**Chapter 2**). Furthermore, more complex models to determine the free concentration of these compounds in an *in vitro* system are also available. These models predict *in vitro* distribution kinetics of chemicals over the medium, proteins, lipids, cell membrane, cellular proteins, cellular lipids, and plastic based on QSAR-predicted partition coefficients (Rodgers et al., 2005; Rodgers & Rowland, 2006) and chemical and *in vitro* system specific inputs (Proença et al., 2021).

## 6.7 Approaches to include biotransformation in the *in vitro* and *in silico* tools

The PBK modelling-facilitated QIVIVE approaches presented in **Chapter 2** were based on the *in vitro* bioactivity data of only the parent compounds. However some compounds are bioactivated or inactivated, often in the liver, and excluding the (absence of) activity of possible relevant metabolites potentially under (or over) predicts the *in vivo* toxicity in humans. In **Chapter 4** and **5** of this thesis, two approaches were examined to include biotransformation in an NGRA context using *in vitro* bioactivity assays and *in silico* tools. These approaches included 1) Using a toxic equivalency factor (TEF) approach in the PBK modelling-facilitated QIVIVE to include the role of an active metabolite and 2) Development of a new *in vitro* technology enabling co-cultivation of metabolically competent cells and reporter gene cells to include the metabolite formation in the *in vitro* bioactivity assays. Regarding the findings, some aspects have to be taken into consideration to affirm and exploit them as practical tools in NGRA which are discussed in the next sections, including i) similar or non-similar concentration-responses in the TEF approach as well as ii) the *in vivo* relevance of 3D HepaRG microtissues compared to other hepatic biotransformation models, iii) the applicability domain of the two-chamber co-culture system, and iv) how to extrapolate findings from the co-culture system to the *in vivo* situation.

### i) Similar or non-similar concentration-responses in the TEF approach

Application of the TEF approach for FLU +HF formally implies that the following criteria should be met i) FLU and HF exhibit the same mode of action, ii) their concentration-response curves in the *in vitro* AR-CALUX assay are parallel, and iii) the activity of FLU and HF in the AR-CALUX assay is additive. In other words, they have a similar *in vitro* pattern of toxicity which is additive and the shape of the concentration-response curves

is similar. Hence, their relative potency is similar at all concentrations. This enables the expression of their relative potency as a constant value based on for example the  $IC_{50}$  to define the TEF. However, for compounds with concentration-response curves that do not have a similar shape, using the TEF based on the  $IC_{50}$  (or  $EC_{50}$ ) may misrepresent their relative potency as this value will vary along the concentration-response curve and a more complex description of how the relative potency changes with the concentration is required. Subsequently, a more statistical complex expression of relative potency as a function of concentration, mean response, or response quantile may be favourable. These functions can be different depending on whether the limits of the concentration-responses are different. When the response limit differences are due to extrinsic (e.g. interlaboratory differences) factors one may choose for a relative potency function of the mean response whereas when these are due to intrinsic (chemical-specific) factors one may choose for the function of concentration or response quantile. These functions could potentially be integrated in the TEF approach (Dinse & Umbach, 2011).

- ii) The *in vivo* relevance of 3D HepaRG microtissues compared to other techniques for executing *in vitro* bioactivity assays in the presence of hepatic biotransformation

In **Chapter 5** of the present thesis 3D HepaRG microtissues were used for *in vitro* hepatic biotransformation. One of the benefits of the agarose-based *in vitro* two-chamber co-culture system is the co-cultivation of liver and target tissue in different chambers sharing the same medium, whereas the agarose hydrogel allows the free diffusion of chemicals between the compartments (Ip et al., submitted). This is preferred compared to other co-culture techniques using for instance organ-on-chips where liver and target cells are separated in plastic wells (Li et al., 2012), only allowing chemical flow and/or diffusion *via* overlaying medium.

Other techniques have been proposed to execute *in vitro* bioactivity assays in the presence of hepatic biotransformation, such as co-incubation of cells of reporter gene assays, like the CALUX assay, with a hepatic S9 fraction and cofactors for phase I and phase II metabolic enzymes (Mollergues et al., 2017; Sumida et al., 2001; van Vugt-Lussenburg et al., 2018). From an NGRA perspective, using human S9 in such an approach is preferred over rat S9, even though rat S9 fractions are often induced with for instance  $\beta$ -naphthoflavone and phenobarbital ( $\beta$ NF/PB) to increase the enzyme expression levels (Mollergues et al., 2017). However, human S9 has been demonstrated to have large interindividual differences in enzyme levels and metabolic activities

(Chiba et al., 2009; Hakura et al., 2003). The advantages of using 3D HepaRG microtissues as biotransformation system compared to human S9 is that they are not prone to interindividual differences being derived from a cancerous cell line, that they can be kept in culture long-term, and have robust liver characteristics such as phase I and phase II metabolizing enzyme expression over time, biliary excretion, and zonation characteristics as in the human liver (Gunness et al., 2013; Jackson et al., 2016; Leite et al., 2012; Ramaiahgari et al., 2017) Ip et al. submitted). Nevertheless, the enzyme expression levels are dependent on culturing conditions as demonstrated in **Chapter 5**, where removing hydrocortisone (HC) from the differentiation medium (DM) resulted in lower enzyme expression levels than when HC was present (Ip et al., submitted), the latter showing relative enzyme expression levels comparable to what was reported in the human *in vivo* liver (Pelkonen et al., 2008). Noteworthy is the fact that using 3D HepaRG microtissues compared to using liver S9 as a biotransformation system, chemical permeability through the cell membrane is taken into consideration and thus metabolism is captured in a more *in vivo* relevant manner. Also other cell-based *in vitro* liver models like 2D HepaRG, HepG2, and induced pluripotent stem cells (iPSCs) derived hepatocytes are available. Compared to 3D HepaRG microtissues, 2D HepaRGs and HepG2 are more easy to culture, but 3D HepaRG microtissues may be preferred due to their higher metabolic activity which is also more comparable to primary hepatocytes (Gunness et al., 2013; Jackson et al., 2016; Leite et al., 2012; Ramaiahgari et al., 2017) Ip et al. submitted). The enzyme levels of iPSCs derived hepatocytes are low and consequently their use is more targeted to a liver disease model for pharmacological research and drug screening (Corbett & Duncan, 2019). Furthermore, a 3D configuration reflects a more complex physiological and *in vivo* relevant structure than a 2D liver structure.

Of course, a 3D HepaRG microtissue is still a simplified reflection of the *in vivo* situation and it may not fully replicate the human liver. Also, the ratio between liver and reporter cells and the measured conversion of T to AD in the two-chamber co-culture system of **Chapter 5** may not reflect the ratio between hepatic tissue mediating DHT and T inactivation and androgen responsive tissues in the body. Free plasma concentrations of T in males range from 0.01 – 0.05 nM (Mayo Clinic Staff 2022; van Tongeren et al., 2023). Converting the nominal T concentrations having significant different responses in the two-chamber co-culture system with human liver and AR reporter cells in the absence and presence of 3D HepaRG microtissues, to the free concentrations using the  $f_{ub}$  *in vitro* of 0.48 (van Tongeren et al., 2021) results in free *in vitro* T concentrations of 0.05 and 0.14 nM T in the AR-INDIGO assay and 1.44 – 4.8 nM in the AR-CALUX assay. Comparing these values to the free plasma concentrations of T in males of 0.01 – 0.05 nM, indicates that the AR response induced by T derived in the two-chamber co-culture system with human liver and AR-INDIGO cells mimics the AR response of T in the male

body to a better extent than the response derived with the two-chamber co-culture system with human liver and AR-CALUX cells

### iii) The applicability domain of the two-chamber co-culture system

Assessing whether metabolites influence the toxicity of a parent compound can also be evaluated for other functional endpoints when the respective *in vitro* bioactivity assay is compatible with the culture conditions in the system. Given that the AR-INDIGO and AR-CALUX systems performed adequately as target tissues in the system, reporter gene assays evaluating other endpoints in similar bioactivity assays will likely also be compatible with the two-chamber co-culture system culture conditions as applied in the present thesis. Both INDIGO and CALUX assays are available for a broad range of other receptors, e.g. the ER-INDIGO and ER-CALUX assay to study e.g. estrogenicity. The two-chamber co-culture system could also be applied beyond *in vitro* reporter gene assays, for example, assessing the proliferative response of MCF-7 cells in the MCF-7/Bos proliferation assay or the development of embryonic ES-D3 cells to beating cardiomyocytes in the embryonic stem cell test. This will generate more proofs of principles for other compounds and endpoints and will contribute to the hazard identification of compounds with unknown metabolites affecting the corresponding bioactivity based on use of two-chamber co-culture system with human liver and target cells that enable detection of an endpoint of interest.

### iv) How to extrapolate findings from the co-culture system to the *in vivo* situation

When the *in vitro* response of a compound increases or decreases in the presence of the 3D HepaRG microtissues in two-chamber co-cultures system, presumably hepatic metabolites were produced which were more bioactive or inactive, respectively, than the parent compound. In subsequent analyses these metabolites should be identified so that their formation and activity can be included when defining a PoD for the parent compound so that the toxic effect would not be under or overpredicted. The *in vitro* concentration-response curve of the parent compound in presence of 3D HepaRG microtissues can however not be used in PBK modelling-facilitated QIVIVE since liver kinetics are already captured in the *in vitro* response, so that application of PBK modelling-facilitated QIVIVE would double account for the biotransformation. For now, the two-chamber co-culture system can be used to identify that a metabolite is affecting the response of the parent compound so that in a next step the TEF-based PBK

modelling-facilitated QIVIVE of the parent compound including the bioactivity of the respective metabolites can be performed to derive the PoD for the safety assessment. This approach will translate the *in vitro* response of the parent compound in the *in vitro* bioactivity assay in the absence of 3D HepaRG microtissues. When the *in vitro* response of a compound remains unaffected in the presence of the 3D HepaRG microtissues in the two-chamber co-culture system, hepatic biotransformation may not play a role in the effects of a compound and may not need to be specifically considered in QIVIVE.

## 6.8 Uncertainty factors in the NGRA approaches

A topic that cannot be left untouched is the application of uncertainty factors (UFs) in the NGRA approaches. In **Chapter 2** and **3**, a DCR cut-off of  $\leq 1$  was set to estimate whether an anti-androgenic or estrogenic exposure can be considered safe. In this DCR approach the BMCL<sub>05</sub> value was used and proven to represent an adequate no effect level of the selected comparator compounds. The conclusion that this approach was valid was based on comparison of the resulting predicted DCR values to known biological outcomes of the respective exposure scenarios. It is however of interest to note that the included literature reported exposure scenarios to the model compounds and the related biological outcomes refer to the reported populations and may show a different outcome in another (more or less sensitive) population. The respective DCR-based safety assessment may thus be indicative for the reporter population but may not be representative for the safety for the general population including sensitive individuals or another specific population of interest. Further research can be performed using PBK modelling with Monte Carlo methods to simulate, upon the reported exposure scenario, the distribution of the predicted internal concentrations over a defined population where interindividual differences are taken into account. PBK modelling can further help identifying for instance a sensitive population for the compound exposure. To also protect sensitive individuals in a population and take into account interindividual variability, an UF could be included in the DCR approach when defining the DCR cut-off value for considering an exposure to be safe. Thus, including the default uncertainty factor of 10 used in human safety assessment for interindividual differences, it could be considered to define only DCR values  $\leq 0.10$  to be safe. Considering that the toxicodynamics for a well-defined AOP may show interindividual differences that are similar for the comparator and test compounds, one could also consider to use only the default uncertainty factor of 4 for interindividual differences in kinetics so that only DCR  $\leq 0.25$  would be considered safe. Furthermore, executing the DCR approach, an extra UF could be used to account for uncertainty using only *in vitro* and *in silico* data, implying the use of an even lower DCR cut-off value resulting in a more conservative safety estimation. In **Chapter 4**, for the TEF-based PBK modelling-

facilitated QIVIVE approach also a re-evaluation of the used UFs as opposed to those traditionally used in animal-based risk assessment can be made. The UF for interspecies differences could be exchanged for an UF capturing the uncertainty using *in vitro* and *in silico* data. Generating more proofs of principle will contribute to a more appropriate estimation of the UF values required for a protective risk assessment.

## 6.9 Future perspectives and conclusion

The present thesis described new approaches in NGRA to define human relevant safe levels of chemical exposure, by integrating *in vitro* and *in silico* approaches for compounds with (anti)androgenic and estrogenic effects. The results obtained showed that these NGRA tools are promising alternative strategies in the toxicity testing of (anti)androgens and estrogens and can be applied to assess the safety of human exposures to for example pharmaceuticals, cosmetics, food constituents, and pesticides with regard to these endpoints. As this field in science continues to advance, the future perspectives of animal free testing include the combination of *in vitro* and *in silico* approaches, next to each other or in a tiered approach for the toxicity screening and prioritization of (anti)androgenic and estrogenic compounds. For example, in a first tier, the *in silico* prediction of the binding affinity of a chemical to a biological target using for instance the MIE ATLAS (Allen et al., 2018) can be made. In a second tier, relevant *in vitro* bioactivity assays like CALUX assays can be executed to derive the corresponding *in vitro* effect concentrations of the chemical. In a third tier, with the DCR approach the derived *in vitro* effect concentrations can be related to an exposure scenario to the chemical under study to determine the corresponding DCR and/or just whether the predicted *in vivo* internal free dose level is below the *in vitro* BMCL<sub>05</sub> or rather in the range of an *in vitro* effect level. When the DCR obtained is  $> 1$ , or the internal concentration exceeds the relevant BMCL<sub>05</sub> the compound could be prioritized for further toxicity testing, whereas when the DCR obtained is  $\leq 1$ , or the internal concentration is below the BMCL<sub>05</sub>, the respective exposure to the compound under study can be considered safe. In the DCR approach, PBK modelling is an essential tool to obtain internal concentrations upon reported external dose levels and to translate the BMCL<sub>05</sub> to its BMDL<sub>05</sub> as safe dose level of the comparator compound. Next to this, when it is expected that hepatic biotransformation affects the *in vivo* toxicity of the compound or whether this is unknown, with the TEF-based PBK modelling-based QIVIVE approach, insight will be obtained on the contribution of potential metabolites to the biological effects induced by exposure to the parent compound and prediction of the dose-response curve in humans becomes feasible. From the predicted dose-response the PoD can be derived to be used in the risk assessment. Alternatively when it is unknown whether metabolites affect the toxicity of a parent compound, the two-

chamber co-culture system with human liver and reporter cells will provide the *in vitro* concentration-response data of the parent compound under study in the presence of hepatic biotransformation and thus information can be obtained regarding the influence of hepatic metabolites on the respective bioactivity. More chemicals and other endpoints are required, for which the *in vivo* activity is affected by hepatic metabolism, in order to increase the level of confidence needed for wider use of these NGRA methods by risk assessors. The validation of the *in vitro* bioassays, the DCR approach, and the PBK models and the acceptance of these tools by regulatory agencies (Punt et al., 2011) is essential and will contribute to the implementation of the NGRA strategies in human safety assessment.

In conclusion, the DCR approach provides a valuable new approach methodology for the safety assessment of human chemical exposures to anti-androgens and estrogens, integrating *in vitro* bioactivity and *in vivo* human exposure data of the compounds under study. Furthermore, when a metabolite is substantially more active than its parent compound and produced in substantial amounts, including the bioactivity of that metabolite in the PBK-modelling facilitated QIVIVE of the parent compound using a TEF approach results in protective and a more appropriate PoD for human safety assessment. The two-chamber co-culture system with human liver and reporter cells is a new technology that will allow the *in vitro* determination of toxicodynamic responses in the presence of hepatic biotransformation, thus identifying the influence of metabolites on the toxic response of a parent compound. The NGRA strategies thus presented in this thesis are demonstrated to be appropriate for the human safety assessment of exposure to (anti)androgens and estrogens in an animal free *in silico/in vitro* 3R compliant way.







# Chapter 7

## Chapter 7. Summary

To assure safe levels of human exposure to chemicals, in toxicological risk assessment advances are made to shift from using animal-based to animal-free testing strategies. This is fuelled by ethical, economic, and legislative issues and the scientific rationale that experimental animals do not adequately represent the human body and animal test guidelines may not cover human pathologies. The development of animal-free testing strategies is highlighted by the 3Rs (replace, reduce, and refine) in the use of experimental animals, including the development of *in vitro* and *in silico* approaches to assess chemical-induced biological changes in human physiology. In Next Generation Risk Assessment (NGRA), the development and use of non-animal based new approach methodologies (NAMs) aims not to predict chemical-induced pathologies in animals but to assure human safety, eliminating the need for animal data. This is described in **Chapter 1** where the aim of this thesis is also provided, namely to perform NGRA to inform human-relevant safe levels of chemical exposure, integrating *in vitro-in silico* approaches for chemicals with putative (anti)androgenic and/or estrogenic effects.

In **Chapter 2**, an NGRA strategy is presented that uses the Dietary Comparator Ratio (DCR) to evaluate the safety of defined exposures to anti-androgenic compounds. The DCR compares the Exposure Activity Ratio (EAR) for the compound of interest, to the EAR of an established safe level of human exposure to a comparator compound with the same putative mode of action. A  $DCR \leq 1$  indicates the exposure evaluated is safe. In **Chapter 2**, the  $EAR_{\text{comparator}}$  values were defined solely based on the *in vitro* androgen receptor (AR)-CALUX assay, using the 95% lower confidence limit of the benchmark concentration (BMC) causing 5% extra response above background level ( $BMCL_{05}$ ) values as alternative safe level of exposure. The adequacy of the newly defined  $EAR_{\text{comparator}}$  values was confirmed by physiologically based kinetic (PBK)-modelling based translation of the  $BMCL_{05}$  values to external exposure levels that were shown to be safe and by comparison of the generated DCR values of the evaluated exposure scenarios for the anti-androgenic test compounds to actual knowledge on (the absence of) their *in vivo* anti-androgenic effects in humans.

In **Chapter 3**, the use of the *in vitro*-based  $EAR_{\text{comparator}}$  is further supported by the adequate DCR-based safety assessment of exposure scenarios to estrogens, based on multiple *in vitro* bioactivity assays. This further affirms the DCR approach as an *in silico/in vitro* 3R compliant strategy for evaluating the safety and efficacy of human exposure scenarios without using animal data in NGRA.

In **Chapter 4**, another NGRA strategy is explored aiming at including hepatic biotransformation by providing a proof of principle for PBK modelling-facilitated quantitative *in vitro* to *in vivo* extrapolation (QIVIVE) using a toxic equivalency factor (TEF) approach. In the PBK modelling-facilitated QIVIVE of the selected anti-androgenic model compound flutamide (FLU), its *in vitro* AR-CALUX derived concentration-response curve was translated to the corresponding *in vivo* dose-response curves, either excluding or including the activity of its more anti-androgenic active metabolite hydroxyflutamide (HF). It was demonstrated that including the bioactivity of the active metabolite in PBK modelling-facilitated QIVIVE provides a better and more appropriate point of departure (PoD) to assure human safe exposure levels to the parent compound, whereas excluding the activity of the metabolite will potentially result in an underestimation of the corresponding risk.

In **Chapter 5**, a two-chamber co-culture system with human liver and reporter cells is developed to assess androgenic responses in the absence and presence of a biotransformation system. The androgenic response of testosterone (T) and 5 $\alpha$ -dihydrotestosterone (DHT), which are hepatically detoxified, were assessed using the AR-CALUX or AR-INDIGO assay in the absence or presence of 3D HepaRG microtissues, that exhibit active hepatic metabolism. Androstenedione, which is an inactivated metabolite, was formed following incubation of T with the 3D HepaRG microtissues which translated in the co-culture system to a significantly reduced T mediated induction of the AR response in both reporter gene assays in the presence of 3D HepaRG microtissues. A similar 3D HepaRG microtissues dependent reduction in the DHT induced AR response was observed in line with the hepatic inactivation of DHT by a similar biotransformation step. The two-chamber co-culture system with human liver and reporter cells may thus provide a screening tool to identify chemicals for which hepatic metabolism affects their bioactivity and thus should be included when setting the PoD of the parent compound.

In **Chapter 6**, a general overview of the results is provided which are then discussed in a wider perspective, followed by future perspectives and conclusions. It is concluded that the DCR approach provides an appropriate NAM for the safety assessment of human chemical exposures to anti-androgenic and estrogenic compounds. Furthermore, biologically active metabolites should be taken into account in the PBK modelling-facilitated QIVIVE for evaluating the safety of a parent compound. Lastly, the two-chamber co-culture system with human liver and reporter cells is a new technology that will allow the identification of hepatic metabolites affecting the *in vitro* bioactivity of a parent compound. Taken together, it is concluded that the NGRA strategies presented in this thesis are appropriate and of value for human safety assessment of

exposure to (anti)androgens and estrogens in an animal *free in silico/in vitro* 3R compliant way.



# Chapter 8

## Chapter 8. Samenvatting

Bij het vaststellen van veilige blootstellingsniveaus van chemische stoffen voor de mens in de toxicologische risicobeoordeling, wordt vooruitgang geboekt in de transitie van het gebruiken van op proefdier gebaseerde naar proefdiervrije teststrategieën. Deze transitie wordt gevoed door ethische, economische en wettelijke overwegingen terwijl tegelijkertijd proefdieren mogelijk niet het menselijke lichaam adequaat vertegenwoordigen en dierproefrichtlijnen mogelijk geen adequaat inzicht verschaffen in menselijke ziektebeelden, wat betekent dat ook wetenschappelijk argumenten een reden zijn voor de verandering van de aanpak. De ontwikkeling van proefdiervrije teststrategieën wordt benadrukt in de 3Vs (vervangen, verminderen en verfijnen) van het gebruik van proefdieren, waarbij de ontwikkeling van *in vitro* en *in silico* benaderingen om chemisch-geïnduceerde biologische veranderingen in de menselijke fysiologie te analyseren een belangrijke rol spelen. In Nieuwe Generatie Risicobeoordeling (Next Generation Risk Assessment) (NGRA) is de ontwikkeling en het gebruik van proefdiervrije nieuwe benaderingsmethodologieën (new approach methodologies) (NAMs) niet gericht op het voorspellen van de ziektebeelden die in dieren veroorzaakt worden door chemische stoffen, maar op het verzekeren van veilige blootstellingen voor de mens, waardoor diergegevens overbodig worden. Deze aanpak wordt verder toegelicht in **Hoofdstuk 1** waar ook het doel van het proefschrift wordt beschreven, namelijk het uitvoeren van NGRA om voor de mens relevante veilige blootstellingsniveaus van chemische stoffen vast te stellen, waarbij *in vitro-in silico* benaderingen worden geïntegreerd voor chemische stoffen met vermoedelijk (anti)androgene en/of oestrogene effecten.

In **Hoofdstuk 2** wordt een NGRA strategie gepresenteerd die gebruik maakt van de zogeheten Dieet Vergelijker Ratio (Dietary Comparator Ratio) (DCR) om de veiligheid voor de mens van gedefinieerde blootstellingen aan anti-androgene stoffen te evalueren. De DCR vergelijkt de Blootstelling Activiteit Ratio (Exposure Activity Ratio) (EAR) van de blootstelling aan de te onderzoeken chemische stof met de EAR van een vastgesteld veilig blootstellingsniveau aan een chemische stof, de comparator, met hetzelfde werkingsmechanisme. Een  $DCR \leq 1$  geeft aan dat de onderzochte blootstelling veilig is. De  $EAR_{\text{comparator}}$  waarden werden in **Hoofdstuk 2** uitsluitend bepaald op basis van de *in vitro* androgeen receptor (AR)-CALUX test, waarbij de ondergrenswaarde van het betrouwbaarheidsinterval van 95% van de benchmark concentratie (BMC) die een extra respons van 5% boven het achtergrondniveau veroorzaakt ( $BMCL_{05}$ ) werd gebruikt als alternatief veilig blootstellingsniveau. De geschiktheid van de nieuw gedefinieerde  $EAR_{\text{comparator}}$  waarden werd bevestigd door de vertaling van de  $BMCL_{05}$  waarden op basis van fysiologisch gebaseerde kinetische (physiologically based kinetic)

(PBK)-modellering naar *in vivo* doseringen die veilig waren en een vergelijking van de gegenereerde DCR waarden van de onderzochte blootstellingsscenario's voor de anti-androgene stoffen met feitelijke kennis over (de afwezigheid van hun *in vivo* anti-androgene effecten in de mens).

In **Hoofdstuk 3** wordt de geschiktheid van een op *in vitro* gegevens gebaseerde  $EAR_{\text{comparator}}$  waarde verder bevestigd in de adequate op DCR gebaseerde veiligheidsbeoordeling van blootstellingsscenario's aan oestrogenen, op grond van meerdere *in vitro* bioactiviteitstesten. Hiermee wordt de DCR-benadering als een *in silico/in vitro* 3V-conforme strategie zonder het gebruik van diergegevens in NGRA verder ondersteund.

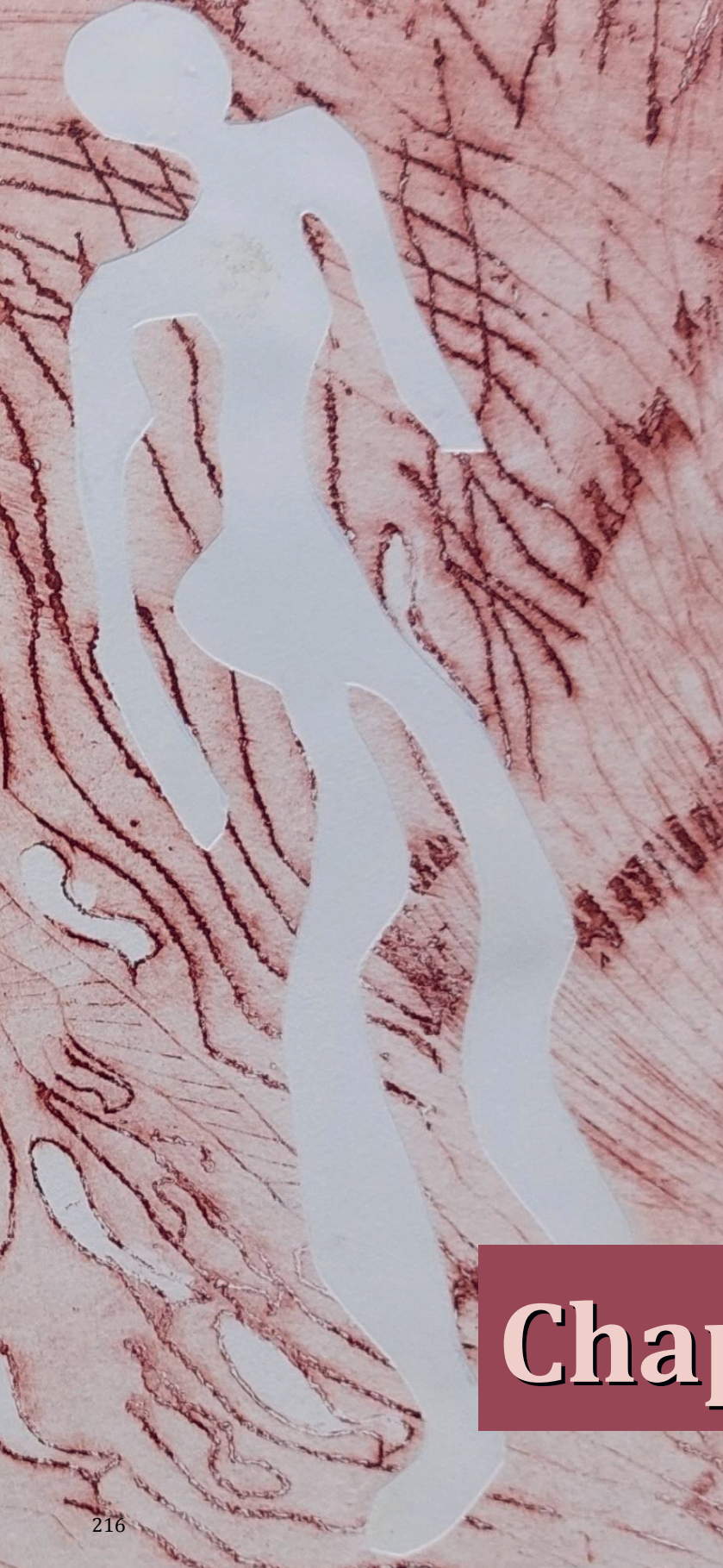
In **Hoofdstuk 4** wordt een NGRA-strategie onderzocht die geschikt is om leverbiotransformatie en de activiteit van gevormde metabolieten op te nemen in de NAM via PBK model-gefaciliteerde kwantitatieve *in vitro* naar *in vivo* extrapolatie (quantitative *in vitro* to *in vivo* extrapolation) (QIVIVE) met behulp van een toxische-equivalentiefactor (TEF). In de PBK model-gefaciliteerde QIVIVE van de geselecteerde anti-androgene modelstof flutamide (FLU) werd de concentratie-responscurve uit de *in vitro* AR-CALUX test vertaald naar de overeenkomstige *in vivo* dosis-responscurves, waarbij de activiteit van de meer anti-androgeen actieve metaboliet hydroxyflutamide (HF) al dan niet werd meegenomen. Het bleek dat het opnemen van de bioactiviteit van de actieve metaboliet in de PBK model-gefaciliteerde QIVIVE een geschikt uitgangspunt (point of departure) (PoD) oplevert om bij de mens veilige blootstellingsniveaus aan de moederstof te bepalen, terwijl het niet meenemen van de activiteit van de metaboliet zou leiden tot een onderschatting van het betreffende risico.

In **Hoofdstuk 5** wordt een twee-compartiment co-cultuursysteem met menselijke lever en reporterzellen ontwikkeld om de androgene respons te meten in de af- en aanwezigheid van een biotransformatie. De androgene respons van testosteron (T) en  $5\alpha$ -dihydrotestosteron (DHT), die hepatisch worden geïnactiveerd, werd beoordeeld met de AR-CALUX of AR-INDIGO assay in af- of aanwezigheid van 3D HepaRG microweefsels. Androsteendion, een inactieve metaboliet van T, werd gevormd na incubatie van T met de 3D HepaRG microweefsels, wat zich in het systeem vertaalde in de significant verminderde T-geïnduceerde AR-respons in beide reporter-gen tests in aanwezigheid van 3D HepaRG microweefsels. Eenzelfde 3D HepaRG microweefsel afhankelijke vermindering in de DHT-geïnduceerde AR-respons werd waargenomen in lijn met de hepatische inactivatie van DHT via eenzelfde biotransformatiestap. De waargenomen respons van het twee-compartiment co-cultuursysteem met menselijke lever en reporterzellen kan dus een screeningsinstrument bieden om chemische stoffen



te identificeren wiens lever metabolieten invloed hebben op hun bioactiviteit en dus meegenomen moeten worden wanneer de PoD van de moederstof wordt bepaald.

In **Hoofdstuk 6** wordt een algemeen overzicht gegeven van de belangrijkste bevinden van dit proefschrift, die vervolgens in een breder perspectief worden bediscussieerd, gevolgd door toekomstperspectieven en conclusies. Geconcludeerd wordt dat de DCR een geschikte nieuwe benaderingsmethodologie biedt voor de veiligheidsbeoordeling van menselijke blootstellingen aan anti-androgenen en oestrogenen. Bovendien zouden ook de biologisch actieve metabolieten meegenomen moeten worden in de PBK model-gefaciliteerde QIVIVE in de veiligheidsbeoordeling van de moederstof. Ten slotte, het twee-compartiment co-cultuursysteem biedt een screeningsinstrument om chemische stoffen te identificeren wiens lever metabolieten invloed hebben op hun bioactiviteit en dus meegenomen moeten worden wanneer de PoD van de moederstof wordt bepaald. Samenvattend, de in dit proefschrift gepresenteerde NGRA-strategieën blijken geschikt en van waarde te zijn voor de veiligheidsbeoordeling van blootstelling aan (anti)androgenen en oestrogenen in de mens op een diervrije *in silico/in vitro* 3R-conforme manier.



# Chapter 9

## Chapter 9. References

- Adir, J., Caplan, Y. H., & Thompson, B. C. (1978). Kepone® serum half-life in humans. *Life Sciences*, 22(8). [https://doi.org/10.1016/0024-3205\(78\)90494-0](https://doi.org/10.1016/0024-3205(78)90494-0)
- Adlercreutz, H. (1998). Epidemiology of phytoestrogens. *Bailliere's Clinical Endocrinology and Metabolism*, 12(4). [https://doi.org/10.1016/S0950-351X\(98\)80007-4](https://doi.org/10.1016/S0950-351X(98)80007-4)
- Aguilar, E., Crebelli, R., Di Domenico, A., Dusemund, B., Frutos, M. J., Galtier, P., Gott, D., Gundert-Remy, U., Lambré, C., Leblanc, J.-C., Lindtner, O., Moldeus, P., Mortensen, A., Mosesso, P., Parent-Massin, D., Oskarsson, A., Stankovic, I., Waalkens-Berendsen, I., Woutersen, R. A., Wright, M., Younes, M. (2015) Risk assessment for peri- and post-menopausal women taking food supplements containing isolated isoflavones. *EFSA J* 13(10). <https://doi.org/10.2903/j.efsa.2015.4246>
- Alexandre, J., Benford, D., Boobis, A., Ceccatelli, S., Cottrill, B., Cravedi, J.-P., Di Domenico, A., Doerge, D., Dogliotti, E., Edler, L., Farmer, P., Filipič, M., Fink-Gremmels, J., Fürst, P., Guérin, T., Knutsen, H. K., Machala, M., Mutti, A., Schlatter, J., Rose, M., van Leeuwen, R. (2011) Scientific Opinion on the risks for public health related to the presence of zearalenone in food. *EFSA J* 9(6). <https://doi.org/10.2903/j.efsa.2011.2197>
- Allen, T. E. H., Goodman, J. M., Gutsell, S., Russell, P. J. (2018). Using 2D Structural Alerts to Define Chemical Categories for Molecular Initiating Events. *Toxicological Sciences*, 165(1). <https://doi.org/10.1093/toxsci/kfy144>
- Almeida, L., Vaz-da-Silva, M., Falcão, A., Soares, E., Costa, R., Loureiro, A. I., Fernandes-Lopes, C., Rocha, J. F., Nunes, T., Wright, L., & Soares-da-Silva, P. (2009). Pharmacokinetic and safety profile of trans-resveratrol in a rising multiple-dose study in healthy volunteers. *Molecular Nutrition and Food Research*, 53(SUPPL. 1). <https://doi.org/10.1002/mnfr.200800177>
- Aneck-Hahn, N. H., Schulenburg, G. W., Bornman, M. S., Farias, P., & De Jager, C. (2007). Impaired semen quality associated with environmental DDT exposure in young men living in a malaria area in the Province, South Africa. *Journal of Andrology*, 28(3). <https://doi.org/10.2164/jandrol.106.001701>
- Aninat, C., Piton, A., Glaise, D., Le Charpentier, T., Langouët, S., Morel, F., Guguen-Guillouzo, C., Guillouzo, A. (2006). Expression of cytochromes P450, conjugating enzymes and nuclear receptors in human hepatoma HepaRG cells. *Drug Metabolism and Disposition*, 34(1). <https://doi.org/10.1124/dmd.105.006759>

- ANSES (French Agency for Food, Environmental and Occupational Health and Safety), 2018b. Note d'appui scientifique et technique de l'Agence nationale de securite sanitaire de l'alimentation, de l'environnement et du travail (ANSES) relative e a la fixation d'une limite maximale de residus de chlordecone dans la graisse pour les denrees carnees (2018b-SA-0202). Available online: <https://www.anses.fr/fr/system/files/ERCA2018bSA0202.pdf>. Accessed 4 Jan 2022
- ANSES (French Agency for Food, Environmental and Occupational Health and Safety), 2019. Avis de l'Agence nationale de securite sanitaire de l'alimentation, de l'environnement et du travail (ANSES) relative e a la fixation d'une limite maximale de residus de chlordecone dans les muscles et dans la graisse pour les denrees carnees (2018-SA-0265).. Available online. <https://www.anses.fr/fr/system/files/ERCA2018SA0265.pdf>. Accessed 4 Jan 2022
- Anton, R., Barlow, S., Boskou, D., Castle, L., Crebelli, R., Dekant, W., Engel, K.-H., Forsythe, S., Grunow, W., Ireland, J., Larsen, J. C., Leclercq, C., Mennes, W., Milana, M.-R., Pratt, I., Rietjens, I., Svensson, K., Tobbacq, P., Toldrá, F. (2004) Opinion of the Scientific Panel on food additives, flavourings, processing aids and materials in contact with food (AFC) related to para hydroxybenzoates (E 214-219). *EFSAJ* 2(9). <https://doi.org/10.2903/j.efs.2004.83>
- Arai, Y., Uehara, M., Sato, Y., Kimira, M., Eboshida, A., Adlercreutz, H., Watanabe, S. (2000). Comparison of isoflavones among dietary intake, plasma concentration and urinary excretion for accurate estimation of phytoestrogen intake. *Journal of Epidemiology*, 10(2). <https://doi.org/10.2188/jea.10.127>
- AstraZeneca Pharmaceuticals, 2005 L.P. AstraZeneca Pharmaceuticals CASODEX (bicalutamide) Manufactured by Caroline, PR 00984: IPR Pharmaceuticals Inc., USA. For Wilmington, DE 19850: AstraZeneca Pharmaceuticals LP (2005).
- Baker, M. E. (2013). What are the physiological estrogens? *Steroids*, 78(3). <https://doi.org/10.1016/j.steroids.2012.12.011>
- Baltazar, M. T., Cable, S., Carmichael, P. L., Cubberley, R., Cull, T., Delagrang, M., Dent, M. P., Hatherell, S., Houghton, J., Kukic, P., Li, H., Lee, M. Y., Malcomber, S., Middleton, A. M., Moxon, T. E., Nathanail, A. V., Nicol, B., Pendlington, R., Reynolds, G., ... Westmoreland, C. (2020). A next-generation risk assessment case study for coumarin in cosmetic products. *Toxicological Sciences*, 176(1). <https://doi.org/10.1093/toxsci/kfaa048>

- Barba, F. J., Nikmaram, N., Roohinejad, S., Khelfa, A., Zhu, Z., Koubaa, M. (2016). Bioavailability of Glucosinolates and Their Breakdown Products: Impact of Processing. In *Frontiers in Nutrition* (Vol. 3). <https://doi.org/10.3389/fnut.2016.00024>
- Basak, S., Das, M. K., Duttaroy, A. K. (2020). Plastics derived endocrine-disrupting compounds and their effects on early development. In *Birth Defects Research* (Vol. 112, Issue 17). <https://doi.org/10.1002/bdr2.1741>
- Bassetto, M., Ferla, S., Pertusati, F., Kandil, S., Westwell, A. D., Brancale, A., McGuigan, C. (2016). Design and synthesis of novel bicalutamide and enzalutamide derivatives as antiproliferative agents for the treatment of prostate cancer. *European Journal of Medicinal Chemistry*, 118. <https://doi.org/10.1016/j.ejmech.2016.04.052>
- B.C. Cancer Agency, 2001 B.C. Cancer Agency Limited Revision (2008 & 2011). Bicalutamide monograph BCCA Cancer Drug Manual. Vancouver, British Columbia (2001).
- Becker, R. A., Friedman, K. P., Simon, T. W., Marty, M. S., Patlewicz, G., & Rowlands, J. C. (2015). An exposure: Activity profiling method for interpreting high-throughput screening data for estrogenic activity-Proof of concept. *Regulatory Toxicology and Pharmacology*, 71(3). <https://doi.org/10.1016/j.yrtph.2015.01.008>
- Bedi, S., Hines, G. V., Lozada-Fernandez, V. v., Piva, C. D. J., Kaliappan, A., Rider, S. D., Hostetler, H. A. (2017). Fatty acid binding profile of the liver X receptor  $\alpha$ . *Journal of Lipid Research*, 58(2). <https://doi.org/10.1194/jlr.M072447>
- Bell, C.C., Dankers, A.C.A., Lauschke, V.M., Sison-Young, R., Jenkins, R., Rowe, C., et al. (2018). Comparison of Hepatic 2D Sandwich Cultures and 3D Spheroids for Long-term Toxicity Applications: A Multicenter Study. *Toxicol Sci.* 162(2):655-666.
- Bergman, Å., Heindel, J. J., Kasten, T., Kidd, K. A., Jobling, S., Neira, M., Zoeller, R. T., Becher, G., Bjerregaard, P., Bornman, R., Brandt, I., Kortenkamp, A., Muir, D., Drisse, M. N. B., Ochieng, R., Skakkebaek, N. E., Byléhn, A. S., Iguchi, T., Toppari, J., & Woodruff, T. J. (2013). The impact of endocrine disruption: A consensus statement on the state of the science. In *Environmental Health Perspectives* (Vol. 121, Issue 4). <https://doi.org/10.1289/ehp.1205448>
- Bessemers, J. G., Loizou, G., Krishnan, K., Clewell, H. J., Bernasconi, C., Bois, F., Coecke, S., Collnot, E. M., Diembeck, W., Farcas, L. R., Geraets, L., Gundert-Remy, U., Kramer, N., Küsters, G., Leite, S. B., Pelkonen, O. R., Schröder, K., Testai, E., Wilk-Zasadna, I., Zaldívar-Comenges, J. M. (2014). PBTK modelling platforms and parameter estimation tools to enable animal-free risk assessment. Recommendations from a joint EPAA -

EURL ECVAM ADME workshop. *Regulatory Toxicology and Pharmacology*, 68(1).  
<https://doi.org/10.1016/j.yrtph.2013.11.008>

- Bhatia, R., Shiao, R., Petreas, M., Weintraub, J. M., Farhang, L., Eskenazi, B. (2005). Organochlorine pesticides and male genital anomalies in the child health and development studies. *Environmental Health Perspectives*, 113(2).  
<https://doi.org/10.1289/ehp.7382>
- Bhatt, D. K., Basit, A., Zhang, H., Gaedigk, A., Lee, S. been, Claw, K. G., Mehrotra, A., Chaudhry, A. S., Pearce, R. E., Gaedigk, R., Broeckel, U., Thornton, T. A., Nickerson, D. A., Schuetz, E. G., Amory, J. K., Steven Leeder, J., Prasad, B. (2018). Hepatic abundance and activity of androgen- and drug-metabolizing enzyme UGT2B17 are associated with genotype, age, and sex. *Drug Metabolism and Disposition*, 46(6).  
<https://doi.org/10.1124/dmd.118.080952>
- Bilotta, M. T., Petillo, S., Santoni, A., Cippitelli, M. (2020). Liver X Receptors: Regulators of Cholesterol Metabolism, Inflammation, Autoimmunity, and Cancer. In *Frontiers in Immunology* (Vol. 11). <https://doi.org/10.3389/fimmu.2020.584303>
- Bolarinwa, A., & Linseisen, J. (2005). Validated application of a new high-performance liquid chromatographic method for the determination of selected flavonoids and phenolic acids in human plasma using electrochemical detection. *Journal of Chromatography B: Analytical Technologies in the Biomedical and Life Sciences*, 823(2).  
<https://doi.org/10.1016/j.jchromb.2005.06.024>
- Bolognesi, C., Castle, L., Cravedi, J.-P., Engel, K.-H., Fowler, P., Franz, R., Grob, K., Gürtler, R., Husøy, T., Mennes, W., Milana, M. R., Penninks, A., Roland, F., Silano, V., Smith, A., de Fátima Tavares Poças, M., Tlustos, C., Toldrá, F., Wölfle, D., Zorn, H. (2015) Scientific Opinion on the risks to public health related to the presence of bisphenol A (BPA) in foodstuffs. *EFSA J* 13(1). <https://doi.org/10.2903/j.efsa.2015.3978>
- Bonn, M., Eydeler, U., Barkworth, M., Rovati, L. C. (2009). Bioequivalence study of generic tablet formulations containing ethinylestradiol and chlormadinone acetate in healthy female volunteers. *Arzneimittel-Forschung/Drug Research*, 59(12).  
<https://doi.org/10.1055/s-0031-1296455>
- Brown, R. P., Delp, M. D., Lindstedt, S. L., Rhomberg, L. R., Beliles, R. P. (1997). Physiological Parameter Values for Physiologically Based Pharmacokinetic Models. *Toxicol. Ind. Health*. 13 (4), 407–484. doi:10.1177/074823379701300401

- Buck Louis, G. M., Rios, L. I., McLain, A., Cooney, M. A., Kostyniak, P. J., Sundaram, R. (2011). Persistent organochlorine pollutants and menstrual cycle characteristics. *Chemosphere*, 85(11). <https://doi.org/10.1016/j.chemosphere.2011.09.027>
- BURTON, K. (1956). A study of the conditions and mechanism of the diphenylamine reaction for the colorimetric estimation of deoxyribonucleic acid. *The Biochemical Journal*, 62(2). <https://doi.org/10.1042/bj0620315>
- Busby, M. G., Jeffcoat, A. R., Bloedon, L. A. T., Koch, M. A., Black, T., Dix, K. J., Heizer, W. D., Thomas, B. F., Hill, J. M., Crowell, J. A., Zeisel, S. H. (2002). Clinical characteristics and pharmacokinetics of purified soy isoflavones: Single-dose administration to healthy men. *American Journal of Clinical Nutrition*, 75(1). <https://doi.org/10.1093/ajcn/75.1.126>
- Calaf, J., López, E., Millet, A., Alcañiz, J., Fortuny, A., Vidal, O., Callejo, J., Escobar-Jiménez, F., Torres, E., Espinós, J. J. (2007). Long-term efficacy and tolerability of flutamide combined with oral contraception in moderate to severe hirsutism: A 12-month, double-blind, parallel clinical trial. *Journal of Clinical Endocrinology and Metabolism*, 92(9). <https://doi.org/10.1210/jc.2006-2798>
- Cannon, S. B., Veazey, J. M., Jackson, R. S., Burse, V. W., Hayes, C., Straub, W. E., Landrigan, P. J., Liddle, J. A. (1978). Epidemic kepone poisoning in chemical workers. *American Journal of Epidemiology*, 107(6). <https://doi.org/10.1093/oxfordjournals.aje.a112572>
- Carmichael, P., Davies, M., Dent, M., Fentem, J., Fletcher, S., Gilmour, N., MacKay, C., Maxwell, G., Merolla, L., Pease, C., Reynolds, F., Westmoreland, C. (2009). Non-animal approaches for consumer safety risk assessments: Unilever's scientific research programme. *ATLA Alternatives to Laboratory Animals*, 37(6). <https://doi.org/10.1177/026119290903700605>
- Carmichael, P. L., Baltazar, M. T., Cable, S., Cochrane, S., Dent, M., Li, H., Middleton, A., Muller, I., Reynolds, G., Westmoreland, C., White, A. (2022). Ready for Regulatory Use: NAMs and NGRA for Chemical Safety Assurance. *Altex*, 39(3). <https://doi.org/10.14573/altex.2204281>
- Chang, H. C., Seng, J. E., Leakey, J. E. A., Gandy, J. (2000). Metabolism of flutamide in diet control fischer 344 and brown Norway x F 344 rats, and its hydroxylation and conjugation by human CYP450s and UDP-glucuronosyltransferases. *Journal of Food and Drug Analysis*, 8(3). <https://doi.org/10.38212/2224-6614.2854>

- Chiba, M., Ishii, Y., Sugiyama, Y. (2009). Prediction of hepatic clearance in human from *in vitro* data for successful drug development. In *AAPS Journal* (Vol. 11, Issue 2). <https://doi.org/10.1208/s12248-009-9103-6>
- Cockshott, I. D. (2004). Bicalutamide: Clinical pharmacokinetics and metabolism. In *Clinical Pharmacokinetics* (Vol. 43, Issue 13). <https://doi.org/10.2165/00003088-200443130-00003>
- Coecke, S., Ahr, H., Blaauboer, B. J., Bremer, S., Casati, S., Castell, J., Combes, R., Corvi, R., Crespi, C. L., Cunningham, M. L., Elaut, G., Eletti, B., Freidig, A., Gennari, A., Gherzi-Egea, J. F., Guillouzo, A., Hartung, T., Hoet, P., Ingelman-Sundberg, M., ... Worth, A. (2006). Metabolism: A bottleneck in *in vitro* toxicological test development. *ATLA Alternatives to Laboratory Animals*, 34(1). <https://doi.org/10.1177/026119290603400113>
- Cooper, G. S., Klebanoff, M. A., Promislow, J., Brock, J. W., Longnecker, M. P. (2005). Polychlorinated biphenyls and menstrual cycle characteristics. *Epidemiology*, 16(2). <https://doi.org/10.1097/01.ede.0000152913.12393.86>
- Corbett, J. L., & Duncan, S. A. (2019). iPSC-Derived Hepatocytes as a Platform for Disease Modeling and Drug Discovery. In *Frontiers in Medicine* (Vol. 6). <https://doi.org/10.3389/fmed.2019.00265>
- Couse, J. F., & Korach, K. S. (1999). Estrogen receptor null mice: What have we learned and where will they lead us? In *Endocrine Reviews* (Vol. 20, Issue 3). <https://doi.org/10.1210/edrv.20.3.0370>
- Damstra, T., Barlow, S., Bergman, A., Kavlock, R., van der Kraak, G. (2002). World Health Organization: Global assessment of the state-of-the-science of endocrine disruptors. *WHO*.
- Dent, M. P., Li, H., Carmichael, P. L., Martin, F. L. (2019). Employing Dietary Comparators to Perform Risk Assessments for Anti-Androgens Without Using Animal Data. *Toxicological Sciences*, 167(2). <https://doi.org/10.1093/toxsci/kfy245>
- Deroo, B. J., & Korach, K. S. (2006). Estrogen receptors and human disease. In *Journal of Clinical Investigation* (Vol. 116, Issue 3). <https://doi.org/10.1172/JCI27987>
- Dinse, G. E., & Umbach, D. M. (2011). Characterizing non-constant relative potency. *Regulatory Toxicology and Pharmacology*, 60(3). <https://doi.org/10.1016/j.yrtph.2011.05.002>



- Doser, K., Guserle, R., Kramer, R., Laufer, S., Lichtenberger, K. (1997). Bioequivalence evaluation of two flutamide preparations in healthy female subjects. *Arzneimittel-Forschung/Drug Research*, 47(2).
- Edler, L., Poirier, K., Dourson, M., Kleiner, J., Mileson, B., Nordmann, H., Renwick, A., Slob, W., Walton, K., Würtzen, G. (2002). Mathematical modelling and quantitative methods. In *Food and Chemical Toxicology* (Vol. 40, Issues 2–3). [https://doi.org/10.1016/S0278-6915\(01\)00116-8](https://doi.org/10.1016/S0278-6915(01)00116-8)
- Elsenbrand, G. (2007). Isoflavones as phytoestrogens in food supplements and dietary foods for special medical purposes. In *Molecular Nutrition and Food Research* (Vol. 51, Issue 10). <https://doi.org/10.1002/mnfr.200700217>
- Emeville, E., Giusti, A., Coumoul, X., Thomé, J. P., Blanchet, P., Multigner, L. (2015). Associations of plasma concentrations of dichlorodiphenyldichloroethylene and polychlorinated biphenyls with prostate cancer: A case–control study in Guadeloupe (French West Indies). *Environmental Health Perspectives*, 123(4). <https://doi.org/10.1289/ehp.1408407>
- Escher, S. E., Aguayo-Orozco, A., Benfenati, E., Bitsch, A., Braunbeck, T., Brotzmann, K., Bois, F., van der Burg, B., Castel, J., Exner, T., Gadaleta, D., Gardner, I., Goldmann, D., Hatley, O., Golbamaki, N., Graepel, R., Jennings, P., Limonciel, A., Long, A., ... Fisher, C. (2022). Integrate mechanistic evidence from new approach methodologies (NAMs) into a read-across assessment to characterise trends in shared mode of action. *Toxicology in vitro*, 79. <https://doi.org/10.1016/j.tiv.2021.105269>
- European Commission. (2006). Regulation (EC) 1907/2006 of the European Parliament and of the Council of 18 December 2006 - REACH. *Official Journal of the European Union*.
- European Food Safety Authority (EFSA) (2012). Guidance on Selected Default Values to Be Used by the EFSA Scientific Committee, Scientific Panels and Units in the Absence of Actual Measured Data. *EFSA J.* 10 (325), 828–835. doi:10.2903/j.efsa.2012.2579
- Extended One-Generation Reproductive Toxicity Study (EOGRTS) (OECD TG 443). (2018). <https://doi.org/10.1787/9789264304741-34-en>
- Fabian, E., Gomes, C., Birk, B., Williford, T., Hernandez, T. R., Haase, C., Zbranek, R., van Ravenzwaay, B., Landsiedel, R. (2019). *In vitro*-to-*in vivo* extrapolation (IVIVE) by PBTK modeling for animal-free risk assessment approaches of potential endocrine-disrupting compounds. *Archives of Toxicology*, 93(2). <https://doi.org/10.1007/s00204-018-2372-z>

- Fan, K., Xu, J., Jiang, K., Liu, X., Meng, J., Di Mavungu, J. D., Guo, W., Zhang, Z., Jing, J., Li, H., Yao, B., Li, H., Zhao, Z., Han, Z. (2019). Determination of multiple mycotoxins in paired plasma and urine samples to assess human exposure in Nanjing, China. *Environmental Pollution*, 248. <https://doi.org/10.1016/j.envpol.2019.02.091>
- Fessler, M. B. (2018). The challenges and promise of targeting the Liver X Receptors for treatment of inflammatory disease. In *Pharmacology and Therapeutics* (Vol. 181). <https://doi.org/10.1016/j.pharmthera.2017.07.010>
- Fragkaki, A. G., Angelis, Y. S., Koupparis, M., Tsantili-Kakoulidou, A., Kokotos, G., Georgakopoulos, C. 2009. Structural characteristics of anabolic androgenic steroids contributing to binding to the androgen receptor and to their anabolic and androgenic activities. Applied modifications in the steroidal structure. *Steroids*. 74(2):172-97.
- Franssen, D., Svingen, T., Lopez Rodriguez, D., van Duursen, M., Boberg, J., Parent, A. S. (2022). A Putative Adverse Outcome Pathway Network for Disrupted Female Pubertal Onset to Improve Testing and Regulation of Endocrine Disrupting Chemicals. *Neuroendocrinology*, 112(2). <https://doi.org/10.1159/000515478>
- Frederiksen, H., Jørgensen, N., Andersson, A. M. (2011). Parabens in urine, serum and seminal plasma from healthy Danish men determined by liquid chromatography-tandem mass spectrometry (LC-MS/MS). *Journal of Exposure Science and Environmental Epidemiology*, 21(3). <https://doi.org/10.1038/jes.2010.6>
- Freire, C., Koifman, R. J., Sarcinelli, P. N., Simões Rosa, A. C., Clapauch, R., Koifman, S. (2013). Long-term exposure to organochlorine pesticides and thyroid status in adults in a heavily contaminated area in Brazil. *Environmental Research*, 127. <https://doi.org/10.1016/j.envres.2013.09.001>
- Freyberger, A., Andrews, P., Hartmann, E., Eiben, R., Loof, I., Schmidt, U., et al. (2003). Testing of Endocrine Active Substances Using an Enhanced OECD Test Guideline 407: Experiences from Studies on Flutamide and Ethinylestradiol. *Pure Appl. Chem.* 75, 2483–2489. doi:10.1351/pac200375112483
- Fujioka, N., Ainslie-Waldman, C. E., Upadhyaya, P., Carmella, S. G., Fritz, V. A., Rohwer, C., Fan, Y., Rauch, D., Le, C., Hatsukami, D. K., Hecht, S. S. (2014). Urinary 3,30-diindolylmethane: A biomarker of glucobrassicin exposure and indole-3-carbinol uptake in humans. *Cancer Epidemiology Biomarkers and Prevention*, 23(2). <https://doi.org/10.1158/1055-9965.EPI-13-0645>
- Fujioka, N., Ransom, B. W., Carmella, S. G., Upadhyaya, P., Lindgren, B. R., Roper-Batker, A., Hatsukami, D. K., Fritz, V. A., Rohwer, C., Hecht, S. S. (2016). Harnessing the power of

cruciferous vegetables: Developing a biomarker for brassica vegetable consumption using urinary 3,3'-diindolylmethane. *Cancer Prevention Research*, 9(10).  
<https://doi.org/10.1158/1940-6207.CAPR-16-0136>

- Gaspari, L., Paris, F., Jandel, C., Kalfa, N., Orsini, M., Dauris, J. P., Sultan, C. (2011). Prenatal environmental risk factors for genital malformations in a population of 1442 French male newborns: A nested casecontrol study. *Human Reproduction*, 26(11).  
<https://doi.org/10.1093/humrep/der283>
- Genschow, E., Spielmann, H., Scholz, G., Pohl, I., Seiler, A., Clemann, N., Bremer, S., Becker, K. (2004). Validation of the embryonic stem cell test in the international ECVAM validation study on three *in vitro* embryotoxicity tests. *ATLA Alternatives to Laboratory Animals*, 32(3). <https://doi.org/10.1177/026119290403200305>
- Genschow, E., Spielmann, H., Scholz, G., Seiler, A., Brown, N., Piersma, A., Brady, M., Clemann, N., Huuskonen, H., Paillard, F., Bremer, S., Becker, K. (2002). The ECVAM international validation study on *in vitro* embryotoxicity tests: Results of the definitive phase and evaluation of prediction models. *ATLA Alternatives to Laboratory Animals*, 30(2).  
<https://doi.org/10.1177/026119290203000204>
- Gilbert-Sandoval, I., Wesseling, S., Rietjens, I. M. C. M. (2020). Predicting the Acute Liver Toxicity of Aflatoxin B1 in Rats and Humans by an *In vitro*-*In silico* Testing Strategy. *Molecular Nutrition and Food Research*, 64(13).  
<https://doi.org/10.1002/mnfr.202000063>
- Goldberg, D. M., Yan, J., Soleas, G. J. (2003). Absorption of three wine-related polyphenols in three different matrices by healthy subjects. *Clinical Biochemistry*, 36(1).  
[https://doi.org/10.1016/S0009-9120\(02\)00397-1](https://doi.org/10.1016/S0009-9120(02)00397-1)
- Goda, R., Nagai, D., Akiyama, Y., Nishikawa, K., Ikemoto, I., Aizawa, Y., et al. (2006). Detection of a New N-Oxidized Metabolite of Flutamide, N-[4-nitro-3-(trifluoromethyl)phenyl]hydroxylamine, in Human Liver Microsomes and Urine of Prostate Cancer Patient. *Drug Metab. Dispos.* 34 (5), 828–835.
- Grace, P. B., Taylor, J. I., Low, Y. L., Luben, R. N., Mulligan, A. A., Botting, N. P., Dowsett, M., Welch, A. A., Khaw, K. T., Wareham, N. J., Day, N. E., Bingham, S. A. (2004). Phytoestrogen concentrations in serum and spot urine as biomarkers for dietary phytoestrogen intake and their relation to breast cancer risk in European Prospective Investigation of Cancer and Nutrition-Norfolk. *Cancer Epidemiology Biomarkers and Prevention*, 13(5). <https://doi.org/10.1158/1055-9965.698.13.5>

- Gripon, P., Rumin, S., Urban, S., Le Seyec, J., Glaise, D., Cannie, I., Guyomard, C., Lucas, J., Trepo, C., Guguen-Guillouzo, C. (2002). Infection of a human hepatoma cell line by hepatitis B virus. *Proceedings of the National Academy of Sciences of the United States of America*, 99(24). <https://doi.org/10.1073/pnas.232137699>
- Gu, X., & Manautou, J. E. (2012). Molecular mechanisms underlying chemical liver injury. In *Expert Reviews in Molecular Medicine* (Vol. 14). <https://doi.org/10.1017/S1462399411002110>
- Gülden, M., Mörchel, S., Tahan, S., Seibert, H. (2002). Impact of protein binding on the availability and cytotoxic potency of organochlorine pesticides and chlorophenols *in vitro*. *Toxicology*, 175(1–3). [https://doi.org/10.1016/S0300-483X\(02\)00085-9](https://doi.org/10.1016/S0300-483X(02)00085-9)
- Guldner, L., Multigner, L., Héraud, F., Monfort, C., Pierre Thomé, J., Giusti, A., Kadhel, P., Cordier, S. (2010). Pesticide exposure of pregnant women in Guadeloupe: Ability of a food frequency questionnaire to estimate blood concentration of chlordecone. *Environmental Research*, 110(2). <https://doi.org/10.1016/j.envres.2009.10.015>
- Gunness, P., Mueller, D., Shevchenko, V., Heinzle, E., Ingelman-Sundberg, M., Noor, F. (2013). 3D organotypic cultures of human heparg cells: A tool for *in vitro* toxicity studies. *Toxicological Sciences*, 133(1). <https://doi.org/10.1093/toxsci/kft021>
- Guzelian, P. S. (1992). The clinical toxicology of chlordecone as an example of toxicological risk assessment for man. *Toxicology Letters*, 64–65(C). [https://doi.org/10.1016/0378-4274\(92\)90236-D](https://doi.org/10.1016/0378-4274(92)90236-D)
- Hakura, A., Suzuki, S., Sawada, S., Sugihara, T., Hori, Y., Uchida, K., Kerns, W. D., Sagami, F., Motooka, S., Satoh, T. (2003). Use of human liver S9 in the Ames test: Assay of three procarcinogens using human S9 derived from multiple donors. *Regulatory Toxicology and Pharmacology*, 37(1). [https://doi.org/10.1016/S0273-2300\(02\)00024-7](https://doi.org/10.1016/S0273-2300(02)00024-7)
- Hargreaves, D. F., Potten, C. S., Harding, C., Shaw, L. E., Morton, M. S., Roberts, S. A., Howell, A., Bundred, N. J. (1999). Two-week dietary soy supplementation has an estrogenic effect on normal premenopausal breast. *Journal of Clinical Endocrinology and Metabolism*, 84(11). <https://doi.org/10.1210/jc.84.11.4017>
- Hardy, A., Benford, D., Halldorsson, T., Jeger, M. J., Knutsen, K. H., More, S., et al. (2017). Update: Use of the Benchmark Dose Approach in Risk Assessment. *EFSA J.* 15 (1), e04658. doi:10.2903/j.efsa.2017.4658
- Hartung, T. (2018). Perspectives on *in vitro* to *in vivo* extrapolations. In *Applied In vitro Toxicology* (Vol. 4, Issue 4). <https://doi.org/10.1089/aivt.2016.0026>

- Hashimoto, M., Kobayashi, K., Yamazaki, M., Kazuki, Y., Takehara, S., Oshimura, M., Chiba, K. (2016). Cyp3a deficiency enhances androgen receptor activity and cholesterol synthesis in the mouse prostate. *Journal of Steroid Biochemistry and Molecular Biology*, 163. <https://doi.org/10.1016/j.jsbmb.2016.04.018>
- Heald, C. L., Bolton-Smith, C., Ritchie, M. R., Morton, M. S., Alexander, F. E. (2006). Phyto-oestrogen intake in Scottish men: Use of serum to validate a self-administered food-frequency questionnaire in older men. *European Journal of Clinical Nutrition*, 60(1). <https://doi.org/10.1038/sj.ejcn.1602277>
- Hess, R. A., & Cooke, P. S. (2018). Estrogen in the male: A historical perspective. In *Biology of Reproduction* (Vol. 99, Issue 1). <https://doi.org/10.1093/biolre/i0y043>
- Hilborn, E., Stål, O., Jansson, A. (2017). Estrogen and androgen-converting enzymes 17 $\beta$ -hydroxysteroid dehydrogenase and their involvement in cancer: With a special focus on 17 $\beta$ -hydroxysteroid dehydrogenase type 1, 2, and breast cancer. In *Oncotarget* (Vol. 8, Issue 18). <https://doi.org/10.18632/oncotarget.15547>
- Högberg, J., Hanberg, A., Berglund, M., Skerfving, S., Remberger, M., Calafat, A. M., Filipsson, A. F., Jansson, B., Johansson, N., Appelgren, M., Håkansson, H. (2008). Phthalate diesters and their metabolites in human breast milk, blood or serum, and urine as biomarkers of exposure in vulnerable populations. *Environmental Health Perspectives*, 116(3). <https://doi.org/10.1289/ehp.10788>
- Hosoda, K., Furuta, T., Ishii, K. (2011). Metabolism and disposition of isoflavone conjugated metabolites in humans after ingestion of kinako. *Drug Metabolism and Disposition*, 39(9). <https://doi.org/10.1124/dmd.111.038281>
- Hyung, S. K., Tae, S. K., Il, H. K., Tae, S. K., Hyun, J. M., In, Y. K., Ki, H., Kui, L. P., Byung, M. L., Sun, D. Y., Han, S. Y. (2005). Validation study of OECD rodent uterotrophic assay for the assessment of estrogenic activity in Sprague-Dawley immature female rats. *Journal of Toxicology and Environmental Health - Part A*, 68(23–24). <https://doi.org/10.1080/15287390500182354>
- Ip, B. C., Cui, F., Wilks, B. T., Murphy, J., Tripathi, A., Morgan, J. R. (2018). Perfused Organ Cell-Dense Macrotissues Assembled from Prefabricated Living Microtissues. *Advanced Biosystems*, 2(8). <https://doi.org/10.1002/adbi.201800076>
- Ip, B. C., Leary, E., Knorlein, B., Reich, D., Van, V., Manning, J., Morgan, J. R. (2022). 3D Microtissues Mimic the Architecture, Estradiol Synthesis, and Gap Junction Intercellular Communication of the Avascular Granulosa. *Toxicological Sciences*, 186(1). <https://doi.org/10.1093/toxsci/kfab153>

- Ip, B. C., et al. (submitted). Development of a human liver microphysiological co-culture system for higher throughput chemical safety assessment.
- Iwasaki, M., Inoue, M., Otani, T., Sasazuki, S., Kurahashi, N., Miura, T., Yamamoto, S., Tsugane, S. (2008). Plasma isoflavone level and subsequent risk of breast cancer among Japanese women: A nested case-control study from the Japan Public Health Center-based prospective study group. *Journal of Clinical Oncology*, 26(10). <https://doi.org/10.1200/JCO.2007.13.9964>
- Jackson, J. P., Li, L., Chamberlain, E. D., Wang, H., Ferguson, S. S. (2016). Contextualizing hepatocyte functionality of cryopreserved HepaRG cell cultures. *Drug Metabolism and Disposition*, 44(9). <https://doi.org/10.1124/dmd.116.069831>
- Jacobs, M., Janssens, W., Bernauer, U., Brandon, E., Coecke, S., Combes, R., Edwards, P., Freidig, A., Freyberger, A., Kolanczyk, R., Mc Ardle, C., Mekenyan, O., Schmieder, P., Schrader, T., Takeyoshi, M., Burg, B. (2008). The Use of Metabolising Systems for *In vitro* Testing of Endocrine Disruptors. *Current Drug Metabolism*, 9(8). <https://doi.org/10.2174/138920008786049294>
- Jarvis, S., Williamson, C., Bevan, C. L. (2019). Liver X receptors and male (In) fertility. In *International Journal of Molecular Sciences* (Vol. 20, Issue 21). <https://doi.org/10.3390/ijms20215379>
- Jones, H. M., Chen, Y., Gibson, C., Heimbach, T., Parrott, N., Peters, S. A., Snoeys, J., Upreti, V. V., Zheng, M., Hall, S. D. (2015). Physiologically based pharmacokinetic modeling in drug discovery and development: A pharmaceutical industry perspective. In *Clinical Pharmacology and Therapeutics* (Vol. 97, Issue 3). <https://doi.org/10.1002/cpt.37>
- Kadhel, P., Monfort, C., Costet, N., Rouget, F., Thomé, J. P., Multigner, L., Cordier, S. (2014). Chlordecone exposure, length of gestation, and risk of preterm birth. *American Journal of Epidemiology*, 179(5). <https://doi.org/10.1093/aje/kwt313>
- Kang, P., Dalvie, D., Smith, E., Zhou, S., Deese, A., Nieman, J. A. (2008). Bioactivation of Flutamide Metabolites by Human Liver Microsomes. *Drug. Metab. Dispos.* 36 (7), 1425–1437. doi:10.1124/dmd.108.020370
- Kaur, G., & Dufour, J. M. (2012). Cell lines: Valuable tools or useless artifacts. *Spermatogenesis*, 2(1). <https://doi.org/10.4161/spmg.19885>
- Kezios, K. L., Liu, X., Cirillo, P. M., Cohn, B. A., Kalantzi, O. I., Wang, Y., Petreas, M. X., Park, J. S., Factor-Litvak, P. (2013). Dichlorodiphenyltrichloroethane (DDT), DDT metabolites

- and pregnancy outcomes. *Reproductive Toxicology*, 35(1).  
<https://doi.org/10.1016/j.reprotox.2012.10.013>
- Khan, S. A., Chatterton, R. T., Michel, N., Bryk, M., Lee, O., Ivancic, D., Heinz, R., Zalles, C. M., Helenowski, I. B., Jovanovic, B. D., Franke, A. A., Bosland, M. C., Wang, J., Hansen, N. M., Bethke, K. P., Dew, A., Coomes, M., Bergan, R. C. (2012). Soy isoflavone supplementation for breast cancer risk reduction: A randomized phase ii trial. *Cancer Prevention Research*, 5(2). <https://doi.org/10.1158/1940-6207.CAPR-11-0251>
- Kim, S., Thiessen, P. A., Bolton, E. E., Chen, J., Fu, G., Gindulyte, A., Han, L., He, J., He, S., Shoemaker, B. A., Wang, J., Yu, B., Zhang, J., Bryant, S. H. (2016). PubChem substance and compound databases. *Nucleic Acids Research*, 44(D1).  
<https://doi.org/10.1093/nar/gkv951>
- Kiyama, R., & Wada-Kiyama, Y. (2015). Estrogenic endocrine disruptors: Molecular mechanisms of action. In *Environment International* (Vol. 83).  
<https://doi.org/10.1016/j.envint.2015.05.012>
- Kolatorova Sosvorova, L., Chlupacova, T., Vitku, J., Vlk, M., Heracek, J., Starka, L., Saman, D., Simkova, M., Hampl, R. (2017). Determination of selected bisphenols, parabens and estrogens in human plasma using LC-MS/MS. *Talanta*, 174.  
<https://doi.org/10.1016/j.talanta.2017.05.070>
- Krewski, D., Acosta, D., Andersen, M., Anderson, H., Bailar, J. C., Boekelheide, K., Brent, R., Charnley, G., Cheung, V. G., Green, S., et al. (2010). Toxicity testing in the 21st century: A vision and a strategy Toxicity testing in the 21st century: A vision and a strategy. *J. Toxicol. Environ. Health B Crit. Rev.* 13, 51–138.
- Kostrubsky, S. E., Strom, S. C., Ellis, E., Nelson, S. D., Mutlib, A. E. (2007). Transport, Metabolism, and Hepatotoxicity of Flutamide, Drug-Drug Interaction With Acetaminophen Involving Phase I and Phase II Metabolites. *Chem. Res. Toxicol.* 20, 1503–1512.
- Kramer, G. F., Walls, C. L., and Perron, M. M. (2021). Chlorothalonil: Revised Human Health Draft Risk Assessment for Registration Review. Washington, DC: USEPA, D45766
- Krüger, T., Long, M., Bonefeld-Jørgensen, E. C. (2008). Plastic components affect the activation of the aryl hydrocarbon and the androgen receptor. *Toxicology*, 246(2–3).  
<https://doi.org/10.1016/j.tox.2007.12.028>
- Kunimatsu, T., Yamada, T., Miyata, K., Yabushita, S., Seki, T., Okuno, Y., et al. (2004). Evaluation for Reliability and Feasibility of the Draft Protocol for the Enhanced Rat

28-day Subacute Study (OECD Guideline 407) Using Androgen Antagonist Flutamide. *Toxicology* 200, 77–89. doi:10.1016/j.tox.2004.03.007

- Legler, J., Van Den Brink, C. E., Brouwer, A., Murk, A. J., Van Der Saag, P. T., Vethaak, A. D., Van Der Burg, B. (1999). Development of a stably transfected estrogen receptor-mediated luciferase reporter gene assay in the human T47D breast cancer cell line. *Toxicological Sciences*, 48(1). <https://doi.org/10.1093/toxsci/48.1.55>
- Leite, S. B., Wilk-Zasadna, I., Zaldivar, J. M., Airola, E., Reis-Fernandes, M. A., Mennecozi, M., Guguen-Guillouzo, C., Chesne, C., Guillou, C., Alves, P. M., Coecke, S. (2012). Three-dimensional HepaRG model as an attractive tool for toxicity testing. *Toxicological Sciences*, 130(1). <https://doi.org/10.1093/toxsci/kfs232>
- Li, A. P., Uzgaré, A., Laforge, Y. S. (2012). Definition of metabolism-dependent xenobiotic toxicity with co-cultures of human hepatocytes and mouse 3T3 fibroblasts in the novel integrated discrete multiple organ co-culture (IdMOC) experimental system: Results with model toxicants aflatoxin B1, cyclophosphamide and tamoxifen. *Chemico-Biological Interactions*, 199(1). <https://doi.org/10.1016/j.cbi.2012.05.003>
- Li, C. Y., Basit, A., Gupta, A., Gáborik, Z., Kis, E., Prasad, B. (2019). Major glucuronide metabolites of testosterone are primarily transported by MRP2 and MRP3 in human liver, intestine and kidney. *Journal of Steroid Biochemistry and Molecular Biology*, 191. <https://doi.org/10.1016/j.jsbmb.2019.03.027>
- Li, H., Yuan, H., Middleton, A., Li, J., Nicol, B., Carmichael, P., Guo, J., Peng, S., Zhang, Q. (2021). Next generation risk assessment (NGRA): Bridging *in vitro* points-of-departure to human safety assessment using physiologically-based kinetic (PBK) modelling – A case study of doxorubicin with dose metrics considerations. *Toxicology in vitro*, 74. <https://doi.org/10.1016/j.tiv.2021.105171>
- Liu, J., Mi, S., Du, L., Li, X., Li, P., Jia, K., Zhao, J., Zhang, H., Zhao, W., Gao, Y. (2018). The associations between plasma phytoestrogens concentration and metabolic syndrome risks in Chinese population. *PLoS ONE*, 13(3). <https://doi.org/10.1371/journal.pone.0194639>
- Loizou, G., & Hogg, A. (2011). MEGen: A physiologically based pharmacokinetic model generator. *Frontiers in Pharmacology*, 2 NOV. <https://doi.org/10.3389/fphar.2011.00056>
- Loizou, G., Spendiff, M., Barton, H. A., Bessems, J., Bois, F. Y., d'Yvoire, M. B., Buist, H., Clewell, H. J., Meek, B., Gundert-Remy, U., Goerlitz, G., Schmitt, W. (2008). Development of good modelling practice for physiologically based pharmacokinetic models for use in risk



- assessment: The first steps. *Regulatory Toxicology and Pharmacology*, 50(3).  
<https://doi.org/10.1016/j.yrtph.2008.01.011>
- Longnecker, M. P., Klebanoff, M. A., Brock, J. W., Zhou, H., Gray, K. A., Needham, L. L., Wilcox, A. J. (2002). Maternal serum level of 1,1-dichloro-2,2-bis(p-chlorophenyl)ethylene and risk of cryptorchidism, hypospadias, and polythelia among male offspring. *American Journal of Epidemiology*, 155(4). <https://doi.org/10.1093/aje/155.4.313>
- Louisse, J., Beekmann, K., Rietjens, I. M. C. M. (2017). Use of physiologically based kinetic modeling-based reverse dosimetry to predict *in vivo* toxicity from *in vitro* data. In *Chemical Research in Toxicology* (Vol. 30, Issue 1).  
<https://doi.org/10.1021/acs.chemrestox.6b00302>
- Ludwig, S., Tinwell, H., Schorsch, F., Cavaillé, C., Pallardy, M., Rouquié, D., et al. (2011). A Molecular and Phenotypic Integrative Approach to Identify a No-Effect Dose Level for Antiandrogen-Induced Testicular Toxicity. *Toxicol. Sci.* 122, 52–63.  
doi:10.1093/toxsci/kfr099
- Madlensky, L., Natarajan, L., Tchu, S., Pu, M., Mortimer, J., Flatt, S. W., Nikoloff, D. M., Hillman, G., Fontecha, M. R., Lawrence, H. J., Parker, B. A., Wu, A. H. B., Pierce, J. P. (2011). Tamoxifen metabolite concentrations, CYP2D6 genotype, and breast cancer outcomes. *Clinical Pharmacology and Therapeutics*, 89(5). <https://doi.org/10.1038/clpt.2011.32>
- Marcocchia, D., Pellegrini, M., Fiocchetti, M., Lorenzetti, S., Marino, M. (2017). Food components and contaminants as (anti)androgenic molecules. In *Genes and Nutrition* (Vol. 12, Issue 1). <https://doi.org/10.1186/s12263-017-0555-5>
- Mathew et al., 2020 J. Mathew, P. Sanker, M. Physiology Varacallo, Blood Plasma [Updated 2020 Mar 23]. In: StatPearls [Internet] StatPearls Publishing, Treasure Island (FL) (2020) Jan-. Available from <https://www.ncbi.nlm.nih.gov/books/NBK531504/>
- Matsumoto, T., Shiina, H., Kawano, H., Sato, T., Kato, S. (2008). Androgen receptor functions in male and female physiology. In *Journal of Steroid Biochemistry and Molecular Biology* (Vol. 109, Issues 3–5). <https://doi.org/10.1016/j.jsbmb.2008.03.023>
- Mayo Clinic Staff. (2022a). Estrogens, Estrone (E1) and Estradiol (E2), Fractionated, Serum. Mayo Clinic, Mayo Foundation for Medical Education and Research.  
<https://pediatric.testcatalog.org/show/ESTF>. Accessed 4 Jan 2022
- Mayo Clinic Staff. (2022b). Testosterone, Total and Free, Serum. Mayo Clinic, Mayo Foundation for Medical Education and Research, <https://testcatalog.org/show/TGRP>. Accessed 4 Jan 2022

- Mazzoleni, G., Di Lorenzo, D., Steimberg, N. (2009). Modelling tissues in 3D: The next future of pharmaco-toxicology and food research? In *Genes and Nutrition* (Vol. 4, Issue 1). <https://doi.org/10.1007/s12263-008-0107-0>
- Mckillop, D., Boyle, G. W., Cockshott, I. D., Jones, D. C., Phillips, P. J., Yates, R. A. (1993). Metabolism and enantioselective pharmacokinetics of casodex in man. *Xenobiotica*, 23(11). <https://doi.org/10.3109/00498259309059435>
- McLeod, D. G. (1993). Antiandrogenic drugs. *Cancer*, 71(3 S). [https://doi.org/10.1002/1097-0142\(19930201\)71:3+<1046::AID-CNCR2820711424>3.0.CO;2-M](https://doi.org/10.1002/1097-0142(19930201)71:3+<1046::AID-CNCR2820711424>3.0.CO;2-M)
- Mescher, 2009 A.L. Mescher Junquiera's Basic Histology: Text and Atlas (Twelfth edition), McGraw-Hill Education / Medical (2009), pp. 203-215 Chapter 12: Blood.
- Mendez-Catala, D. M., Wang, Q., Rietjens, I. M. C. M. (2021). PBK Model-Based Prediction of Intestinal Microbial and Host Metabolism of Zearalenone and Consequences for its Estrogenicity. *Molecular Nutrition and Food Research*, 65(23). <https://doi.org/10.1002/mnfr.202100443>
- Metzner, J. E., Frank, T., Kunz, I., Burger, D., Riegger, C. (2009). Study on the pharmacokinetics of synthetic genistein after multiple oral intake in post-menopausal women. *Arzneimittel-Forschung/Drug Research*, 59(10). <https://doi.org/10.1055/s-0031-1296435>
- Meyer, H., Bolarinwa, A., Wolfram, G., Linseisen, J. (2006). Bioavailability of apigenin from apiin-rich parsley in humans. *Annals of Nutrition and Metabolism*, 50(3). <https://doi.org/10.1159/000090736>
- Middleton, A. M., Reynolds, J., Cable, S., Baltazar, M. T., Li, H., Bevan, S., Carmichael, P. L., Dent, M. P., Hatherell, S., Houghton, J., Kukic, P., Liddell, M., Malcomber, S., Nicol, B., Park, B., Patel, H., Scott, S., Sparham, C., Walker, P., White, A. (2022). Are Non-animal Systemic Safety Assessments Protective? A Toolbox and Workflow. *Toxicological Sciences : An Official Journal of the Society of Toxicology*, 189(1). <https://doi.org/10.1093/toxsci/kfac068>
- Minelli, E. V., & Ribeiro, M. L. (1996). DDT and HCH residues in the blood serum of malaria control sprayers. *Bulletin of Environmental Contamination and Toxicology*, 57(5). <https://doi.org/10.1007/s001289900245>
- Mollergues, J., Van Vugt-Lussenburg, B., Kirchnawy, C., Bandi, R. A., Van Der Lee, R. B., Marin-Kuan, M., Schilter, B., Fussell, K. C. (2017). Incorporation of a metabolizing system in

- biodetection assays for endocrine active substances. *Altex*, 34(3).  
<https://doi.org/10.14573/altex.1611021>
- Moxon, T. E., Li, H., Lee, M. Y., Piechota, P., Nicol, B., Pickles, J., Pendlington, R., Sorrell, I., Baltazar, M. T. (2020). Application of physiologically based kinetic (PBK) modelling in the next generation risk assessment of dermally applied consumer products. *Toxicology in vitro*, 63. <https://doi.org/10.1016/j.tiv.2019.104746>
- Müderris, I. I., Bayram, F., Özçelik, B., Güven, M. (2002). New alternative treatment in hirsutism: Bicalutamide 25 mg/day. *Gynecological Endocrinology*, 16(1).  
<https://doi.org/10.1080/gye.16.1.63.66>
- Multigner, L., Kadhel, P., Huc-Terki, F., Thome, J. P., Janky, E., Auger, J. (2006). Exposure to Chlordecone and Male Fertility in Guadeloupe (French West Indies). *Epidemiology*, 17(Suppl). <https://doi.org/10.1097/00001648-200611001-00989>
- Multigner, L., Kadhel, P., Pascal, M., Huc-Terki, F., Kercret, H., Massart, C., Janky, E., Auger, J., Jégou, B. (2008). Parallel assessment of male reproductive function in workers and wild rats exposed to pesticides in banana plantations in Guadeloupe. *Environmental Health: A Global Access Science Source*, 7. <https://doi.org/10.1186/1476-069X-7-40>
- Multigner, L., Kadhel, P., Rouget, F., Blanchet, P., Cordier, S. (2016). Chlordecone exposure and adverse effects in French West Indies populations. *Environmental Science and Pollution Research*, 23(1). <https://doi.org/10.1007/s11356-015-4621-5>
- Nair, S. G., Patel, D. P., Gonzalez, F. J., Patel, B. M., Singhal, P., Chaudhary, D. v. (2018). Simultaneous determination of etonogestrel and ethinyl estradiol in human plasma by UPLC-MS/MS and its pharmacokinetic study. *Biomedical Chromatography*, 32(5).  
<https://doi.org/10.1002/bmc.4165>
- Najjar, A., Punt, A., Wambaugh, J. et al. Towards best use and regulatory acceptance of generic physiologically based kinetic (PBK) models for in vitro-to- in vivo extrapolation (IVIVE) in chemical risk assessment. *Arch Toxicol* 96, 3407–3419 (2022). <https://doi.org/10.1007/s00204-022-03356-5>
- Natarajan, N., Shambaugh, G. E., Elseth, K. M., Haines, G. K., Radosevich, J. A. (1994). Adaptation of the diphenylamine (DPA) assay to a 96-well plate tissue culture format and comparison with the MTT assay. *BioTechniques*, 17(1).
- Niculescu, M. D., Pop, E. A., Fischer, L. M., Zeisel, S. H. (2007). Dietary isoflavones differentially induce gene expression changes in lymphocytes from postmenopausal

women who form equal as compared with those who do not. *Journal of Nutritional Biochemistry*, 18(6). <https://doi.org/10.1016/j.jnutbio.2006.06.002>

- Nilsson, M., Stulnig, T. M., Lin, C. Y., Ai, L. Y., Nowotny, P., Liu, E. T., Steffensen, K. R. (2007). Liver X receptors regulate adrenal steroidogenesis and hypothalamic- pituitary-adrenal feedback. *Molecular Endocrinology*, 21(1). <https://doi.org/10.1210/me.2006-0187>
- NRC. (2007). Toxicity Testing in the 21st Century: A Vision and a Strategy | The National Academies Press. *Reproductive Toxicology*, 25(1).
- Nyffeler et al., (2023) Application of Cell Painting for chemical hazard evaluation in support of screening-level chemical assessments. *Tox. And applied pharma.*
- OECD. (2006). The use of metabolising systems for in vitro testing of endocrine disruptors.
- OECD. 2008. Test No. 407: Repeated Dose 28-day Oral Toxicity Study in Rodents, OECD Guidelines for the Testing of Chemicals, Section 4, OECD Publishing, Paris.
- OECD. 2009. Test No. 441: Hershberger Bioassay in Rats: A Short-term Screening Assay for (Anti)Androgenic Properties, OECD Guidelines for the Testing of Chemicals, Section 4, OECD Publishing, Paris.
- OECD. (2016). OECD Guideline for the Testing of Chemicals No. 455: Performance-Based Test Guideline for Stably Transfected Transactivation *In vitro* Assays to Detect Estrogen Receptor Agonists and Antagonists. *OECD Guidelines for the Testing of Chemicals*, 2006(January).
- OECD. (2016). Test No. 421: Reproduction/Developmental Toxicity Screening Test. Paris: OECD Publishing.
- OECD. (2018a). Guidance Document on Good *In vitro* Method Practices ( GIVIMP ) 4 September 2018. *OECD Guideline for the Testing of Chemicals*, 1(286).
- OECD. (2018b). Revised Guidance Document 150 on Standardised Test Guidelines for Evaluating Chemicals for Endocrine Disruption, OECD Series on Testing and Assessment. In *OECD Publishing* (Issue 286). <https://doi.org/10.1787/9789264304796-en>
- OECD. DRP 97. (2008). Detailed Review Paper on the use of metabolising systems for *in vitro* testing of endocrine disruptors. In *OECD Series on Testing and Assessment*.
- OECD-407. (2008). OECD. Guidelines for Testing of Chemicals. Repeated Dose 28-day Oral Toxicity. Organization for Economic Co-operation and Development. Guide No. 407

- (2008). [Revised Draft Guideline October 2008]. (<http://www.oecd.org>). [Accessed 29.11.18]. *OECD Guidelines for the Testing of Chemicals, October*.
- Paini, A., Leonard, J. A., Joossens, E., Bessems, J. G. M., Desalegn, A., Dorne, J. L., Gosling, J. P., Heringa, M. B., Klaric, M., Kliment, T., Kramer, N. I., Loizou, G., Louisse, J., Lumen, A., Madden, J. C., Patterson, E. A., Proença, S., Punt, A., Setzer, R. W., ... Tan, Y. M. (2019). Next generation physiologically based kinetic (NG-PBK) models in support of regulatory decision making. In *Computational Toxicology* (Vol. 9). <https://doi.org/10.1016/j.comtox.2018.11.002>
- Paini, A., Tan, Y. M., Sachana, M., Worth, A. (2021). Gaining acceptance in next generation PBK modelling approaches for regulatory assessments – An OECD international effort. In *Computational Toxicology* (Vol. 18). <https://doi.org/10.1016/j.comtox.2021.100163>
- Paterni, I., Granchi, C., Katzenellenbogen, J. A., Minutolo, F. (2014). Estrogen receptors alpha (ER $\alpha$ ) and beta (ER $\beta$ ): Subtype-selective ligands and clinical potential. In *Steroids* (Vol. 90). <https://doi.org/10.1016/j.steroids.2014.06.012>
- Paul Friedman, K., Gagne, M., Loo, L. H., Karamertzanis, P., Netzeva, T., Sobanski, T., Franzosa, J. A., Richard, A. M., Lougee, R. R., Gissi, A., Lee, J. Y. J., Angrish, M., Dorne, J. Lou, Foster, S., Raffaele, K., Bahadori, T., Gwinn, M. R., Lambert, J., Whelan, M., ... Thomas, R. S. (2020). Utility of *in vitro* Bioactivity as a Lower Bound Estimate of *in vivo* Adverse Effect Levels and in Risk-Based Prioritization. *Toxicological Sciences*, 173(1). <https://doi.org/10.1093/toxsci/kfz201>
- Pearce, R. G., Setzer, R. W., Strobe, C. L., Sipes, N. S., Wambaugh, J. F. (2017). Httk: R package for high-throughput toxicokinetics. *Journal of Statistical Software*, 79. <https://doi.org/10.18637/jss.v079.i04>
- Pelkonen, O., Turpeinen, M., Hakkola, J., Honkakoski, P., Hukkanen, J., Raunio, H. (2008). Inhibition and induction of human cytochrome P450 enzymes: Current status. In *Archives of Toxicology* (Vol. 82, Issue 10). <https://doi.org/10.1007/s00204-008-0332-8>
- Petrakis, N. L., Barnes, S., King, E. B., Lowenstein, J., Wiencke, J., Lee, M. M., Miike, R., Kirk, M., Coward, L. (1996). Stimulatory influence of soy protein isolate on breast secretion in pre- and postmenopausal women. *Cancer Epidemiology Biomarkers and Prevention*, 5(10).
- Proença, S., Escher, B. I., Fischer, F. C., Fisher, C., Grégoire, S., Hewitt, N. J., Nicol, B., Paini, A., Kramer, N. I. (2021). Effective exposure of chemicals in *in vitro* cell systems: A review

- of chemical distribution models. In *Toxicology in vitro* (Vol. 73).  
<https://doi.org/10.1016/j.tiv.2021.105133>
- Punt, A., Aartse, A., Bovee, T. F. H., Gerssen, A., van Leeuwen, S. P. J., Hoogenboom, R. L. A. P., Peijnenburg, A. A. C. M. (2019). Quantitative *in vitro*-to-*in vivo* extrapolation (QIVIVE) of estrogenic and anti-androgenic potencies of BPA and BADGE analogues. *Archives of Toxicology*, 93(7). <https://doi.org/10.1007/s00204-019-02479-6>
- Punt, A., Schiffelers, M. J. W. A., Jean Horbach, G., van de Sandt, J. J. M., Groothuis, G. M. M., Rietjens, I. M. C. M., Blaauboer, B. J. (2011). Evaluation of research activities and research needs to increase the impact and applicability of alternative testing strategies in risk assessment practice. *Regulatory Toxicology and Pharmacology*, 61(1). <https://doi.org/10.1016/j.yrtph.2011.06.007>
- Radwanski, E., Parentesis, G., Symchowicz, S., Zampaglione, N. (1989). Single and Multiple Dose Pharmacokinetic Evaluation of Flutamide in Normal Geriatric Volunteers. *The Journal of Clinical Pharmacology*, 29(6). <https://doi.org/10.1002/j.1552-4604.1989.tb03381.x>
- Ramaiahgari, S. C., Waidyanatha, S., Dixon, D., DeVito, M. J., Paules, R. S., Ferguson, S. S. (2017). Three-dimensional (3D) HepaRG spheroid model with physiologically relevant xenobiotic metabolism competence and hepatocyte functionality for liver toxicity screening. *Toxicological Sciences*, 159(1).  
<https://doi.org/10.1093/toxsci/kfx122>
- REACH (2006). REGULATION (EC) No 1907/2006 OF THE EUROPEAN PARLIAMENT AND OF THE COUNCIL of 18 December 2006 concerning the Registration, Evaluation, Authorisation and Restriction of Chemicals (REACH), establishing a European Chemicals Agency, amending Directive 1999/45/EC and repealing Council Regulation (EEC) No 793/93 and Commission Regulation (EC) No 1488/94 as well as Council Directive 76/769/EEC and Commission Directives 91/155/EEC, 93/67/EEC, 93/105/EC and 2000/21/EC. Official Journal of the European Union, L 396/1-849.
- Reed, G. A., Sunega, J. M., Sullivan, D. K., Gray, J. C., Mayo, M. S., Crowell, J. A., Hurwitz, A. (2008). Single-dose pharmacokinetics and tolerability of absorption-enhanced 3,3'-diindolylmethane in healthy subjects. *Cancer Epidemiology Biomarkers and Prevention*, 17(10). <https://doi.org/10.1158/1055-9965.EPI-08-0520>
- Repeated Dose 90-Day Oral Toxicity Study in Rodents (OECD TG 408). (2018).  
<https://doi.org/10.1787/9789264304741-23-en>

- Rietjens, I. M. C. M., Louisse, J., Punt, A. (2011). Tutorial on physiologically based kinetic modeling in molecular nutrition and food research. *Molecular Nutrition and Food Research*, 55(6). <https://doi.org/10.1002/mnfr.201000655>
- Rietjens, I. M. C. M., Sotoca, A. M., Vervoort, J., Louisse, J. (2013). Mechanisms underlying the dualistic mode of action of major soy isoflavones in relation to cell proliferation and cancer risks. In *Molecular Nutrition and Food Research* (Vol. 57, Issue 1). <https://doi.org/10.1002/mnfr.201200439>
- Risk assessment for peri- and post-menopausal women taking food supplements containing isolated isoflavones. (2015). *EFSA Journal*, 13(10). <https://doi.org/10.2903/j.efsa.2015.4246>
- Ritchie, M. R., Morton, M. S., Deighton, N., Blake, A., Cummings, J. H. (2004). Plasma and urinary phyto-oestrogens as biomarkers of intake: validation by duplicate diet analysis. *British Journal of Nutrition*, 91(3). <https://doi.org/10.1079/bjn20031062>
- Rizzello, F., Spisni, E., Giovanardi, E., Imbesi, V., Salice, M., Alvisi, P., Valerii, M. C., Gionchetti, P. (2019). Implications of the westernized diet in the onset and progression of IBD. In *Nutrients* (Vol. 11, Issue 5). <https://doi.org/10.3390/nu11051033>
- Rochat, B., Morsman, J. M., Murray, G. I., Figg, W. D., and McLeod, H. L. (2001). Human CYP1B1 and Anticancer Agent Metabolism: Mechanism for Tumor-specific Drug Inactivation? *J. Pharmacol. Exp. Ther.* 296, 537–541.
- Rodgers, T., Leahy, D., Rowland, M. (2005). Physiologically based pharmacokinetic modeling 1: Predicting the tissue distribution of moderate-to-strong bases. *Journal of Pharmaceutical Sciences*, 94(6). <https://doi.org/10.1002/jps.20322>
- Rodgers, T., & Rowland, M. (2006). Physiologically based pharmacokinetic modelling 2: Predicting the tissue distribution of acids, very weak bases, neutrals and zwitterions. *Journal of Pharmaceutical Sciences*, 95(6). <https://doi.org/10.1002/jps.20502>
- Rovida, C., & Hartung, T. (2009). Re-evaluation of animal numbers and costs for *in vivo* tests to accomplish REACH legislation requirements for chemicals - A report by the transatlantic think tank for toxicology (t4). *Altex*, 26(3). <https://doi.org/10.14573/altex.2009.3.187>
- Rowe, C., Gerrard, D. T., Jenkins, R., Berry, A., Durkin, K., Sundstrom, L., Goldring, C. E., Park, B. K., Kitteringham, N. R., Hanley, K. P., et al. 2013. Proteome-wide analyses of human hepatocytes during differentiation and dedifferentiation. *Hepatology* 58, 799–809.

- Rouquié, D., Friry-Santini, C., Schorsch, F., Tinwell, H., Bars, R. (2009). Standard and Molecular NOAELs for Rat Testicular Toxicity Induced by Flutamide. *Toxicol. Sci.* 109, 59–65. doi:10.1093/toxsci/kfp056
- Rumph, J. T., Stephens, V. R., Archibong, A. E., Osteen, K. G., Bruner-Tran, K. L. (2020). Environmental Endocrine Disruptors and Endometriosis. In *Advances in Anatomy Embryology and Cell Biology* (Vol. 232). [https://doi.org/10.1007/978-3-030-51856-1\\_4](https://doi.org/10.1007/978-3-030-51856-1_4)
- Russell, W., & Burch, R. (1959). The Principles of Humane Experimental Technique by W.M.S. Russell and R.L. Burch. *John Hopkins Bloomberg School of Public Health*.
- Safe, S. (2020). Recent advances in understanding endocrine disruptors: DDT and related compounds. *Faculty Reviews*, 9. <https://doi.org/10.12703/b/9-7>
- Sager, J. E., Yu, J., Ragueneau-Majlessi, I., Isoherranen, N. (2015). Physiologically based pharmacokinetic (PBPK) modeling and simulation approaches: A systematic review of published models, applications, and model verification. In *Drug Metabolism and Disposition* (Vol. 43, Issue 11). <https://doi.org/10.1124/dmd.115.065920>
- Schellhammer, P. F., Sharifi, R., Block, N. L., Soloway, M. S., Venner, P. M., Patterson, A. L., Sarosdy, M. F., Vogelzang, N. J., Schellenger, J. J., Kolvenbag, G. J. C. M. (1998). Erratum: Clinical benefits of bicalutamide compared with flutamide in combined androgen blockade for patients with advanced prostatic carcinoma: Final report of a double-blind, randomized, multicenter trial (*Urology* (September 1997) 50 (330-336)). In *Urology* (Vol. 51, Issue 2). [https://doi.org/10.1016/S0090-4295\(98\)00091-0](https://doi.org/10.1016/S0090-4295(98)00091-0)
- Schiffer, L., Arlt, W., & Storbeck, K. H. (2018). Intracrine androgen biosynthesis, metabolism and action revisited. In *Molecular and Cellular Endocrinology* (Vol. 465). <https://doi.org/10.1016/j.mce.2017.08.016>
- Schulz, M., Schmoldt, A., Donn, F., Becker, H. (1988). The pharmacokinetics of flutamide and its major metabolites after a single oral dose and during chronic treatment. *European Journal of Clinical Pharmacology*, 34(6). <https://doi.org/10.1007/BF00615229>
- Scientific Opinion on the risks for public health related to the presence of zearalenone in food. (2011). *EFSA Journal*, 9(6). <https://doi.org/10.2903/j.efsa.2011.2197>
- Setchell, K. D. R., Brown, N. M., Zhao, X., Lindley, S. L., Heubi, J. E., King, E. C., Messina, M. J. (2011). Soy isoflavone phase II metabolism differs between rodents and humans: Implications for the effect on breast cancer risk. *American Journal of Clinical Nutrition*, 94(5). <https://doi.org/10.3945/ajcn.111.019638>



- Setchell, K. D. R., Faughnan, M. S., Avades, T., Zimmer-Nechemias, L., Brown, N. M., Wolfe, B. E., Brashear, W. T., Desai, P., Oldfield, M. F., Botting, N. P., Cassidy, A. (2003). Comparing the pharmacokinetics of daidzein and genistein with the use of <sup>13</sup>C-labeled tracers in premenopausal women. *American Journal of Clinical Nutrition*, 77(2). <https://doi.org/10.1093/ajcn/77.2.411>
- She, J., Gu, T., Pang, X., Liu, Y., Tang, L., Zhou, X. (2022). Natural Products Targeting Liver X Receptors or Farnesoid X Receptor. In *Frontiers in Pharmacology* (Vol. 12). <https://doi.org/10.3389/fphar.2021.772435>
- Shet, M. S., McPhaul, M., Fisher, C. W., Stallings, N. R., Estabrook, R. W. (1997). Metabolism of the antiandrogenic drug (flutamide) by human CYP1A2. *Drug Metabolism and Disposition*, 25(11).
- Shi, M., Bouwmeester, H., Rietjens, I. M. C. M., Strikwold, M. (2020). Integrating *in vitro* data and physiologically based kinetic modeling-facilitated reverse dosimetry to predict human cardiotoxicity of methadone. *Archives of Toxicology*, 94(8). <https://doi.org/10.1007/s00204-020-02766-7>
- Shimazu, T., Inoue, M., Sasazuki, S., Iwasaki, M., Sawada, N., Yamaji, T., Tsugane, S. (2011). Plasma isoflavones and the risk of lung cancer in women: A nested case-control study in Japan. *Cancer Epidemiology Biomarkers and Prevention*, 20(3). <https://doi.org/10.1158/1055-9965.EPI-10-1025>
- Shoham, Z., & Schachter, M. (1996). Estrogen biosynthesis - Regulation, action, remote effects, and value of monitoring in ovarian stimulation cycles. *Fertility and Sterility*, 65(4). [https://doi.org/10.1016/s0015-0282\(16\)58197-7](https://doi.org/10.1016/s0015-0282(16)58197-7)
- Silano, V., Barat Baviera, J. M., Bolognesi, C., Chesson, A., Cocconcelli, P. S., Crebelli, R., Gott, D. M., Grob, K., Lampi, E., Mortensen, A., Rivière, G., Steffensen, I. L., Tlustos, C., van Loveren, H., Vernis, L., Zorn, H., Cravedi, J. P., Fortes, C., Tavares Poças, M. de F., ... Castle, L. (2019). Update of the risk assessment of di-butylphthalate (DBP), butylbenzyl-phthalate (BBP), bis(2-ethylhexyl)phthalate (DEHP), di-isononylphthalate (DINP) and di-isodecylphthalate (DIDP) for use in food contact materials. *EFSA Journal*, 17(12). <https://doi.org/10.2903/j.efsa.2019.5838>
- Sohoni, P., & Sumpter, J. P. (1998). Several environmental oestrogens are also anti-androgens. *Journal of Endocrinology*, 158(3). <https://doi.org/10.1677/joe.0.1580327>
- Sonneveld, E., Jansen, H. J., Riteco, J. A. C., Brouwer, A., van der Burg, B. (2005). Development of androgen- and estrogen-responsive bioassays members of a panel of human cell

line-based highly selective steroid-responsive bioassays. *Toxicological Sciences*, 83(1).  
<https://doi.org/10.1093/toxsci/kfi005>

- Sonneveld, E., J.A. Riteco, H.J. Jansen, B. Pieterse, A. Broywer, W.G. Schooner, B. van der Burg (2006). Comparison of in vitro and in vivo screening models for androgenic and estrogenic activities. *Toxicol. Sci.* 89(1), 173-187.
- Sonneveld, E., Pieterse, B., Schoonen, W. G., van der Burg, B. (2011). Validation of *in vitro* screening models for progestagenic activities: Inter-assay comparison and correlation with *in vivo* activity in rabbits. *Toxicology in vitro*, 25(2).  
<https://doi.org/10.1016/j.tiv.2010.11.018>
- Soto, A. M., Sonnenschein, C., Chung, K. L., Fernandez, M. F., Olea, N., Olea Serrano, F. (1995). The E-SCREEN assay as a tool to identify estrogens: An update on estrogenic environmental pollutants. *Environmental Health Perspectives*, 103(SUPPL. 7).  
<https://doi.org/10.1289/ehp.95103s7113>
- Soule, H. D., Vazquez, J., Long, A., Albert, S., Brennan, M. (1973). A human cell line from a pleural effusion derived from a breast carcinoma<sup>1,2</sup>. *Journal of the National Cancer Institute*, 51(5). <https://doi.org/10.1093/jnci/51.5.1409>
- Srivilai, J., Minale, G., Scholfield, C. N., Ingkaninan, K. (2019). Discovery of natural steroid 5 alpha-reductase inhibitors. In *Assay and Drug Development Technologies* (Vol. 17, Issue 2). <https://doi.org/10.1089/adt.2018.870>
- Stanley, L. A., & Wolf, C. R. (2022). Through a glass, darkly? HepaRG and HepG2 cells as models of human phase I drug metabolism. In *Drug Metabolism Reviews* (Vol. 54, Issue 1). <https://doi.org/10.1080/03602532.2022.2039688>
- Sumida, K., Ooe, N., Nagahori, H., Saito, K., Isobe, N., Kaneko, H., Nakatsuka, I. (2001). An *in vitro* reporter gene assay method incorporating metabolic activation with human and rat S9 or liver microsomes. *Biochemical and Biophysical Research Communications*, 280(1). <https://doi.org/10.1006/bbrc.2000.4071>
- Suzuki, T., Sasano, H., Andersson, S., Mason, J. I. (2000). 3 $\beta$ -Hydroxysteroid dehydrogenase/ $\Delta$ (5 $\rightarrow$ 4)-isomerase activity associated with the human 17 $\beta$ -hydroxysteroid dehydrogenase type 2 isoform. *Journal of Clinical Endocrinology and Metabolism*, 85(10). <https://doi.org/10.1210/jcem.85.10.6918>
- Takashima, N., Miyanaga, N., Komiya, K., Mori, M., Akaza, H. (2004). Blood isoflavone levels during intake of a controlled hospital diet. *Journal of Nutritional Science and Vitaminology*, 50(4). <https://doi.org/10.3177/jnsv.50.246>

- Tang, H., Hussain, A., Leal, M., Mayersohn, M., Fluhler, E. (2007). Interspecies prediction of human drug clearance based on scaling data from one or two animal species. *Drug Metabolism and Disposition*, 35(10). <https://doi.org/10.1124/dmd.107.016188>
- Testai, E., Bechaux, C., Buratti, F. M., Darney, K., Di Consiglio, E., Kasteel, E. E. J., Kramer, N. I., Lautz, L. S., Santori, N., Skaperda, Z., Kouretas, D., Turco, L., Vichi, S. (2021). Modelling human variability in toxicokinetic and toxicodynamic processes using Bayesian meta-analysis, physiologically-based modelling and *in vitro* systems. *EFSA Supporting Publications*, 18(4). <https://doi.org/10.2903/sp.efsa.2021.en-6504>
- Tevell, A., Lennernäs, H., Jönsson, M., Norlin, M., Lennernäs, B., Bondesson, U., Hedeland, M. (2006). Flutamide metabolism in four different species *in vitro* and identification of flutamide metabolites in human patient urine by high performance liquid chromatography/tandem mass spectrometry. *Drug Metabolism and Disposition*, 34(6). <https://doi.org/10.1124/dmd.105.008516>
- Thakkar, Y., Moustakas, H., Moelijker, N., Hendriks, G., Brandsma, I., Pfuhler, S., Api, A. M. (2023). Utility of ToxTracker in animal alternative testing strategy for fragrance materials. *Environmental and Molecular Mutagenesis*. <https://doi.org/10.1002/em.22532>
- The Endocrine Disruptor Screening and Testing Advisory Committee. (1998). Endocrine disruptor screening and testing advisory committee (EDSTAC) final report. Retrieved from <https://www.epa.gov/endocrine-disruption/endocrine-disruptor-screening-and-testingadvisory-committee-edstac-final>
- Thomson, C. A., Ho, E., Strom, M. B. (2016). Chemopreventive properties of 3,30-diindolylmethane in breast cancer: Evidence from experimental and human studies. *Nutrition Reviews*, 74(7). <https://doi.org/10.1093/nutrit/nuw010>
- Toyoda, K., Shibutani, M., Tamura, T., Koujitani, T., Uneyama, C., and Hirose, M. (2000). Repeated Dose (28 Days) Oral Toxicity Study of Flutamide in Rats, Based on the Draft Protocol for the 'Enhanced OECD Test Guideline 407' for Screening for Endocrine-Disrupting Chemicals. *Archives Toxicol.* 74, 127–132. doi:10.1007/s002040050664
- Two-Generation Reproduction Toxicity Study (OECD TG 416). (2018). <https://doi.org/10.1787/9789264304741-33-en>
- Tyrrell, C., Denis, L., Newling, D., Soloway, M., Channer, K., Cockshott, I. (1998). Casodex TM 10–200 mg daily, used as monotherapy for the treatment of patients with advanced prostate cancer. *European Urology*, 33.

- [US EPA] US Environmental Protection Agency. 2011\_ref 1. Uterotrophic Assay OCSP Guideline 890. 1600 Standard Evaluation Procedure ( SEP ) ENDOCRINE DISRUPTOR SCREENING PROGRAM.
- [US EPA] US Environmental Protection Agency. 2011\_ref 2. Androgen receptor binding (rat ventral prostate cytosol); standard evaluation procedure, 1-12.
- [US EPA] US Environmental Protection Agency. (2012) Benchmark Dose Technical Guidance. Washington, DC: U.S. Environmental protection Agency, Risk Assessment Forum. EPA/100/R-12/001. Environmental Protection Agency, Risk Assessment Forum. Available online at <https://www.epa.gov/risk/benchmark-dosE-technical-guidance>.
- [US EPA] US Environmental Protection Agency. (2018). Strategic Plan to Promote the Development and Implementation of Alternative Test Methods Within the TSCA Program. [https://www.epa.gov/sites/production/files/2018-06/documents/epa\\_alt\\_strat\\_plan\\_6-20-18\\_clean\\_final.pdf](https://www.epa.gov/sites/production/files/2018-06/documents/epa_alt_strat_plan_6-20-18_clean_final.pdf).
- Usmani, K. A., & Tang, J. (2004). Human cytochrome P450: metabolism of testosterone by CYP3A4 and inhibition by ketoconazole. *Current Protocols in Toxicology / Editorial Board, Mahin D. Maines (Editor-in-Chief) ... [et Al.], Chapter 4*. <https://doi.org/10.1002/0471140856.tx0413s20>
- Van Breemen, R. B., & Li, Y. (2005). Caco-2 cell permeability assays to measure drug absorption. In *Expert Opinion on Drug Metabolism and Toxicology* (Vol. 1, Issue 2). <https://doi.org/10.1517/17425255.1.2.175>
- van der Burg, B., Winter, R., Man, H. yen, Vangenechten, C., Berckmans, P., Weimer, M., Witters, H., van der Linden, S. (2010). Optimization and prevalidation of the *in vitro* AR CALUX method to test androgenic and antiandrogenic activity of compounds. *Reproductive Toxicology*, 30(1). <https://doi.org/10.1016/j.reprotox.2010.04.012>
- van der Burg, B., Winter, R., Weimer, M., Berckmans, P., Suzuki, G., Gijsbers, L., Jonas, A., van der Linden, S., Witters, H., Aarts, J., Legler, J., Kopp-Schneider, A., Bremer, S. (2010). Optimization and prevalidation of the *in vitro* ER $\alpha$  CALUX method to test estrogenic and antiestrogenic activity of compounds. *Reproductive Toxicology*, 30(1). <https://doi.org/10.1016/j.reprotox.2010.04.007>
- Van der Linden, S. C., von Bergh, A. R. M., van Vught-Lussenburg, B. M. A., Jonker, L. R. A., Teunis, M., Krul, C. A. M., et al. (2014). Development of a Panel of High-Throughput Reporter-Gene Assays to Detect Genotoxicity and Oxidative Stress. *Mutat.*

- Research/Genetic Toxicol. Environ. Mutagen. 760 (760), 23–32.  
doi:10.1016/j.mrgentox.2013.09.009
- Van Der Velpen, V., Geelen, A., Hollman, P. C. H., Schouten, E. G., Van 't Veer, P., Afman, L. A. (2014). Isoflavone supplement composition and equol producer status affect gene expression in adipose tissue: A double-blind, randomized, placebo-controlled crossover trial in postmenopausal women. *American Journal of Clinical Nutrition*, 100(5). <https://doi.org/10.3945/ajcn.114.088484>
- van Liempd, S., Morrison, D., Sysmans, L., Nelis, P., Mortishire-Smith, R. (2011). Development and validation of a higher-throughput equilibrium dialysis assay for plasma protein binding. *Journal of Laboratory Automation*, 16(1).  
<https://doi.org/10.1016/j.jala.2010.06.002>
- van Tongeren, T. C. A., Carmichael, P. L., Rietjens, I. M. C. M., Li, H. (2022). Next Generation Risk Assessment of the Anti-Androgen Flutamide Including the Contribution of Its Active Metabolite Hydroxyflutamide. *Frontiers in Toxicology*, 4.  
<https://doi.org/10.3389/ftox.2022.881235>
- van Tongeren, T. C. A., Moxon, T. E., Dent, M. P., Li, H., Carmichael, P. L., Rietjens, I. M. C. M. (2021). Next generation risk assessment of human exposure to anti-androgens using newly defined comparator compound values. *Toxicology in vitro*, 73.  
<https://doi.org/10.1016/j.tiv.2021.105132>
- van Vugt-Lussenburg, B. M. A., van der Lee, R. B., Man, H. Y., Middelhof, I., Brouwer, A., Besselink, H., van der Burg, B. (2018). Incorporation of metabolic enzymes to improve predictivity of reporter gene assay results for estrogenic and anti-androgenic activity. *Reproductive Toxicology*, 75. <https://doi.org/10.1016/j.reprotox.2017.11.005>
- Vandenberg, L. N. (2021). Toxicity testing and endocrine disrupting chemicals. In *Advances in Pharmacology* (Vol. 92). <https://doi.org/10.1016/bs.apha.2021.05.001>
- Varma, M. V., Steyn, S. J., Allerton, C., El-Kattan, A. F. (2015). Predicting Clearance Mechanism in Drug Discovery: Extended Clearance Classification System (ECCS). In *Pharmaceutical Research* (Vol. 32, Issue 12). <https://doi.org/10.1007/s11095-015-1749-4>
- Varnell, R. R., Arnold, T. J., Quandt, S. A., Talton, J. W., Chen, H., Miles, C. M., Daniel, S. S., Sandberg, J. C., Anderson, K. A., Arcury, T. A. (2021). Menstrual Cycle Patterns and Irregularities in Hired Latinx Child Farmworkers. *Journal of Occupational and Environmental Medicine*, 63(1). <https://doi.org/10.1097/JOM.0000000000002065>

- Vermet H, Raoust N, Ngo R, Esserméant L, Klieber S, Fabre G, Boulenc X. 2016. Evaluation of Normalization Methods To Predict CYP3A4 Induction in Six Fully Characterized Cryopreserved Human Hepatocyte Preparations and HepaRG Cells. *Drug Metab Dispos.* 44(1):50-60.
- Wambaugh, J. F., Wetmore, B. A., Pearce, R., Strope, C., Goldsmith, R., Sluka, J. P., Sedykh, A., Tropsha, A., Bosgra, S., Shah, I., Judson, R., Thomas, R. S., Setzer, R. W. (2015). Toxicokinetic triage for environmental chemicals. *Toxicological Sciences*, 147(1). <https://doi.org/10.1093/toxsci/kfv118>
- Wang, D., Rietdijk, M. H., Kamelia, L., Boogaard, P. J., Rietjens, I. M. C. M. (2021). Predicting the *in vivo* developmental toxicity of benzo[a]pyrene (BaP) in rats by an *in vitro*-*in silico* approach. *Archives of Toxicology*, 95(10). <https://doi.org/10.1007/s00204-021-03128-7>
- Wang, Q., Spenkelink, B., Boonpawa, R., Rietjens, I. M. C. M. (2022). Use of Physiologically Based Pharmacokinetic Modeling to Predict Human Gut Microbial Conversion of Daidzein to S-Equol. *Journal of Agricultural and Food Chemistry*, 70(1). <https://doi.org/10.1021/acs.jafc.1c03950>
- Wang, Q., Spenkelink, B., Boonpawa, R., Rietjens, I. M. C. M., Beekmann, K. (2020). Use of Physiologically Based Kinetic Modeling to Predict Rat Gut Microbial Metabolism of the Isoflavone Daidzein to S-Equol and Its Consequences for ER $\alpha$  Activation. *Molecular Nutrition and Food Research*, 64(6). <https://doi.org/10.1002/mnfr.201900912>
- Wang, S., Aarts, J. M. M. J. G., de Haan, L. H. J., Argyriou, D., Peijnenburg, A. A. C. M., Rietjens, I. M. C. M., Bovee, T. F. H. (2014). Towards an integrated *in vitro* strategy for estrogenicity testing. *Journal of Applied Toxicology*, 34(9). <https://doi.org/10.1002/jat.2928>
- Wetmore, B. A., Wambaugh, J. F., Allen, B., Ferguson, S. S., Sochaski, M. A., Setzer, R. W., Houck, K. A., Strope, C. L., Cantwell, K., Judson, R. S., LeCluyse, E., Clewell, H. J., Thomas, R. S., Andersen, M. E. (2015). Incorporating high-throughput exposure predictions with dosimetry-adjusted *in vitro* bioactivity to inform chemical toxicity testing. *Toxicological Sciences*, 148(1). <https://doi.org/10.1093/toxsci/kfv171>
- WHO, ILO, UNEP, IOMC. (2005). Chemical-Specific Adjustment Factors for Interspecies Differences and Human Variability : Guidance Document for Use of Data in Dose / Concentration – Response Assessment. *World Health Organisation*, 2.

- WHO. (2010) Characterization and application of physiologically based pharmacokinetic models in risk assessment. IPCS harmonization project document ; no. 9. World Health Organization, Geneva
- Wilson, V. S., & LeBlanc, G. A. (2000). The contribution of hepatic inactivation of testosterone to the lowering of serum testosterone levels by ketoconazole. *Toxicological Sciences*, 54(1). <https://doi.org/10.1093/toxsci/54.1.128>
- Wiraagni, I. A., Mohd, M. A., Rashid, R. A., Haron, D. E. B. M. (2020). Trace Level Detection of Bisphenol A Analogues and Parabens by LC-MS/MS in Human Plasma from Malaysians. *BioMed Research International*, 2020. <https://doi.org/10.1155/2020/2581287>
- Wishart, D. S., Tzur, D., Knox, C., Eisner, R., Guo, A. C., Young, N., Cheng, D., Jewell, K., Arndt, D., Sawhney, S., Fung, C., Nikolai, L., Lewis, M., Coutouly, M. A., Forsythe, I., Tang, P., Shrivastava, S., Jeroncic, K., Stothard, P., ... Querengesser, L. (2007). HMDB: The human metabolome database. *Nucleic Acids Research*, 35(SUPPL. 1). <https://doi.org/10.1093/nar/gkl923>
- Wu, T. Y., Huang, Y., Zhang, C., Su, Z. Y., Boyanapalli, S., Khor, T. O., Wang, H., Lin, H., Gounder, M., Kagan, L., Androulakis, I. P., Kong, A. N. T. (2015). Pharmacokinetics and pharmacodynamics of 3,3'-diindolylmethane (DIM) in regulating gene expression of phase II drug metabolizing enzymes. *Journal of Pharmacokinetics and Pharmacodynamics*, 42(4). <https://doi.org/10.1007/s10928-015-9421-5>
- Yamada, T., Kunimatsu, T., Sako, H., Yabushita, S., Sukata, T., Okuno, Y., et al. (2000). Comparative Evaluation of a 5-Day Hershberger Assay Utilizing Mature Male Rats and a Pubertal Male Assay for Detection of Flutamide's Antiandrogenic Activity. *Toxicol. Sci.* 53, 289–296. doi:10.1093/toxsci/53.2.289
- Yoon, M., Campbell, J. L., Andersen, M. E., Clewell, H. J. (2012). Quantitative *in vitro* to *in vivo* extrapolation of cell-based toxicity assay results. In *Critical Reviews in Toxicology* (Vol. 42, Issue 8). <https://doi.org/10.3109/10408444.2012.692115>
- Yuan, B., Zhen, H., Jin, Y., Xu, L., Jiang, X., Sun, S., Li, C., Xu, H. (2012). Absorption and plasma disposition of genistin differ from those of genistein in healthy women. *Journal of Agricultural and Food Chemistry*, 60(6). <https://doi.org/10.1021/jf204421c>
- Zacharia, L. C. (2017). Permitted daily exposure of the androgen receptor antagonist flutamide. *Toxicological Sciences*, 159(2). <https://doi.org/10.1093/toxsci/kfx135>

- Zanelli, U., Caradonna, N. P., Hallifax, D., Turlizzi, E., Houston, J. B. (2012). Comparison of cryopreserved HepaRG cells with cryopreserved human hepatocytes for prediction of clearance for 26 drugs. *Drug Metabolism and Disposition*, 40(1).  
<https://doi.org/10.1124/dmd.111.042309>
- Zhang, H., Basit, A., Busch, D., Yabut, K., Bhatt, D. K., Drozdik, M., Ostrowski, M., Li, A., Collins, C., Oswald, S., Prasad, B. (2018). Quantitative characterization of UDP-glucuronosyltransferase 2B17 in human liver and intestine and its role in testosterone first-pass metabolism. *Biochemical Pharmacology*, 156.  
<https://doi.org/10.1016/j.bcp.2018.08.003>
- Zhang, H., Chen, H., Li, X. J., Zhang, Q., Sun, Y. F., Liu, C. J., Yang, L. Z., Ding, Y. H. (2014). Pharmacokinetics and safety profiles of novel diethylstilbestrol orally dissolving film in comparison with diethylstilbestrol capsules in healthy Chinese male subjects. *International Journal of Clinical Pharmacology and Therapeutics*, 52(5).  
<https://doi.org/10.5414/CP201989>
- Zhang, H., Gao, N., Tian, X., Liu, T., Fang, Y., Zhou, J., Wen, Q., Xu, B., Qi, B., Gao, J., Li, H., Jia, L., Qiao, H. (2015). Content and activity of human liver microsomal protein and prediction of individual hepatic clearance *in vivo*. *Scientific Reports*, 5.  
<https://doi.org/10.1038/srep17671>
- Zhang, M., van Ravenzwaay, B., Fabian, E., Rietjens, I. M. C. M., Louisse, J. (2018). Towards a generic physiologically based kinetic model to predict *in vivo* uterotrophic responses in rats by reverse dosimetry of *in vitro* estrogenicity data. *Archives of Toxicology*, 92(3). <https://doi.org/10.1007/s00204-017-2140-5>
- Zhang, Q., Li, J., Middleton, A., Bhattacharya, S., and Conolly, R. B. (2018). Bridging the Data Gap from In Vitro Toxicity Testing to Chemical Safety Assessment through Computational Modeling. *Front. Public Health* 6, 261. doi:10.3389/fpubh.2018.00261
- Zhao, S., Wesseling, S., Spenkelink, B., Rietjens, I. M. C. M. (2021). Physiologically based kinetic modelling based prediction of *in vivo* rat and human acetylcholinesterase (AChE) inhibition upon exposure to diazinon. *Archives of Toxicology*, 95(5).  
<https://doi.org/10.1007/s00204-021-03015-1>
- Zuo, Z., Kwon, G., Stevenson, B., Diakur, J., Wiebe, L. I. (2000). Flutamide-hydroxypropyl-beta-chyclodextrin complex: formulation, physical characterization, and absorption studies using the Caco-2 *in vitro* model. *Journal of Pharmacy & Pharmaceutical Sciences : A Publication of the Canadian Society for Pharmaceutical Sciences, Société Canadienne Des Sciences Pharmaceutiques*, 3(2).







# Appendix

# **Appendix**

**Acknowledgment**

**Biography**

**List of Publications**

**Overview of completed training activities**

## Acknowledgment

I cannot believe my 4 year-long PhD journey is now finally completed. It were 4 of the most meaningful and exciting years full of growth, as well as the most challenging and insecure years full of self-exploration. An experience which has shaped me in both my scientific skills and my being, and which I could never had carried out without all of you. I would love to take these pages to express my forever gratitude and appreciation.

First of all, my supervisors Ivonne, Paul, and Hequn. Ivonne, I am forever grateful for your exquisite, inexhaustible, and inimitable knowledge. Your guidance and encouragement led me through the challenges of my PhD. Your valuable advice in both the science and process gave me direction when I was stuck. Your quick, sharp, detailed, and highly expert insights are an inspiration to us all, and I am grateful that I could witness and learn from it. I thank you for the trust you have put in me and for all the support you gave me to growing into the scientist I am today.

Paul, thank you for your everlasting knowledge, humour, and support. I am very grateful for the trust and all the opportunities you gave me during the time we worked together. The invitation to work a few months at SEAC made me get acquainted with the company and its people. I had a very pleasant collaboration and expanded my network with many great and knowledgeable people because if this. I also feel that my work was appreciated at SEAC which meant a great deal to me and motivated me. Unfortunately we did not get to meet very often face-to-face, that's why it was even more fun seeing you at SOT in San Diego. It was great catching up over a good IPA and always a pleasure to lead the group to The Tippy Crow for assessing another angle of toxicology. Paul, you have been a very important figure during my PhD. Listening and assisting me when I struggled scientifically or personally. The way you can pin point essential and put into perspective other things contributes to the joy I find in my work today, for which I will be forever grateful. I am positive we will meet in the toxicology world and am looking forward continuing our conversations.

Hequn, a biggest thank you for all the knowledge, help, shared visions, and conversations. The insights you gave me content, career, and personal wise will keep helping me in my life. The in-depth supervision during our weekly meetings and patience with which you tackled problems were indispensable for the success of my PhD. Your calmness and infinite support during challenging and stressful periods were invaluable to keep going. I learned true problem solving from you and for that I am very grateful. The way you combine raising your family with your work in such an energetic

and ambitious way is inspirational. I wish you all the best in your next adventure as PBK modeller and look forward to meet you again somewhere in the toxicology world.

I also gratefully thank the members of the thesis committee for their precious time to evaluate my thesis. Your efforts are highly appreciated.

Then to my co-authors, without you this thesis would not have existed. I would like to extend my deepest gratitude to all of you, for the insightful discussions and comments valuable to the projects and the hard work you put into reviewing the manuscripts.

I cannot begin to express my thanks and appreciation to my technicians, Laura, Bert, Hans, Sebas, and Wouter. I think I am not only speaking for myself but also for all the other PhD'ers and students if I say that you are the engines of the department and you make the lab work pleasant and fun. Laura, your technical guidance and, even more valuable, your warmth and personal guidance has pulled me through all the cell culture work and PhD as a whole. Your endless knowledge on everything which has to do with a cell or bioassay and your creative in-depth problem solving has deeply impressed me and you taught me countless skills. Bert and Hans, thank you for all the handy tips and good talks we had in the lab, it made me gain more technical confidence in my first years. Sebas and Wouter, thank you for all the work and support in the analytics. Without your tips, tricks and humour, making endless dilution series and running endless numbers of samples would have been unbearable.

Thanks to the team at SEAC, Alistair, Beate, Carl, Ian, Iris, Lisa, Maria, Matt, Predrag, Richard, Sandrine, Sarah, Sophie, Tom and the other wonderful people for all the knowledge you shared with me. The time you have taken to meet with me and discuss and explain complex matters made that I did not see those subjects as problems anymore but as interesting and exciting challenges.

I would like to express my heartfelt gratitude and appreciation to the team at Brown, Kim, Sue, Blanche, and Sam. Thank you for having me and making my time overseas one of the most exciting, informative, and, most important, fun periods during my PhD. I am impressed by your professionalism and the constructive and considerate way you work together, it must be an example for all work places. Kim, your knowledge, expertise, enthusiasm, dedication, and kindness have taught me a lot and made a significant impact on how I will pursue the norms and values of how I want to work and collaborate in the future. I am forever grateful for your scientific and personal mentorship which has shaped me to be confident and determined entering the next phase after my PhD. Sue, I cannot begin to express that pipetting those cells very slooowly into those little

wells became actually so much fun with you next to me, as well as all the other lab journeys we had together. It was great having you around for all the handy lab-tips, happy chats, and good conversations. Thank you for letting me enjoy the warmth and comfort of you, your family and your home. You truly are the lab mom and I truly miss you. Blanche, your inexhaustible energy, expertise, and motivation are indispensable for the positive atmosphere and success of the project. I think I never saw anyone work so meticulously as you, which I deeply respect. You go above and beyond helping and supporting your colleagues and it is a joy learning from you. Thank you for your time and efforts mentoring me and teaching me skills which I will forever value. Sam, good times chatting with you during lab work and thanks for showing me the ins and outs of the techniques. Your positive and practical attitude towards challenges is praiseworthy and it is a joy to see you talk with so much love about your family. I am very much looking forward meeting you all in person again somewhere in Rhode Island, Utrecht or for a good hike in Switzerland!

Then a big thank you to my amazing colleagues at Tox for the great years at the department and your companionship. The PhD trip in the UK being the grand finale. Thanks to my office mates for all the nice chats and brainstorming. To the SOT meiden, Annelies, Katja and Véronique, thank you for the incredible week in San Diego! It was great to end a full conference day in our loft, and only have to take the elevator for a “good” dose of fun in the comedy club. And Salsa dancing in Club Sevilla cannot be complete without over-priced tequila. To Jing, the endless hours of pipetting were fun because of you and I am glad we could laugh at each other when we had to redo an experiment for the how-maniest of time. It was always good to know that there was someone even more sleepy (you) and please get a puppy. I will miss our chats and lunches! To Merel, so much fun being hotel roomies in London. I will miss our chats and the peptalks and it was always fun to hear about your worms. To Aafke, your enthusiasm and passion in science is contagious. It is an inspiration to see how you stand in life with your positivity and resilience. To Katharina, thank you for the endless hours of chatting in our office and your openness. You have a way of motivating people and showing us again what our passion in our work was. To Jingxuan and Qiuhui, thanks for being great lab-and science buddies and making the lab tasks fun together. To Maartje, my “enige maat uit Wageningen”. Luckily we didn’t stay that way and it was great diving together in the world of toxicology. Already in the masters we worked “met trots” and we continued that at the Tox department. But maybe can you explain one more time about the lion and the cage? I admire how you tackle things with your positivity, strength, sharpness, and humour. I won’t forget “de letteren” and hope we will one day find out what peerlie means.

A big thanks for the greatest paranympths, Geert and Wieke. Geert, wat ben ik blij dat we over fietstochten, lunchwandelingetjes, planten, borrels in Café de Haard en dansjes in Club Tegel vrienden zijn geworden. Je bent een prachtmens en dank je dat je me altijd weet op te vrolijken en dat gedoe naar de achtergrond weet te brengen. Zonder jouw droogheid en oneindige grapjes was ik niet door die PhD heen gekomen. Om Wulfgang te quoten zijn we “ein sehr nettes Paar” en laten we snel samen een eind nemen. Wieke, toen ik je ontmoette vond ik je een leuk en gevat mens en ben enorm blij dat we al zo lang vriendinnen zijn. Het is fantastisch om van jouw scherpzinnigheid, humor en warmte te genieten. Het is prachtig om met jou alles te kunnen ondernemen van een klassiek concert tot een all-inclusive in Almelo. Met jou eindeloos keuvelen over onzin en belangrijke zaken op persoonlijk- en wereldtoneel was essentieel om niet knettergek te worden deze 4 jaar, bedankt daarvoor.

Dan aan iedereen die er over de jaren waren. Karlijn, Lotte, Nynke, Rian, Nynke en Wieke, dank jullie dat ik al 10 jaar van Rowdeo kan genieten. Wat begon met een A-finale roeiwedstrijdje verliep al snel naar een avond-finale biercantus, en ergens op dat spectrum hebben we elkaar helemaal gevonden. Ze zeggen dat je in je studententijd de vrienden van je leven maakt en jullie zijn de belichaming van dat. In jullie bijzijn heb ik veel van mijn mooiste herinneringen gemaakt, van tappen als eerstejaars broekies tot een drijvende kaasplank in de hottub vlak nadat ik mijn PhD thesis inleverde. Jullie zijn rotsen en een baken van vrolijkheid in tijden dat ik het allemaal even niet meer zag en bedankt voor jullie schouders om op uit te huilen en alle onderbroekenlol. Jullie zijn stuk voor stuk enorm sterke, inspirerende, prachtige en verschrikkelijk grappige vrouwen en heb dikke mazzel dat ik jullie in mijn leven heb. Tim en Eva, jullie hebben mijn Orca jaren nog beter gemaakt. Allebei knettergek, op de beste manier. Tim, jouw humor in combinatie met je intelligentie zijn fantastisch. Eva, jouw oneindige interesse in mensen en prachtige dance moves zijn heerlijk om mee te maken. Bedankt voor alle feestjes, festivals en avonturen tussen de PhD struggles door en die door jullie altijd schitterend zijn. Floor en Sara, wat ben ik blij dat ik door mijn slechte handschrift met jullie in de Hiërogliefenclub kwam! Dank jullie voor de waardevolle vriendschap. Floor, dank je voor je gezelligheid, luisterend oor en je onuitputtelijke optimisme. Er zouden meer mensen zo constructief en empathisch in het leven moeten staan als jij. Sara, dank je voor je scherpzinnigheid, nuchterheid en humor, en alle slappe lachbuien die jij en Gerda me bezorgen. Met jou door de VS karren (we moeten door!) was een van de beste en mooiste reizen. Sanne, vanaf onze hospiteeravond maten en bedankt voor de ontelbare feestjes die we hebben gehad. Die ene alleen met zijn tweeën samen dat de politie moest komen is mijn favoriet. Jouw gezelligheid, positiviteit en doorzettingsvermogen zijn fantastisch om mee te maken. Je bent een mooie sterke vrouw en niet kapot te krijgen. Dank je wel voor alle lol, dansjes, gesprekken, luisterend oor en warmte die je me geeft. Het Kamperhuis, dank jullie voor alle

proefondervindelijke intoxicatie en de mooie tijd. Moppiegozerwijven, Gijsje, Ine en Jamie, wat een tornado sinds we elkaar ontmoetten in Here Hostel en altijd weer chaos als we elkaar zien. Dank jullie voor alle mooie feestjes, enerverende uitspraken en acute feedback. Met jullie en Fredlars kan ik me geen betere familie Broekmans wensen! Dakterraspeople (de naam is even discreet veranderd), bedankt voor de prachtige middelbare school jaren op het dakterras en in de pub. Celine en Blom, bedankt voor al jullie hilariteit, gesprekken en vriendschap. Bente en Suzanne, jullie zijn er langs de hele linie geweest sinds het klimrek op de basisschool en bedankt dat ik nog steeds van jullie gezelligheid en warmte mag genieten.

Rick, lieve schat, bedankt voor je liefde, warmte en steun. Ik kan met niet voorstellen hoe ik dit zonder jou had moeten doen. Jouw onvoorwaardelijk vermogen om me te kalmeren, te vertroetelen, op te vrolijken, me eruit te fietsen, om dingen te relativeren en dingen leuk te maken is het beste wat er is. Jouw geduld en begrip zijn oneindig en woorden schieten te kort om te zeggen hoe belangrijk die voor me zijn. Zonder jou zijn deze jaren niet zo kleurrijk en was er geen mooi en leesbaar boek geweest. Je maakt me gelukkig en kan niet wachten tot het volgende avontuur, met jou aan mijn zijde.

Lieve Piet en Lindert, ik ben onbeschrijfelijk dankbaar voor een familie zoals jullie. Jullie zijn mijn basis en door jullie liefde en steun ben ik wie ik ben. Door jullie vasthoudendheid en vertrouwen in mij heb ik geleerd me niet uit het veld te laten slaan. Jullie intelligentie en nieuwsgierigheid hebben me geleerd om altijd afvragen te waarom iets is zoals het is, en waarom het niet anders zou kunnen zijn. Jullie kijk op de wereld met verwondering, compassie en ook met kritiek, inspireert mij om te ontdekken en leert me wanneer me te verwonderen en wanneer niet naïef te zijn. Jullie pragmatisme, humor en kalmte helpen me te relativeren en zijn onmisbaar voor mij en dit succes. Zonder jullie was ik hier nooit gekomen. Met jullie, Marleen en Pleun heb ik een warm en veilig nest waarop ik altijd kan terugvallen, en daarmee prijs ik mezelf immens gelukkig.

Lieve Marjo, dank je voor de liefde en basis die je me hebt gegeven. Je bent de vrouw die ik ooit hoop te zijn en ik mis je. Dank je voor je kunst waarmee je ons raakte en inspireerde, en die me dit proefschrift op een prachtige manier laat afsluiten.

Tessa,  
July 2023



## Biography

Tessa van Tongeren was born on August 16<sup>th</sup> 1995 in Haarlem, The Netherlands. She completed her Bachelor in Biomedical Sciences at the Utrecht University in 2016, including the successful completion of its honours program. She continued with her Masters Molecular Nutrition and Toxicology at Wageningen University and Research and conducted her thesis at the Division of Toxicology. She finalized her second thesis at Unilever Safety and Environmental Assurance Centre (SEAC) in the United Kingdom and obtained her Master's degree in 2019. In that same year, she started her PhD at Division of Toxicology, Wageningen University, under supervision of prof. dr. ir. Ivonne M.C.M Rietjens as well as prof. dr. Paul L. Carmichael and dr. Hequn Li from the project sponsor company Unilever SEAC in the United Kingdom. During her PhD, she followed the postgraduate education program in Toxicology which facilitates her to register as a European Toxicologist (ERT). In 2020, she was awarded runner-up in the annual Unilever SEAC PhD Award for Science Communication. In 2022, she spend 6 months as a Visiting Research Fellow at the Department of Pathology and Laboratory Medicine, Brown University, USA.

## List of publications

**van Tongeren TCA**, Moxon TE, Dent MP, Li H, Carmichael PL, Rietjens IMCM. (2021). Next generation risk assessment of human exposure to anti-androgens using newly defined comparator compound values. *Toxicology in Vitro*. 73, 105132.

**van Tongeren TCA**, Carmichael PL, Rietjens IMCM, Li H. (2022). Next generation risk assessment of the anti-androgen flutamide including the contribution of its active metabolite hydroxyflutamide. *Frontiers in Toxicology*. 4, 881235.

**van Tongeren TCA**, Wang S, Carmichael PL, Rietjens IMCM, Li H. (2023). Next generation risk assessment of human exposure to estrogens using safe comparator compound values based on in vitro bioactivity assays. *Archives of Toxicology*. 97, 1547-75.

**van Tongeren TCA**, Hall SJ, Madnick SJ, Ip BC, Carmichael PL, Li H, Chen W, Breitweiser LA, Pence H, Ames DM, Bowling AJ, Johnson KJ, Cubberley R, Sherf B, Morgan JR, Boekelheide K. (Submitted). A two-chamber co-culture system with human liver and reporter cells for evaluating androgenic responses.

## Overview of completed training activities

### Discipline specific activities

NGRA workshop, Unilever (Sharnbrook, UK, 2019)  
Risk Assessment, PET (Wageningen, 2019)  
Medical and Forensic Toxicology, PET (Utrecht, 2019)  
Pathobiology, PET (Online, 2020)  
Reproduction Toxicology, PET (Online, 2020)  
Cell Toxicology, PET (Online, 2021)  
Molecular Toxicology, PET (Online, 2021)  
Organ Toxicology, PET (Online, 2021)  
Epidemiology, PET (Online, 2021)  
Visiting Scholar, Brown University (Providence, RI, USA, 2023)

### General courses

VLAG PhD week, VLAG (Baarlo, 2019)  
Philosophy and Ethics of Food Science and Technology, VLAG (Wageningen, 2020)  
Introduction to R, VLAG (Wageningen, 2020)  
Bridging across Cultural Differences, WGS (Wageningen, 2020)  
Reviewing a Scientific Manuscript, WGS (Wageningen, 2020)  
Laboratory Animal Science, PET (Online, 2021)  
VLAG online lectures, VLAG (Online, 2020)

### Optional courses and other activities

Preparation of Research Proposal, Wageningen  
Group meetings and scientific discussions/presentations, TOX  
General Toxicology, WUR (Wageningen, 2019)  
Environmental Toxicology, PET (Online, 2020)  
PhD study tour to the UK (UK, 2023)

### Conferences and meetings

11<sup>th</sup> World Congress on Alternatives and Animal Use in the Life Sciences (poster presentation), WC11 (Online, 2021)  
60<sup>th</sup> Annual meeting Society of Toxicology, SOT (Online, 2021)

61<sup>st</sup> Annual meeting Society of Toxicology (poster presentation), SOT (San Diego, CA, USA, 2022)

Annual meeting Dutch Endocrine Meeting (oral presentation), NVE (Noordwijk, 2023)

Annual meeting European Society for Sexual Medicine, ESMM (Rotterdam, 2023)

Annual meeting British Toxicology Society (oral presentation), BTS (Birmingham, UK, 2023)



This research described in this thesis was financially supported by Unilever.

Financial support from Wageningen University for printing this thesis is gratefully acknowledged.

Design by Rick Waasdorp

Art by Marjo J. Alkemade



